



UNIVERSITY OF  
**TEXAS**  
ARLINGTON

TxDOT Report 0-7008-1

**Advanced Geophysical Tools for Geotechnical Analysis**  
**Final Report**

Mohsen Shahandashti, Ph.D., P.E.

Sahadat Hossain, Ph.D., P.E.

Mina Zamanian

Md. Asif Akhtar

---

Report Publication Date: Submitted: August 2021  
Published: September 2021

Project: 0-7008

Project Title: Advanced Geophysical Tools for Geotechnical Analysis

Technical Report Documentation Page

1. Report No. FHWA/TX-20/0-7008-1		2. Government Accession No.		3. Recipient's Catalog No.	
4. Title and Subtitle Advanced Geophysical Tools for Geotechnical Analysis: Final Report				5. Report Date August 2021; published September 2021	
7. Author(s) Mohsen Shahandashti ( <a href="https://orcid.org/0000-0002-2373-7596">https://orcid.org/0000-0002-2373-7596</a> ), Sahadat Hossain, Mina Zamanian, Md. Asif Akhtar				6. Performing Organization Code	
9. Performing Organization Name and Address The University of Texas at Arlington Department of Civil Engineering P.O. Box 19308 Arlington, TX 76019				8. Performing Organization Report No. 0-7008-1	
12. Sponsoring Agency Name and Address Texas Department of Transportation Research and Technology Implementation Division P.O. Box 5080 Austin, TX 78763-5080				10. Work Unit No. (TRAIS)	
				11. Contract or Grant No. 0-7008	
				13. Type of Report and Period Covered Research Report June 2019–August 2021	
				14. Sponsoring Agency Code	
15. Supplementary Notes Project performed in cooperation with the Texas Department of Transportation and the Federal Highway Administration. Study Title: Advanced Geophysical Tools for Geotechnical Analysis					
16. Abstract Texas Department of Transportation (TxDOT) encounters a considerable and yet increasing number of claims and change orders every year that negatively affects project costs and schedules. Insufficient and inaccurate information about the subsurface condition is a critical factor contributing to these cost overruns and delays. The annual cost of change orders resulting from insufficient subsurface information is commonly in order of millions of dollars. This lack of sufficient information is primarily due to the inherent limitation of the conventional geotechnical site investigation methods to provide continuous assessment of subsurface conditions. The primary objectives of this research project were to (1) develop an easy-to-use comprehensive manual that provides TxDOT staff with the Electrical Resistivity Imaging (ERI) technique procedures and guidelines for safe and correct implementation of ERI technology, (2) develop sets of equations and charts to investigate the relationship between the soil electrical resistivity and geotechnical properties in Texas, (3) demonstrate the ERI technique in the five TxDOT districts to cover different geotechnical conditions and operational environments, (4) create easy-to-use and instructive text and video training materials for learning workshops and provide TxDOT staff with information about the ERI survey, data collection, and data processing, and (5) perform training workshops in the TxDOT districts to convey the information about the ERI technology and share the research project's findings. The ERI technology provides a unique opportunity to reduce the cost overruns and delays related to inadequate subsurface information by providing (1) continuous subsurface images along with estimated soil properties and potential anomalies (e.g., karst, void) between the boreholes, and (2) additional information about the required drilling and sampling intervals.					
17. Key Words Electrical Resistivity Imaging, Continuous Assessment, Geotechnical Properties				18. Distribution Statement No restrictions. This document is available to the public through the National Technical Information Service, Springfield, Virginia 22161; <a href="http://www.ntis.gov">www.ntis.gov</a> .	
19. Security Classif. (of report) Unclassified		20. Security Classif. (of this page) Unclassified		21. No. of pages xv, 172	
				22. Price	

**ADVANCED GEOPHYSICAL TOOLS FOR GEOTECHNICAL ANALYSIS**  
**FINAL REPORT**

by:

Mohsen Shahandashti, Ph.D., P.E.

Sahadat Hossain, Ph.D., P.E.

Mina Zamanian

Md. Asif Akhtar

The University of Texas at Arlington

Report 0-7008-1

Project 0-7008

Project Title: Advanced Geophysical Tools for Geotechnical Analysis

Performed in cooperation with  
Texas Department of Transportation and Federal Highway Administration

August 2021

Published: September 2021



425 Nedderman Dr., 416 Yates St.

Box 19308, Arlington, TX 76019

## **DISCLAIMER**

The contents of this report reflect the views of the authors, who are responsible for the facts and the accuracy of the data presented herein. The contents do not necessarily reflect the official view or policies of the Federal Highway Administration (FHWA) or the Texas Department of Transportation (TxDOT). This report does not constitute a standard, specification, or regulation.

This report is not intended for construction, bidding, or permit purposes.

The United States Government and the State of Texas do not endorse products or manufacturers. Trade or manufacturers' names appear herein solely because they are considered essential to the object of this report.

## **ACKNOWLEDGEMENT**

This project was conducted in cooperation with TxDOT. The authors are grateful for the support and guidance provided by Ms. Jade Adediwura, Project Manager of Research and Technology Implementation (RTI). The authors are thankful for the technical guidance provided by the TxDOT staff Natnael Asfaw, Prakash Chavda, Trenton Ellis, Haijian Fan, Jimmy Si, Boon Thian, Clover Clamons, Kenneth Wiemers, Hugo Hernandez, Sydney Newman, and Sheetal Patel. Their prompt assistance and advice have been central to the successful completion of this project.

# TABLE OF CONTENTS

TABLE OF CONTENTS.....	iii
LIST OF TABLES.....	vii
LIST OF FIGURES .....	viii
EXECUTIVE SUMMARY .....	xiv
CHAPTER 1 INTRODUCTION .....	1
CHAPTER 2 OVERVIEW ANALYSIS of CONVENTIONAL AND GEOPHYSICAL TOOLS IN SITE CHARACTERIZATION.....	4
2.1. Introduction.....	4
2.2. Current State of Practice of Geotechnical Investigation in TxDOT.....	4
2.2.1. Soil Drilling .....	5
2.2.2. Texas Cone Penetration Test (TCP) .....	6
2.2.3. Standard Penetration Test (SPT).....	7
2.2.4. Vane Shear Test (VST).....	8
2.2.5. Torvane and Pocket Penetrometer .....	9
2.3. EDC-5 SUGGESTED GEOPHYSICAL METHODS.....	10
2.3.1. Electrical Methods .....	11
2.3.2. Seismic Methods.....	14
2.3.3. Optical and Acoustic Tele-Viewers .....	21
2.3.4. Seismic Cone Penetration Test (SCPT) .....	23
2.3.5. Measurement While Drilling (MWD) .....	25
CHAPTER 3 ELECTRICAL RESISTIVITY IMAGING TECHNIQUE .....	27
3.1. Introduction.....	27
3.2. Applications .....	27

3.2.1.	Providing Continuous Image of Subsurface .....	27
3.2.2.	Determining Boring and Sampling Intervals .....	28
3.2.3.	Estimating Geotechnical Parameters .....	29
3.3.	Electrical Resistivity Imaging Survey .....	29
3.3.1.	Field Survey Equipment .....	32
3.3.2.	Survey Planning.....	37
3.3.3.	Field Survey Implementation.....	46
3.4.	Survey Considerations .....	52
3.5.1.	Operational Environments .....	52
3.5.2.	Weather Conditions .....	54
3.5.3.	Safety Hazards and Precautions.....	55
3.5.	Common Mistakes in Implementation.....	56
3.6.1.	Use of Untrained Operators .....	56
3.6.2.	Inappropriate Selection of Electrode Configuration.....	56
3.6.3.	Deeply Buried Electrodes .....	57
3.6.4.	Incorrect Order of Attached Cable Sections .....	57
3.6.5.	Unconnected Cable Take-out In Between .....	58
3.6.6.	Ignorance of High Contact Resistance.....	58
3.6.7.	Insufficient Battery Charge.....	58
CHAPTER 4	DATA COLLECTION IN TXDOT DISTRICTS .....	59
4.1.	Introduction.....	59
4.2.	Selection Criteria of TxDOT Districts.....	59
4.3.	Field Data Collection .....	62
4.4.	Laboratory Data Collection.....	67

4.4.1.	Soil Physical Property Testing.....	70
4.4.2.	Laboratory Electrical Resistivity Imaging.....	74
CHAPTER 5	DATA PROCESSING AND ANALYSIS.....	76
5.1.	Introduction.....	76
5.2.	Continuous Resistivity Images of Subsurface .....	76
5.2.1.	Data Processing.....	76
5.2.2.	Examples of Resistivity Images of Subsurface.....	82
5.3.	Empirical Equations and Charts for Estimation of Geotechnical Properties .....	90
3.3.4.	Statistical Method .....	90
5.3.1.	Corrected Electrical Resistivity .....	90
5.3.2.	Empirical Equations for Estimation of Geotechnical Properties .....	92
5.3.3.	Empirical Charts for Estimation of Geotechnical Properties.....	95
5.3.4.	Geoparameter Estimator Application .....	99
CHAPTER 6	TRAINING WORKSHOPS.....	102
6.1.	Introduction.....	102
6.2.	Performed Training Workshops.....	102
CHAPTER 7	SUMMARY AND CONCLUSION .....	104
APPENDIX A	2D RESISTIVITY INVERSION SOFTWARE SETTINGS .....	112
A.1.	Initial Settings .....	113
A.1.1.	Criteria for Removing Noisy Readings.....	113
A.1.2.	Inversion Method Selection .....	117
A.2.	Forward Modeling Settings.....	118
A.3.	Inversion Modeling Settings.....	119
APPENDIX B	BORHOLE LOGS .....	123



APPENDIX C	WORKSHOP SUMMARY .....	163
APPENDIX D	VALUE OF RESEARCH ON ADVANCED GEOPHYSICAL TOOLS IN GEOTECHNICAL ANALYSIS.....	164
D.1.	Reduced Construction Operations and Maintenance Cost.....	165
D.2.	Environmental Sustainability.....	167
D.3.	Level of Knowledge.....	167
D.4.	Safety .....	167
D.5.	Infrastructure Condition.....	167
D.6.	Material and Pavements.....	168
D.7.	System Reliability and Increase Service Life .....	168
D.8.	Management and Policy.....	168
D.9.	Reduced Administrative Costs.....	168
D.10.	Traffic and Congestion Reduction.....	169
D.11.	Customer Satisfaction.....	169
APPENDIX E	TECHNOLOGY READINESS LEVEL ASSESSMENT .....	170

## LIST OF TABLES

<b>Table 3.1</b> Characteristics of different 2D electrode configurations .....	38
<b>Table 3.2</b> Median depth of investigation based on different electrode configurations (Loke, 1999) .....	44
<b>Table 4.1</b> Number of visited locations, drilled boreholes, collected samples, and the performed electrical resistivity imaging surveys.....	68
<b>Table 4.2</b> Number of boreholes and depths of sampling - Beaumont district.....	68
<b>Table 4.3</b> Number of boreholes and depths of sampling - Corpus Christi district.....	69
<b>Table 4.4</b> Number of boreholes and depths of sampling - Dallas district.....	69
<b>Table 4.5</b> Number of boreholes and depths of sampling - El Paso district.....	69
<b>Table 4.6</b> Number of boreholes and depths of sampling - Fort Worth district .....	69
<b>Table 5.1</b> Examples of software programs along with available algorithms for processing of electrical resistivity data .....	78
<b>Table 5.2</b> Typical ranges of electrical resistivity of different earth material .....	80
<b>Table 5.3</b> Equations for estimating the geotechnical parameters using electrical resistivity for clayey soil .....	93
<b>Table 5.4</b> Equations for estimating the geotechnical parameters using electrical resistivity for sandy soil .....	94
<b>Table 6.1</b> Scheduled workshops in the selected districts .....	103

## LIST OF FIGURES

<b>Figure 1.1</b> A comparison of the number of applications of EDC-suggested geophysical methods .....	2
<b>Figure 2.1</b> Conical probe for the TCP (TxDOT, 1999) .....	7
<b>Figure 2.2</b> SPT penetrometer (Vipulanandan et al., 2008) .....	8
<b>Figure 2.3</b> Examples of different sizes of vane shear blades (johnmorrisgroup.com).....	9
<b>Figure 2.4</b> Torvane device (left); Pocket penetrometer with different sizes of the adaptor (right) 9	9
<b>Figure 2.5</b> EDC-5 suggested subsurface investigation methods.....	10
<b>Figure 2.6</b> Direct and refracted ray paths in the case of a two-layer model (Adapted from Kearey et al., 2013) .....	15
<b>Figure 2.7</b> Reflected ray paths in the case of a one-layer model (Adapted from Kearey et al., 2013) .....	16
<b>Figure 2.8</b> (a) A schematic crosshole tomography procedure; (b) Crosshole data acquisition layout (Adapted from ASTM Standard D4428-07, 2007; Wightman et al., 2004) .....	18
<b>Figure 2.9</b> Seismic downhole tomography procedure (Adapted from ASTM Standard D7400-19, 2019).....	19
<b>Figure 2.10</b> Diagram of a spectral analysis of surface wave test (Adapted from Astarita et al., 2014).....	20
<b>Figure 2.11</b> Diagram of a multichannel analysis of surface wave test (geosigma.com).....	21
<b>Figure 2.12</b> (a) Acoustic tele-viewer head (lim.eu); (b) Optical tele-viewer head (openei.org) .	22
<b>Figure 2.13</b> An example of the acoustic tele-viewer images. (A) Fixed high frequency transducer, and (B) Rotating low-frequency transducer (Williams and Johnson, 2004) .....	22
<b>Figure 2.14</b> An example of tele-viewer images of a borehole using (a) Acoustic and (b) Optical tele-viewers (Adapted from Williams et al., 2002).....	23
<b>Figure 2.15</b> Schematic layout of SCPT (Campanella et al., 1986) .....	24

<b>Figure 2.16</b> A mud-telemetry system; (a) Positive pulser; (b) Negative pulser; and (c) Continuous wave (Adapted from Fontenot, 1986).....	26
<b>Figure 3.1</b> Illustration of the heterogeneity of subsurface materials and locating a critical zone by resistivity image of the subsurface - Fort Worth district .....	28
<b>Figure 3.2</b> Approximate locations of boreholes to properly investigate the subsurface condition along the survey line .....	28
<b>Figure 3.3</b> Missing the critical zone on the left side .....	29
<b>Figure 3.4</b> Misinterpretation of the subsurface condition.....	29
<b>Figure 3.5</b> Arrangement of the electrodes and sequence of measurements used to obtain a 2D pseudo-section.....	31
<b>Figure 3.6</b> Required equipment for the implementation of an electrical resistivity survey in the field.....	32
<b>Figure 3.7</b> AGI Supersting R8 resistivity meter .....	33
<b>Figure 3.8</b> Data measurement procedures using (a) single-channel system and (b) multi-channel system .....	33
<b>Figure 3.9</b> (a) a stainless-steel electrode and (b) multi-electrode cable sections each includes 14 take-outs.....	35
<b>Figure 3.10</b> Cable take-out and label .....	35
<b>Figure 3.11</b> External marine 12 V battery.....	36
<b>Figure 3.12</b> AGI switch box.....	36
<b>Figure 3.13</b> Sensitivity sections of Wenner (alpha, beta, gamma), Schlumberger, dipole-dipole, pole-pole, and pole-dipole arrays (Dahlin and Zhou, 2004).....	39
<b>Figure 3.14</b> Schematic instrumentation of the Wenner-alpha array (“k” is the geometric factor of the array).....	40
<b>Figure 3.15</b> Schematic instrumentation of the dipole-dipole array (“k” is the geometric factor of the array).....	40

<b>Figure 3.16</b> Schematic instrumentation of the Schlumberger array (“k” is the geometric factor of the array).....	41
<b>Figure 3.17</b> Schematic instrumentation of the pole-pole array (“k” is the geometric factor of the array).....	42
<b>Figure 3.18</b> Schematic instrumentation of the pole-dipole array (“k” is the geometric factor of the array).....	43
<b>Figure 3.19</b> Equally spaced electrodes.....	45
<b>Figure 3.20</b> (a) determining the length of the whole survey using a tape measure, (b) laying down the electrodes in specific spacings, and (c) driving the electrodes into the ground using a hammer .....	47
<b>Figure 3.21</b> Theoretical relation between the depth of burial of electrode and contact resistance (ABEM Instrument, 2010).....	47
<b>Figure 3.22</b> (a) attachment of a cable to an electrode using a stainless-steel spring and (b) the appropriate connection of a cable take-out to an electrode.....	48
<b>Figure 3.23</b> Proper connection of resistivity meter to an external battery, a switching system, and a laptop.....	48
<b>Figure 3.24</b> (a), (b), and (c) general layout of the 2D electrical resistivity imaging survey line.	50
<b>Figure 3.25</b> An example of a measurement sequence of a roll-along survey using two cable sections for a survey with 28 electrodes .....	51
<b>Figure 3.26</b> (a), (b), and (c) the soil around the electrode is wetted to reduce the contact resistance .....	53
<b>Figure 3.27</b> Distribution of current flow from a point source in a homogeneous soil (Samouëlian et al., 2005) .....	57
<b>Figure 3.28</b> Correct order of cable section’s connections for 56 electrodes with two 28-electrode cable sections .....	58
<b>Figure 4.1</b> Expansive clay soil map of Texas (Adapted from Olive et al., 1989).....	60
<b>Figure 4.2</b> Physiographic map of Texas (Adapted from Bureau of Economic Geology, 1996)..	61

<b>Figure 4.3</b> Average annual precipitation map of Texas (Adapted from PRISM Climate Group, 2019) .....	62
<b>Figure 4.4</b> Location of the proposed site on the map, number of collected samples at each borehole, and the instrumentation of electrical resistivity surveys in Beaumont district .....	63
<b>Figure 4.5</b> Locations of the boreholes along with the depth of borings in Beaumont district.....	63
<b>Figure 4.6</b> Locations of electrical resistivity survey lines with respect to the boreholes in Beaumont district.....	64
<b>Figure 4.7</b> Location of the proposed site on the map, number of collected samples at each borehole, and the instrumentation of electrical resistivity surveys in Corpus Christi district .....	65
<b>Figure 4.8</b> Locations of resistivity lines with respect to the boreholes along with the depth of borings in Corpus Christi district.....	65
<b>Figure 4.9</b> Location of the proposed site on the map, number of collected samples at each borehole, and the instrumentation of electrical resistivity surveys in Fort Worth district.....	66
<b>Figure 4.10</b> Locations of the proposed sites on the map in the Fort Worth district.....	66
<b>Figure 4.11</b> Locations of resistivity lines with respect to the boreholes along with the depth of borings in Fort Worth district .....	67
<b>Figure 4.12</b> Soil testing; (a) Liquid limit testing, (b) hydrometer analysis, (c) Specific gravity testing, (d) plastic limit testing, and (e) sieve analysis (UTA laboratory).....	70
<b>Figure 4.13</b> Liquid limit testing: (a) the soil is flattened in the device cup, and (b) a groove was made at the center (UTA laboratory) .....	71
<b>Figure 4.14</b> Plastic limit testing (a) Rolling device and (b) cracked and broken threads of 3 mm (UTA laboratory) .....	72
<b>Figure 4.15</b> Particle size distribution testing using the hydrometer procedure (UTA laboratory) .....	73
<b>Figure 4.16</b> Specific gravity testing of soil (UTA laboratory).....	74
<b>Figure 4.17</b> (a) and (b) preparation of soil specimens, (c) a schematic setup of laboratory electrical resistivity test, and (d) experimental setup of laboratory resistivity test .....	75

<b>Figure 5.1</b> Typical flowchart of data processing (Adapted from Watanabe and Takeuchi, 2004)	77
<b>Figure 5.2</b> Example of an inverted electrical resistivity image of the subsurface using the EarthImager software program. RMS of 4.27% is achieved after 4 iterations.	79
<b>Figure 5.3</b> Example of pseudo-sections for an electrical resistivity survey using the EarthImager software program	81
<b>Figure 5.4</b> Resistivity profiles and location of boreholes along the survey lines for the Beaumont district	83
<b>Figure 5.5</b> Resistivity profiles and location of boreholes along the survey lines for the Beaumont district	84
<b>Figure 5.6</b> Resistivity profiles and location of boreholes along the survey lines for the Corpus Christi district.	85
<b>Figure 5.7</b> Resistivity profiles and location of boreholes along the survey lines 1 through 5 for the Fort Worth district.	86
<b>Figure 5.8</b> Resistivity profiles and location of boreholes along the survey lines of 6 through 8 for the Fort Worth district.	87
<b>Figure 5.9</b> Resistivity profiles and location of boreholes along the survey lines of 9 through 12 for the Fort Worth district.	88
<b>Figure 5.10</b> Resistivity profiles and location of boreholes along the survey lines of 13 through 15 for the Fort Worth district	89
<b>Figure 5.11</b> Variations of electrical resistivity measurements with soil temperature during the experiment for a soil sample at different moisture contents	91
<b>Figure 5.12</b> Variations of temperature-corrected electrical resistivity of compacted clay with moisture content for different dry unit weights	95
<b>Figure 5.13</b> Variations of temperature-corrected electrical resistivity of compacted clay with moisture content	96

<b>Figure 5.14</b> Variations of temperature-corrected electrical resistivity of sandy soil with moisture content for different dry unit weights .....	97
<b>Figure 5.15</b> Variations of temperature-corrected electrical resistivity of sandy soil with moisture content.....	98
<b>Figure 5.16</b> User interface of the GeoParameter estimator.....	99
<b>Figure 5.17</b> Example of completed sections for the estimation of moisture content using minimum input from the user .....	100
<b>Figure 5.18</b> Example of the estimation results in the print preview window .....	101



## EXECUTIVE SUMMARY

Texas Department of Transportation (TxDOT) encounters a considerable and yet increasing number of claims and change orders every year that has a detrimental effect on project costs and schedules. Insufficient and inaccurate information about the subsurface condition is one of the critical factors that contribute to these cost overruns and delays in 20 to 50% of all infrastructure projects (Baynes, 2010). The annual cost of change orders resulting from the insufficient subsurface information is commonly in order of millions of dollars (Boeckmann and Loehr, 2016). This lack of sufficient information is primarily due to the inherent limitation of the conventional geotechnical site investigation methods to provide continuous assessment of subsurface condition (Hossain et al., 2018). In other words, the conventional methods only sample and provide information about a small percentage of a total sample space. The primary objectives of this research project were to (1) develop an easy-to-use comprehensive manual that provides TxDOT staff with the Electrical Resistivity Imaging (ERI) technique procedures and guidelines for safe and correct implementation of ERI technology, (2) develop sets of equations and charts to investigate the relationship between the soil electrical resistivity and geotechnical properties in Texas, (3) demonstrate the electrical resistivity imaging technique in the five TxDOT districts to cover different geotechnical conditions and operational environments, (4) create easy-to-use and instructive text and video training materials for learning workshops and provide TxDOT staff with information about the electrical resistivity imaging survey, data collection, and data processing, and (5) perform training workshops in the TxDOT districts to convey the information about the electrical resistivity imaging technology and share the research project's findings.

These research project's findings were obtained through an extensive literature review, data collection, and statistical analysis. A thorough review of the literature was conducted to assess and document the current state of knowledge and practice pertaining to the electrical resistivity imaging technology. The gained experiences from demonstrating the electrical resistivity imaging in various operational environments and geotechnical conditions across the selected TxDOT districts (Beaumont, Corpus Christi, El Paso, Dallas, and Fort Worth) were translated into a comprehensive, instructive, and practical research manual to offer guidelines and tools for a rapid and continuous assessment of subsurface conditions. Extensive laboratory testing (1093 laboratory electrical resistivity tests) was performed on the collected samples from different locations in the

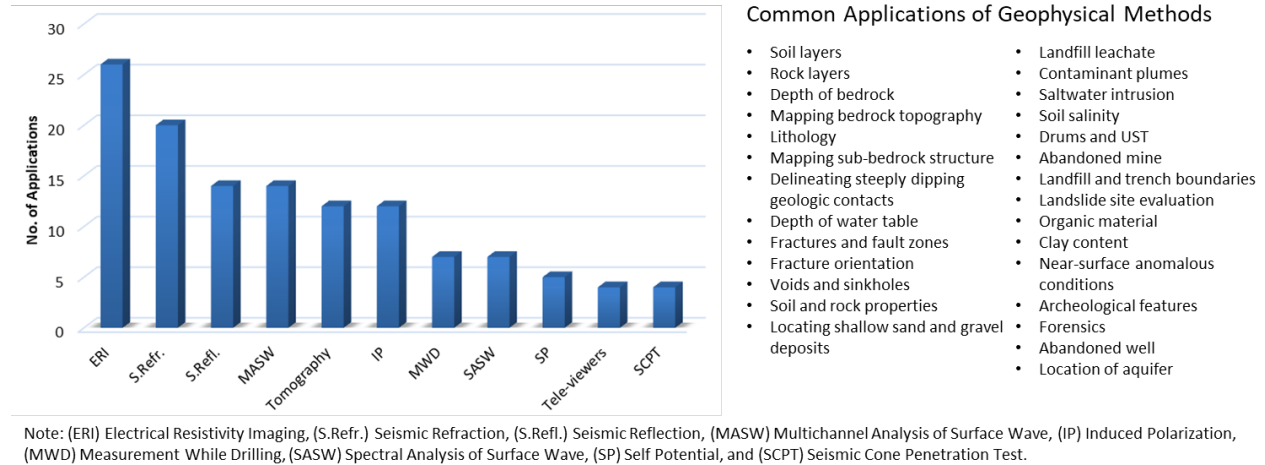
selected TxDOT districts. The results of the laboratory testing were later analyzed to investigate the relationships between the geoelectrical and geotechnical parameters and to provide sets of empirical equations and charts using linear regression models. These tools allow for estimating the geotechnical parameters (e.g., moisture content, dry unit weight, plasticity index, percent of fines, and clay content) using the field electrical resistivity values. An Excel-based application was also developed and introduced to facilitate the computation steps of geotechnical parameters from the proposed equations. This research offered training workshops in Beaumont, El Paso, Fort Worth, and Paris districts to disseminate the knowledge of the applications, data collection, and data interpretation of electrical resistivity imaging technology to TxDOT staff.

The electrical resistivity imaging technology provides a unique opportunity to reduce the cost overruns and delays related to inadequate subsurface information by providing (1) continuous subsurface images along with estimated soil properties and potential anomalies (e.g., karst, void) between the boreholes, and (2) additional information about the required drilling and sampling intervals. The electrical resistivity imaging technology helps TxDOT staff prevent inadequate/conservative designs and mitigate risks and unexpected failures due to the lack of adequate subsurface information.

## CHAPTER 1 INTRODUCTION

Texas Department of Transportation (TxDOT) encounters a considerable and yet increasing number of claims and change orders every year that has a detrimental effect on project costs and schedules (Shrestha and Maharjan, 2018). Insufficient and inaccurate information about the subsurface condition is one of the critical factors that contribute to these cost overruns and delays in 20 to 50% of all infrastructure projects (Baynes, 2010). A national survey of 55 U.S. transportation agencies showed that the annual cost of change orders resulting from the insufficient subsurface investigation is commonly in order of millions of dollars (Boeckmann and Loehr, 2016). The lack of sufficient site investigation may also contribute to inadequate or conservative designs, leading to costly failures or increased project's costs (Adhikari et al. 2021; Sirles 2006). The repairing of damages to buildings, highways, and other infrastructure systems resulting from inadequate subsurface information is a significant national cost. For example, the average repairing cost of karst-related damages to the infrastructures was estimated to be at least \$300 million per year in the U.S. (Weary, 2015). This lack of sufficient information is due to the inherent limitation of the conventional geotechnical site investigation methods to provide continuous assessment of the subsurface. In other words, the conventional methods only sample and provide information about a small percentage of a total sample space.

Electrical Resistivity Imaging (ERI) offers a unique opportunity to mitigate these costs and limitations of conventional geotechnical site investigation methods by providing a rapid and continuous assessment of subsurface condition using a non-invasive, and cost-effective method. The main benefit of this method over the other advanced geophysical tools is its wide range of applications in determining various subsurface anomalies and soil properties. Figure 1.1 shows a comparison of the number of applications of advanced geophysical tools in subsurface investigation (Campanella et al., 1986; Ward, 1988; Ward, 1990; Fenning and Donnelly, 2004; Wightman et al., 2004; Williams and Johnson, 2004; Sirles, 2006; Anderson et al., 2008; Edet, 2009; Rogers, 2009; British Standards Institution, 2010; ASTM Standard D6429-99, 2011; ASTM Standard D5778-12, 2012; Li et al., 2014; ASTM Standard 6285-99, 2016; Rivers, 2016; ASTM Standard D5753-18, 2018; ASTM Standard D7400-19, 2019).



**Figure 1.1** A comparison of the number of applications of EDC-suggested geophysical methods

This technical report is organized in 7 chapters and 5 appendices as follows:

Chapter 1 presents the significance of this research project and the organization of the technical report.

Chapter 2 reviews the current state of TxDOT geotechnical practices and presents an overview analysis of the advanced geophysical tools that are not commonly used in Texas.

Chapter 3 describes the electrical resistivity imaging technology, its application, survey procedure, practical considerations, limitation of the method, and common mistakes in performing the survey.

Chapter 4 describes the selection criteria of the TxDOT districts, and the laboratory and field data collection procedures.

Chapter 5 elaborates on the electrical resistivity data processing and modeling. It also presents sets of equations and charts for estimating the geotechnical parameters.

Chapter 6 reviews the training workshops that were held in the TxDOT districts to convey the information about the electrical resistivity imaging technology and share the project’s findings.

Chapter 7 provides a summary and conclusion of this research project.

Appendix A presents available tools and settings of EarthImager software program for processing the electrical resistivity data.

Appendix B provides borehole logs where the soil samples were collected in different TxDOT districts.

Appendix C presents a summary of the performed workshops.

Appendix D presents the value of research on this project by determining the qualitative and economic benefits of electrical resistivity imaging technology for geotechnical analysis.

Appendix E describes the process of assessing the readiness level of electrical resistivity imaging technology.

## **CHAPTER 2      OVERVIEW ANALYSIS OF CONVENTIONAL AND GEOPHYSICAL TOOLS IN SITE CHARACTERIZATION**

### **2.1. Introduction**

A continuous evaluation and characterization of subsurface condition is required for any construction project or development activity to have a reliable and cost-effective design (Shahandashti et al., 2020; Baral et al., 2021). The Texas Department of Transportation (TxDOT) uses several conventional geotechnical site investigation methods such as soil drilling and sampling, Texas cone penetration test, standard penetration test, vane shear test, and Torvane or pocket penetrometer to characterize the subsurface conditions (TxDOT, 2018). Despite the accurate and reliable information that these methods provide, these methods only sample and provide information about a small percentage of a total sample space and do not yield to a continuous overview of the subsurface condition. Federal Highway Administration (FHWA) identified several promising subsurface exploration technologies through the fifth round of its “Every Day Counts” initiative (EDC-5) that improve site characterization and maximum return-on-investment (FHWA, 2018). These technologies include electrical and seismic geophysics, seismic cone penetration test, measurement while drilling, and optical and acoustic tele-viewers. The method selection depends on several factors such as site accessibility, required accuracy, available time, the extent of investigation (area), budget, and investigation application (e.g., moisture variation, depth of bedrock, unknown utilities, location of foundations) (ASTM Standard D6429-99, 2011). This chapter reviews the current state of TxDOT geotechnical practices and presents an overview analysis of the EDC-suggested geophysical tools that are not used (or commonly used) in Texas.

### **2.2. Current State of Practice of Geotechnical Investigation in TxDOT**

Currently, soil drilling and various in-situ tests are employed to determine subsoil properties in TxDOT geotechnical investigations. The commonly used in-situ tests include Texas Cone Penetration (CPT) test, Standard Penetration Test (SPT), Vane Shear Test (VST), and Torvane and Pocket Penetrometer tests (TxDOT, 2018). These methods can help geotechnical engineers and designers to obtain information about the subsurface condition immediately on the project site.

However, some of these methods require soil sampling. Stratigraphy and characteristics of subsurface materials are interpreted based on the types of information recorded and using empirical correlations between the test measurements and soil properties. The objective of the in-situ testing is to measure the subsoil response and correlate it to the geotechnical properties such as strength and stiffness (Hossain et al., 2018). A brief description of common practices in TxDOT site investigations is presented in the following subsections.

### **2.2.1. Soil Drilling**

Drilling and sampling methods cover those conventional geotechnical site investigation methods that characterize the subsurface conditions by laboratory tests on disturbed or undisturbed samples. Disturbed samples are usually obtained by hand excavating methods or by mechanical digging or drilling techniques. The disturbed samples are tested to acquire information such as soil type, Atterberg limits, moisture content, density, stratification, and presence of contaminants. On the other hand, undisturbed samples are used to determine geotechnical characteristics such as in-situ density, strength, permeability, discontinuities, fractures, and fissures of subsurface formations (ASTM Standard D7015–04, 2004). Selection of proper method of drilling depends on the geology, hydrology, available equipment, and monitoring design. The common drilling methods for subsurface investigations include Solid Stem Auger, Hollow Stem Auger, and Rotary Wash Borings, which are described further in the following paragraphs. The less commonly used drilling methods include Bucket Auger, Reverse-Air Rotary, and Cable tool (Mayne et al., 2002; SD DENR, 2003).

#### **Solid Stem Auger**

Solid stem continuous flight augers excavate and transport the soil to the land surface mechanically and are available in diameters of 4 to 12 inches (Mayne et al., 2002). This method is only applicable to lithified sediments, stable earth materials, and stiff cohesive soils. The boring walls for the entire depth of boring are stable in these kinds of soils and will not collapse when the augers are removed from the hole to obtain soil samples. The soil sampling using this method is rapid and straightforward for the shallow depths, but deeper investigations are labor-intensive because the augers must be removed from the hole before each sampling (Mayne et al., 2002; SD DENR, 2003).

## **Hollow Stem Auger**

Hollow stem continuous flight augers are available in large outside diameters up to 17.5 inches and axial opening up to 12.25 inches to allow access to the bottom of the hole without removing the auger for sampling (Mayne et al., 2002). The applications of the hollow stem augers are limited to drilling in poorly lithified to unlithified sediments, clay soils, and granular soils above the groundwater level, where the boring walls may be unstable. The obtained samples can significantly be disturbed by hydrostatic water pressure below the groundwater level. The stratigraphy of the subsurface determines the depth of investigation which can be up to 150 ft. Soil sampling using this method is rapid, especially for shallow applications (Mayne et al., 2002; SD DENR, 2003).

## **Rotary Wash Boring**

Rotary wash boring is advanced by the rapid rotation of a drill bit mounted upon the end of drill rods. The boring walls need to be supported either with casing or with the use of a drilling fluid (water mixed with bentonite or polymer additives) since drill rods need to be removed prior to sampling. The casings for rotary wash are typically available with inside diameters in the range of 2.4 to 5.1 inches (Mayne et al., 2002). This method applies to a wide range of geologic conditions, especially if the target is below the groundwater level. An adequate water head should be maintained in the case of drilling below the groundwater level to avoid loosening or heaving of the soil to be sampled beneath the casing. Rotary wash boring is also a rapid sampling technique (Mayne et al., 2002, SD DENR, 2003).

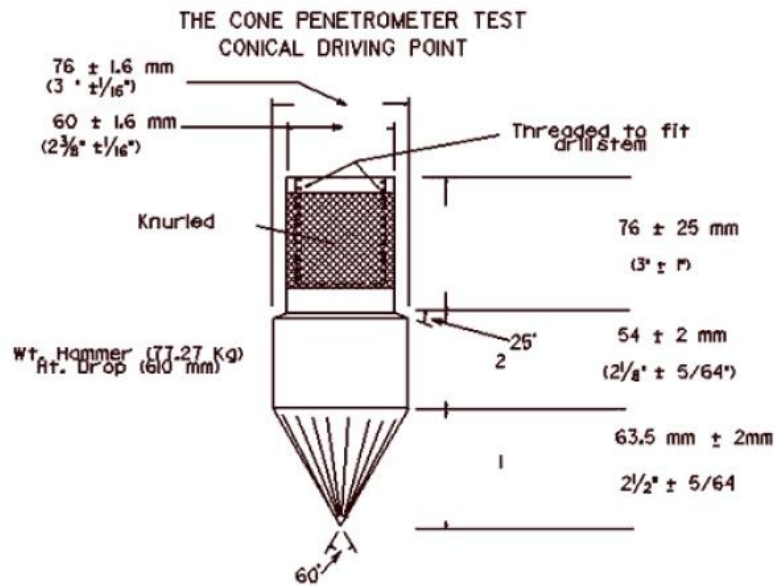
### **2.2.2. Texas Cone Penetration Test (TCP)**

Texas Cone Penetration (TCP) test is developed by TxDOT to explore the geotechnical subsurface conditions of Texas. The TCP is used for foundation investigations to determine the relative density, consistency, and load-bearing capacity of all types of soil and rock (TxDOT, 2018).

This test consists of pushing a cylindrical cone shape steel probe into the subsoil using a 170 lb (77 kg) hammer which drops from a height of 24 inches (0.6 m) in a repeated manner. In soft materials, the numbers of blows for driving the penetrometer cone for the first 6 inches (150 mm) and the second 6 inches (150 mm) are counted, while in hard materials, the increment of penetration (in inches) is recorded for 100 blows, representing the penetration resistance or blow counts (N-value) (TxDOT, 2018; Hossain et al., 2018; Vipulanandan et al., 2008). The standard



test procedures for the TCP test are described in the Texas designation Tex-132-E. A conical probe conforming to the TxDOT specifications for the TCP test is shown in Figure 2.1.

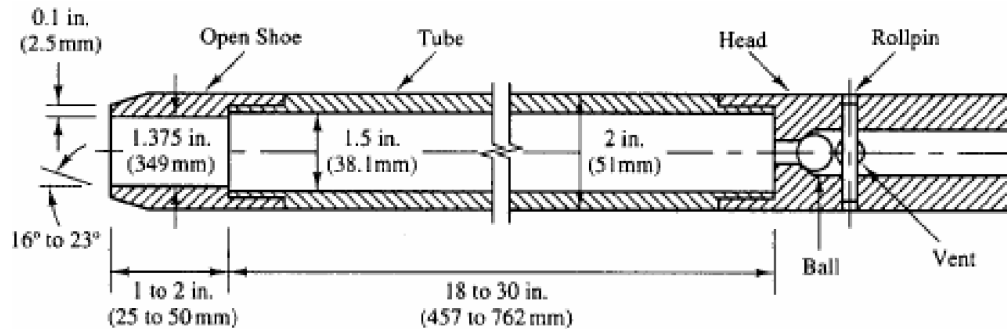


**Figure 2.1** Conical probe for the TCP (TxDOT, 1999)

### 2.2.3. Standard Penetration Test (SPT)

Standard Penetration Test (SPT) has been commonly used for foundation design to determine the soil resistance at different depths. Disturbed samples are also obtained during SPT using a split spoon. This method is widely used in various subsurface conditions and weak rocks. The SPT is a very fast technique, and the accuracy of the obtained data is highly dependent on the type of equipment and competence of the operator (Hossain et al., 2018).

The test consists of driving a hollow thick-walled tube into the ground. A 140 lb (63.5 kg) hammer is repeatedly pounded from a height of 30 inches (0.76 m) to achieve three successive increments of 6 inches (150 mm). The SPT blow count requires penetrating the first 6 inches, which is known as “seating” blow counts. The number of blows required to penetrate successive 1 foot (300 mm) is known as SPT blow counts, i.e., N-value or SPT-resistance (blows/ft or blows/0.3 m). When the penetration of 6 inches is not achieved, the increment of penetration is recorded for 50 blow counts. In the case of shallow bedrock, very dense gravel, or any obstacle such as a boulder, the boring should be extended below this depth, under the direction of a geotechnical engineer. The standard test procedures for SPT are described in ASTM Standard D1586. A Split-barrel sampler conforming to the ASTM Standard D1586 for SPT is shown in Figure 2.2.



**Figure 2.2** SPT penetrometer (Vipulanandan et al., 2008)

#### 2.2.4. Vane Shear Test (VST)

Vane Shear Test (VST) is used to evaluate the undrained shear strength of very soft to medium stiff clays and silts that are free of gravel and shell particles. The strength and consistency of soil materials determine the size, shape, and configuration of the vane blade. The VST test is simple, but it has a slow and time-consuming testing procedure (Hossain et al., 2018).

The test consists of driving a four-bladed vane into the clayey soil and rotating about the vertical axis slowly at a rate of 0.1 degrees per second (Hossain et al., 2018). While rotating, the resisting torque evolving from soil shearing is measured. Two shear strengths are determined from the VST: peak shear strength and remolded shear strength. The peak torque is related to the peak shear in a cylindrical failure surface by a constant and depends on the dimensions and shape of the vane. After obtaining the peak torque, the vane is rotated about ten (10) times to determine the torque associated with remolded shear strength. The sensitivity of the clayey soil is determined by calculating the ratio of peak strength to remolded shear strength (Hossain et al., 2018; TxDOT, 2018; Mayne et al., 2002). The standard test procedure is described in ASTM Standard D2573. Examples of different sizes of vane shear blades are shown in Figure 2.3.



**Figure 2.3** Examples of different sizes of vane shear blades (johnmorriscgroup.com)

### 2.2.5. Torvane and Pocket Penetrometer

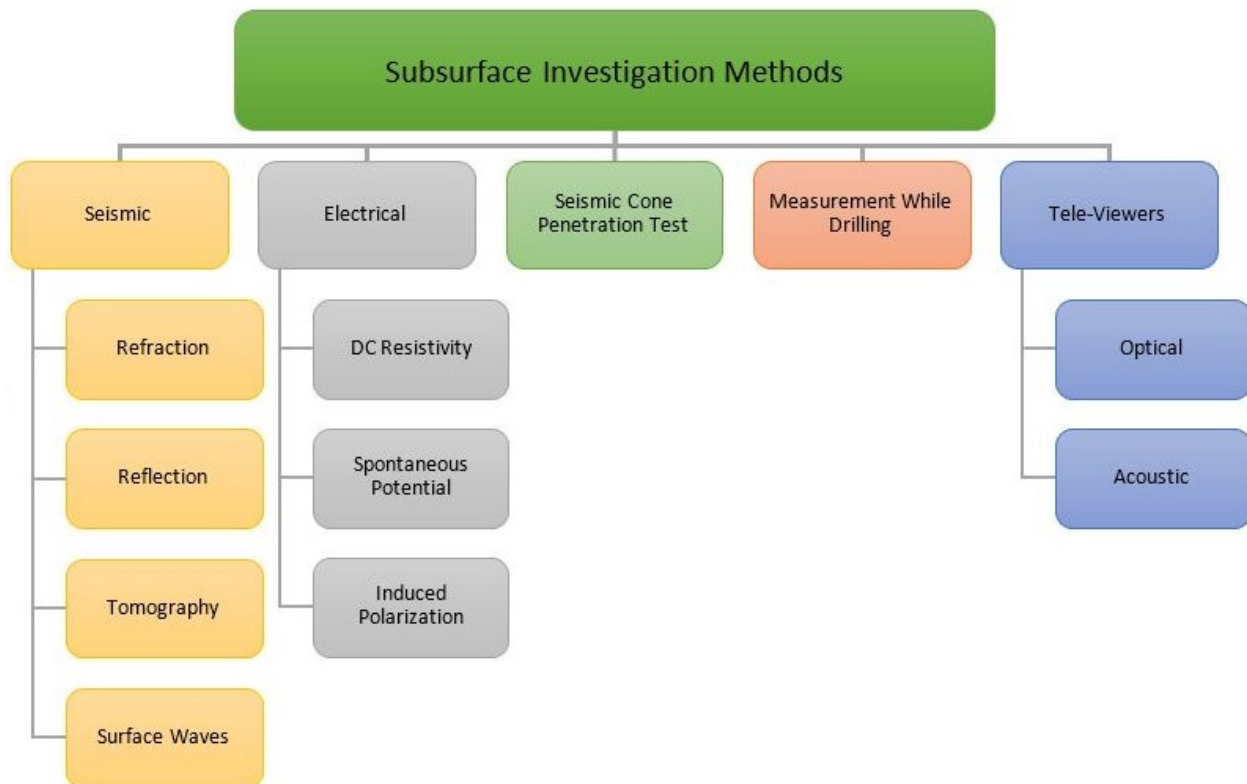
Torvane and Pocket Penetrometer are two test devices that are used to determine approximate shear and unconfined strength of cohesive soils (very soft to very stiff clay soil). The tests are not suitable for geotechnical analysis or design purposes and should be only used as a guide for a comparison of the results. The devices must be applied to the center of the top or bottom end of the undisturbed soil samples to properly conduct the tests (Mayne et al., 2002; TxDOT, 2018). Figure 2.4 shows examples of Torvane and pocket penetrometer devices with different sizes of the adaptor.



**Figure 2.4** Torvane device (left); Pocket penetrometer with different sizes of the adaptor (right)

### 2.3. EDC-5 SUGGESTED GEOPHYSICAL METHODS

The FHWA has identified several subsurface exploration technologies through the EDC-5 program that are proven effective in evaluating geological, hydrological, geotechnical, and environmental site assessments. Despite the evident advantages of these technologies that can potentially transform existing subsurface investigations, many of these technologies are underutilized by many state departments of transportation because of lack of proven implementation details for different applications, geotechnical conditions, and operational environments (FHWA, 2018; Rosenblad and Boeckmann, 2020). These methods provide a unique opportunity to overcome the inherent limitations of the conventional geotechnical site investigation methods and thoroughly investigate the subsurface condition. These technologies are electrical and seismic geophysics, seismic cone penetration test, measurement while drilling, and optical and acoustic tele-viewers (FHWA, 2018). A brief description of each method and their related techniques (listed in Figure 2.5) are presented in the following subsections.



**Figure 2.5** EDC-5 suggested subsurface investigation methods

### **2.3.1. Electrical Methods**

The electrical methods can be divided into two types based on the source of the electrical currents: some of those need an artificial current flow to be introduced into the ground and some of those uses the low-frequency electrical currents that exist between subsurface materials (Wightman et al., 2004; Kearey et al., 2013). The three main electrical techniques including Electrical Resistivity Imaging (ERI), Induced Polarization (IP), and Spontaneous Potential (SP) are described in the following paragraphs.

#### **Electrical Resistivity Imaging (ERI)**

Electrical Resistivity Imaging (ERI) method employs the fundamental physics principles of Ohm's law to measure the horizontal and vertical discontinuities in the electrical properties of the ground. The ERI method is used to determine the resistance of soil, rock, and groundwater to the flow of electrical current (Kearey et al., 2013; Hossain et al., 2018). The resistivity of materials is a function of the soil and rock matrix, moisture content, unit weight, porosity, pore fluid conductivity, degree of saturation, organic content, clay content, fabric structure, temperature, salinity, and acidity (Yang, 2002; Rinaldi and Cuestas, 2002; Giau et al., 2003; Ekwue and Bartholomew, 2010; Kibria and Hossain, 2012; Kibria and Hossain, 2017; Samouëlian et al., 2005). The most common geotechnical conditions affecting the performance of the ERI data are subsurface stratigraphy, resistivity contrast, groundwater, and soil compressibility.

As a rule of thumb, three to five times the desired depth of investigation is needed on the ground surface to implement the ERI method, far away from power lines and grounded metallic structures. The current is transmitted into the ground through the electrodes. A poor connection between the electrodes and the ground results in low or erratic current measurement and noise. The electrical property can be studied by injecting a direct current or a very low-frequency current using a transmitter into the ground. The current is injected across two electrodes (current electrodes) into the ground, and then the resulting voltage is received by the other two electrodes (potential electrodes) (ASTM Standard D6429-99, 2011; ASTM Standard D6431-18, 2018). The electrical resistivity data is collected in a short amount of time and stored in the resistivity box. Finally, the results are plotted as profiles and contoured maps. Batteries or an external generator and simple analog voltmeters or microcomputer-controlled systems may be needed during the surveying (Schoenleber, 2005).

The resistivity measurements can be made in one, two, and three dimensions to determine the subsurface characteristics, depending on site conditions and project objectives. There are some parameters related to the implementation of the survey that affect the RI data, such as current and potential electrode spacing, current frequency, the spacing between the station measurements, and target depth. Typically, the ERI technique can map three to four layers to a depth of a hundred meters or more. The electrical resistivity measurements are susceptible to interferences from nearby metal pipes, cables, or fences. The resolution of the obtained results decreases with depth. The electrical resistivity measurements are made as profiling or as sounding. Profiling data is used to map the lateral variations in resistivity and can be plotted as resistivity versus distance along a profile line with little processing. Sounding data is used to map the vertical variations in resistivity, must be processed to obtain depth, thickness, and resistivity of layers (ASTM Standard D6429-99, 2011; Anderson and Ismail, 2003). The field procedure of resistivity method is straightforward and sounding to a depth of about 50 meters (165 ft) can be made in less than one hour (Wightman et al., 2004).

The arrangements of the electrodes vary based on the required application or depth of interest. The three most frequently used collinear electrode configurations for different applications are Wenner, dipole-dipole, Schlumberger arrays (Wightman et al., 2004; ASTM Standard D6431-18, 2018; Hossain et al., 2018). Electrode spacing could be relatively large in the case of deep investigation with less detailed data, or small when more detailed data in shallower depth is needed (ASTM Standard D6431-18, 2018). The electrical resistivity imaging technique requires a single survey with three or four persons depending on site conditions and schedule. The ERI equipment is portable, and its implementation is cheap and cost-effective (Anderson et al., 2007; Wightman et al., 2004). More information about the ERI method, its application, and data processing are provided in Chapters 3, 4, and 5.

### **Induced Polarization (IP)**

The Induced Polarization (IP) method measures the resistivity variations of the subsurface with frequency and is often performed along with the ERI measurements (Wightman et al., 2004; Schoenleber, 2005). Two approaches are used to measure the induced polarization data: time domain and frequency domain. In the time domain, an electrical current is introduced into the ground through two electrodes, and then the current is rapidly turned off. The rate of decay in

potential difference is measured by two other electrodes. In the frequency domain, different current frequencies are propagated to the subsurface through the electrodes, and then the resulting voltage is measured (Anderson and Ismail, 2003; Wightman et al., 2004).

Like the ERI surveys, a long distance on the surface is needed for the implementation of the induced polarization survey. All the array configurations used in the electrical resistivity imaging can also be used in induced polarization surveying. The electrodes should be driven into the ground at a greater depth than the ERI electrodes. A poor connection between the electrodes and the ground results in low or erratic current measurement and noise. The induced polarization implementation is a labor-intensive process (Wightman et al., 2004). The resolution of data is a function of electrode spacing, target depth and resistivity, the sensitivity of investigation target to induced polarization, and magnitude of background noise (Anderson and Ismail, 2003). More power needs to be provided in the induced polarization surveys rather than ERI surveys to diminish the effects of cultural interferences (buildings, vehicles, underground utilities, overhead powerlines, etc.) on the induced polarization measurements. Therefore, heavier and bulkier power sources and equipment are needed than ERI technique (Schoenleber, 2005; Wightman et al., 2004). The resolution of induced polarization data decreases with depth. All geotechnical conditions that affect the performance of the ERI surveys have some effects on the induced polarization surveys. Like the ERI method, the results of the induced polarization survey are plotted as profiles and contoured maps.

### **Spontaneous Potential (SP)**

The Spontaneous/Self Potential (SP) method measures the natural potential differences that exist in the subsurface. Spontaneous potential voltages are mainly generated by electrochemical differences between soils, rock, pore fluids, or minerals as well as the electrokinetic effect of the presence of flowing water (Kearey et al., 2013; Loehr et al., 2017; ASTM Standard D6429-99, 2011).

The spontaneous potential measurements can be obtained by two different approaches. One requires an electrode (porous pot or stainless-steel spike) at a fixed location (remote electrode) and a second electrode which is moved along the desired traverse while reading the voltages between the two electrodes. The second approach is more applicable in the field. In this approach, the two electrodes are fixed in a permanent distance, and the system is moved in increments along the

desired traverse (Loehr et al., 2017). Non-polarized electrodes must be used since metal electrodes produce their own spontaneous potential effects. The source parameters do not have any effect on the depth of spontaneous potential investigations since it is a potential field technique. The depth of investigation is usually less than 100 ft (Kearey et al., 2013; ASTM Standard D6429-99, 2011). The degree of saturation, temperature, chemical activities of the fluids, clay content, and salinity of the fluids are among the most important geotechnical conditions that have an impact on the performance of the spontaneous potential survey. The effects of porosity and permeability of the materials on the spontaneous potential measurements are negligible (Wightman et al., 2004).

Like the ERI method, the electrodes need to be in good electrical contact with the ground. However, the spontaneous potential data is measured in a fast and straightforward process (ASTM Standard D6429-99, 2011). The resolution of data is a function of voltmeter electrode spacing, target size and depth, the magnitude of naturally occurring potential differences, and magnitude of background noise (Anderson and Ismail, 2003). The resolution of the spontaneous potential results also decreases with depth. Like the induced polarization method, spontaneous potential measurements are susceptible to cultural interferences (buildings, vehicles, underground utilities, overhead powerlines, etc.) since these interferences may generate potentials due to corrosion. Therefore, surveying near the electrical groundings will probably be ineffective (Wightman et al., 2004).

### **2.3.2. Seismic Methods**

Seismic methods are used to obtain subsurface velocity data by measuring the travel time of propagated waves from an energy source back to receivers. These techniques include Refraction, Reflection, Tomography (Downhole and Crosshole), and Surface Wave Methods (Spectral Analysis of Surface Wave (SASW), Multichannel Analysis of Surface Wave (MASW)) which are described in the following paragraphs.

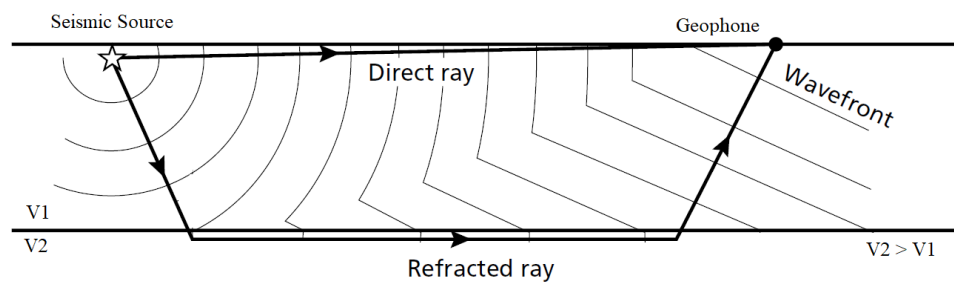
#### **Refraction**

In seismic refraction, the travel time of an acoustic wave to travel down through a layer and along with an interface and then back to the surface receivers (geophones) is measured (Kearey et al., 2013; Schoenleber, 2005; ASTM Standard D5777-00, 2011). In the refraction survey, the attention



is only on the first arrival of the seismic waves received by the geophones. The first arrival represents the refracted ray or direct ray (Kearey et al., 2013).

The refraction measurements require three to five times the desired depth of investigation to be implemented. The investigation depth can be calculated using the travel time and the distance between the source of energy and the geophones, which is typically less than 100 ft (30 m). The geophones and energy sources need to be in contact with the ground. In shallow surveys, the layers with only a significant velocity contrast (e.g., bedrock, water table) could be detected by refraction technique, and the velocity of layers must increase with depth (Mayne et al., 2002; Anderson and Ismail, 2003; ASTM Standard D6429-99, 2011). Direct and refracted ray paths from a near-surface source to a geophone is illustrated in Figure 2.6.



**Figure 2.6** Direct and refracted ray paths in the case of a two-layer model (Adapted from Kearey et al., 2013)

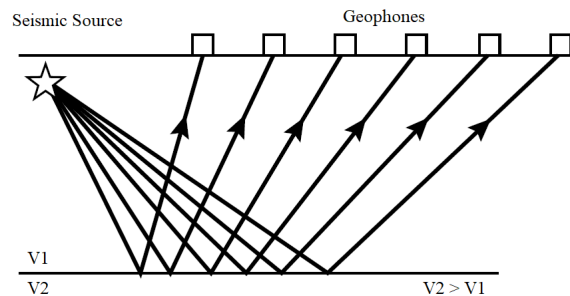
For deeper measurements, more powerful sources are needed to transmit the energy waves along the entire length of the survey (Kearey et al., 2013). Therefore, different sources of energy such as sledgehammers, mechanical weight drops or impact devices, projectile (gun) sources, and explosives could be applied in the refraction surveys for different applications (ASTM Standard D5777-00, 2011). The resolution of the refraction data is a function of source frequency, layer thickness, propagation velocities, velocity contrasts, receiver spacing, and background noise levels. The most common geotechnical conditions affecting the performance of the refraction method are homogeneity, degree of saturation, particle size, and the existence of highly fractured areas (Anderson and Ismail, 2003; ASTM Standard D6429-99, 2011). The results of the refraction survey can be plotted as profiles and contoured maps to display the stratigraphic layers. This method is ineffective in delineating the low-velocity and thin layers. Lateral resolution is typically 5 to 20 ft or more (2 to 6 m) which decreases with depth. Refraction data acquisition is labor-

intensive, and it requires extensive cable handling and moving the source of energy (Anderson and Ismail, 2003; ASTM Standard D6429-99, 2011).

The surface seismic refraction survey requires a single survey with three or five persons depending on site conditions and schedule. The refraction technique equipment is portable, and the implementation of this method is often cheap and cost-effective (Anderson et al., 2007; Wightman et al., 2004).

## Reflection

In seismic reflection, the travel time of acoustic waves to travel down to the subsurface interfaces (change in velocity or density) and then back to the surface receivers (geophones) is measured (Wightman et al., 2004; Kearey et al., 2013). The depth of investigation depends on the source of energy and could be up to 1000 ft (300 m) (ASTM Standard D6429-99, 2011). One to two times of the desired depth of investigation is required to implement the reflection surveys, which is less than the required distance for the refraction surveys. Unlike the refraction, low- and high-velocity layers can be mapped using reflection technique. However, the acquisition of data in a reflection survey is more complicated and time-consuming than refraction, and it requires significant data processing (ASTM Standard D6429-99, 2011; Anderson and Ismail, 2003; Wightman et al., 2004). The results can be plotted as profiles and contoured maps to display the stratigraphic layers. A reflected ray path from a near-surface source to a geophone is illustrated in Figure 2.7.



**Figure 2.7** Reflected ray paths in the case of a one-layer model (Adapted from Kearey et al., 2013)

The energy sources for the reflection survey are the same for the refraction method. However, less energy source is needed for a given depth than refraction method (Wightman et al., 2004). The resolution of the reflection measurements is a function of source frequency, propagation velocities, layer thickness, velocity and density contrasts, receiver spacing, and background noise levels.

Homogeneity, degree of saturation, particle size, and existence of highly fractured areas are among the most geotechnical conditions that affect the performance of the reflection survey (ASTM Standard D6429–99, 2011; Anderson and Ismail, 2003; BOEM, 2017). Lateral resolution is commonly 1 to 10 ft (0.3 to 3 m) which decreases with depth. Like the refraction surveys, seismic reflection is a labor-intensive technique, and it requires extensive cable handling and moving the source of energy (ASTM Standard D6429-99, 2011; Anderson and Ismail, 2003).

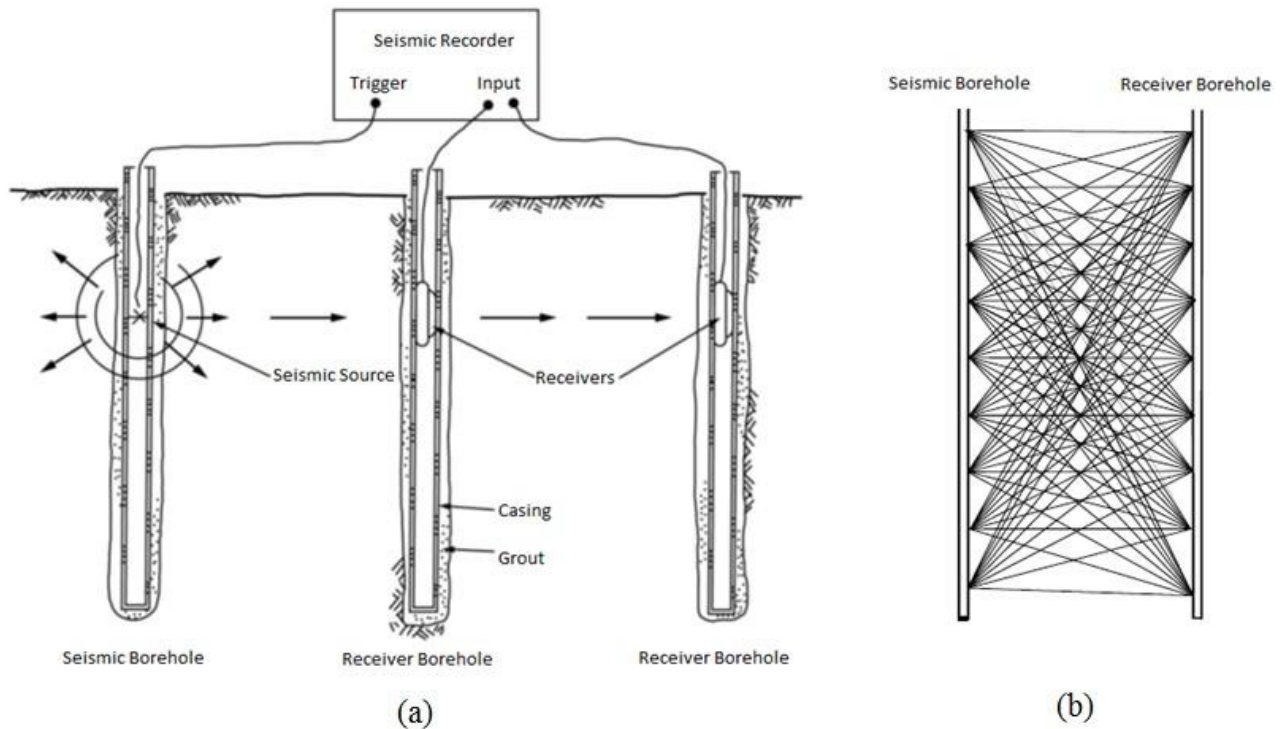
The surface seismic reflection survey requires a single survey with three or five persons depending on site conditions and schedule. The reflection technique equipment is portable, and the implementation of this method is more costly than the refraction technique (Anderson et al., 2007; Wightman et al., 2004).

### **Tomography**

Seismic tomography is used to obtain more detailed compressional and shear wave velocity profiles than the other seismic methods and provide high-resolution images of the near subsurface (Wightman et al., 2004). In contrast to the other seismic techniques, which are surface-based methods, tomography methods require cased boreholes with plastic pipes and grouted in-place which makes it a time-consuming process (Anderson et al., 2008; Mayne et al., 2002). The following paragraphs describe commonly used tomography techniques which are Crosshole (CH) and Downhole (DH) tomography.

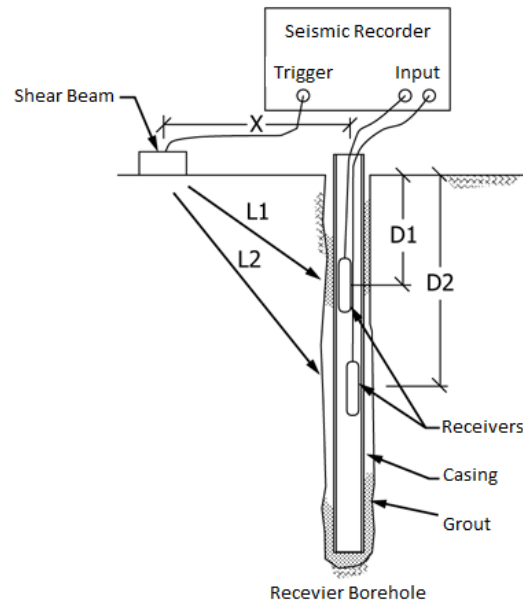
In crosshole surveys, two or more collinear boreholes are drilled. A seismic energy source is placed in a borehole (source borehole) at a depth of a stratum being investigated which can be up to 980 ft (300 m) (Mayne et al., 2002). The spacing between the source borehole and the first receiver borehole should be 5 to 10 ft (1.5 to 3 m), and the distance between the next boreholes should be 10 to 20 ft (3 to 6 m) (ASTM Standard D4428-07, 2007). The deviation of the drilled boreholes should be checked using an inclinometer to determine changes in horizontal distances with depth. Seismic waves are generated by the same equipment used by the other seismic methods. The amplitude and arrival time of the seismic waves are received by the geophones which are placed in the subsequent boreholes (receiver borehole). This procedure is repeated for the different depth of the borehole by moving the source of energy along the source borehole (Anderson et al., 2008; Wightman et al., 2004). Therefore, crosshole tomography is a data-intensive technique due to many combinations of source and receiver depth locations. Figure 2.8 illustrates a schematic

procedure and data acquisition layout of the seismic crosshole tomography technique. Since the compressional waves move faster and are received by the geophones, it might mask the arrivals of the shear waves. So, it is useful to perform the crosshole tomography in two separate tests for different waves (ASTM Standard D4428-07, 2007).



**Figure 2.8** (a) A schematic crosshole tomography procedure; (b) Crosshole data acquisition layout (Adapted from ASTM Standard D4428-07, 2007; Wightman et al., 2004)

In downhole surveys, only one cased borehole is needed, and the seismic source is placed on a fixed position on the surface instead of a borehole (Mayne et al., 2002). A horizontal beam (metal or wood) is placed at the ground surface with an offset from the top of the drilled receiver borehole (ASTM Standard D7400-19, 2019). A shear beam is loaded by a vehicle wheel (to increase normal stress and avoid sliding of the beam) and struck lengthwise (using 1 to 15 kg hammer at both ends) to provide an excellent shear wave source. The direction of the beam should be parallel with the direction of the receivers in the borehole. Vertical path distance is measured using the source to borehole offset and depth, so no inclinometer is needed in the downhole tomography (Mayne et al., 2002). Figure 2.9 shows the seismic downhole tomography procedure. Like the crosshole tomography, compressional and shear wave collection should be conducted separately to obtain the best results.



**Figure 2.9** Seismic downhole tomography procedure (Adapted from ASTM Standard D7400-19, 2019)

Compared to reflection and refraction methods, tomography requires more power and therefore higher resolution is expected. The resolution of the data is a function of source frequency, propagation velocities, source/receiver spacing, the multiplicity of travel paths, and background noise levels. Soil velocity/density contrasts, homogeneity, and degree of saturation are among the most common geotechnical conditions that affect the performance of these methods (Anderson and Ismail, 2003; ASTM Standard D7400-19, 2019). The tomography data collection is a labor-intensive procedure, and it requires extensive data processing (Wightman et al., 2004; Anderson and Ismail, 2003).

The cost of tomography methods is high compared to the other seismic techniques due to several reasons, including high costs of drilling, casing the boreholes with PVC materials, and equipment transportation costs (Anderson et al., 2007).

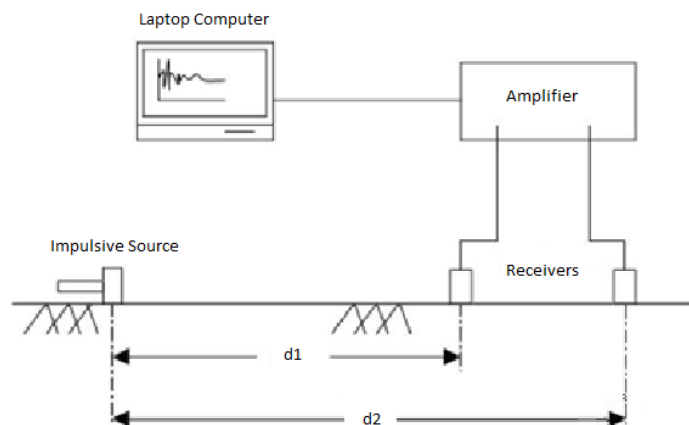
### Surface Wave Methods

A detailed shear wave velocity profile can be obtained using analysis of surface waves (Rayleigh waves) which are generated by an acoustic source on the ground. The surface wave arrival-time is recorded by geophones using two techniques: Spectral Analysis of Surface Wave (SASW) and Multichannel Analysis of Surface Wave (MASW). A full range of frequencies must be applied in these methods to obtain the velocity profile since, each wavelength propagates to a specific depth

(Gucunski and Woods, 1991). The surveys require three persons to operate, coordinate the source, and to monitor the results (Wightman et al., 2004). The degree of saturation and irregular soil profiles of the subsurface are among the most common geotechnical parameters affecting the performance of these methods (Wightman et al., 2004; Gucunski and Wood, 1991).

In the spectral analysis of surface waves, the surface waves are applied by a vertical impact on the ground surface and received by a pair of receivers placed linearly with an offset to the source of energy. Geophones are repositioned at varying distances from the source to develop a dispersion curve (Mayne et al., 2002). A general configuration of the spectral analysis of the surface wave technique is shown in Figure 2.10.

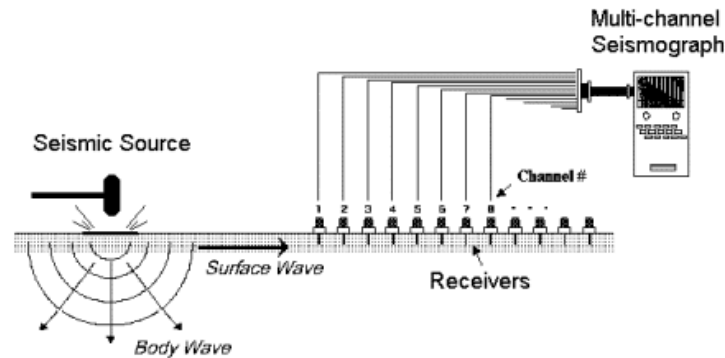
Various frequencies are generated for surveying using the spectral analysis of surface wave technique. Different arrival times and different shapes of signals are generated in media with different layers. However, in homogenous media, the same signal shapes are generated by the transducer (Luna and Jadi, 2000; Gazetas, 1991). In some cases, the sources are located on both sides of the receivers called the forward and reverse configuration. The transient (such as sledgehammers and dropped weights) and continuous (such as an electromagnetic vibrator, eccentric mass oscillator, bulldozers, and vibroseis truck) sources could be used for subsurface investigation to a depth of up to 390 ft (120 m). The thickness of a layer must be at least one-fifth of the layer depth to be recognized (Wightman et al., 2004).



**Figure 2.10** Diagram of a spectral analysis of surface wave test (Adapted from Astarita et al., 2014)

In the multi-channel analysis of surface wave technique, a couple of receivers (usually 12 or more geophones) with multi-channel seismograph are used with even spacing to get information on all

the subsurface layers. The channels are connected to a seismograph as shown in Figure 2.11. The source offset and the receiver spacing depend on the depth of investigation and the average stiffness of near-surface materials (Wightman et al., 2004). An impulsive source of energy is used on the ground to generate the surface waves. The waves are received by the geophones and recorded by the seismograph (Park, 1995).

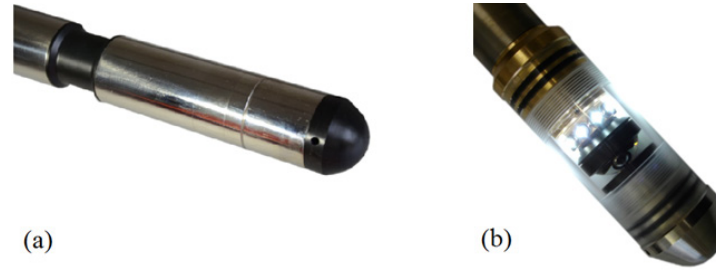


**Figure 2.11** Diagram of a multichannel analysis of surface wave test (geosigma.com)

Implementation of the spectral analysis of the surface wave survey is much slower than the multichannel analysis of surface wave technique since the former technique uses only two receivers to record the propagated surface waves. Therefore, it requires multiple field setups to conduct the survey which makes it a time-consuming process (Park, 1995).

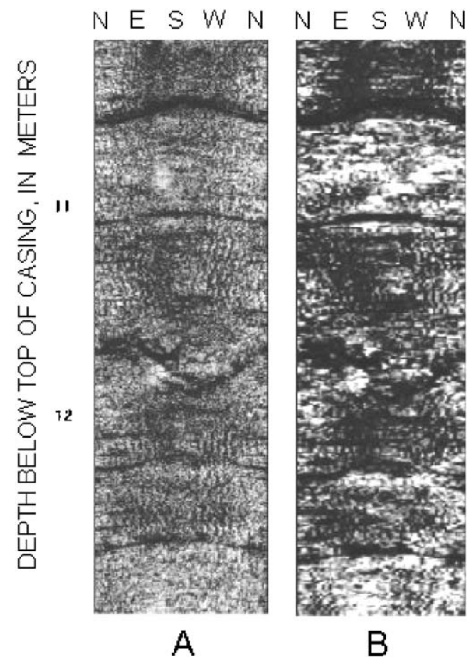
### 2.3.3. Optical and Acoustic Tele-Viewers

Optical and acoustic tele-viewers have been successfully used in geotechnical investigations and mineral explorations to produce continuous and oriented 360° views of the subsurface as it exists (Schepers et al., 2001; Wightman et al., 2004; Williams and Johnson, 2004). To obtain the subsurface images, the centralized probes within the borehole are slowly lowered at a rate of 1-3 m/min into the boreholes, and the optical images or acoustic reflected sounds are recorded by the receivers (Wightman et al., 2004; Williams and Johnson, 2004). Tele-viewer probes produce a full, in-situ, and oriented images of the boreholes under natural temperature and pressure conditions by capturing a layer of samples around the circumference of the hole. Image orientation can be affected by magnetic material within the near vicinity of the borehole (Wightman et al., 2004). Examples of acoustic and optical tele-viewer probes are shown in Figure 2.12. The most common approach is a combined application of acoustic and optical tele-viewers imaging with integrated interpretation (Williams and Johnson, 2004).



**Figure 2.12** (a) Acoustic tele-viewer head (lim.eu); (b) Optical tele-viewer head (openei.org)

Acoustic Tele-Viewers (ATV) use an ultrasonic pulse-echo configuration with a 0.5 to 1.5 MHz transducer (Williams and Johnson, 2004). Two transducer systems are used to perform the acoustic method: a rotating low-frequency transducer and a fixed high-frequency transducer. In the former system, the transducer was rotated on a motor-driven shaft while the tool is pulled up-hole. In the latter system, the acoustic beam is bounced off a rotating convex reflector (Williams and Johnson, 2004). An example of the received images using two transducers is depicted in Figure 2.13.



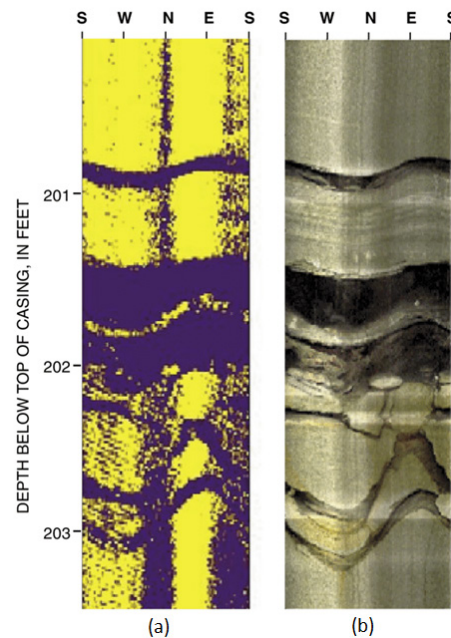
**Figure 2.13** An example of the acoustic tele-viewer images. (A) Fixed high frequency transducer, and (B) Rotating low-frequency transducer (Williams and Johnson, 2004)

The amplitude and travel time of the reflected sound waves are recorded to produce high-resolution images. The vertical resolution of a fixed high-frequency and a rotating low-frequency transducer is about 1 to 2 mm and 5 to 7.5 mm, respectively. The ATV logging requires a liquid medium



between the probe and the borehole wall to couple the signal to the borehole wall (Wightman et al., 2004; Williams and Johnson, 2004).

Optical Tele-Viewers (OTV) use a ring of lights to illuminate the borehole, a Charged-Coupled Device (CCD) camera, and a conical or hyperbolic reflector housed in a transparent cylindrical window (Williams and Johnson, 2004). Common vertical and horizontal resolutions of the OTV images are 0.5, 1, or 2 mm and 180, 360, or 720 pixels per line, respectively. The OTV imaging requires a transparent medium between the probe and the borehole wall (Wightman et al., 2004; Williams and Johnson, 2004). Figure 2.14 illustrates examples of acoustic and optical images of a borehole.



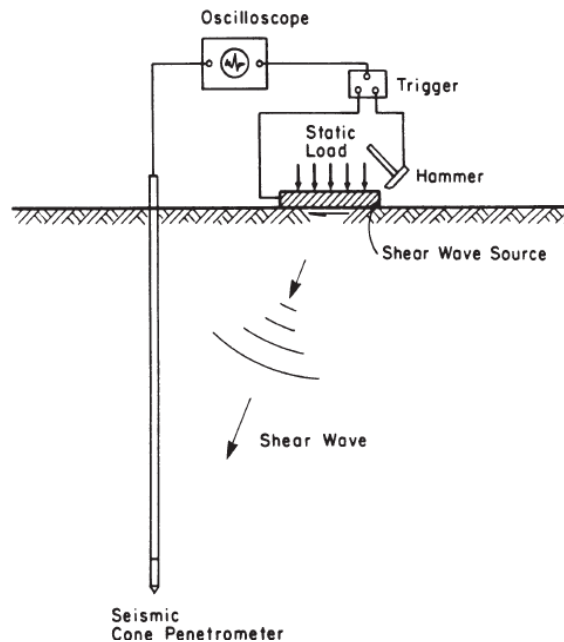
**Figure 2.14** An example of tele-viewer images of a borehole using (a) Acoustic and (b) Optical tele-viewers (Adapted from Williams et al., 2002)

The drilling and casing a borehole to implement the tele-viewer methods is a time-consuming process. Besides, the cost of implementing the tele-viewer techniques is high due to several reasons, including high costs of drilling, casing the boreholes with PVC materials, and equipment transportation costs (Anderson et al., 2007).

#### 2.3.4. Seismic Cone Penetration Test (SCPT)

Seismic Cone Penetration Test (SCPT) is a combination of the seismic downhole method and the CPT logging which provides a rapid means of determining continuous data including stratigraphy,

strength, and modulus information in one survey (Campanella et al., 1986). In this technique, no borehole is needed, and the seismic energy source is placed perpendicular to the cone probe on the surface. The conical probe is pushed into the desired depth at a rate of  $20 \pm 5$  mm/s, and the measurement for the shear wave velocity is conducted at the same depth simultaneously (generally 1 m intervals). A small rugged velocity seismometer has been incorporated into the cone penetrometer to obtain the measurement of dynamic shear modulus. After the velocity measurement is completed, the cone is advanced to the next depth, and the measurement is repeated. The seismic cone penetration test is conducted in couple of hours at each site (Loehr et al., 2017; Campanella et al., 1986; Anderson et al., 2007). A schematic layout of the SCPT is shown in Figure 2.15. The resistance against the penetration at the tip and sleeve of the probe, as well as shear wave velocity are measured by this method.



**Figure 2.15** Schematic layout of SCPT (Campanella et al., 1986)

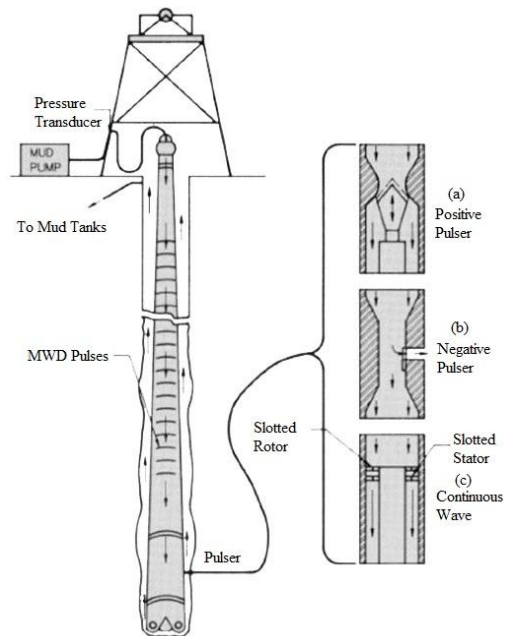
The most common geotechnical conditions affecting the performance of the SCPT method are soil anisotropy, degree of consolidation, very stiff soils, particle size, pore water pressure, and temperature (Stewart and Campanella, 1993; Campanella et al., 1986; Lunne et al., 2002; BOEM, 2017; Robertson et al., 1986; Anderson et al., 2007). The seismic cone penetration test is costly in terms of the high capital cost of the equipment and transporting the equipment to the field. The cost of the seismic cone penetration test is less than the tomography and tele-viewer techniques since it does not require any drilled borehole (Anderson et al., 2007; Robertson et al., 1986).

### 2.3.5. Measurement While Drilling (MWD)

Measurements While Drilling (MWD) has been used in mining and construction industries to collect the geotechnical subsurface data. The drilling is performed using sensors that are in the bottom-hole assembly (Li et al., 2014; Dowell and Mills). The terms Logging While Drilling (LWD) or Monitoring While Drilling may also be used to refer to measurement while drilling technique. Measurement while drilling can be implemented in the harshest operating environments (Dowell and Mills).

There are different sensors for different purposes. Surface equipment for measurement while drilling includes a pressure transducer for signal detection, analog pressure recorder, electronic signal decoding equipment, and digital and analog readouts and plotters (Gravley, 1983). The measurement while drilling logging rate depends on the rate of penetration that could be between 0.08-1 m/min. The results are interpreted using software and displayed in real-time on continuous multi-scale logs at a rate of once per foot, and presented digitally on video displays (Gravley, 1983; Dowell and Mills).

The data are transferred using one or more telemetry approaches, including mud-pulse, electromagnetic, acoustic, and hardwire. Mud-pulse telemetry is the economical and standard method in measurement while drilling systems (Desbrandes and Clayton, 1994; Fontenot, 1986). Mud-pulse telemetry is a method of transmitting information through a flowing column of drilling mud. In this process, the pressure in the flowing mud column at a point downhole is modulated by a mechanical means (mud-pulse valve), and the resulting pressure pulses appearing at the surface end of the mud column are detected by a pressure transducer conveniently located in the standpipe (shown in Figure 2.16). The pulses in the flowing mud column are generated by several different devices which are categorized into three ways: positive pulse, negative pulse, and continuous wave or mud siren (Fontenot, 1986). A mud-pulse telemetry, along with its three different devices is shown in Figure 2.16.



**Figure 2.16** A mud-telemetry system; (a) Positive pulser; (b) Negative pulser; and (c) Continuous wave (Adapted from Fontenot, 1986).

## CHAPTER 3 ELECTRICAL RESISTIVITY IMAGING TECHNIQUE

### 3.1. Introduction

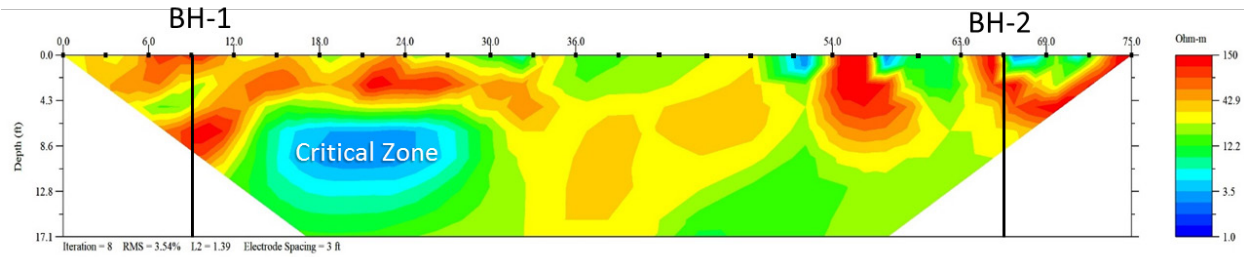
This chapter describes the applications of ERI technique in TxDOT site investigations. The required information and guidelines for performing a successful ERI survey along with the limitations, practical considerations, and common mistakes are also presented in this chapter.

### 3.2. Applications

The electrical resistivity imaging method is a complementary method to the conventional geotechnical soil investigation methods to provide information about subsurface heterogeneity, help locating the required boreholes and samples, and provide estimates of the geotechnical parameters to overcome the inherent limitations (e.g., point-specific data) and problems (e.g., limited accessibility of drill rigs) of the conventional geotechnical site investigation methods.

#### 3.2.1. Providing Continuous Image of Subsurface

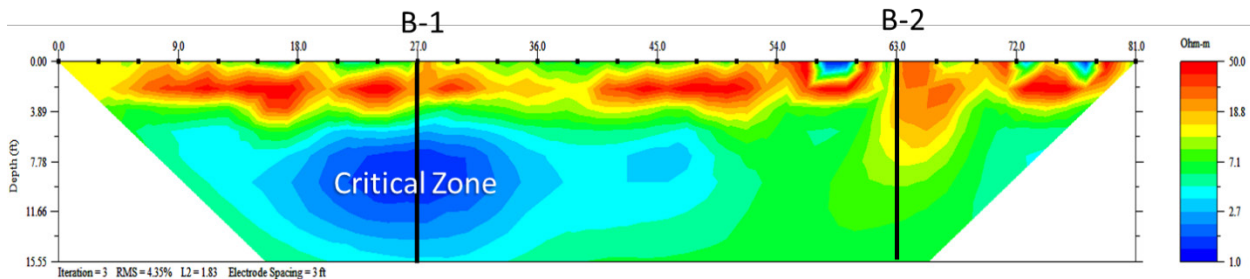
The electrical resistivity imaging method could be used along with conventional geotechnical site investigations to help geotechnical engineers confirm the obtained results and augment them by providing additional data between the boreholes. Figure 3.1 illustrates a continuous resistivity image of subsurface between two boreholes obtained after completion of soil boring and sampling operations in Fort Worth, Texas. This subsurface resistivity image illustrates the heterogeneity of subsurface materials and a critical zone (very low resistivity area) between the two boreholes. The subsurface heterogeneity shown in Figure 3.1 provides valuable insights for geotechnical engineers to reduce risk and uncertainty resulting from the lack of adequate site investigation. However, the conventional geotechnical investigation is incapable of providing a continuous view of the subsurface and miss the anomalous conditions between the boreholes.



**Figure 3.1** Illustration of the heterogeneity of subsurface materials and locating a critical zone by resistivity image of the subsurface - Fort Worth district

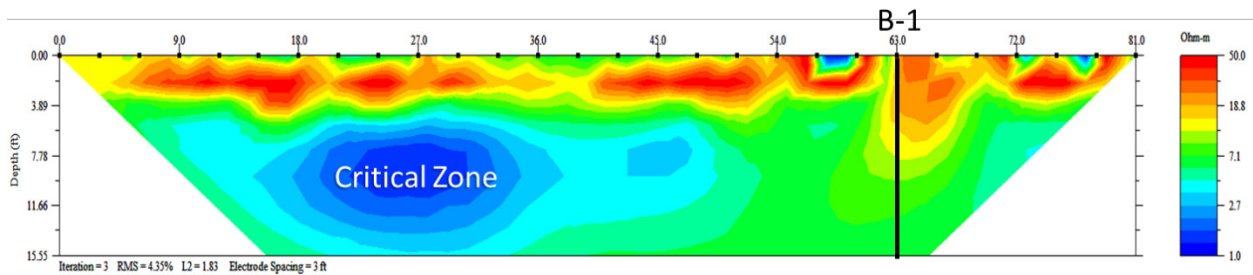
### 3.2.2. Determining Boring and Sampling Intervals

Conducting electrical resistivity imaging surveys provides a continuous view of the subsurface to geotechnical engineers before performing conventional site investigations. The continuous subsurface resistivity images help to locate the approximate locations of boreholes and samples that are good representatives of the subsurface condition. For example, Figure 3.2 shows the recommended locations of boreholes along a survey line that could lead to a proper assessment of the subsurface condition. The number of required samples could be approximated based on the different zones in the resistivity image.

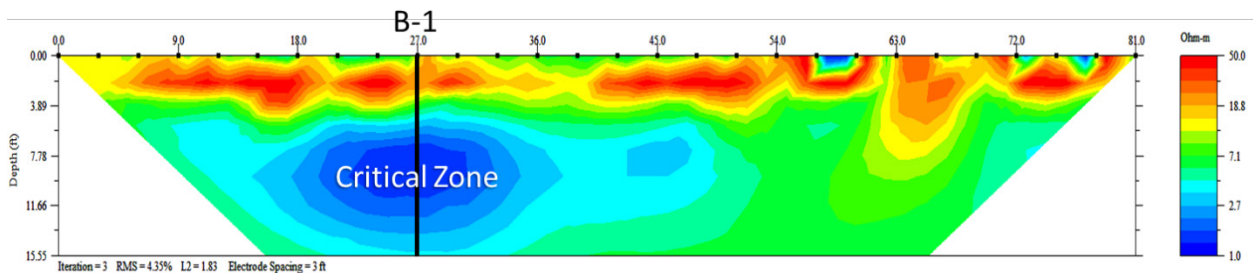


**Figure 3.2** Approximate locations of boreholes to properly investigate the subsurface condition along the survey line

An investigation without having an overall view of the subsurface condition could lead to misleading interpretations. Figure 3.3 and Figure 3.4 illustrate conditions when only one borehole is considered along the survey line to investigate the subsurface condition. However, neither of them can adequately represent the actual subsurface condition. The interpretation only based on the boring results shown in Figure 3.3, will ignore the critical zone at the left side of the resistivity image, leading to inadequate design and potential failure of a project. Likewise, the interpretation only based on the boring results shown in Figure 3.4, may lead to incorrect designs.



**Figure 3.3** Missing the critical zone on the left side



**Figure 3.4** Misinterpretation of the subsurface condition

### 3.2.3. Estimating Geotechnical Parameters

The electrical resistivity values depend on some geotechnical parameters such as moisture content, unit weight, porosity, pore fluid conductivity, clay content, and temperature. Therefore, quantifying the geotechnical parameters using electrical resistivity values enables the geotechnical engineers to interpret the electrical resistivity data and benefit from them in the analyses and designs. This research manual provides sets of empirical equations and charts using the data obtained from extensive laboratory experiments (1093 laboratory electrical resistivity tests) on the soil samples collected from five selected TxDOT districts (Beaumont, Corpus Christi, El Paso, Dallas, and Fort Worth districts). These tools allow for the estimation of known geotechnical parameters (e.g., moisture content, dry unit weight, plasticity index, percent of fines, and clay content) using the field electrical resistivity values.

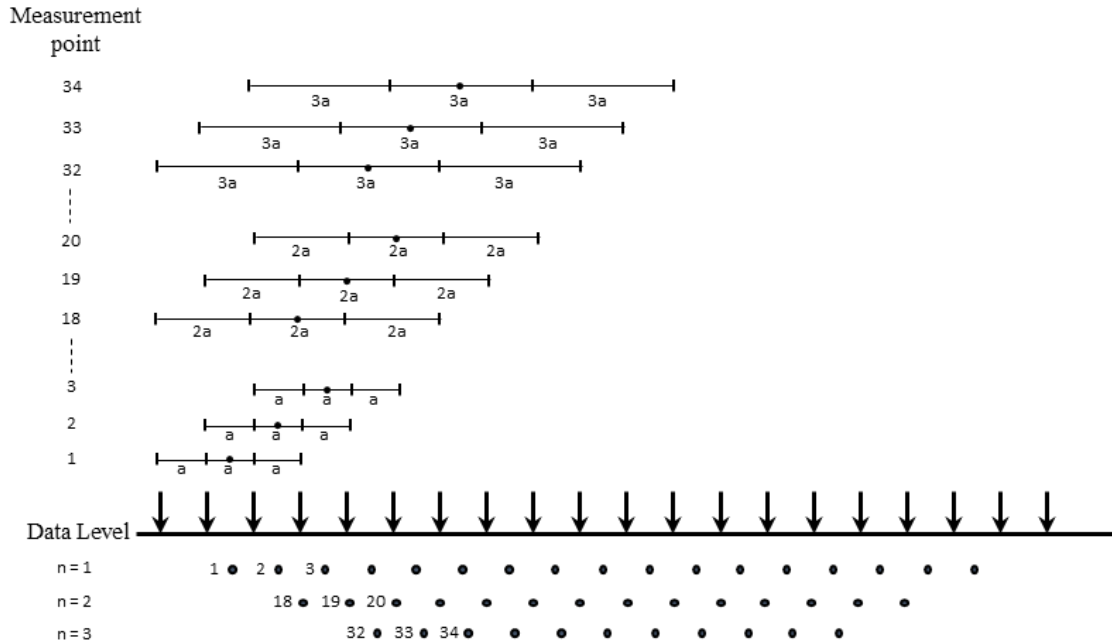
### 3.3. Electrical Resistivity Imaging Survey

Depending on the site condition and project objectives (i.e., determination of either horizontal or vertical resistivity variations), the field electrical resistivity surveys can be performed using one-, two-, or three-dimensional survey methods. A One-dimensional electrical resistivity survey, also known as Vertical Electrical Sounding (VES), is used to resolve the vertical resistivity variations

with depth (i.e., used to detect horizontal structures). In this method, the electrical resistivity of subsurface materials is measured at a single location. Then at each step, the spacing between the electrodes is increased gradually to reach the higher depths (the center of electrodes remains constant until the end of the survey) (Hossain et al., 2018; Wightman et al., 2004). One of the most significant drawbacks of the VES method is that it only captures the vertical resistivity variations and does not consider the horizontal variations of subsurface materials (Loke, 1999). Therefore, 2D and 3D surveys are utilized to obtain more realistic results.

A two-dimensional electrical resistivity survey is used to resolve the vertical and horizontal resistivity variations through the depth. In this method, the variations of resistivity with depth are measured at grid locations or along the lines of traverse (Wightman et al., 2004). In this method, several measurements are recorded simultaneously using multi-electrode arrays. At each step, the spacing of the electrodes is increased by a factor of “n”. Each measurement is recorded at the intersection of two 45° lines through the centers of the quadrupole (Loke, 2004). In this method, the electrical resistivity of subsurface material perpendicular to the survey line is assumed to be constant. This assumption results in a cost-effective survey, along with reasonable accuracy in the results (Loke, 1999). Based on the measured (apparent) resistivity, continuous 2D images (pseudo-section) of the subsurface can be developed using software programs that illustrate both horizontal and vertical variations in subsurface electrical resistivity. Figure 3.5 illustrates the arrangement of electrodes and the sequence of measurements to obtain a 2D pseudo-section.





**Figure 3.5** Arrangement of the electrodes and sequence of measurements used to obtain a 2D pseudo-section

A three-dimensional electrical resistivity survey provides the most accurate results of the subsurface electrical resistivity and is performed using two different approaches. The first method uses different 2D images measured in parallel and perpendicular lines to build up a 3D profile (Hossain et al., 2018; Arjwech, 2011). The accuracy of this approach depends on the orientation of in-line measurement electrodes to the anomalies (should be perpendicular) (Samouëlian, 2005). The second method uses a square array of four electrodes that provides measurements that are orientation-dependent. Also, the in-line measurements can be done in concentric circles on the surface to obtain 3D images of the subsurface (Brunner et al., 1999). The 3D survey implementation is a time-consuming process, and the cost of the survey is relatively high compared to the 2D survey (Loke, 1999).

### 3.3.1. Field Survey Equipment

A resistivity meter, electrodes, cables, a power supply, a switching box, and a laptop are required on the site to perform the electrical resistivity survey. Besides, a tape measure and a hammer are needed to locate and place the electrodes into the ground. Figure 3.6 shows the equipment required for the implementation of the electrical resistivity survey in the field. Although resistivity measurements can be made using common electronic instruments, it is recommended by ASTM Standard D6431-18 to use the commercial resistivity instruments designed for the electrical resistivity measurements in the field (ASTM Standard D6431-18, 2018).



**Figure 3.6** Required equipment for the implementation of an electrical resistivity survey in the field

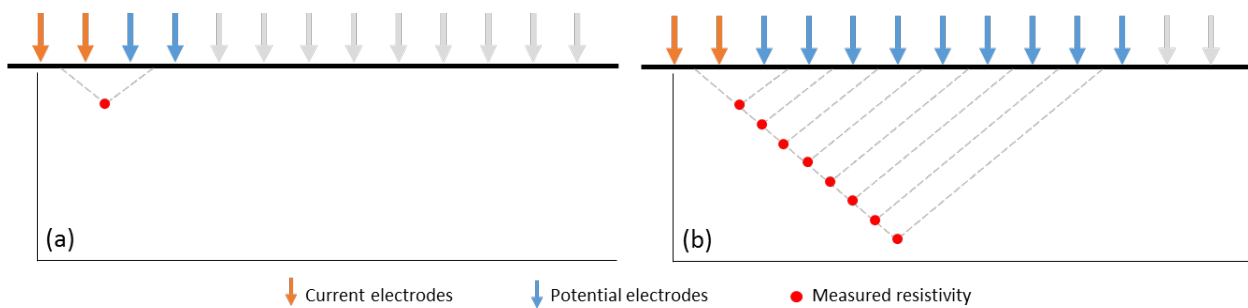
#### Resistivity Meter

The resistivity meters measure the resistance value of earth materials and usually contain both transmitter (which controls and measures the current) and receiver (which measures the voltage) in one device. An example of a resistivity meter manufactured by Advanced Geoscience Inc. is shown in Figure 3.7.



**Figure 3.7** AGI Supersting R8 resistivity meter

Resistivity meters are classified into single-channel (one receiver) and multi-channel (more than one receiver) systems. In a single-channel system, for each time that the current is transmitted through the electrodes, only one measurement is recorded using the four electrodes. However, in multi-channel systems, for each current injection, several measurements are recorded simultaneously using multiple electrodes, which accelerate the measurement process (Hossain et al., 2018; Advanced Geoscience Inc., 2011). The data measurement procedures using the single-channel and multi-channel measurement systems are illustrated in Figure 3.8.



**Figure 3.8** Data measurement procedures using (a) single-channel system and (b) multi-channel system

### Electrodes and Cables

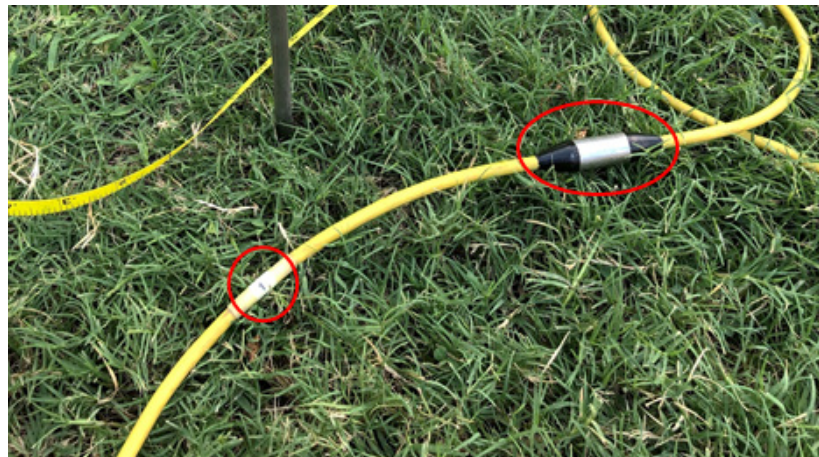
The current is transmitted into the ground through the electrodes. The electrodes must be made of corrosive-resistant metal such as copper, hot-galvanized steel, stainless steel, aluminum, and lead (Wightman et al., 2004; Milsom, 2003). The stainless-steel electrodes with lengths in the range of 12 to 40 in (30 to 100 cm) and diameter in the range of 7/16 to 45/64 in (10 to 18 mm) are commonly used in the field electrical resistivity imaging (IRIS Instruments; Advanced Geoscience

Inc.; Geomatics CO. LTD.; Seidel and Lange, 2007). The effect of the electrode's diameter on the electrical resistivity measurements is negligible; however, larger diameters could be utilized in the case of hard materials to provide extra rigidity (Megger, 2010). Non-polarizing electrodes are rarely used in electrical resistivity surveys (Milsom, 2003). The polarization voltages generated in metal electrodes in contact with groundwater, could cause problems in the potential electrodes. The magnitude of these voltages can be reduced using stainless-steel electrodes. Threaded electrodes are not used in the resistivity imaging surveys.

To connect the resistivity meter and the electrodes, multi-stranded or single-core copper wires insulated by plastic or rubber coatings are commonly used to eliminate noisy readings resulting from the crosstalk of members of a cable (Advanced Geoscience Inc., 2011; Milsom, 2003). The need for mechanical strength determines the thickness of the cables (cable resistance is negligible rather than contact resistance) (Seidel and Lange, 2007; Milsom, 2003). Therefore, a 16 AWG cable (with a cross-section of about 1.5 mm<sup>2</sup>) works sufficiently for the field electrical resistivity imaging. There are different types of cables for various applications, such as land surveys, underwater measurements, and borehole surveys. The multi-electrode cables are used for automatic measurements and are divided into several sections to make it easier to carry. The cable sections can be connected to form a continuous cable that is used in the field surveys (Advanced Geoscience Inc., 2011). Figure 3.9 shows examples of a stainless-steel electrode and two multi-electrode cable sections for a survey with 28 electrodes. The cables have take-outs at specific intervals and are labeled, which are shown in Figure 3.10.



**Figure 3.9** (a) a stainless-steel electrode and (b) multi-electrode cable sections each includes 14 take-outs



**Figure 3.10** Cable take-out and label

### External Battery

The resistivity meter requires one or two external batteries to ensure that adequate power is provided for the transmitter to carry out the measurements (Advanced Geoscience Inc., 2011). The external batteries are mainly delivered with the purchased instruments. The deep cycle marine 12 V batteries are recommended by Advanced Geosciences Inc. (2011) to be used in the field surveys because of their ability to discharge and recharge without losing their capacity. Lead-acid car batteries are also used. However, they lose their capacity to be fully charged in a shorter period

(Advanced Geoscience Inc., 2011; ABEM Instrument, 2010). Figure 3.11 shows an example of an external marine 12 V battery.



**Figure 3.11** External marine 12 V battery

### Switch Box

A switch box (also known as electrode selector) is usually used with multi-electrode cables to automatically switch and select the relevant four electrodes for each measurement based on the electrode labels. The electrode switching capabilities of switch boxes are different depending on the number of used electrodes (e.g., for an AGI system comes in 28, 48, 56, 64, 84, and 112 electrodes) (Advanced Geoscience Inc., 2011; Loke, 1999). Several switch boxes can be connected in a linear series to increase the capability of a switch box. Figure 3.12 illustrates an example of the Advanced Geoscience Inc. switch box.



**Figure 3.12** AGI switch box

### **3.3.2. Survey Planning**

A practical and detailed plan for the survey leads to the appropriate use of the electrical resistivity imaging method (ASTM Standard D6431-18, 2018). Therefore, in this section, instructions for preliminary evaluation of the site, selecting the electrode configuration, determining the electrode spacing, and evaluating penetration depth are provided.

#### **Preliminary Evaluation of Site**

The site characteristics and purpose of an electrical resistivity survey should be assessed beforehand since they are essential factors in selecting a survey approach, electrode configuration, needed equipment, needed operators, required interpretation method, and required budget to obtain the desired results. The geological and hydrological models of the site, the topography of the site, the desired depth of penetration, and accessibility of the site are among the most important considerations (ASTM Standard D6431-18, 2018). The resistivity contrast of geologic or hydrologic units of interest should be assessed using previous studies in the area. Preliminary fieldwork at the location of known stratigraphy (e.g., borehole) might be needed, if the earlier studies are insufficient, to determine the resistivity contrast and assess the feasibility of the method (ASTM Standard D6431-18, 2018). The location of the survey should be visually inspected in advance to check for the feasibility of the survey. A flat area far away from any source of electric or electromagnetic fields (e.g., buried manmade structures and utilities) can be a desirable location for the implementation of electrical resistivity surveys (Milsom, 2003).

#### **Selection of Electrode Configuration**

The type of electrode configuration should be selected carefully to obtain reliable results with high-resolution and provide more information about the subsurface characteristics along with sufficient coverage (Dahlin and Zhou, 2004). The most commonly used electrode configurations in electrical surveys are Wenner, dipole-dipole, Wenner-Schlumberger, pole-pole, and pole-dipole (Loke, 2004; Reynolds, 1997). Some considerations should be taken into account in selecting the most appropriate configuration for the field survey. These considerations include the type of anomaly to be investigated, the sensitivity of electrode configuration to vertical or horizontal changes in resistivity, depth of investigation, horizontal coverage needed, and background noise level (Loke, 1999). Moreover, the heterogeneity of earth materials affects the potential distribution and measured electrical resistivity values (Loke, 2004). The characteristics of different 2D electrode

configurations have been compared and summarized in Table 3.1 (Reynolds, 2011; Samouëlian et al., 2005; Dahlin and Zhou, 2004; Loke, 2001; Griffiths and Barker, 1993).

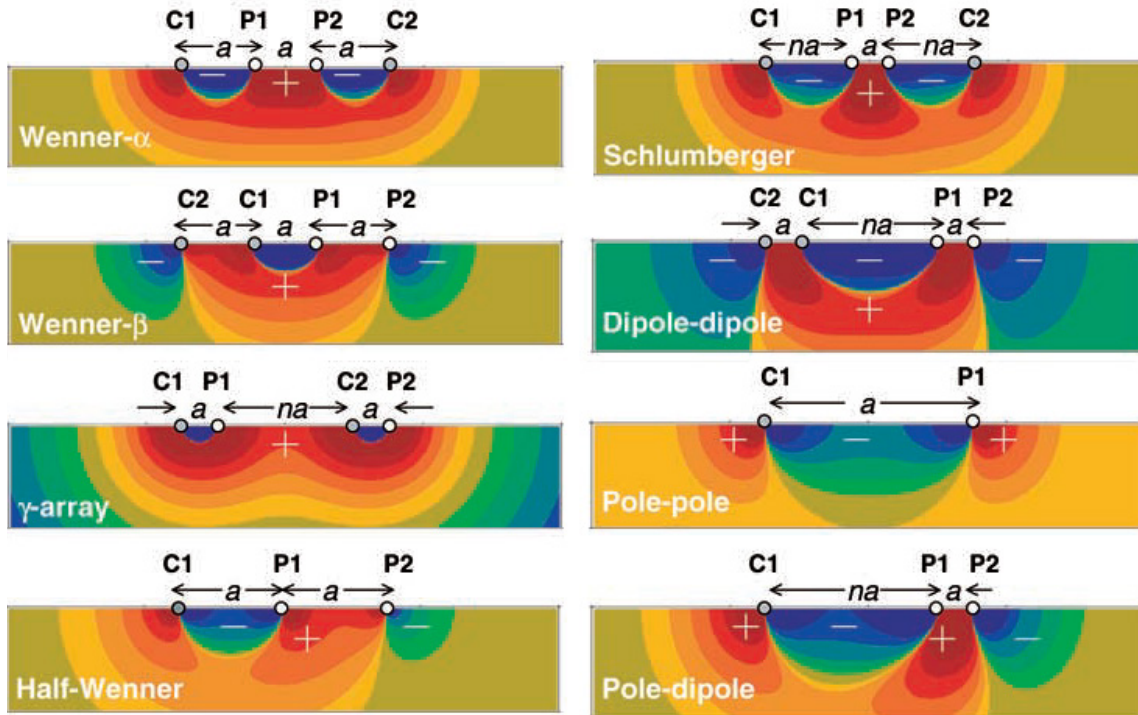
**Table 3.1** Characteristics of different 2D electrode configurations

	Wenner	Dipole-dipole	Wenner-Schlumberger	Pole-pole	Pole-dipole
Sensitive to horizontal structures	****	*	**	**	**
Sensitive to vertical structures	*	****	**	**	*
Depth of investigation	*	***	**	****	***
Signal strength	****	*	***	*	**
Horizontal data coverage	*	***	**	****	***
Sensitive to background noise	*	***	*	****	***
Sensitive to line orientation	****	***	****		

Note: symbols \* to \*\*\*\* represent the relative sensitivity of electrode configurations from low to high.

The sensitivity of the electrode configurations to vertical or horizontal changes in resistivity differs according to the location of current and potential electrodes. Sensitivity is defined as the degree to which a change in the subsurface electrical resistivity will affect the measured potential by the electrode configuration. Figure 3.13 illustrates the sensitivity sections of different electrode configurations for a homogeneous media. The regions with positive and negative signs will increase and decrease the potential measurements, respectively (Milsom, 2003). For all the electrode configurations, the sensitivity has the highest values close to the electrodes. Considering the sensitivity sections, the applicability of a specific electrode configuration for investigating a particular anomaly can be assessed for different electrode configurations (Dahlin and Zhou, 2004; Loke, 2004; Furman et al., 2003). For example, the sensitivity section for the Wenner-alpha array in Figure 3.13 has almost horizontal closely spaced contours below the center of the array, indicating that the array is more sensitive to changes of electrical resistivity in the vertical direction rather than the horizontal direction. On the contrary, the sensitivity section for the dipole-dipole array has almost vertical contours, indicating that the array is more sensitive to horizontal changes in electrical resistivity rather than vertical changes (Milsom, 2003). These sections are solely dependent on the electrode configuration characteristics and are independent of body characteristics. They could be reproduced in any plane which passes through the line of four electrodes (Barker, 1979).





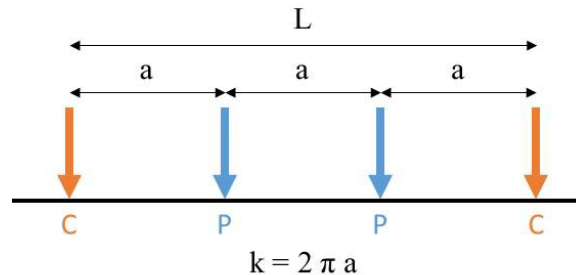
**Figure 3.13** Sensitivity sections of Wenner (alpha, beta, gamma), Schlumberger, dipole-dipole, pole-pole, and pole-dipole arrays (Dahlin and Zhou, 2004)

Here, the instrumentation and characteristics of the most common electrode configurations are described in more detail:

### ***Wenner array***

In the Wenner array, the length of a survey is divided into equal sections, and the electrodes are driven into the ground in those places (ASTM Standard D6431-18, 2018). The schematic instrumentation of the Wenner array (technically called Wenner-alpha) is depicted in Figure 3.14. The Wenner array is more sensitive to vertical changes of resistivity than horizontal variations. Therefore, it is an appropriate electrode configuration to map the horizontal structures (detecting vertical changes). The performance of the Wenner array is poor in mapping narrow vertical structures (detecting horizontal changes) (Hossain et al., 2018; Milsom, 2003). Wenner array consists of three-electrode configurations: Wenner-alpha, Wenner-beta, which is a special case of the dipole-dipole array with equally spaced electrodes ( $n=1$ ), and Wenner-gamma in which the electrodes are spaced with an unusual arrangement (Loke, 2004). Since the Wenner-alpha array has the strongest signal strength among all electrode configurations, it is preferred for surveys where substantial noise is anticipated in the field condition (ASTM Standard D6431-18, 2018;

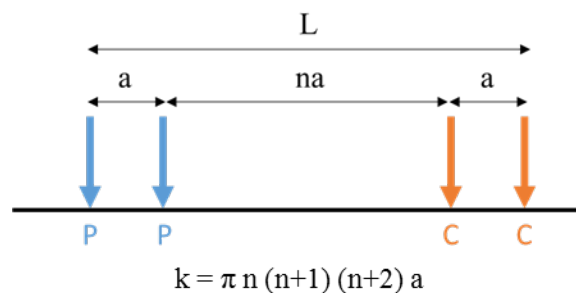
Hossain et al., 2018). If the electrode spacing is increased (in case of a limited number of electrodes), a poorly horizontal coverage will be resulted (Loke, 2004). The depth of investigation using Wenner arrays depends on the electrode spacing “a”.



**Figure 3.14** Schematic instrumentation of the Wenner-alpha array (“k” is the geometric factor of the array)

### *Dipole-dipole array*

In the dipole-dipole array, the identical electrodes are closely spaced at the same distance for current and potential electrodes. The distance between the inner electrodes is a function of the distance between the current or potential electrodes and is expressed by a factor called “n” (ASTM Standard D6431-18, 2018). The schematic instrumentation of dipole-dipole array geometry is depicted in Figure 3.15. “n” values vary depending on the desired depth of penetration and have the value between 1 to 6 (Loke, 2004).



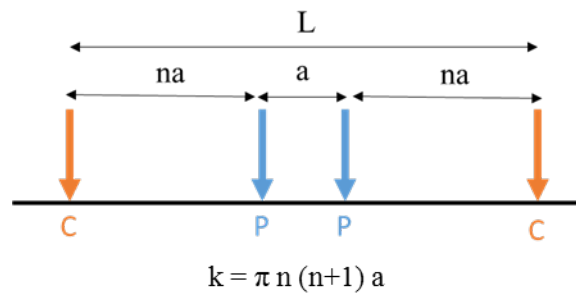
**Figure 3.15** Schematic instrumentation of the dipole-dipole array (“k” is the geometric factor of the array)

The dipole-dipole array has been widely used in field surveying because the electromagnetic coupling between the current and potential electrodes is low for the array (Hossain et al., 2018; Loke, 2004). The dipole-dipole array is more sensitive to variations in the horizontal direction than to the vertical resistivity changes. Therefore, it is an appropriate electrode configuration to map the vertical structures like cavities. However, its performance is poor in mapping horizontal

structures like sedimentary layers (ASTM Standard D6431-18, 2018; Hossain et al., 2018). The dipole-dipole array has a very small signal strength. Moreover, this array is suitable for the survey of large areas with detailed information in shallow depth (Milsom, 2003). Compared to the Wenner array, the horizontal coverage of the dipole-dipole array is better in case of using a limited number of electrodes. The depth of investigation has different values depending on the electrode spacing “a” and factor of “n”. However, it underestimates the depth of subsurface anomalies in “n” factors greater than 2 (Loke, 2004).

### ***Schlumberger array***

In the Schlumberger array, the electrodes are spaced unequally, where the distance between current electrodes is greater than five times the distance between potential electrodes (ASTM Standard D6431-18, 2018). It means that the factor of “n” is greater than 2 for this electrode configuration. The schematic instrumentation of the Schlumberger array is depicted in Figure 3.16. Indeed, the Wenner array is a special case of Schlumberger array when “n” factor is equal to one.

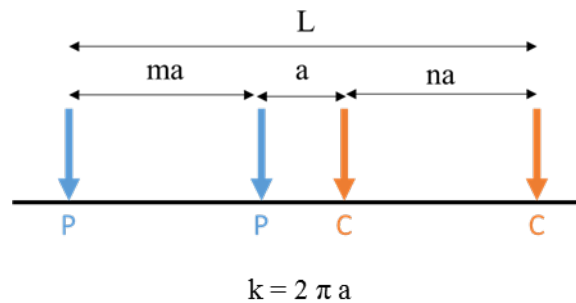


**Figure 3.16** Schematic instrumentation of the Schlumberger array (“k” is the geometric factor of the array)

For lower values of “n”, the Schlumberger array is more sensitive to vertical changes in resistivity than to horizontal variations. However, for higher values of “n”, it is more sensitive to horizontal variations in resistivity. The Schlumberger array is an appropriate electrode configuration for surveying a combination of horizontal and vertical structures (Loke, 2004). The horizontal coverage is decreased with an increase in the electrode spacing (Aizebiokhai, 2010; Hossain et al., 2018). Compared to the Wenner array, the Schlumberger array has a higher depth of investigation for “n” values greater than 3, weaker signal strength, and slightly wider horizontal coverage (higher signal strength and narrower horizontal coverage than the dipole-dipole array) (Loke, 2004). Recently, the Wenner-Schlumberger array has been used in electrical resistivity imaging surveys.

### ***Pole-pole array***

In the pole-pole array, a current and a potential electrode are closely spaced. The second current and potential electrodes are located at a distance greater than 20 times the separation between the first electrodes (Loke, 2004; Hossain et al., 2018). The schematic instrumentation of the pole-pole array is depicted in Figure 3.17.

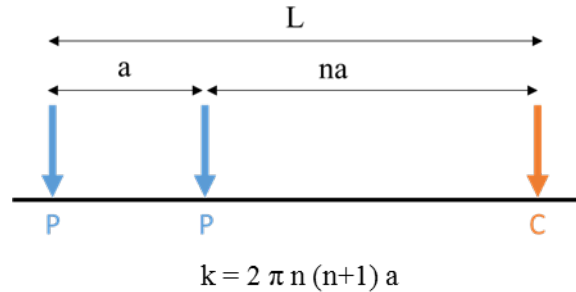


**Figure 3.17** Schematic instrumentation of the pole-pole array (“k” is the geometric factor of the array)

The pole-pole array is very sensitive to the background noises due to large distances between the identical potential electrodes. The pole-pole array is mostly used in the surveys with small electrode spacing (less than a few meters) because it requires a relatively large area to place the secondary electrodes (Loke, 2004). Although the pole-pole array has the highest horizontal coverage and the maximum depth of investigation in comparison to the other electrode configurations, the resolution of its results is not satisfactory. Therefore, this array is not commonly used as Wenner, dipole-dipole, and Schlumberger arrays in electrical resistivity imaging surveys.

### ***Pole-dipole array***

In the pole-dipole array, two potential electrodes are spaced closely, and a current electrode is placed at a larger distance to potential electrodes. The pole-dipole array has significantly higher signal strength than the dipole-dipole array, as well as it is less sensitive to background noises than the pole-pole array (Loke, 2004; Hossain et al., 2018). The schematic instrumentation of the pole-dipole array is depicted in Figure 3.18. It is not recommended to use “n” values greater than 8 to 10 unless the spacing between the potential electrodes “a” increases (Loke, 2004).



**Figure 3.18** Schematic instrumentation of the pole-dipole array (“k” is the geometric factor of the array)

To eliminate the effects of array asymmetry on the inverted electrical resistivity values, one should conduct the forward and reverse order measurements that resolve the asymmetry problem on the electrical resistivity data. Consequently, it doubles the data points and duration of the survey (Loke, 2004). The pole-dipole array is more sensitive to the vertical variations in electrical resistivity compared to the dipole-dipole array. It also has a higher signal strength rather than the dipole-dipole array. This electrode configuration is suitable for the reconnaissance survey of large areas with minimum electrode movement and a shallow investigation with a relatively limited number of electrodes (Loke, 2004).

### Evaluation of Depth of Penetration

The depth of penetration can be estimated by the median depth of investigation with a particular electrode configuration. The median depth “ $Z_e$ ” is determined using the sensitivity section of the electrode configuration. It is defined as the depth in which the upper part of the earth above the median depth has the same effect on the measurements as the lower part (Loke, 1999). Table 3.2 presents the values for the median depth of investigation for different electrode configurations. It is worth noting that these values have been developed for homogenous media. However, they can be applied in a heterogeneous media to give a rough estimation of the maximum depth of investigation (Loke, 1999). The maximum depth of investigation is estimated either by multiplying the values in Table 2 by the maximum length of the survey line “L” or by maximum electrode spacing “a”. Besides, the factor of “n” needs to be considered in estimating the depth of investigation for the dipole-dipole, Wenner-Schlumberger, and pole-dipole arrays. It is easier to use the maximum length of the survey for the electrode configurations with four active electrodes (e.g., dipole-dipole, Wenner, and Wenner-Schlumberger arrays) to estimate the maximum depth of penetration. For example, if a dipole-dipole array is used with a maximum electrode spacing of

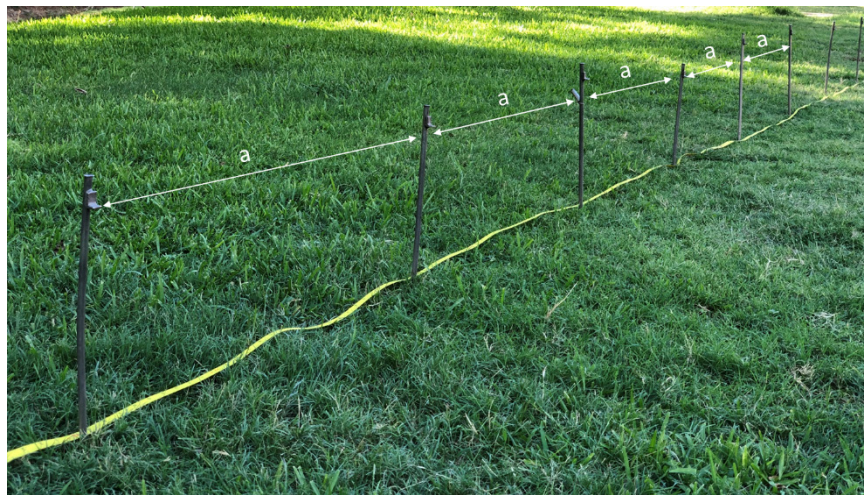
3 ft. ( $a=3$  ft.) with a value of 4 for the factor of “n”, then the maximum length of the survey is 30 ft. ( $L=30$  ft.). Therefore, the maximum depth of penetration would be  $0.203 \times 30$  or about 6 ft. The actual depth of investigation can vary in case of having sizeable electrical resistivity contrasts near the surface. Typically, the length of a survey line must be three to five times the desired depth of investigation (ASTM Standard D6429-99, 2011).

**Table 3.2** Median depth of investigation based on different electrode configurations (Loke, 1999)

Electrode Configuration	n	$Z_e/a$	$Z_e/L$
Wenner-alpha		0.519	0.173
Wenner-beta		0.416	0.139
Wenner-gamma		0.598	0.198
Dipole-dipole	1	0.416	0.139
	2	0.697	0.174
	3	0.962	0.192
	4	1.220	0.203
	5	1.476	0.211
	6	1.730	0.216
Wenner-Schlumberger	1	0.519	0.173
	2	0.925	0.186
	3	1.318	0.189
	4	1.706	0.190
	5	2.093	0.190
	6	2.178	0.191
Pole-dipole	1	0.519	
	2	0.925	
	3	1.318	
	4	1.706	
	5	2.093	
	6	2.478	
Pole-pole		0.867	

### Determination of Electrode Spacing

Generally, the length of the profile, the desired depth of penetration, and the required resolution determine the electrode spacing (Griffiths and Barker, 1993). Therefore, the electrode spacing could be determined using the desired depth of penetration and median depth (Table 3.2). For example, assume that the desired depth of penetration is 30 ft, and the Wenner-alpha configuration is selected for a survey. Based on Table 3.2, the length of the profile would be  $30 \text{ ft.}/0.173$  or 174 ft. Typically, a constant electrode spacing is considered between the adjacent electrodes (Loke, 1999), as shown in Figure 3.19. Therefore, if 56-electrodes' system is used, the electrode spacing would be  $174/55 \text{ ft.}$  or 3 ft. (the answer should be rounded to the nearest feet to be practical). The spacing between the electrodes can be relatively large for investigating deep depth with less detailed data and small when more detailed data in shallower depth is needed (ASTM Standard D6431-18, 2018). For example, the electrode spacings employed in the landslide studies can range from 16 to 130 ft. (5 to 40 m). However, for the study of buried cavities and karst features, narrower electrode spacings in the range of 1 to 16 ft. (0.5 to 5 m) have been utilized. The electrode spacing should not exceed twice the size of the anomaly or feature to be investigated. Otherwise, the method is unable to detect the subsurface anomaly (Hossain et al., 2018).



**Figure 3.19** Equally spaced electrodes

### Coverage Consideration

Orientation and offset of the survey lines, as well as the electrode spacings, play a vital role in achieving reliable and accurate results, especially to investigate the subsurface voids and bedrock

fractures (Roth and Nyquist, 2003). Therefore, several surveys with different orientations could be performed to avoid misleading interpretations of the result. The planner must consider the orientation and offset of survey lines regarding the type of anomaly to be investigated. For instance, several surveys can be performed in equally spaced parallel lines to determine the extent of a subsurface anomaly (e.g., extent of an underground void).

### 3.3.3. Field Survey Implementation

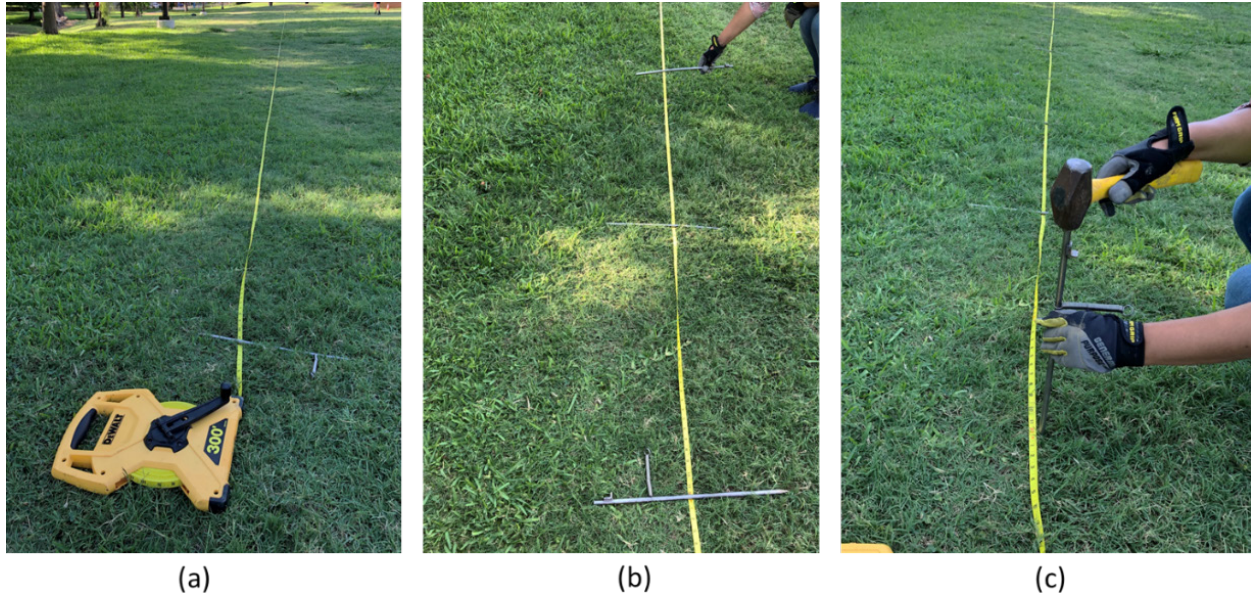
In this section, instructions for laying out the survey line, performing preliminary tests, measuring the earth resistivity, and common mistakes that operators may encounter in the field implementation are presented.

#### Layout of the Survey Line

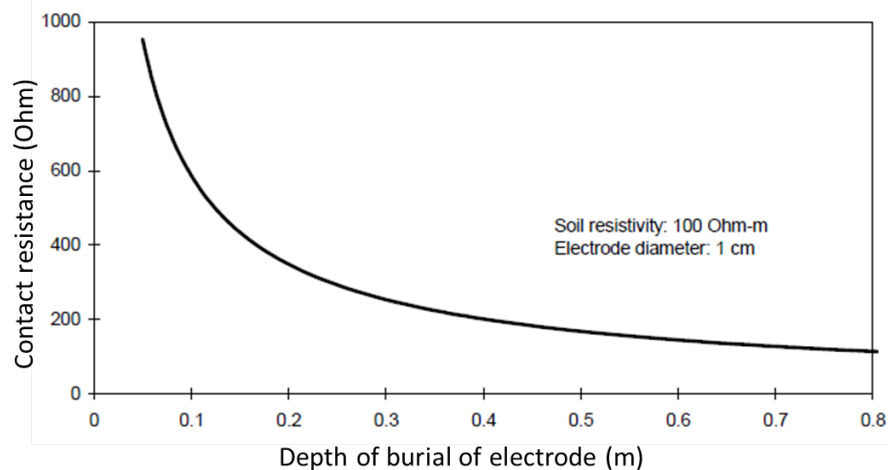
Generally, field electrical resistivity surveys are carried out using multiple electrodes (e.g., 28, 56, 64, 84, and 112 electrodes for AGI systems). The proper placement of electrodes (especially the current electrodes) into the ground is essential in an electrical resistivity survey to eliminate low or erratic current measurement and noise (ASTM Standard D6431-18, 2018; ABEM Instrument, 2010). First, a tape measure is laid out, and the whole length of the survey and electrode locations are specified. Second, a specific number of electrodes are laid out on the ground along a straight line with the known spacing depending on the survey requirements (i.e., the desired depth of investigation, required resolution, and size of an anomaly to be investigated). The number of electrodes should be adjusted with the number of cable take-outs. Any deviation from the straight line leads to noisy readings. Third, the electrodes are driven into the ground using a hammer (e.g., polyurethane covered hammer) without damaging the electrodes. Figure 3.20 illustrates the steps to locate and drive the electrodes into the ground. In practice, the depth of burial of electrodes should be about 4 to 8 in (10 to 20 cm) to eliminate the problem of contact resistance (Advanced Geoscience Inc., 2011). Figure 3.21 shows the theoretical relation between the depth of burial of electrode and contact resistance. Theoretically, the ideal depth of burial of the electrodes into the ground is about 8 to 12 in (20 to 30 cm) (ABEM Instrument, 2010). In dry soils, the minimum depth of burial of electrodes may have to be more than 20 inches (50 cm) (Milsom, 2003). In saturated soils, the ability of soil to hold the electrode upright determines the depth of burial of electrode (the contact resistance in saturated soils is negligible). In shallow surveys with small electrode spacing, the electrodes should not be driven deep into the ground (the burial depth should



not exceed 5% of the electrode spacing) to avoid any changes in the subsurface geometry (Advanced Geoscience Inc., 2011). The stickup depth of electrodes does not have any effect on the electrical resistivity imaging results.



**Figure 3.20** (a) determining the length of the whole survey using a tape measure, (b) laying down the electrodes in specific spacings, and (c) driving the electrodes into the ground using a hammer



**Figure 3.21** Theoretical relation between the depth of burial of electrode and contact resistance (ABEM Instrument, 2010)

After setting up all the electrodes, the cable section(s) needs to be connected to the electrodes. The operator should attach the first take-out at the free cable end to the first electrode in line and continue until all cable take-outs are connected to the electrodes. The cable take-outs are usually

attached to the electrodes by stainless-steel springs or crocodile clips. Figure 3.22 shows the attachment of a cable to an electrode using stainless-steel springs and an example of the appropriate connection of a cable take-out to an electrode. By attaching the cable take-outs to the electrodes, each electrode will be assigned to a unique number in the system used by the resistivity meter to control the measurement process. Therefore, it is crucial to attach the cable take-outs to the electrodes in the correct order. Then, the cables are linked to a switching unit, which is connected to the resistivity meter. It is preferred to place the resistivity meter in the middle of the electrodes (between the two cable sections) to minimize the voltage drop (Advanced Geoscience Inc., 2011). A proper connection of a resistivity meter to an external battery, a switching system, and a laptop is shown in Figure 3.23.



**Figure 3.22** (a) attachment of a cable to an electrode using a stainless-steel spring and (b) the appropriate connection of a cable take-out to an electrode



**Figure 3.23** Proper connection of resistivity meter to an external battery, a switching system, and a laptop

## **Preliminary Tests**

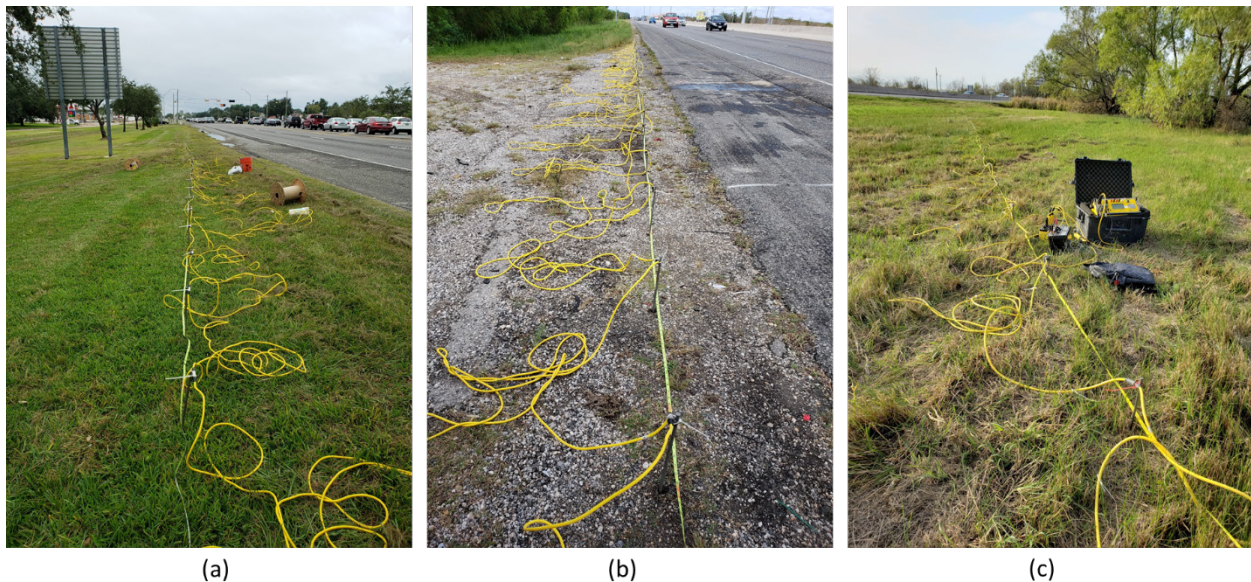
It is always worthwhile to perform preliminary measurements after placing the electrodes to check for electrical current leakage, missing connections, and contact resistance before conducting the actual survey. The resistivity meters automatically perform the contact resistance testing; the resistivity meter measures the contact resistance for each pair of electrodes (e.g., electrodes 1 and 2, electrodes 2 and 3, electrodes 3 and 4, and so on) and shows the value on its screen. Accurate electrical resistivity measurements will be obtained if the threshold value for the contact resistance sets to 2000 ohm (ideally 1800 ohm) (Allied Associates LTD., 2019; Advanced Geoscience Inc.). The operator uses the contact resistance values to detect the electrodes that have loose connections with the ground. For example, if the contact resistance values for electrodes 2 and 3 and electrodes 3 and 4 are above the threshold value, but the contact resistance values for electrodes 1 and 2 and electrodes 4 and 5 are below the threshold value, it is concluded that the third electrode should be inspected to improve its contact with the ground. The ground contact could be improved by pushing the electrodes deeper into the ground or wetting the soil around the electrodes. The contact resistance test could be performed once again to ensure that the electrode contact has been improved. The contact resistance test will be stopped, and an error message will be shown on the screen if an electrode pair is improperly attached to cable take-outs or too loosely placed into the ground (minute vibrations from traffic or wind might also change the contact condition) (Advanced Geoscience Inc., 2011).

## **Measurement Procedure**

The electrical resistivity measurement process can be performed either manually with four cables and electrodes (one reading per current injection) or automatically with multi-electrode cable and multiple electrodes (simultaneous readings per current injection). There are many electrodes that can be used in the automatic mode (e.g., typically 28 to 224 electrodes for the AGI system). During the measurement process, the resistivity meter must be connected to an external battery.

The resistivity meter needs at least one command file to perform the electrical resistivity measurements. The command files, that control the resistivity meter on how to conduct the measurements, are created before the field survey. The inputs to the command files are survey parameters, such as the number of electrodes, electrode configuration, electrode spacing, and desired depth of penetration. The resistivity meters have different formats and settings to create

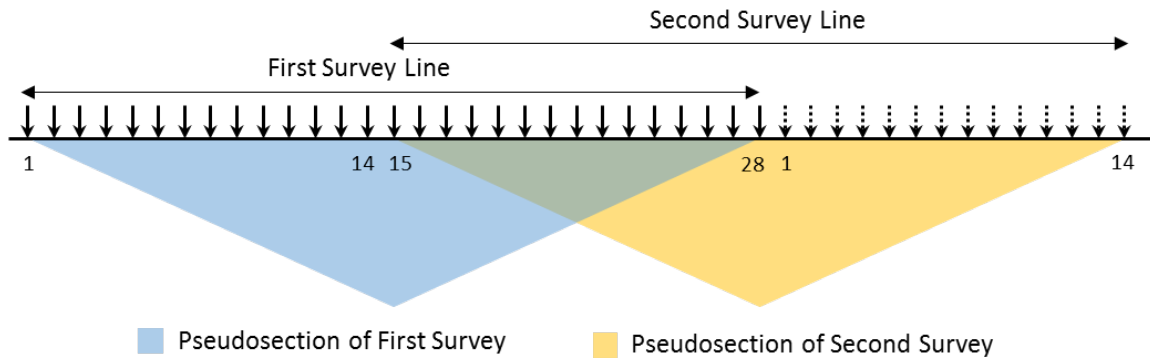
and control the command file. These formats and settings are explained in detail in their user manuals. The sequence of measurements and expected duration of the survey can be simulated using the command file before the field survey. These files will be stored in the resistivity meter RAM. Using the command file, the resistivity meter will automatically select different combinations of current and potential electrodes for each measurement and read the measurements (Advanced Geoscience Inc., 2011). Therefore, the resistivity meter stores the readings in a data file that is readable by a program on the computer. The data files are used for generating the electrical resistivity images of the subsurface (Advanced Geoscience Inc., 2011). The number of measurements, which depends on the type of array, decreases as the electrode spacing increases (Loke, 1999). A general layout of the 2D electrical resistivity imaging survey line is illustrated in Figure 3.24.



**Figure 3.24** (a), (b), and (c) general layout of the 2D electrical resistivity imaging survey line

When the survey line is longer than the available electrode spread, a roll-along system might extend the coverage of the survey. In this method, after completing the initial measurements, if the electrode cable is divided into sections and each cable section has connectors at each end, the extension is achieved by detaching the first cable section of the electrodes and moving it to the end of the cable system. An example of a measurement sequence of a roll-along survey using two cable sections with 28 electrodes is illustrated in Figure 3.25. In Figure 3.25, after the first electrical resistivity measurements using cable sections of 1-14 and 15-28, the cable section of 1-14 is moved to the right side of the cable section of 15-28. Then, the measurement procedure is repeated. The

two triangular sections in Figure 3.25 illustrate the generated pseudo-section of each measurement. Then, the repeated measurements (overlap of the two triangles) can be disregarded. The data for each roll is recorded and combined with the other surveys to obtain a complete data set (Advanced Geoscience Inc., 2011; Loke, 1999).



**Figure 3.25** An example of a measurement sequence of a roll-along survey using two cable sections for a survey with 28 electrodes

The electrical resistivity imaging method has some limitations:

- The horizontal variations in resistivity are not considered in a 2D electrical resistivity data processing. Therefore, it would lead to misleading interpretations if only a single line is surveyed, especially to investigate the subsurface voids and bedrock fractures (Wightman et al., 2004). Therefore, the survey planner must consider the orientations and offsets of survey lines regarding the type of anomaly to be investigated.
- Cultural interferences (i.e., manmade obstruction) originated from electric conductors in the ground such as metal pipes, utilities, or fences in the vicinity of survey line could influence the electrical resistivity measurements and lead to inaccurate results (ASTM Standard D6429-99, 2011; Wightman et al., 2004). Therefore, the survey planner must locate the survey line far away from any sources of electric or electromagnetic fields as possible.
- The practical depth of investigation depends on the elevation of the groundwater table, meaning that the subsurface layers are hard to be differentiated because the electrical resistivity of materials has very low values in saturated materials (Hunt, 2005).

- The thin subsurface layers with relatively similar electrical resistivity values are hard to be detected (ASTM Standard D6431-18, 2018).
- It is unlikely to investigate the anomalies which are embedded deep in the ground (i.e., more than 30 ft.), because not only the resolution of results decreases exponentially through the depth but also it requires a long survey line which sometimes makes it difficult to find sufficient accessible space for the implementation (ASTM Standard D6429-99, 2011; Loke, 2004).
- The electric current is poorly transmitted through highly resistive materials. So, an alternative method (i.e., Electromagnetic method) could be used in such conditions (ASTM Standard D6431-18, 2018).
- The software programs could produce different models based on a set of data meaning that the electrical resistivity imaging method provides non-unique result, like all other geophysical methods. Therefore, a complete assessment of subsurface conditions will be accomplished if the geotechnical data are combined with the electrical resistivity results (ASTM Standard D6431-18, 2018).

### **3.4. Survey Considerations**

In this section, the practical considerations regarding different operational environments and weather conditions are discussed to eliminate noisy readings and prevent equipment failure. Some safety precautions are also presented to maintain a safe workplace.

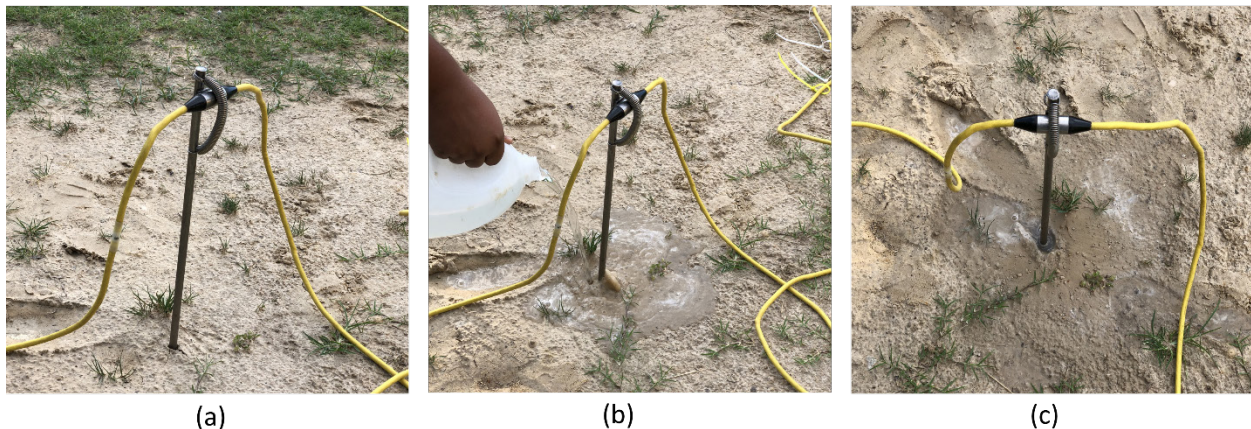
#### **3.5.1. Operational Environments**

Extreme ground conditions and various sources of natural/cultural (manmade) noise can generate noisy readings that lead to misinterpretation of the results.

#### **Ground Conditions**

The high resistance ground materials, such as dry and frozen soils, impede the proper connection for transferring the current through the electrodes and cause polarization problems at the receiving electrodes (ASTM Standard D6431-18, 2018; ABEM Instrument, 2010; Loke, 2004). Typically, in the case of dry soils, the soil around the electrodes is wetted using water/saltwater to decrease the contact resistance and provide a good connection to the electrodes. Then the contact resistance test could be performed to make sure that the electrode contact has been improved (refer to Section

2.5.2). Figure 3.26 illustrates how to wet the soil around the electrodes to reduce the contact resistance. Care must be taken to avoid wetting the connection between the electrodes and cable take-outs (if so, they should be cleaned using dry compressed air). It is necessary to wait for a while after wetting the ground to allow the electrodes to adapt to the wetted soil environment (ASTM Standard D6431-18, 2018; Advanced Geoscience Inc., 2011). In the case of permeable soils, some mixing materials, such as bentonite, polymer, or starch compounds, are added to the water to decrease the infiltration rate and keep the water in place for a longer time (ABEM Instrument, 2010; Reynolds, 1997). In stony surface, water/saltwater saturated sponges are utilized between rocks and electrodes to provide appropriate ground contact (Kneisel, 2006; Sass, 2006a). Three or more electrodes also can be used in one end of the cable in parallel to reduce the problem of high contact resistance so that the total resistance of multiple electrodes becomes less than the resistance of one electrode (ABEM Instrument, 2010; Reynolds, 1997). If the survey site is covered with resistive materials (i.e., concrete or asphalt), the surface needs to be drilled at the electrode locations. Then the electrodes are driven into the ground.



**Figure 3.26** (a), (b), and (c) the soil around the electrode is wetted to reduce the contact resistance

### Sources of Natural and Cultural Noises

Various sources of natural (e.g., lightning or natural earth currents) and cultural (e.g., buried utilities, radio stations, or cathodic pipeline protection) noise could short circuit the measured current or induce a voltage in electrical resistivity cables that result in inaccurate measurements (ASTM Standard D6431-18, 2018). These problems can be mitigated by avoiding large electrode spacings and long cables, as well as increasing the signal strength to improve the signal to noise

ratio (Milsom, 2003). The Wenner array can be an appropriate choice for performing the electrical resistivity imaging survey in a noisy area (Loke, 2004).

### **3.5.2. Weather Conditions**

Instructions for addressing unusual and unexpected weather conditions in the fieldwork are provided in the following paragraphs.

#### **Rain**

Exposing the resistivity meter and connectors to water causes electrical leakage between the current and potential lines and leads to inaccurate data. Although the electrical resistivity equipment and electrodes are waterproof, they should not be exposed to rain for long periods. It is also recommended to wait for about one day after heavy rains to avoid creating noisy images of subsurface characteristics (ABEM Instrument, 2010; Advanced Geoscience Inc., 2011).

#### **Hot Weather**

Placing the resistivity meter in an ambient temperature of above 100° F (+40° C) causes a break down in the insulation performance of plastic materials and leads to electrical leakage problems. The situation is aggravated when the device is utilized at full power. Therefore, it is necessary to lower the device temperature by 18 to 27° F (10 to 15° C). It is recommended to keep the device as cool as possible by placing it in the shade from direct sun, in camping coolers, or on the cooling mats during the survey (ABEM Instrument, 2010; Advanced Geoscience Inc., 2011).

#### **Cold Weather**

Cold weather condition does not affect the electrical resistivity results. The electrodes work correctly in temperatures down to -4° F (-20° C). The only difficulty is that the resistivity meter display works slowly or might stop working in temperatures below 32° F (0° C). It is recommended to keep the resistivity meter warm while using it in extremely cold weather (Advanced Geoscience Inc., 2011).

#### **Thunderstorms**

Thunderstorms could damage the equipment. It is also dangerous for the operators to work in the field in this scenario. It is recommended to immediately stop working in case of hearing the thunder



or observing lightning in the distance and disconnect all the cables, and pick up the equipment (Advanced Geoscience Inc., 2011; ABEM Instrument, 2010).

### **3.5.3. Safety Hazards and Precautions**

Some safety instructions are presented here to be followed to avoid injury or damage to the equipment. However, these instructions do not guarantee the absence of any risks (IRIS Instruments, 2018; ASTM Standard D6431-18, 2018; Advanced Geoscience Inc., 2011; ABEM Instrument, 2010).

- The electrical resistivity equipment should be operated by trained operators.
- The operators who work in the field should wear electric insulating gloves and boots during the survey.
- The cables should be inspected before the field survey and be replaced in the case of damaged isolation or exposed wiring.
- The electrical resistivity survey line is a tripping hazard and should be protected using safety cones and/or warning tapes.
- The resistivity meter should be placed on a flat surface (to avoid falling) and must have good ventilation (to avoid overheating).
- The personnel should be informed when the equipment is operating. They should monitor the equipment to keep the personnel or animals away from the equipment.
- The personnel should stay at least 3 ft. (1 m) away from the electrodes and cables while the equipment is operating in damp environments because of the high risk of electrical leakage.
- The electrical resistivity imaging survey should not be conducted in the case of hearing thunder or observing lightning in the distance.
- The cables should not be left overnight because a thunderstorm may occur unless adequate lightning protection is used.
- The electrical current source should be physically disconnected from the other equipment before and after the measurement procedure.
- The resistivity meter should be shut down before attempting to fix the electrodes or connections that are loosely placed or attached during the preliminary tests.

- The resistivity meter should not be powered with a vehicle battery while it is still within or connected to the vehicle.
- A right voltage source should be connected to the resistivity meter to avoid irreversible damages to the device.
- The batteries should be stored at an ambient temperature of  $-40^{\circ}$  to  $149^{\circ}\text{F}$  ( $-40^{\circ}$  to  $+65^{\circ}\text{C}$ ) and disconnected from all the instruments.
- The connectors must be kept clean and dry to avoid noisy readings and irreversible damages to the connectors.

### **3.5. Common Mistakes in Implementation**

In this section, common mistakes in the implementation of electrical resistivity imaging surveys are described. It is essential to keep them in mind to avoid mistakes and perform a successful survey.

#### **3.6.1. Use of Untrained Operators**

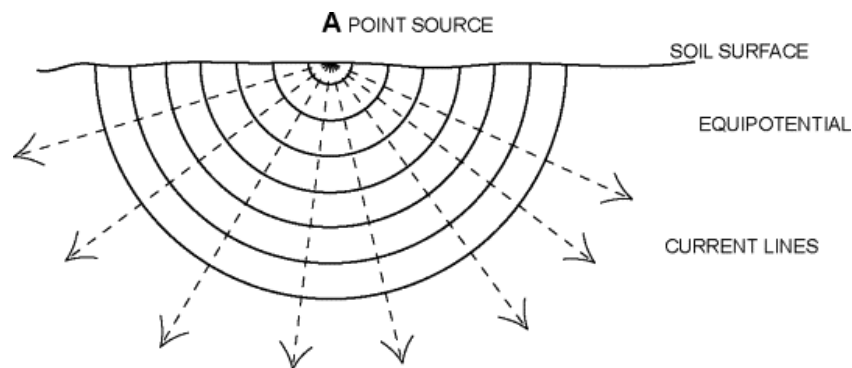
The competence of the operators is critical to ensure that the survey will be successfully implemented. The operators must be educated about the basic principle of the method, field procedures, methods to interpret the resistivity data, and site geology. Besides, the operators should be trained to work with the resistivity meter. Implementing the survey with unqualified operators may result in inaccurate measurements and delay in the survey schedule.

#### **3.6.2. Inappropriate Selection of Electrode Configuration**

The electrode configuration should be selected carefully based on the guidelines presented in Section 3.3.2. to ensure the quality of the results regarding the purpose of the survey. For example, the dipole-dipole array could be the most appropriate electrode configuration in investigating a vertical structure. On the other hand, the Wenner array could be the most appropriate electrode configuration for investigating a horizontal structure with high background noise. Inappropriate selection of electrode configuration leads to unreliable results and misleading interpretation of the subsurface condition.

### 3.6.3. Deeply Buried Electrodes

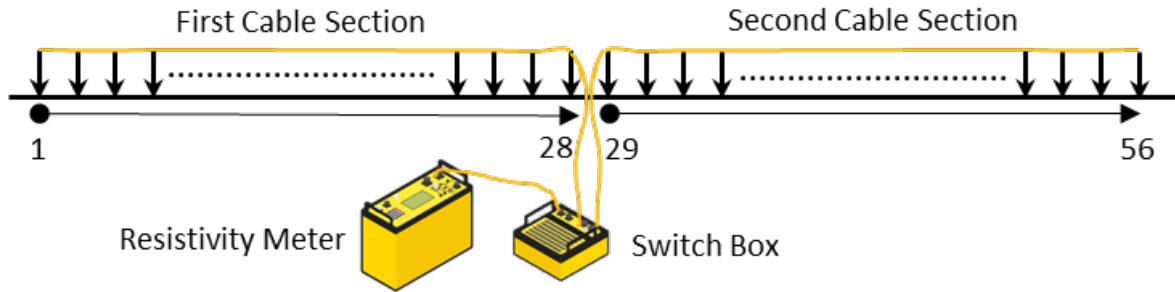
The electrical resistivity imaging method assumes that the current flow is transmitted into the ground through the point sources (i.e., electrodes in the field condition). This assumption will remain valid when the electrodes are not buried deep into the ground. Therefore, the operator needs to consider it to limit the driven depth of electrodes to the recommended ranges presented in Section 3.3.3. Figure 3.27 shows the distribution of current flow from a point source in a homogeneous soil.



**Figure 3.27** Distribution of current flow from a point source in a homogeneous soil (Samouëlian et al., 2005)

### 3.6.4. Incorrect Order of Attached Cable Sections

The cable sections should be attached to the electrodes in the correct order while using more than one cable section so that the cable take-outs are numbered consecutively. Besides, none of the electrodes should remain unconnected. In some cases, the cable sections might be attached in the incorrect order, or an electrode remains unconnected. For instance, if two 28-electrode cable sections are used (i.e., each having 28 electrode take-outs) in a survey with 56 electrodes, the first section will be attached to the first 28 electrodes in the survey line (from the first to 28<sup>th</sup> electrode) and the second section will be attached to the next 28 electrodes in the survey line (from 29<sup>th</sup> to 56<sup>th</sup> electrodes). Figure 3.28 illustrates the correct order of the cable section's connections. Therefore, the order of cable sections must be taken into consideration while using more than one cable section. The electrode numbers could be written beside the electrodes to ensure that each electrode is attached to the cables by matching numbers.



**Figure 3.28** Correct order of cable section's connections for 56 electrodes with two 28-electrode cable sections

### 3.6.5. Unconnected Cable Take-out In Between

The cable take-outs should be attached to the electrodes without leaving none of them unconnected. The operator must also ensure that the metallic parts of the cable and electrode are connected to provide a good connection and avoid reading noisy data. It is common for a new operator to miss a few of the cable connections in between and continue attaching the remaining take-outs. However, it should be corrected before performing the measurements. Therefore, the operator should consider it while attaching the cable to the electrodes to avoid the mistake that causes delays in the survey schedule.

### 3.6.6. Ignorance of High Contact Resistance

By lowering the contact resistance, more current will be transmitted into the ground (i.e., it improves the signal to noise ratio), which leads to measuring less noisy data. The contact resistance could be checked before the actual survey (refer to Section 3.3.3.) to ensure that the contact resistance values are reasonably low and even from an electrode pair to the other. The noisy reading will be obtained if the data are measured, ignoring the high contact resistance. Therefore, the contact resistance needs to be checked and lowered as much as possible before the actual survey is conducted.

### 3.6.7. Insufficient Battery Charge

The external batteries are needed to be fully charged before going to the field. Besides, the operator needs to ensure that the batteries are in good condition by performing regular checks (for more specifications on the type of external batteries, refer to Section 3.3.1.). If the batteries run out of charge in the field, it will cause delays in the survey implementation.

## CHAPTER 4 DATA COLLECTION IN TXDOT DISTRICTS

### 4.1. Introduction

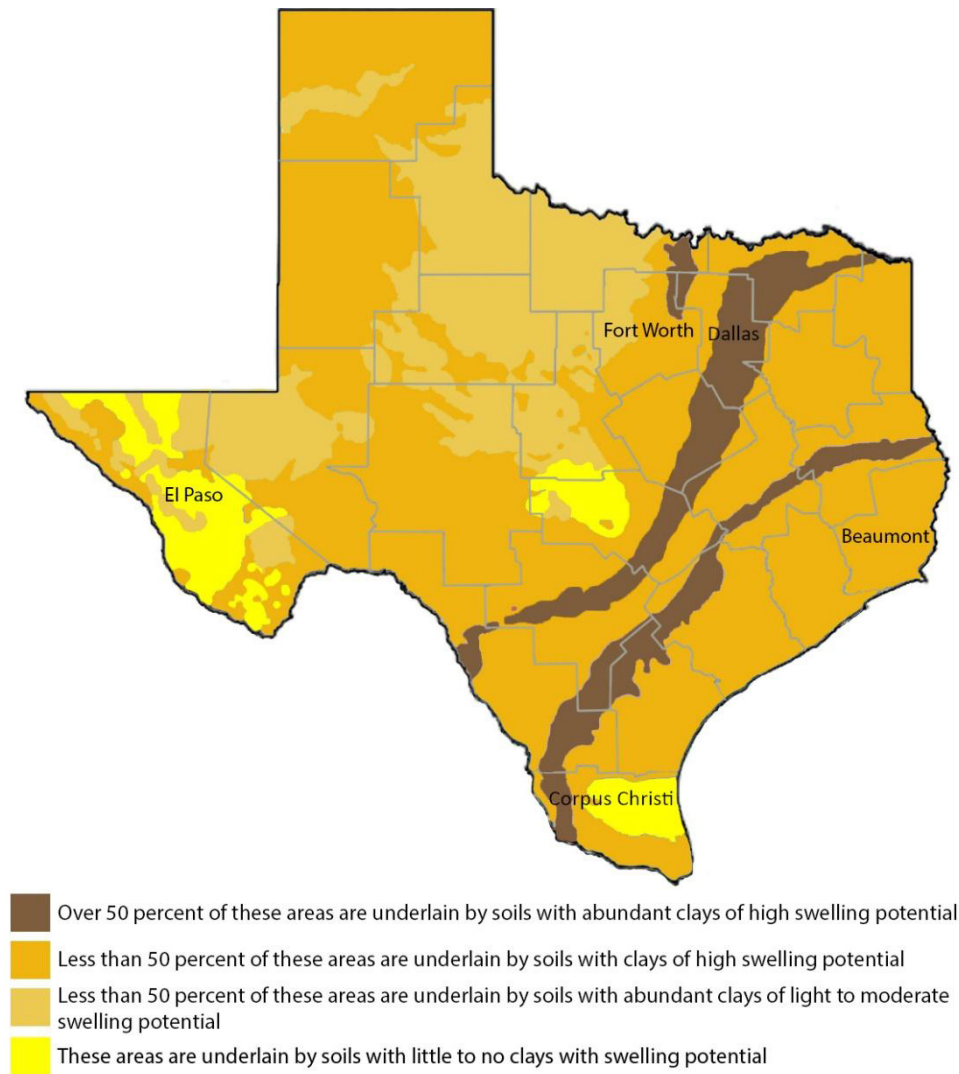
In collaboration with the TxDOT advisory committee appointed to this research project, a list of five districts was selected to demonstrate electrical resistivity imaging surveys and collect soil samples to investigate the relationship between the geoelectrical and geotechnical properties. In this chapter, the selection criteria of the TxDOT districts, the laboratory and field data collection procedures are elaborated.

### 4.2. Selection Criteria of TxDOT Districts

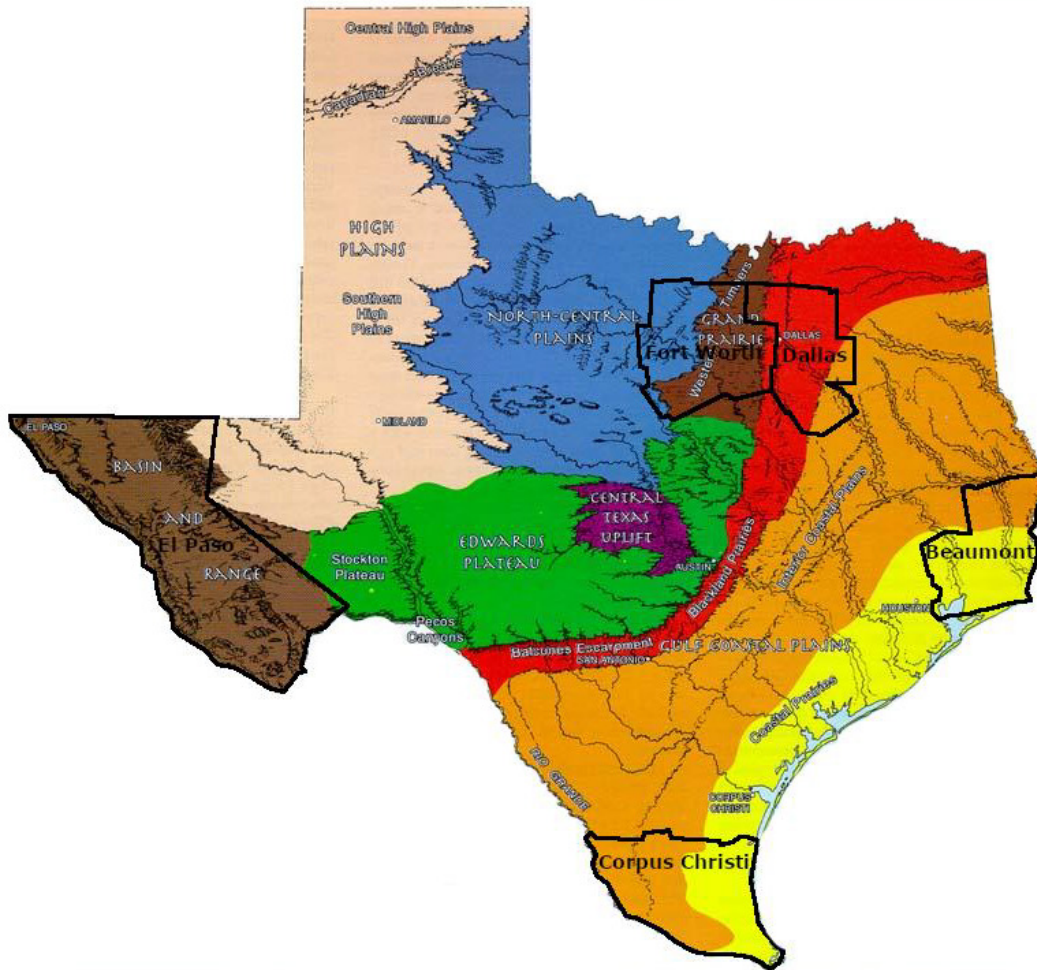
Five districts located at the East, West, South, and North of Texas (Beaumont, Corpus Christi, Fort Worth, Dallas, and El Paso) were selected to be the focus of this research project representing various TxDOT operational environments and geotechnical conditions. The criteria for selection of these districts include but not limited to:

- diverse geotechnical characteristics (e.g., soil type, topography, etc.)
- various levels of rainfalls or frequent wetting and drying cycles
- limited experience in using the advanced geophysical tools
- having the most recent projects, which included subsurface investigation (especially those that have problems with the subsurface investigation)

Figure 4.1, 4.2, and 4.3 illustrates the expansive clay soil map, physiographic map, and average annual precipitation map of Texas, respectively, along with the location of the selected TxDOT districts.

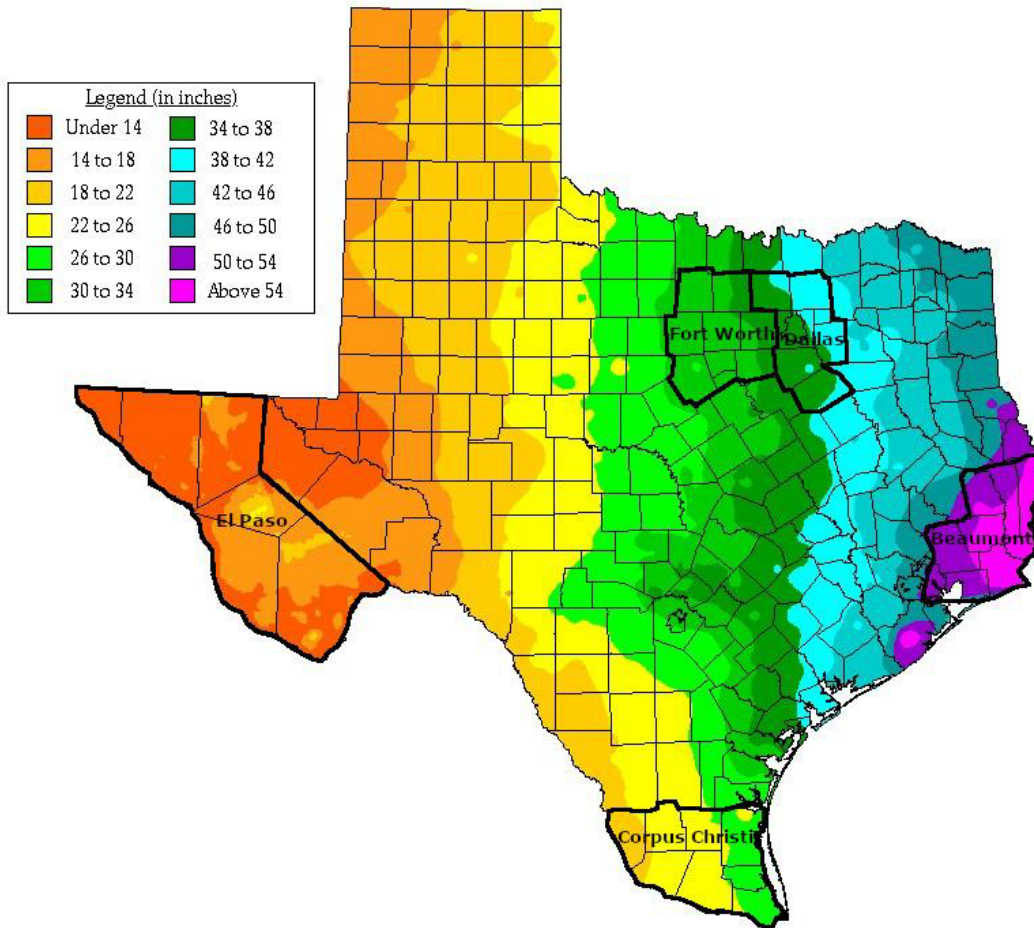


**Figure 4.1** Expansive clay soil map of Texas (Adapted from Olive et al., 1989)



PROVINCE	MAX. ELEV. (ft)	MIN. ELEV. (ft)	TOPOGRAPHY	GEOLOGIC STRUCTURE	BEDROCK TYPES
<b>Gulf Coastal Plains</b>					
Coastal Prairies	300	0	Nearly flat prairie, <1 ft/mi to Gulf	Nearly flat strata	Deltaic sands and muds
Interior Coastal Plains	800	300	Parallel ridges (questas) and valleys	Beds tilted toward Gulf	Unconsolidated sands and muds
Blackland Prairies	1000	450	Low rolling terrain	Beds tilted south and east	Chalks and marls
Grand Prairie	1250	450	Low stairstep hills west; plains east	Strata dip east	Calcareous east; sandy west
<b>Edwards Plateau</b>					
Principal	3000	450	Flat upper surface with box canyons	Beds dip south; normal faulted	Limestones and dolomites
Pecos Canyons	2000	1200	Steep-walled canyons		Limestones and dolomites
Stockton Plateau	4200	1700	Mesa-formed terrain; highs to west	Unfaulted, near-horizontal beds	Carbonates and alluvial sediments
Central Texas Uplift	2000	800	Knobby plain; surrounded by questas	Centripetal dips, strongly faulted	Granites; metamorphics; sediments
North-Central Plains	3000	900	Low north-south ridges (questas)	West dip; minor faults	Limestones; sandstones; shales
<b>High Plains</b>					
Central	4750	2900	Flat prairies slope east and south	Slight dips east and south	Eolian silts and fine sands
Canadian Breaks	3800	2350	Highly dissected; local solution valleys		
Southern	3800	2200	Flat; many playas; local dune fields		
Basin and Range	8750	1700	North-south mountains and basins	Some complex folding and faulting	Igneous; metamorphics; sediments

Figure 4.2 Physiographic map of Texas (Adapted from Bureau of Economic Geology, 1996)



**Figure 4.3** Average annual precipitation map of Texas (Adapted from PRISM Climate Group, 2019)

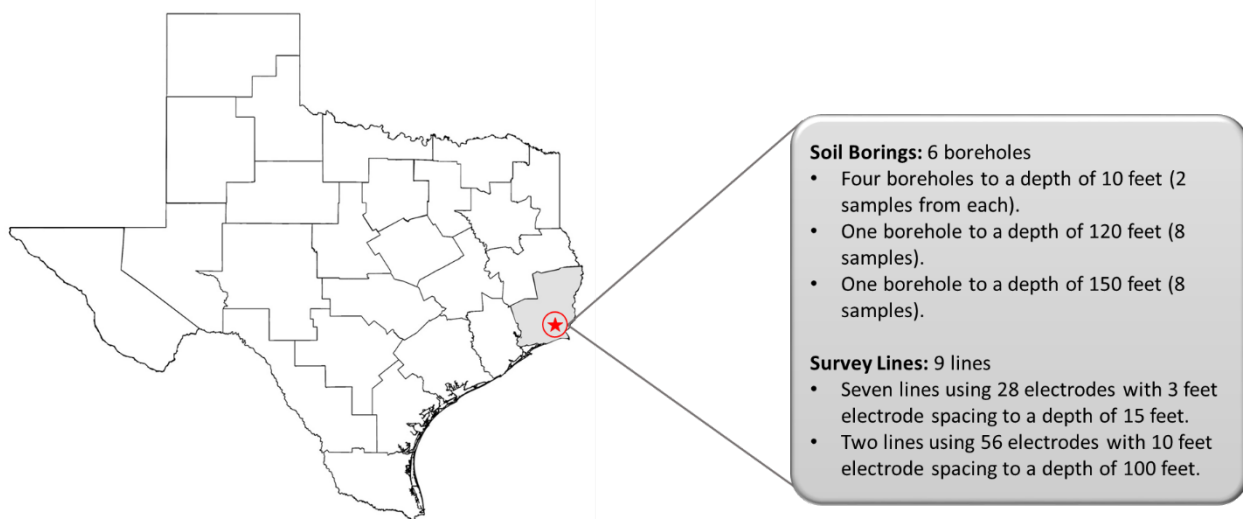
#### 4.3. Field Data Collection

In coordination with the receiving agency district contacts, several locations were finalized to implement and demonstrate the electrical resistivity imaging technique. In total, twenty-seven (27) electrical resistivity imaging surveys were performed and demonstrated to the TxDOT personnel in the proposed locations in the Beaumont, Corpus Christi, and Fort Worth districts. The minimum and maximum lengths of resistivity lines were about 78 ft. (advanced to a depth of 15 ft.) and 550 ft. (advanced to a depth of 60 ft.), respectively. The specification and instrumentation of each line are presented in the following paragraphs.



## Beaumont District

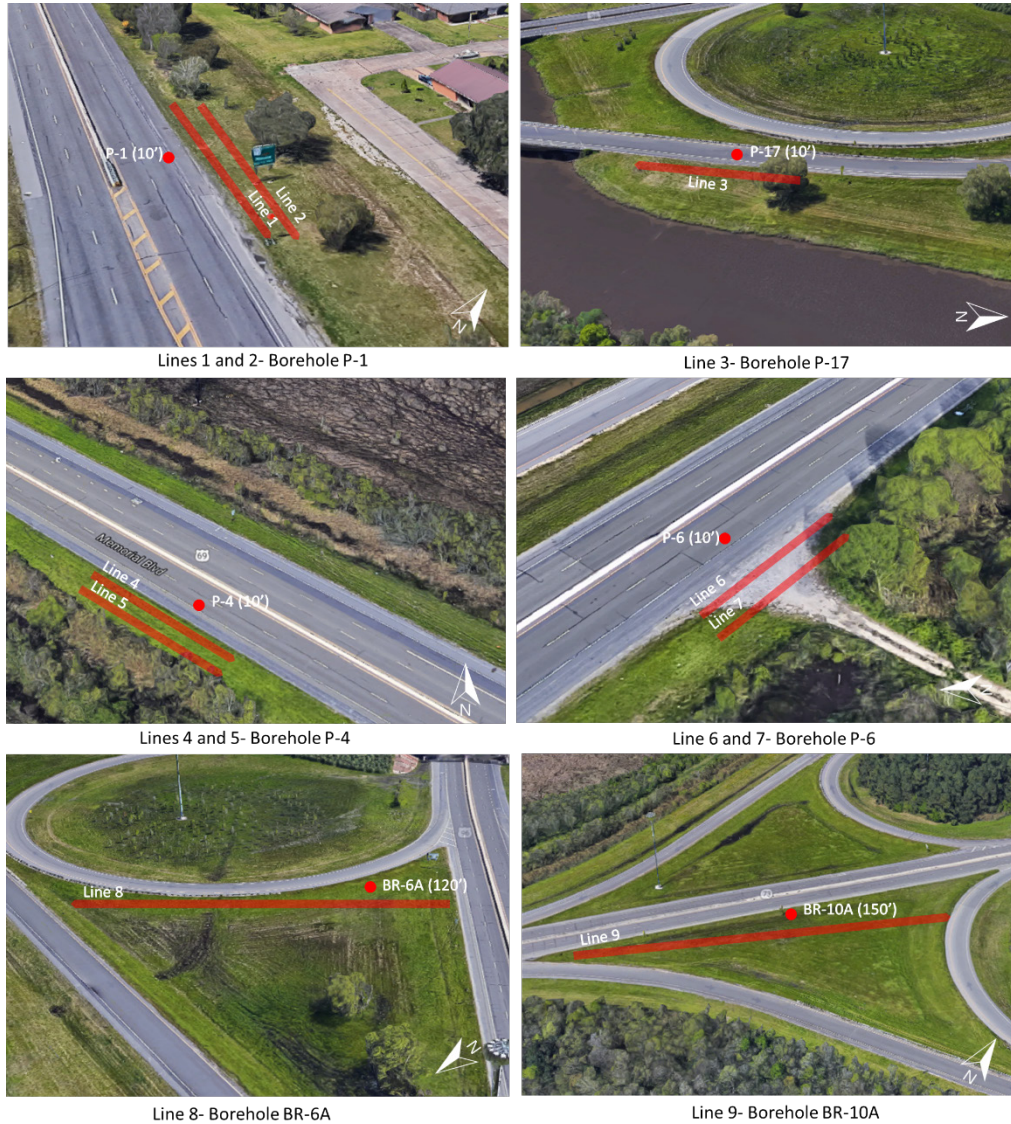
The proposed site for the subsurface geotechnical investigation was located along the roadside of “Highway US96-SH73” in the Beaumont district in Texas. The electrical resistivity survey was implemented in seven (7) and two (2) lines in October and December 2019, respectively. Figure 4.4 shows the location of the proposed site on the map, number of collected samples at each borehole, and the instrumentation of electrical resistivity surveys. Figure 4.5 shows the locations of boreholes along with the depth of borings. Figure 4.6 illustrates the approximate locations of resistivity lines with respect to the boreholes.



**Figure 4.4** Location of the proposed site on the map, number of collected samples at each borehole, and the instrumentation of electrical resistivity surveys in Beaumont district



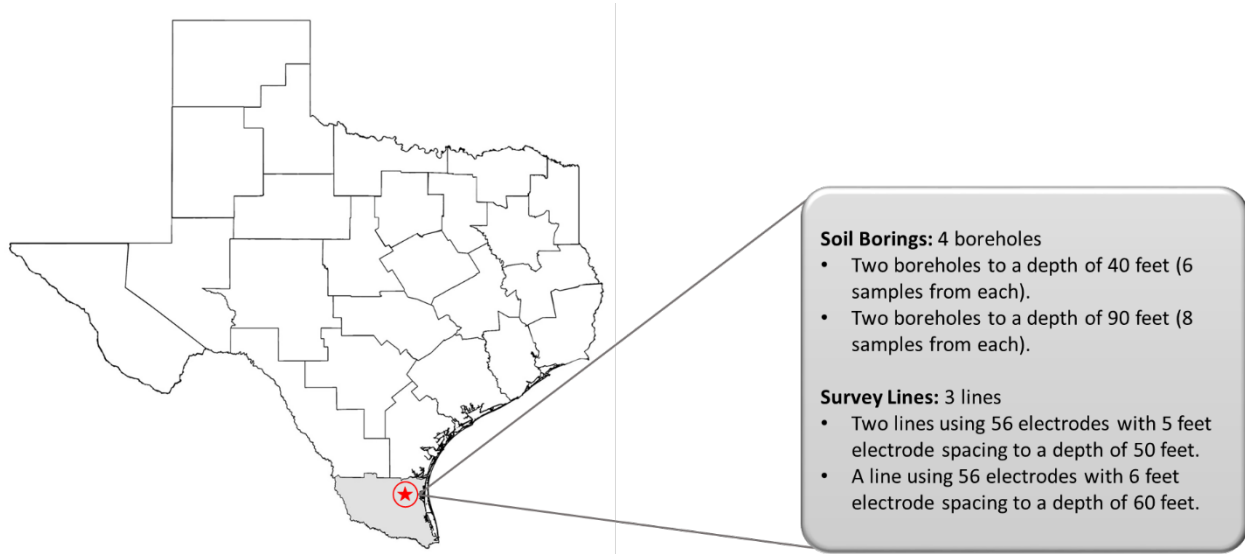
**Figure 4.5** Locations of the boreholes along with the depth of borings in Beaumont district



**Figure 4.6** Locations of electrical resistivity survey lines with respect to the boreholes in Beaumont district

### Corpus Christi District

The proposed site for the subsurface geotechnical investigation was located along the roadside of “Highway I37” in the Corpus Christi district in Texas. The electrical resistivity survey was implemented in three (3) lines in February 2020. Figure 4.7 shows the location of the proposed site on the map, number of collected samples at each borehole, and the instrumentation of electrical resistivity surveys. Figure 4.8 shows the approximate locations of resistivity lines with respect to the boreholes along with the depth of borings.



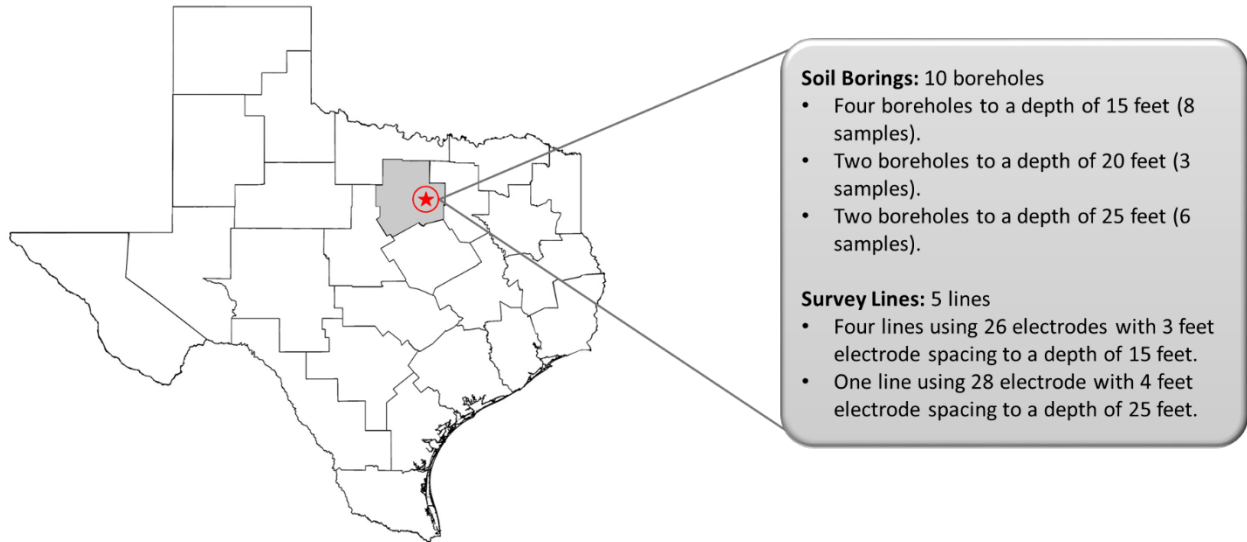
**Figure 4.7** Location of the proposed site on the map, number of collected samples at each borehole, and the instrumentation of electrical resistivity surveys in Corpus Christi district



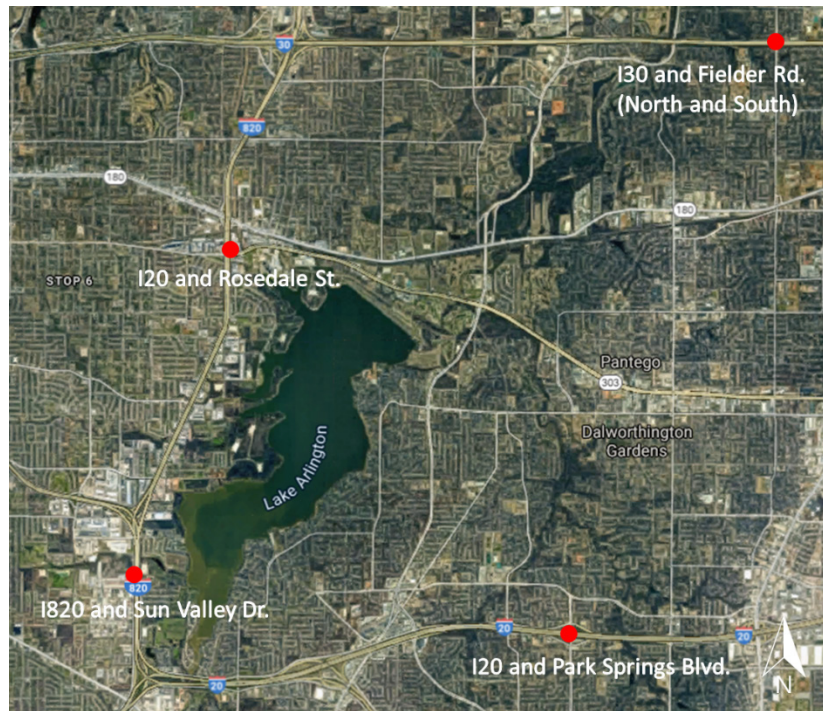
**Figure 4.8** Locations of resistivity lines with respect to the boreholes along with the depth of borings in Corpus Christi district

### Fort Worth District

The proposed sites for the subsurface geotechnical investigation were located at “Highway I30 and Fielder Rd.”, “I820 and Sun Valley Dr.”, “I20 and Park Springs Blvd.”, and “I820 and Rosedale St.” in the Fort Worth district in Texas. The electrical resistivity survey was implemented in six (6) lines in July 2019. Figure 4.9 shows the location of the proposed site on the map, number of collected samples at each borehole, and the instrumentation of electrical resistivity surveys. Figure 4.10 demonstrates the locations of the proposed sites on the map in the Fort Worth district. Figure 4.11 illustrates the approximate locations of resistivity lines with respect to the boreholes along with the depth of borings.



**Figure 4.9** Location of the proposed site on the map, number of collected samples at each borehole, and the instrumentation of electrical resistivity surveys in Fort Worth district



**Figure 4.10** Locations of the proposed sites on the map in the Fort Worth district








**Figure 4.11** Locations of resistivity lines with respect to the boreholes along with the depth of borings in Fort Worth district

#### 4.4. Laboratory Data Collection

The performing agency conducted laboratory testing to identify the influencing soil parameters on the electrical resistivity values and later develop equations and charts for the estimation of geotechnical parameters using the electrical resistivity values.

The performing agency collected 121 disturbed and undisturbed samples, in collaboration with the drilling companies, from thirty-six (36) drilled boreholes in the Beaumont, Corpus Christi, Dallas, El Paso, and Fort Worth districts. Table 4.1 summarizes the number of visited locations, drilled boreholes, collected samples, and the performed electrical resistivity imaging surveys in each district. The soil sampling was performed continuously throughout the borings. Tables 4.2 to 4.6 lists the number of samples per borehole and the depths at which samples were taken from the proposed sites in the selected districts (borehole logs are attached in the Appendix B). The minimum and maximum drilling depths were about 10 and 120 feet (in Beaumont), respectively.

**Table 4.1** Number of visited locations, drilled boreholes, collected samples, and the performed electrical resistivity imaging surveys

District	Data Collection
	<ul style="list-style-type: none"> <li>● One location at the intersection of US96 and SH73</li> <li>● Six boreholes</li> <li>● Thirty-four soil samples</li> <li>● Nine ERI surveys</li> </ul>
	<ul style="list-style-type: none"> <li>● One location along Highway I37</li> <li>● Four boreholes</li> <li>● Twenty soil samples</li> <li>● Three ERI surveys</li> </ul>
	<ul style="list-style-type: none"> <li>● Five different locations along Highway US80, US183, I35, and in the city of Irving</li> <li>● Six boreholes</li> <li>● Eleven soil samples</li> </ul>
	<ul style="list-style-type: none"> <li>● Seven different locations at Highway I30 and Fielder Road, I820 and Sun Valley Drive, I20 and Park Springs Boulevard, I820 and Rosedale Street, Highway I35 W and W Cotter Ave., and Highway US67 and W Henderson Street</li> <li>● Eighteen boreholes</li> <li>● Forty-one soil samples</li> <li>● Fifteen ERI surveys</li> </ul>
	<ul style="list-style-type: none"> <li>● One location along Wyoming Ave. (eastbound)</li> <li>● Two boreholes</li> <li>● Fourteen soil samples</li> </ul>

**Table 4.2** Number of boreholes and depths of sampling - Beaumont district

Borehole No.	Depth of Sampling (ft)
P-1	5 and 8
P-4	5 and 8
P-6	5 and 8
P-17	5 and 8
BR-6A	5, 20, 30, 40, 50, 60, 70, and 80
BR-10A	5, 20, 30, 40, 50, 60, 70, and 80

**Table 4.3** Number of boreholes and depths of sampling - Corpus Christi district

Borehole No.	Depth of Sampling (ft)
BR-201	5, 8, 14, 18, 28, 38, 52, and 60
BR-202	5, 10, 13, 17, 30, 40, 50, and 60
RW-214	5, 10, 15, 20, 30, and 39
RW-215	5, 10, 15, 22, 30, and 40

**Table 4.4** Number of boreholes and depths of sampling - Dallas district

Borehole No.	Depth of Sampling (ft)
BH-1 (Irving-1)	80
BH-1 (Irving-2)	15
BH-1 (US80)	5
BH-2 (US80)	10
BH-1 (US183)	10
BH-1 (I35)	10

**Table 4.5** Number of boreholes and depths of sampling - El Paso district

Borehole No.	Depth of Sampling (ft)
BH-2	5, 10, 15, 20, 30, 40, and 50
BH-4	5, 10, 15, 20, 30, 40, and 50

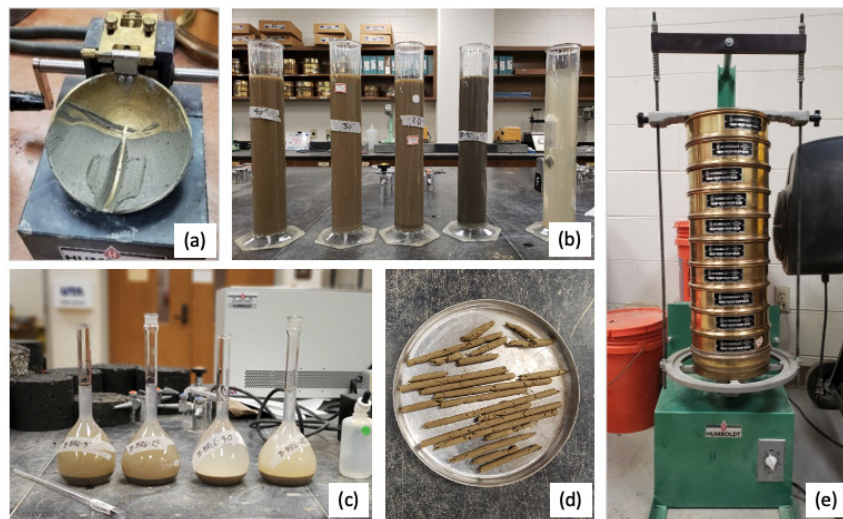
**Table 4.6** Number of boreholes and depths of sampling - Fort Worth district

Borehole No.	Depth of Sampling (ft)
BH-1 (FN)	7 and 13
BH-2 (FN)	6, 7, and 12
BH-1 (FS)	7, 11, and 13
BH-1 (SV)	6, 12, 17, and 24
BH-2 (SV)	10 and 20
BH-2 (PS)	6, 8, and 13
BH-1 (RD)	7, 9, 12, and 17
BH-1 (US67-1)	5, and 10
BH-2 (US67-1)	5, 10, and 15
BH-3 (US67-1)	5, 10, 15, 20, and 25
BH-4 (US67-1)	5, and 10
BH-1 (US67-2)	5, 10, 15, and 20
BH-2 (US67-2)	5, 10, and 15
BH-1 (I35W)	5, 10, 15, 20, and 25
BH-2 (I35W)	5, 10, 15, 20, and 25

Note: (FN) I30 and Fielder Rd. (North), (FS) I30 and Fielder Rd. (South), (SV) I820 and Sun Valley Dr., (PS) I20 and Park Springs Blvd., (RD) I820 and Rosedale St., (US67-1) US67 and W Henderson Street (South), (US67-2) US67 and W Henderson Street (North), and (I35W) I35 W and W Cotter Ave.

#### 4.4.1. Soil Physical Property Testing

The performing agency conducted laboratory tests on the collected soil samples in accordance with the American Society for Testing and Materials (ASTM) procedures to determine the Atterberg limits, particle size distribution for fine-grained soil, sieve analysis for coarse-grained soil, and specific gravity. The testing procedures are briefly explained in the following paragraphs. The soluble sulfate content and PH of soil samples were also measured according to Tex-145-E. Figure 4.12 shows the conducted soil testing to determine the physical property of soils.



**Figure 4.12** Soil testing; (a) Liquid limit testing, (b) hydrometer analysis, (c) Specific gravity testing, (d) plastic limit testing, and (e) sieve analysis (UTA laboratory)

#### Atterberg Limits

The performing agency determined the Atterberg limit (liquid limit and plastic limit) of the soil samples according to ASTM D4318-17 standard test method. These tests were conducted on materials passing the No. 40 (0.475-mm) sieve.

#### *Liquid Limit (LL)*

Liquid limit is defined as the water content, in percent, of a cohesive soil at the arbitrarily defined boundary between the semi-liquid and plastic states (ASTM D4318-17). First, to conduct the test, small increments of distilled water was added into the soil using a spray bottle to apply a uniform mist of water to the sample. Then, a sufficient amount of soil was placed in the liquid limit device cup, flattened, and finally divided using a grooving tool at the point of maximum thickness. The cup was lifted and dropped at a rate of 2 drops per second until the groove closure was about 13



mm (appropriate moisture contents should yield to 15 to 35 number of blows). The test was repeated three times with different moisture contents. Then to determine the moisture content, samples were dried in the oven at 100-110 degrees of Centigrade for 24 hours. The moisture content corresponding to 25 blows was considered as the liquid limit of the soil specimen. Figure 4.13 illustrates the testing procedure using the liquid limit device.



**Figure 4.13** Liquid limit testing: (a) the soil is flattened in the device cup, and (b) a groove was made at the center (UTA laboratory)

### ***Plastic Limit (PL)***

Plastic limit is defined as the lowest moisture content, in percent, of a cohesive soil at the boundary between the plastic and semi-solid states (ASTM D4318-17). First, to determine the plastic limit, distilled water was added into the soil and kneaded repeatedly. Then a sufficient amount of soil was placed on a glass plate and rolled back and forth until threads of about one-eighth inch in diameter (3 mm) were formed and broken into pieces. Then to determine the moisture content, samples were placed and dried in the oven at 100-110 degrees of Centigrade for 24 hours. The moisture content corresponding to this stage was considered as the plastic limit of the soil specimen. Figure 4.14 illustrates the rolling device and the state of cracked threads resulted from the experiment.



**Figure 4.14** Plastic limit testing (a) Rolling device and (b) cracked and broken threads of 3 mm (UTA laboratory)

### Particle Size Distribution

The performing agency determined the particle size distribution of fine-grained soil using the hydrometer method according to ASTM D7928-17 standard test method. The test was performed on material passing the No. 10 (2.0-mm) or finer sieve.

First, approximately 5.0 grams of sodium hexametaphosphate was dissolved in water and added to the sedimentation specimen. The contents were completely mixed with a spatula until all of the soil aggregations are broken-up. The slurry should be soaked overnight (at least 12 hours). Then the slurry was dispersed using a stirring device and transferred into the hydrometer cylinder. A sufficient amount of distilled water was added to bring the level of the water to 1000 ml. Then the cylinder was placed in a constant temperature water bath.

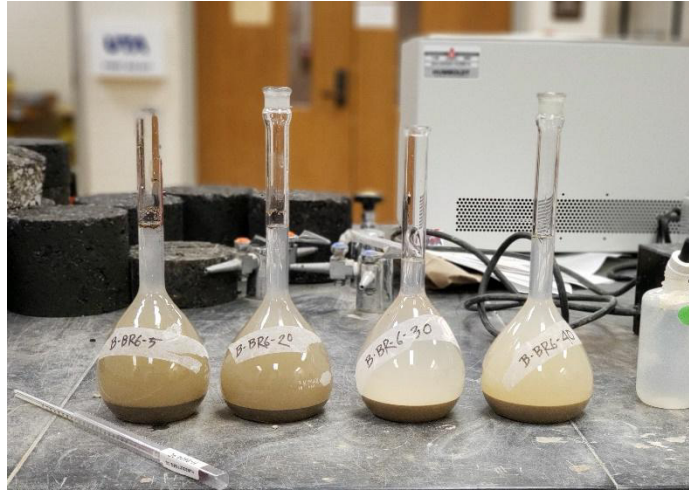
When the soil suspension reaches the temperature of the bath, its contents were completely agitated for about one minute. Then the hydrometer cylinder was placed on the table, and immediately the hydrometer was lowered into the suspension, and the time was recorded. The peak of the meniscus formed on the stem of hydrometer was read to the nearest 0.5 g per liter at the end of two minutes from the time the graduate was set on the table. The cylinder was removed and again placed into the constant temperature bath. The hydrometer readings were obtained at time intervals of 1, 2, 4, 15, 30, 60, 240, and 1440 minutes after the beginning of sedimentation. Figure 4.15 shows the hydrometer test on the clayey soil specimens. Using the equations presented in ASTM D7928-17, particle diameters and the percent finer than a specific diameter were determined.



**Figure 4.15** Particle size distribution testing using the hydrometer procedure (UTA laboratory)

### **Specific Gravity**

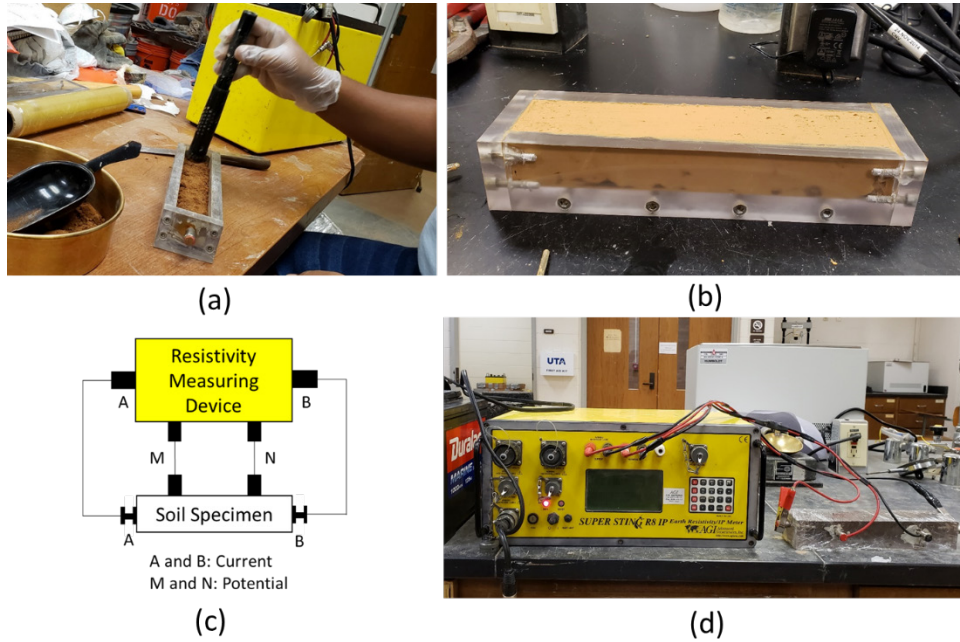
The performing agency determined the specific gravity of soil samples using a water pycnometer according to ASTM D854-14 standard test method. About 50 grams of dried soil material passing the No. 10 (2.00 mm) sieve used in the test. The soil was added to the pycnometer, and the pycnometer was filled about one-half with distilled water. The weights of the empty pycnometer and pycnometer with specimens were measured separately. To remove the entrapped air between the soil particles, a partial vacuum was applied. It is started by applying a low vacuum and then the vacuum level was increased gradually until the water in the flash boils. Then, water was added up to the graduation mark of the pycnometer and weighted. The distilled water was poured in a clean pycnometer, and the combined weight was measured. Using the equations presented in ASTM D54-14, the specific gravity of soil was determined. Figure 4.16 shows the testing procedure on the clayey soil specimens.



**Figure 4.16** Specific gravity testing of soil (UTA laboratory)

#### **4.4.2. Laboratory Electrical Resistivity Imaging**

The performing agency conducted laboratory electrical resistivity tests on the collected soil samples in accordance with the ASTM G187-05, considering different moisture contents (in the range of 6 to 45 percent) and dry unit weights (in the range of 50 to 100 pounds per cubic feet). A four-electrode soil box, current source, resistance measuring equipment, and electrical connections were used to conduct the laboratory testing. First, a specific amount of water was added to the soil and mixed. Then, the soil was placed in the resistivity box and compacted to reach the desired compaction. After the installation of equipment, direct current was applied using two electrodes located at the end of the resistivity box, and the potential drop was measured between two points at the specimen. The preparation of soil specimens and experimental setup of laboratory resistivity testing are illustrated in Figure 4.17.



**Figure 4.17** (a) and (b) preparation of soil specimens, (c) a schematic setup of laboratory electrical resistivity test, and (d) experimental setup of laboratory resistivity test

## CHAPTER 5 DATA PROCESSING AND ANALYSIS

### 5.1. Introduction

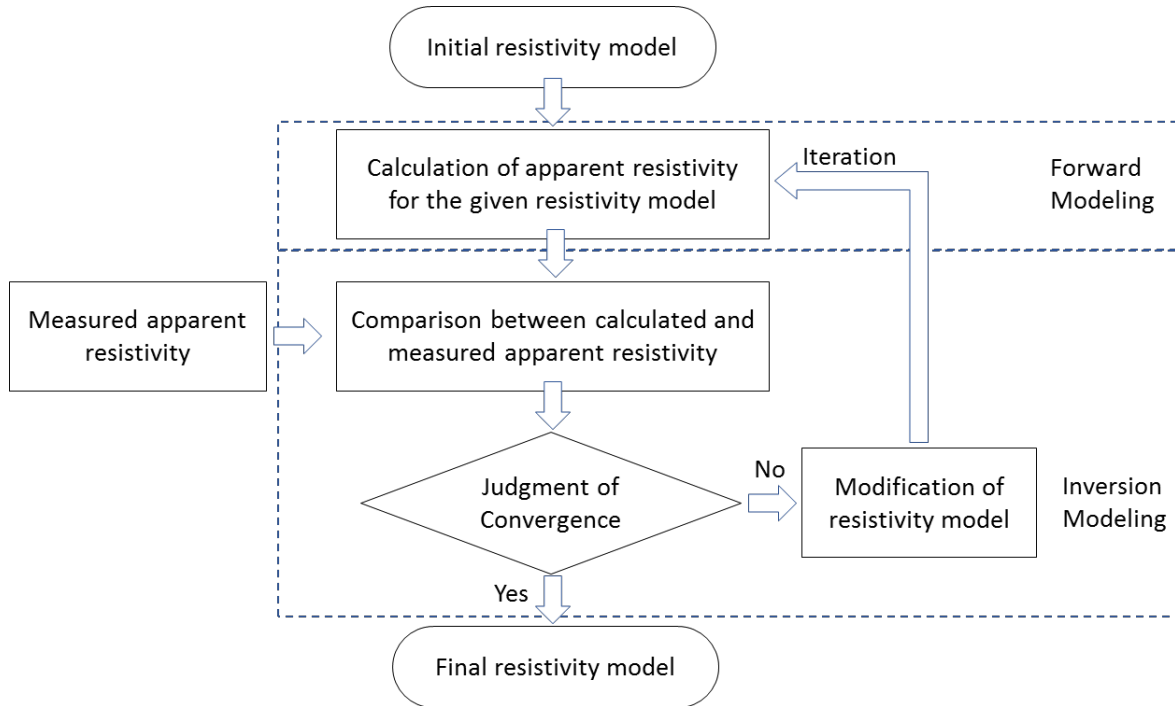
This chapter describes the ERI data processing using software programs. It also discusses the obtained subsurface resistivity images from the demonstrative electrical resistivity imaging surveys to illustrate how different zones in a subsurface resistivity image can be interpreted. This chapter describes the data analysis procedure and provides sets of equations and charts to characterize geotechnical parameters using the electrical resistivity values. It also introduces an Excel-based application developed by the receiving agency to facilitate the computation of the geotechnical parameters from the proposed equations.

### 5.2. Continuous Resistivity Images of Subsurface

In this section, a general procedure for processing of the measured data from the field surveys is explained to obtain the electrical resistivity images of the subsurface using software programs.

#### 5.2.1. Data Processing

After the field survey, the resistance measurements are reduced to apparent resistivity by multiplying the measurements by a geometric factor specific to the used electrode configuration. The apparent resistivity is the electrical resistivity of a homogenous subsurface, which will give the same resistance for the same electrode configuration. In other words, it is the weighted average of the resistivity of the subsurface under the four measuring electrodes. Generally, the software programs perform this conversion. Then, they use the measured apparent resistivity data to derive the true resistivity (calculated apparent resistivity) and accurate images of the subsurface through an inversion process. A typical flowchart of data processing is illustrated in Figure 5.1.



**Figure 5.1** Typical flowchart of data processing (Adapted from Watanabe and Takeuchi, 2004)

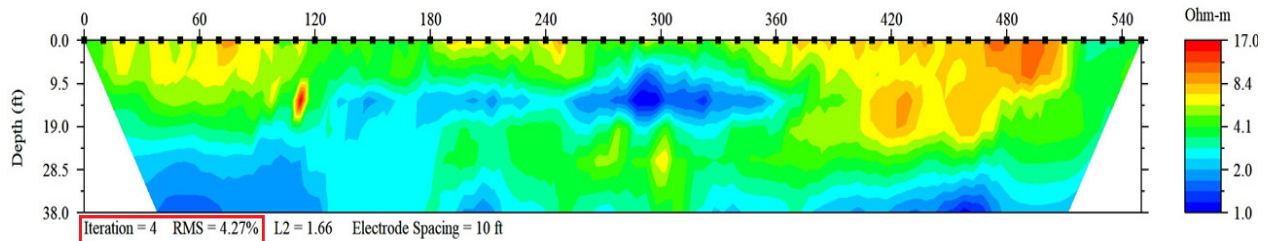
There are several software programs available for 2D modeling of electrical resistivity data such as RES2DINV, EarthImager, DC2DINVRES, ZondRes2D, and RTomo. These software programs use different techniques such as finite difference, finite element, and integral equation algorithms to process the field electrical resistivity data (Schoenleber, 2005; Loke, 1999). Table 5.1 lists examples of software programs along with available algorithms for processing of electrical resistivity data. Using the finite difference and finite element modeling approaches, the program divides the subsurface area into a large number of similar rectangular blocks in the fixed locations beneath the location of the measurements. The depth of the bottom row of the blocks is approximately set to the median depth of investigation of the data points with the largest electrode spacing (Loke, 2015). A finer mesh results in more accurate results, but it extends the duration of the data processing and requires a larger memory space (Loke, 2015; Advanced Geoscience Inc., 2009). The horizontal and vertical sizes of the mesh could be determined in the software programs (e.g., see Appendix A.2.). The finite element method is a better algorithm to model the data which contains earth topography. Besides, the finite element method is more accurate than the finite difference method. However, the finite difference data processing method is faster than the finite element method (Loke, 2015; Advanced Geoscience Inc., 2009).

**Table 5.1** Examples of software programs along with available algorithms for processing of electrical resistivity data

Software Name	Data Processing Algorithm		Description
	Finite Element	Finite Difference	
2D EarthImager	<input checked="" type="checkbox"/>	<input checked="" type="checkbox"/>	License is required (www.agiusa.com)
RES2DINV	<input checked="" type="checkbox"/>	<input checked="" type="checkbox"/>	Free demo version for 2D datasets with up to 84 electrodes (www.geotomosoft.com)
DC2DINVRES	-	<input checked="" type="checkbox"/>	Licenses are free for academic and non-commercial use (www.resistivity.net)
ZondRes2D	<input checked="" type="checkbox"/>	-	License is required (zond-geo.com/English)
RTomo	<input checked="" type="checkbox"/>	-	License is required (www.geogiga.com)

After the blocks are constructed, least-square optimization method is used to estimate the theoretical apparent resistivity value for each block under certain conditions (Arjwech, 2011). The iterative process is continued until an improved subsurface pseudo-section model is constructed whose calculated resistivity values are close enough to the measured resistivity values (Loke and Barker, 1996). The inversion model reduces a quantity in each iteration that is expressed by Root Mean Squared (RMS) error in percent. The model that gives the lowest possible measure for RMS (less than 5%) is identified as the best fit that typically obtains after 3 to 6 iterations for a good quality data set (Loke, 2015; Advanced Geoscience Inc., 2009; Arjwech, 2011). An example of an inverted electrical resistivity image of the subsurface using the EarthImager software program is shown in Figure 5.2.





**Figure 5.2** Example of an inverted electrical resistivity image of the subsurface using the EarthImager software program. RMS of 4.27% is achieved after 4 iterations.

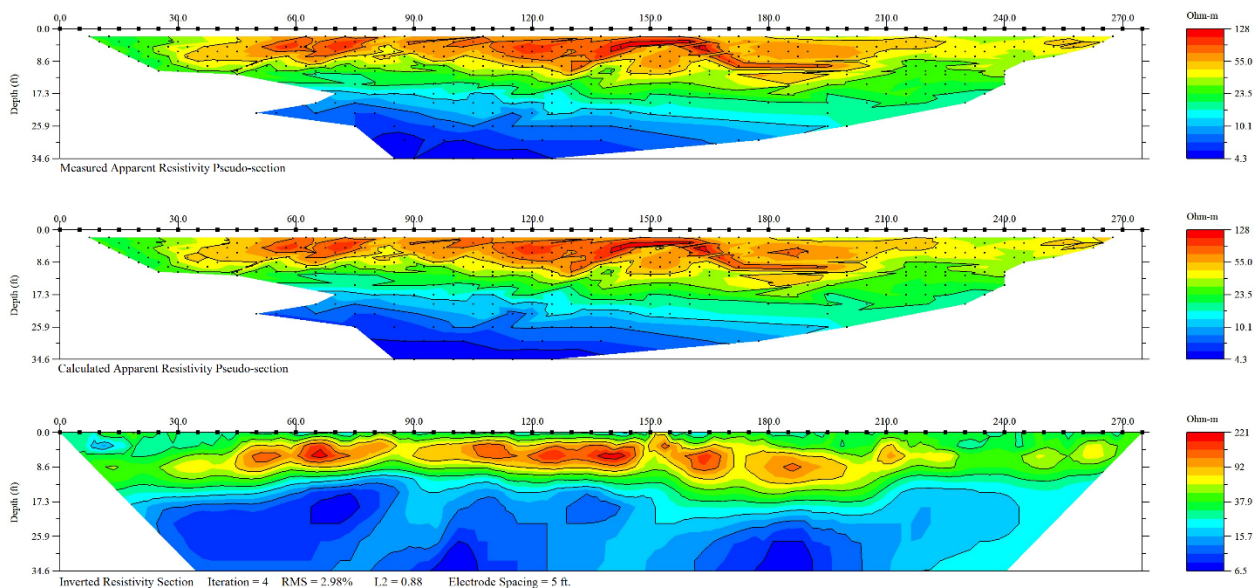
Some assumptions must be made concerning the nature of the subsurface to minimize the sum of the square of errors and the number of possible models that give the same calculated apparent resistivity values. For instance, to create models of subsurface bodies that are internally homogenous with sharp boundaries (e.g., igneous intrusive in sedimentary rocks), a robust (also known as  $l_1$ -norm or blocky) inversion method efficiently minimizes the sum of the absolute values of the data misfit (Dahlin and Zhou, 2004; Ellis and Oldenburg, 1994). On the other hand, by assuming the gradual variation in resistivity of subsurface material (e.g., bedrock with a thick transitional weathered layer), the more realistic model will result using the smoothness-constrained inversion method (also known as  $l_2$ -norm) (Arjwech, 2011).

The typical ranges for electrical resistivity of earth materials are listed in Table 5.2 (Reynolds, 2011; Arjwech, 2011; Loke, 2004; Telford et al., 1990). The electrical resistivity values are overlapped for different materials because the electrical resistivity is influenced by various geological parameters such as water content, clay content, void ratio, concentration of dissolved salt, and temperature of earth materials. Comparatively, the electrical resistivity of igneous rocks is more than metamorphic rocks. Due to the more porous media of sedimentary rocks and their higher water content, they normally have lower electrical resistivity values compared to the igneous and metamorphic rocks. Terrain materials have the least electrical resistivity values compared to the igneous, metamorphic, and sedimentary rocks. Depending on the concentration of dissolved salt, the electrical resistivity of fresh groundwater varies between 10 and 100 ohm-m (Arjwech, 2011; Loke, 1999).

**Table 5.2** Typical ranges of electrical resistivity of different earth material

	<b>Earth Material</b>	<b>Resistivity (ohm-m)</b>
Sedimentary rocks	Conglomerate	$2 \times 10^3 - 10^4$
	Sandstone	$8 - 7.4 \times 10^8$
	Consolidated shale	$20 - 2 \times 10^3$
	Limestone	$50 - 10^7$
	Dolomite	$3.5 \times 10^2 - 5 \times 10^3$
Terrain materials	Unconsolidated wet clay	20
	Clays (moist to dry)	1 - 100
	Alluvium and sands	10 - 800
	Clay and marl	1 - 100
	Loam	5 - 80
	Gravel (moist to dry)	$100 - 1.4 \times 10^3$
	Top soil	50 - 120
	Clayey soil	100 - 150
	Sandy soil	$8 \times 10 - 5 \times 10^3$
	Loose sands	$10^3 - 10^5$
	River sand and gravel	$10^2 - 9 \times 10^4$
Igneous rock	Glacial till	50 - 100
	Granite (weathered to unweathered)	$3 \times 10^2 - 1.3 \times 10^6$
	Diorite	$1.9 \times 10^3 - 10^5$
	Andesite	$4.5 \times 10^4 - 1.7 \times 10^7$
	Basalt	$10 - 1.3 \times 10^7$
Metamorphic rock	Gabbro	$10^2 - 10^6$
	Hornfels	$8 \times 10^3 - 6 \times 10^7$
	Schist (calcareous and mica)	$20 - 10^4$
	Schist (graphite)	$10 - 5 \times 10^2$
	Marble	$10^2 - 2.5 \times 10^8$
	Quartzite	$2.5 \times 10^2 - 2.5 \times 10^8$
	Gneiss	$6.8 \times 10^4 - 3 \times 10^6$
Water	Slate	$5 \times 10^2 - 4 \times 10^7$
	Fresh groundwater	10 - 100
	Seawater	$2 \times 10^{-1}$
Permafrost	Ice	$10^3 - 10^5$
		$10^2 <$

The software program reads the data file from the resistivity meter to provide an inverted electrical resistivity image of the subsurface. By loading the data file to the software program, it can automatically carry out the conversion process of the measured data with minimal input from the user. The data processing requires a set of parameters to determine the noisy readings and perform the forward and inversion modeling. Typically, the software programs have a set of default parameters, which are estimated from the measured data. Processing of the data using the default parameters mostly leads to reasonable electrical resistivity images of the subsurface. However, a user can change the default parameters for each data set based on the subsurface (e.g., geometry, minimum and maximum values of material's electrical resistivity) and survey (e.g., minimum voltage, ratio of voltage to transmitted current) characteristics. When the data processing is completed, the measured and calculated apparent resistivity pseudo-sections and the inverted section would be provided by the software program. The electrical resistivity values and depth of pseudo-sections are calculated in ohm-m and meter, respectively. Figure 5.3 shows an example of pseudo-sections for an electrical resistivity survey using the EarthImager software program. In Appendix A, the EarthImager software program tools for processing the electrical resistivity data are presented. Other software programs usually come with similar settings.



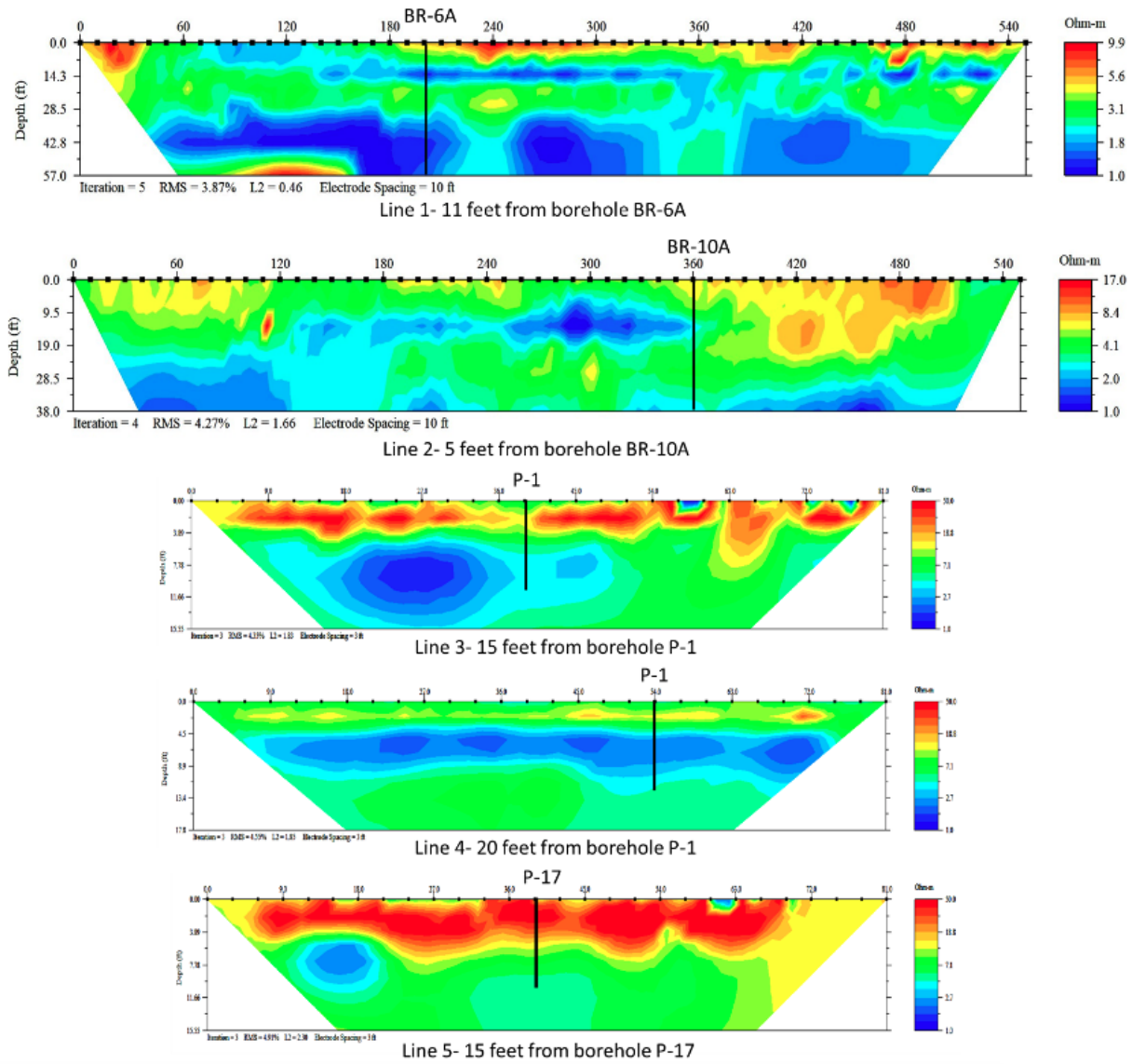
**Figure 5.3** Example of pseudo-sections for an electrical resistivity survey using the EarthImager software program

### 5.2.2. Examples of Resistivity Images of Subsurface

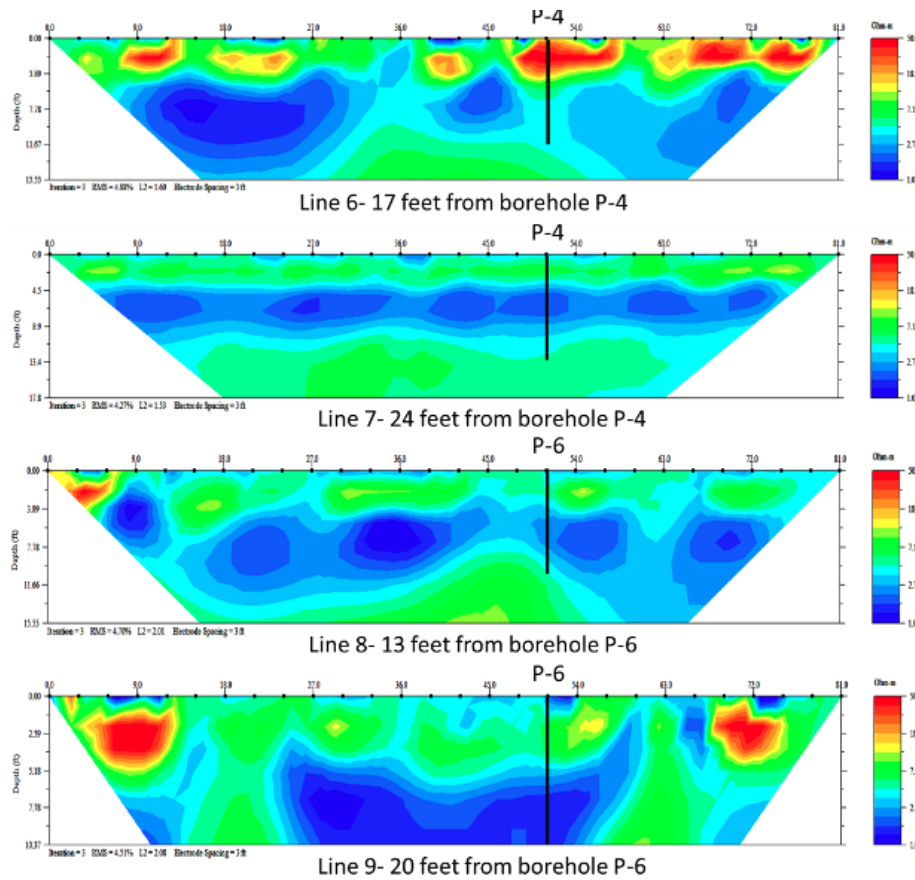
The processed subsurface resistivity images obtained from twenty-seven (27) field electrical resistivity imaging surveys in Beaumont, Corpus Christi, and Fort Worth districts are discussed in this section. The collected resistivity data was processed using “EarthImager” software to obtain resistivity images.

#### Beaumont District

Figures 5.4 and 5.5 show the resistivity images of the subsurface in the Beaumont district, along with the location of boreholes with respect to the survey lines. The maximum resistivity value is 50 ohm-m in all images, indicating that the dominant soil type is clay in this area. There is a thin layer at the top of all images with relatively higher resistivity values, which is attributed to dryer soil. Due to very low resistivity values (<17 ohm-m) in Lines 1 and 2, it is concluded that either the moisture content is relatively high through the entire depth of profiles, or it is an indication of the water table at a depth of around 10 feet. In Lines 3 and 4, a relatively high resistive layer is observed on top, which is associated with the sandy clay. This layer is thicker in Line 3 than Line 4 (further away from the roadway). This suggests that the soil moisture in Line 3 is less than the moisture content in Line 4 or the soil has a higher void ratio than the soil in Line 4. The low resistivity areas beneath the high resistive layer are associated with moist clay. A similar interpretation to Line 3 can be made in Line 5. The subsurface resistivity images in Lines 6 to 9 show slight variations in the electrical resistivity values. Considering the maximum electrical resistivity values (50 ohm-m) in these lines, the subsurface material can be characterized as moist to relatively dry clay soil. The results are consistent with the borehole data.



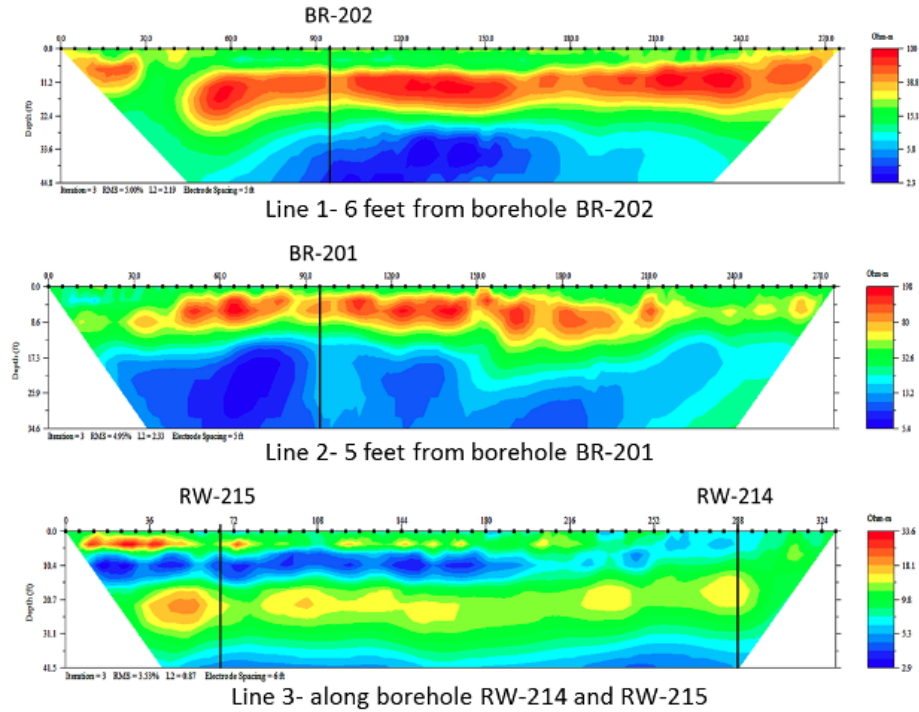
**Figure 5.4** Resistivity profiles and location of boreholes along the survey lines for the Beaumont district



**Figure 5.5** Resistivity profiles and location of boreholes along the survey lines for the Beaumont district

**Corpus Christi District**

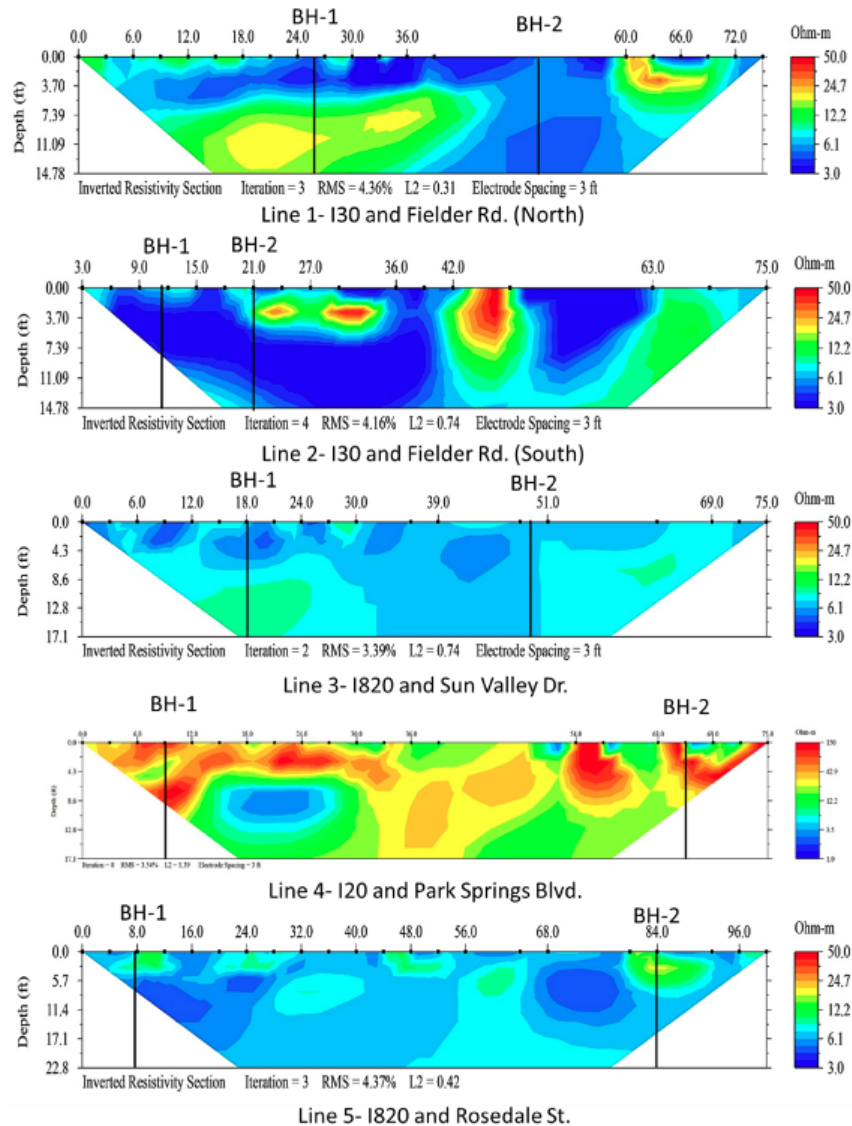
Figure 5.6 shows the resistivity images of the subsurface in the Corpus Christi district, along with the locations of boreholes with respect to the survey lines. The low resistivity areas in Lines 1 and 2 are associated with the groundwater level observed at the approximate depth of 15 feet. The shallow, highly resistive layers in the two images are due to the presence of sandy soils. In Line 3 (with a maximum resistivity value of 33.6 ohm-m), there is a low resistive layer, which is an indication of the groundwater table at a depth of 10 feet. This layer is underlain by a relatively high resistive layer attributed to the saturated sandy soil. The results of the survey are consistent with the borehole data.



**Figure 5.6** Resistivity profiles and location of boreholes along the survey lines for the Corpus Christi district

### Fort Worth District

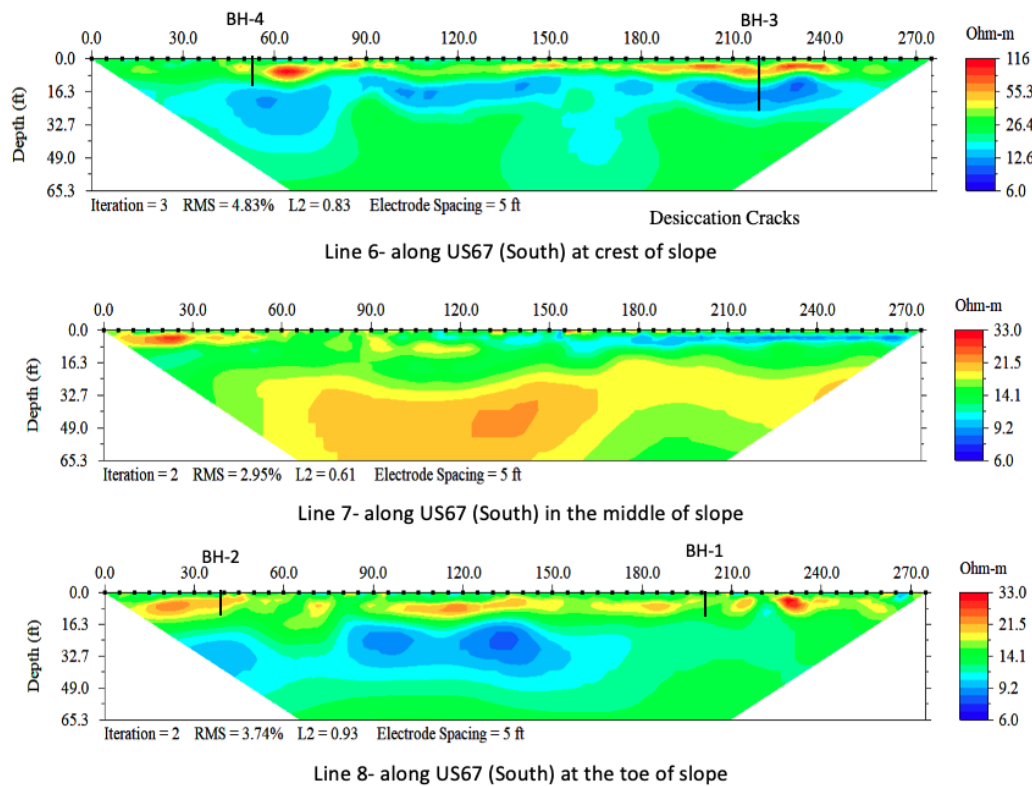
Figure 5.7 to 5.10 show the resistivity images of the subsurface for different locations in the Fort Worth district, along with the location of boreholes with respect to the survey lines. The low resistivity zones are observed in Lines 1, 2, and 3 through the depth of profiles associated with the high moisture content, leading to instability of slopes. In Line 4, the zones of high resistivity ( $>100$  ohm-m) in the shallow depth are interpreted as sandy soil or dry clayey soil with a high void ratio. An oval shape low resistivity area ( $<10$  ohm-m) is observed in the middle of Line 4, indicating a zone with high moisture content. The pockets of relatively high resistivity values in Line 5 represent the presence of loose material in shallow depth.



**Figure 5.7** Resistivity profiles and location of boreholes along the survey lines 1 through 5 for the Fort Worth district

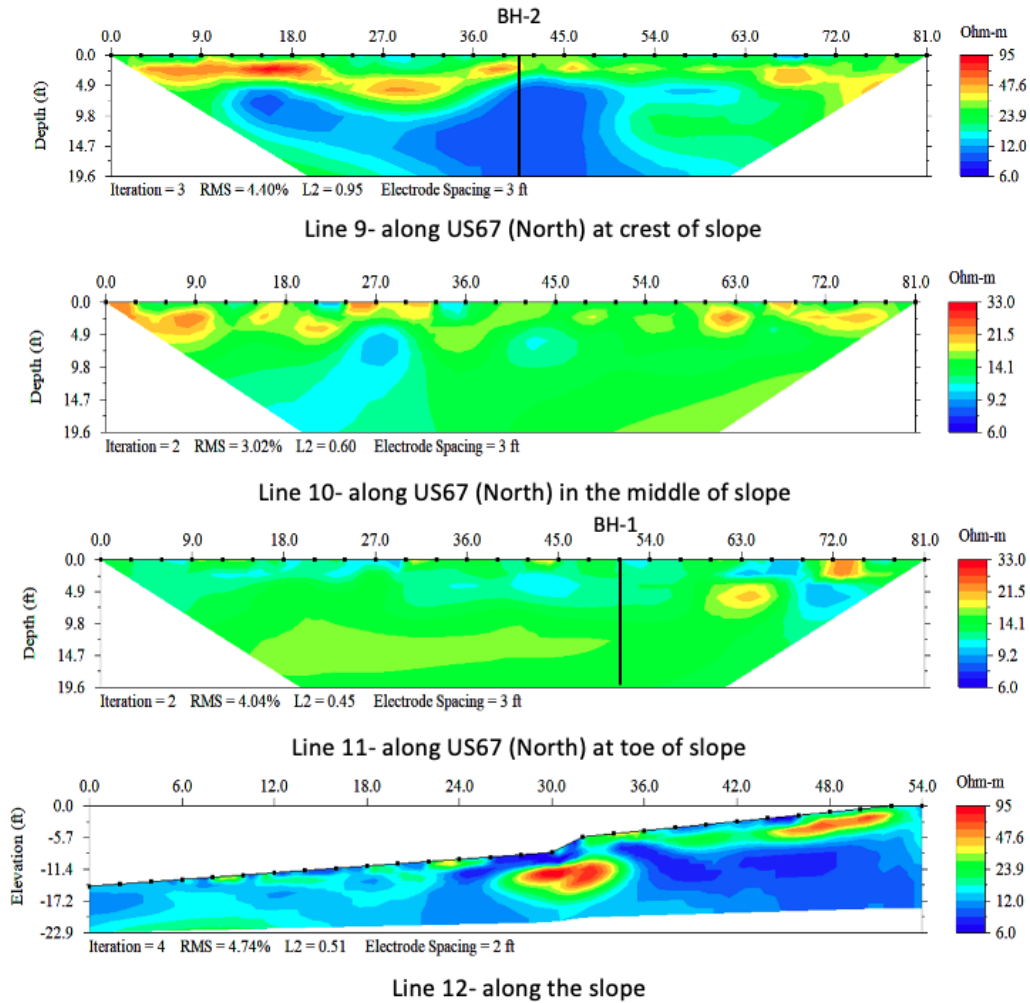
High contrast to the background resistivity is observed at the shallow depths of Line 6 (the background resistivity is about 26 ohm-m). The zones of relatively high resistivity close to the surface are associated with either porous materials or desiccation cracks, through which the water seeps to deeper depths and result in emerging very low resistivity areas right below these high resistivity areas. Similar conclusions can be made by observing Lines 7 and 8. However, the resistivity contrasts are less severe as moving from the crest to the toe of the slope. The low resistivity areas in the middle of Line 8 are indications of moisture pockets in the subsurface.





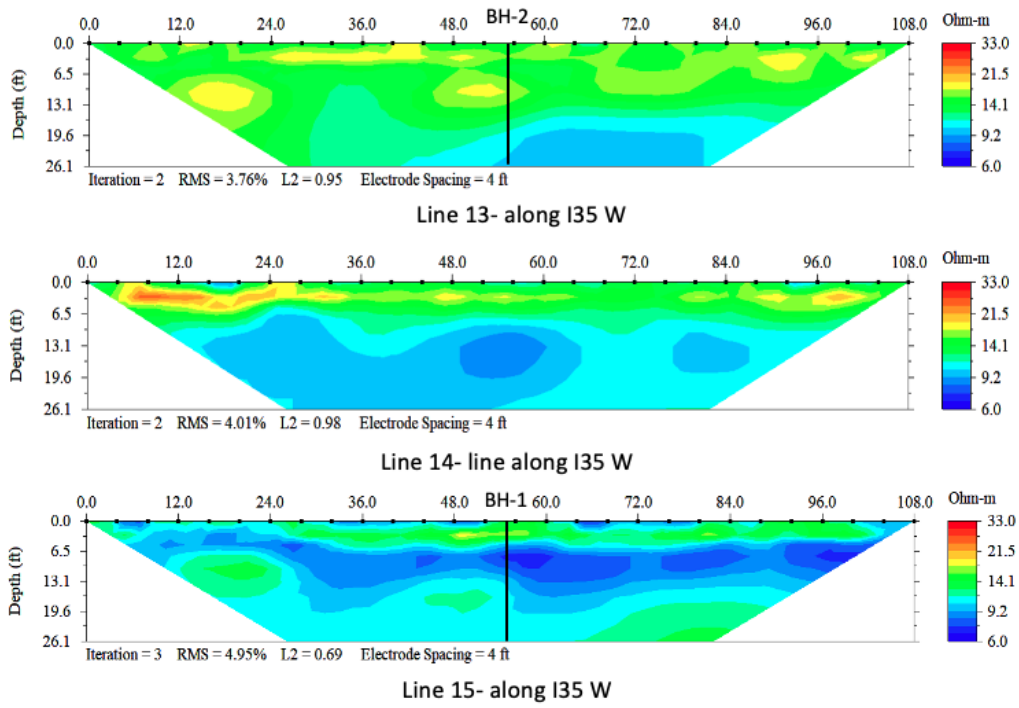
**Figure 5.8** Resistivity profiles and location of boreholes along the survey lines of 6 through 8 for the Fort Worth district

A large area with low resistivity values can be observed in Line 9, which indicates high moisture content in the subsurface material at 5 to 19.6 ft depths. The resistivity images of Lines 10 and 11 are quite homogenous with low resistivity values (about 14 ohm-m) through the depth of profiles, implying the presence of moist materials except at the shallow depths. The high and low resistivity areas at the top are most likely caused by the formation of desiccation cracks and seepage of water through the depth. As shown in Line 12, as moving from the crest to the toe of the slope, the thickness of the high resistivity areas at the shallow depths decreases, meaning that the resistivity contrast through the depth of the profile decreases. A zone of high resistivity (>50 ohm-m) is also observed in the middle of Line 12, which can be attributed to the presence of dry clay or porous materials. The results are consistent with the borehole data.



**Figure 5.9** Resistivity profiles and location of boreholes along the survey lines of 9 through 12 for the Fort Worth district

The resistivity images of Lines 13, 14, and 15 show approximately similar patterns at which relatively low resistivity areas are observed in the bottom of the images, indicating the presence of possible water table at the depths of 20 and 10 ft., respectively (the water table was observed at the depths of 20 to 22 ft by boring). Since the electrical resistivity values range from 6 to 33 ohm-m, the subsurface material can be identified as moist to relatively dry clayey soil, which is consistent with the boring results.



**Figure 5.10** Resistivity profiles and location of boreholes along the survey lines of 13 through 15 for the Fort Worth district

### **5.3. Empirical Equations and Charts for Estimation of Geotechnical Properties**

A set of equations and charts were developed by analyzing the collected data from the laboratory tests. These tools help TxDOT engineers to determine the approximate ranges of known geotechnical parameters (e.g., moisture content, dry unit weight, and plasticity index), using the field temperature-corrected electrical resistivity values. In this section, the equations and charts for the estimation of geotechnical parameters using corrected-electrical resistivity values are presented and an Excel-based application developed for facilitating the computation of the geotechnical parameters from the equations is introduced.

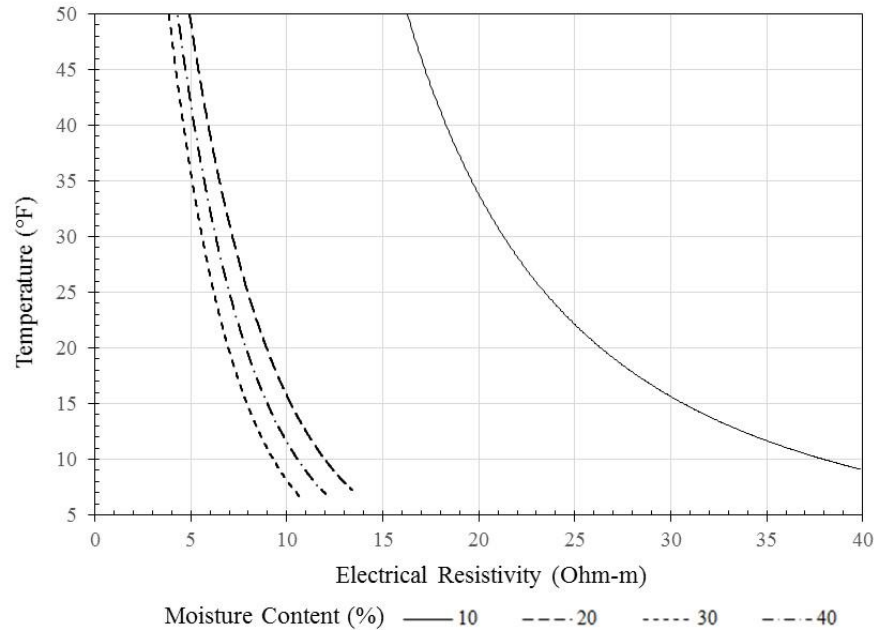
#### **3.3.4. Statistical Method**

The Simple Linear Regression (SLR) and Multiple Linear Regression (MLR) models were used to develop relationships between the geoelectrical and geotechnical parameters. The geotechnical parameters with the most insignificant test statistics that showed high correlations with other parameters were removed from the model to avoid multicollinearity. These parameters are the degree of saturation, void ratio, specific gravity, and liquid limit. Besides, different types of transformation of the dependent and independent variables were used to ensure that the critical assumptions of the linear model, including linearity, normality, and homoscedasticity are satisfied. The analyses were conducted using R statistical software.

The collected data from the physical property tests (e.g., specific gravity, grain size distribution, and Atterberg limit) and 1093 laboratory electrical resistivity tests on the 81 disturbed soil samples taken from different locations in Texas (Beaumont, Corpus Christi, Dallas, El Paso, and Fort Worth districts) were considered in the modeling.

#### **5.3.1. Corrected Electrical Resistivity**

The soil temperature during the electrical resistivity survey influences the electrical resistivity measurements (Kouchaki et al., 2019; Abu Hassanein et al., 1996). The variations of electrical resistivity measurements with soil temperature during the laboratory electrical resistivity tests for a soil sample at different moisture contents are illustrated in Figure 5.11. Figure 5.11 shows that, at different moisture contents, the electrical resistivity of the soil decreases as the temperature increases. However, there are significantly larger differences between the measured electrical resistivity values in different temperatures when the soil contains low moisture content.



**Figure 5.11** Variations of electrical resistivity measurements with soil temperature during the experiment for a soil sample at different moisture contents

Therefore, to eliminate the variability of electrical resistivity values resulting from temperature variations, the field electrical resistivity measurements should be corrected at a reference temperature of 15.5°C (59.9°F) using the following equation (ASTM G187-05):

$$R_{15.5} = R_T \frac{(24.5+T)}{40} \quad (1)$$

where  $R_{15.5}$  is the corrected electrical resistivity at a reference temperature of 15.5°C,  $R_T$  is the measured resistivity at the temperature  $T$ °C. Then, the corrected electrical resistivity parameter can be used in the equations and charts to estimate the geotechnical parameters.

### 5.3.2. Empirical Equations for Estimation of Geotechnical Properties

Simple and multiple linear regression were used to identify the relationship between the electrical resistivity property and geotechnical engineering parameters. Sets of equations for the two dominant soil types (clayey and sandy soils) in the study areas are presented separately in the following paragraphs.

#### Equations for Clayey Soil

The developed equations for clayey soil are based on four geotechnical parameters: moisture content, dry unit weight, plasticity index, and percent of fines (i.e., percent of soil finer than sieve No. 200). The data relating to the clayey soil, collected from the Beaumont, Dallas, Corpus Christi, and Fort Worth districts, were used in the modeling. General relationships were created using the multiple linear regression model that relates electrical resistivity to moisture content, dry unit weight, plasticity index, and percent of fines and have the forms of:

$$R_{15.5}^{-0.5} = -0.8601 + 0.2317 \times \ln w + 0.0058 \times \gamma_d + 0.0033 \times PI - 0.0008 \times F$$

$$R_{adj}^2 = 0.79 \quad (2)$$

where “ $R_{15.5}$ ” is temperature-corrected electrical resistivity (ohm-m), “ $w$ ” is moisture content (percent), “ $\gamma_d$ ” is the dry unit weight (pcf), “ $PI$ ” is the plasticity index (percent), and “ $F$ ” is the percent of fines (%). The relationship between the electrical resistivity, moisture content, dry unit weight, and plasticity index can be defined as:

$$R_{15.5}^{-0.5} = -0.9212 + 0.2312 \times \ln w + 0.0059 \times \gamma_d + 0.0030 \times PI, \quad R_{adj}^2 = 0.78$$

$$(3)$$

Likewise, the relationship between the electrical resistivity, moisture content, and dry unit weight is defined as:

$$R_{15.5}^{-0.5} = -0.7955 + 0.2320 \times \ln w + 0.0053 \times \gamma_d, \quad R_{adj}^2 = 0.75 \quad (4)$$

The relationship between the electrical resistivity, moisture content, and plasticity index has the form of:

$$R_{15.5}^{-0.5} = -0.3992 + 0.2130 \times \ln w + 0.0021 \times PI, \quad R_{adj}^2 = 0.68 \quad (5)$$

Finally, the relationship between electrical resistivity and moisture content is defined as:

$$R_{15.5}^{-0.5} = -0.3267 + 0.2149 \times \ln w , \quad R_{adj}^2 = 0.66 \quad (6)$$

Table 5.3 summarizes all the models for clayey soils to predict the known geotechnical parameters using electrical resistivity values.

**Table 5.3** Equations for estimating the geotechnical parameters using electrical resistivity for clayey soil

Potential Influencing Parameters	Relationship
R, w, $\gamma_d$ , PI, and F	$R_{15.5}^{-0.5} = -0.8601 + 0.2317 \times \ln w + 0.0058 \times \gamma_d + 0.0033 \times PI - 0.0008 \times F$
R, w, $\gamma_d$ , and PI	$R_{15.5}^{-0.5} = -0.9212 + 0.2312 \times \ln w + 0.0059 \times \gamma_d + 0.0030 \times PI$
R, w, and $\gamma_d$	$R_{15.5}^{-0.5} = -0.7955 + 0.2320 \times \ln w + 0.0053 \times \gamma_d$
R, w, and PI	$R_{15.5}^{-0.5} = -0.3992 + 0.2130 \times \ln w + 0.0021 \times PI$
R and w	$R_{15.5}^{-0.5} = -0.3267 + 0.2149 \times \ln w$

Note: “ $R_{15.5}$ ” denotes temperature-corrected electrical resistivity (ohm-m), “w” denotes moisture content (percent), “ $\gamma_d$ ” denotes the dry unit weight (pcf), “PI” denotes the plasticity index (percent), and “F” denotes the percent of fines (percent).

### Equations for Sandy Soil

The developed equations for sandy soil are based on three geotechnical parameters: moisture content, dry unit weight, clay content (i.e., percent of soil finer than 2 microns), and percent of fines (i.e., percent of soil finer than sieve No. 200). The data related to sandy soil, collected from the Corpus Christi and El Paso districts, were used in the modeling. General relationships were developed using multiple linear regression approach between electrical resistivity, moisture content, dry unit weight, percent of fines, and clay content as follow:

$$R_{15.5}^{-0.5} = -0.3151 + 0.1039 \times \ln w + 0.0058 \times C + 0.0018 \times \gamma_d , \quad R_{adj}^2 = 0.76 \quad (7)$$

$$R_{15.5}^{-0.5} = -0.3115 + 0.1037 \times \ln w + 0.0027 \times F + 0.0015 \times \gamma_d , \quad R_{adj}^2 = 0.69 \quad (8)$$

where “ $R_{15.5}$ ” is the temperature-corrected electrical resistivity (ohm-m), “w” is moisture content (percent), “ $\gamma_d$ ” is the dry unit weight (pcf), “F” is the percent of fines (percent), and “C” is the clay content (percent). The relationship between electrical resistivity, moisture content, and clay content is as follow:

$$R_{15.5}^{-0.5} = -0.1719 + 0.1088 \times \ln w + 0.0051 \times C, \quad R_{adj}^2 = 0.73 \quad (9)$$

$$R_{15.5}^{-0.5} = -0.1883 + 0.1080 \times \ln w + 0.0023 \times F, \quad R_{adj}^2 = 0.67 \quad (10)$$

The relationship between electrical resistivity and moisture content is defined as:

$$R_{15.5}^{-0.5} = -0.1198 + 0.1133 \times \ln w, \quad R_{adj}^2 = 0.58 \quad (11)$$

Table 5.4 summarizes all the models for sandy soils to estimate the known geotechnical parameters using electrical resistivity values.

**Table 5.4** Equations for estimating the geotechnical parameters using electrical resistivity for sandy soil

Potential Influencing Parameters	Relationship
R, w, $\gamma_d$ , and C	$R_{15.5}^{-0.5} = -0.3151 + 0.1039 \times \ln w + 0.0058 \times C + 0.0018 \times \gamma_d$
R, w, $\gamma_d$ , and F	$R_{15.5}^{-0.5} = -0.3115 + 0.1037 \times \ln w + 0.0027 \times F + 0.0015 \times \gamma_d$
R, w, and C	$R_{15.5}^{-0.5} = -0.1719 + 0.1088 \times \ln w + 0.0051 \times C$
R, w, and F	$R_{15.5}^{-0.5} = -0.1883 + 0.1080 \times \ln w + 0.0023 \times F$
R and w	$R_{15.5}^{-0.5} = -0.1198 + 0.1133 \times \ln w$

Note: “ $R_{15.5}$ ” denotes temperature-corrected electrical resistivity (ohm-m), “w” denotes moisture content (percent), “ $\gamma_d$ ” denotes the dry unit weight (pcf), “C” denotes the clay content (percent), and “F” denotes the percent of fines (percent).

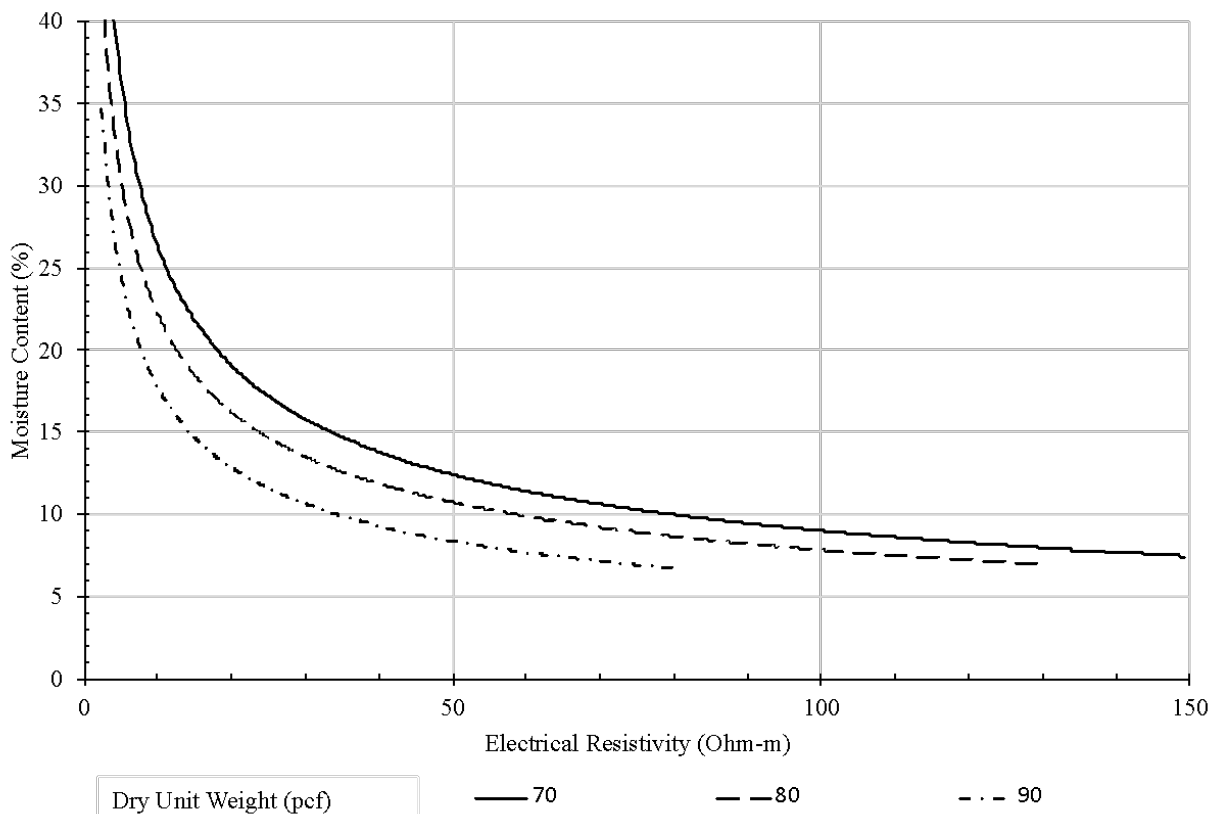


### 5.3.3. Empirical Charts for Estimation of Geotechnical Properties

Several empirical charts were developed for the two dominant soil types (clayey and sandy soils) in the study areas to illustrate the variations of temperature-corrected electrical resistivity with some geotechnical parameters such as moisture content and dry unit weight.

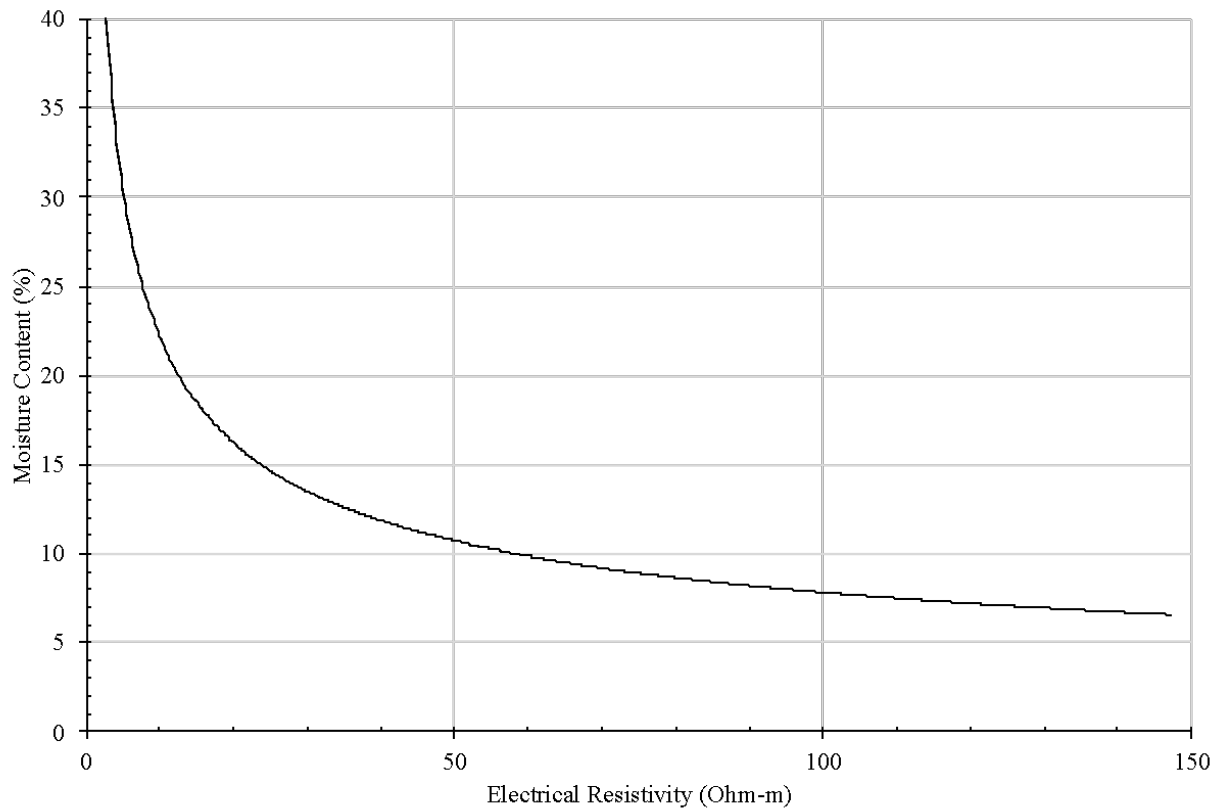
#### Charts for Clayey Soil

Figure 5.12 illustrates the variations of temperature-corrected electrical resistivity of compacted clayey soil with the moisture content at different dry unit weights. Using the electrical resistivity values, the approximate ranges of moisture content at different dry unit weights can be predicted. According to Figure 5.12, it is perceived that there is an inverse relationship between the electrical resistivity and moisture content of the soil. As the moisture content increases, the electrical resistivity decreases, and vice versa. Similarly, keeping the moisture content constant, the lower values for the electrical resistivity correspond to the higher values of dry unit weights.



**Figure 5.12** Variations of temperature-corrected electrical resistivity of compacted clay with moisture content for different dry unit weights

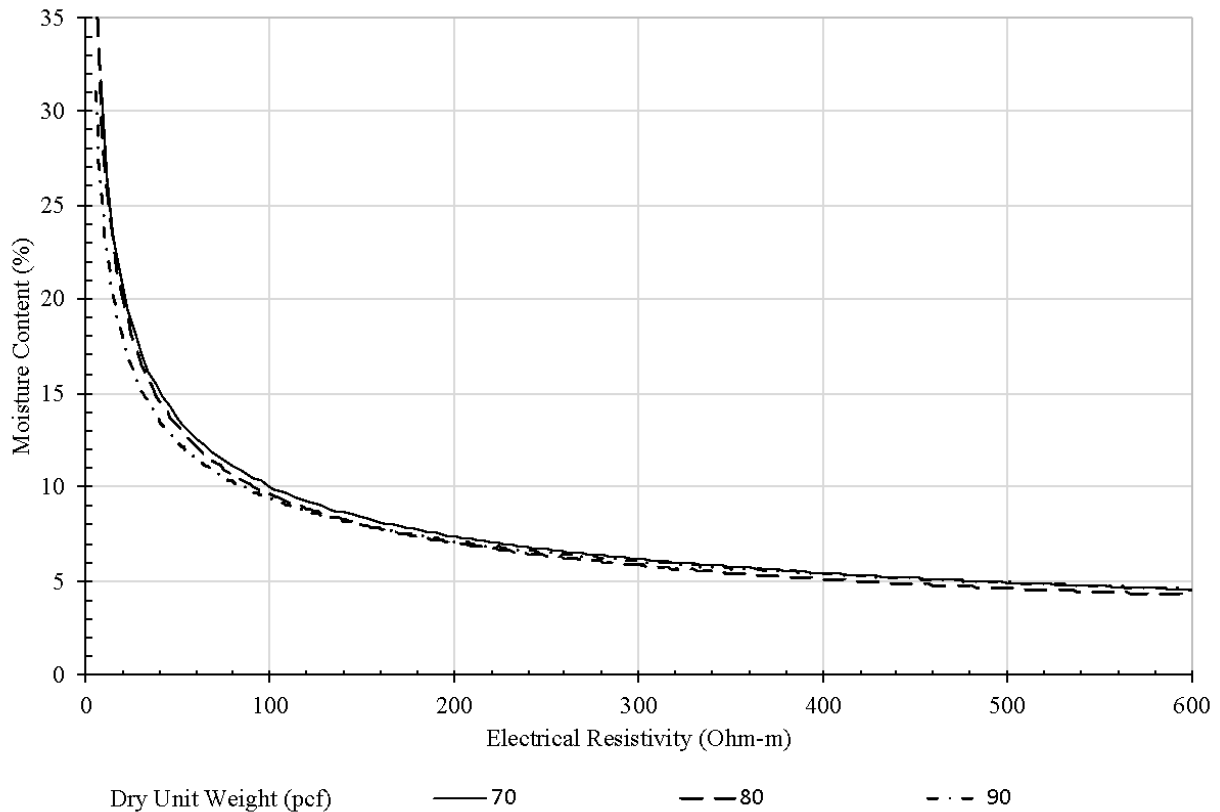
Similarly, Figure 5.13 shows the variations of temperature-corrected electrical resistivity of compacted clayey soil with the moisture content (without considering dry unit weights).



**Figure 5.13** Variations of temperature-corrected electrical resistivity of compacted clay with moisture content

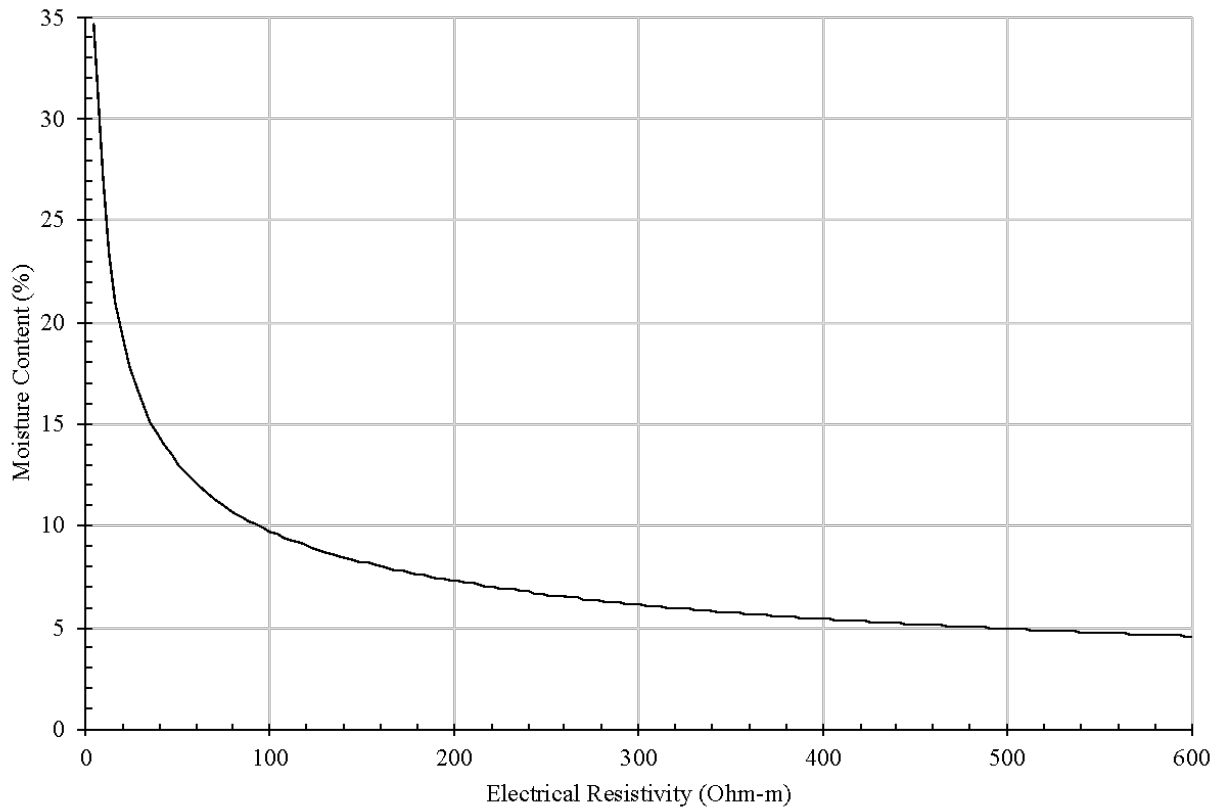
## Charts for Sandy Soil

Figure 5.14 illustrates the variations of temperature-corrected electrical resistivity of sandy soil with the moisture content at different dry unit weights. Using the electrical resistivity values, the approximate ranges of moisture content at different dry unit weights can be predicted. Similar to Figure 5.12 for clayey soils, there is an inverse relationship between the electrical resistivity values and dry unit weight of sandy soils. However, for sandy soils, there are insignificant differences in electrical resistivity values among different dry unit weights.



**Figure 5.14** Variations of temperature-corrected electrical resistivity of sandy soil with moisture content for different dry unit weights

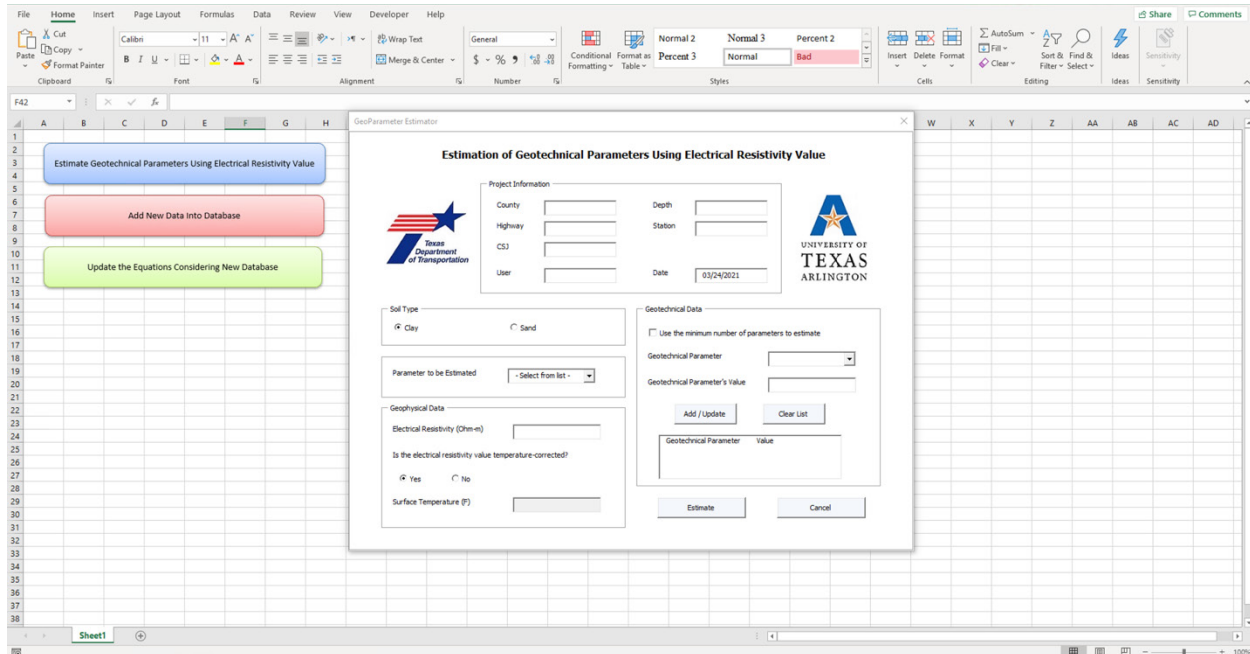
Figure 5.15 shows the variations of temperature-corrected electrical resistivity of sandy soil with the moisture content (without considering dry unit weights).



**Figure 5.15** Variations of temperature-corrected electrical resistivity of sandy soil with moisture content

### 5.3.4. Geoparameter Estimator Application

GeoParameter Estimator is an Excel-based application developed by the performing agency to facilitate the computation of the geotechnical parameters using the electrical resistivity values from the proposed equations in the previous subsection. Figure 5.16 shows the user interface of the GeoParameter estimator.



**Figure 5.16** User interface of the GeoParameter estimator

As shown in Figure 5.16, multiple sections are designed in the application to enable the user to have an estimation for the geotechnical parameters by providing the required information with regard to the “Soil Type,” “Parameter to be Estimated,” “Geophysical Data,” and “Geotechnical Data” sections and to have a complete record of project information by entering the information of a specific project in the “Project Information” section (optional). At a minimum, the soil type should be selected, and the geophysical data should be provided; among the geotechnical parameters, moisture content can be estimated with having the minimum input from the user. Figure 5.17 shows an example of completed sections to estimate moisture content using minimum input from the user. The surface temperature at the time of survey should be provided in a text box in the Geophysical Data section if the electrical resistivity value is not corrected at the reference temperature before.

The screenshot shows the 'GeoParameter Estimator' window with the following data entered:

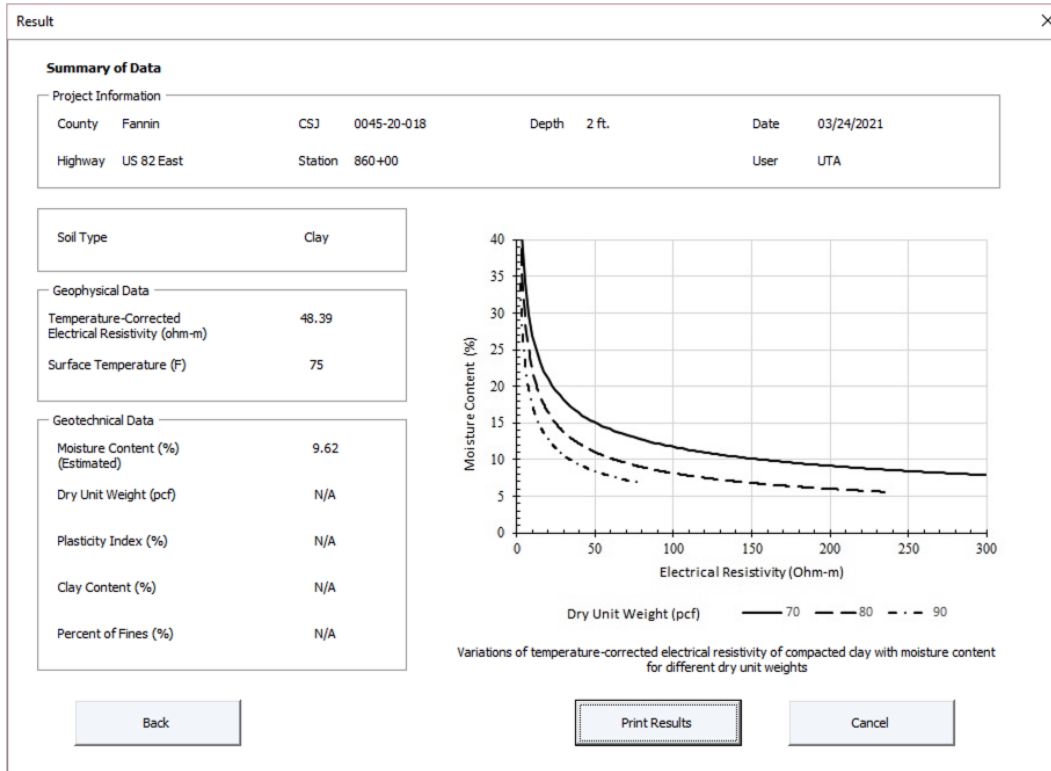
- Project Information:**
  - County: Fannin
  - Highway: US 82 East
  - CSJ: 0045-20-018
  - User: UTA
  - Depth: 2 ft.
  - Station: 860+00
  - Date: 03/24/2021
- Soil Type:** Clay (selected)
- Parameter to be Estimated:** Moisture Content
- Geophysical Data:**
  - Electrical Resistivity (Ohm-m): 40
  - Is the electrical resistivity value temperature-corrected? No (selected)
  - Surface Temperature (F): 75
- Geotechnical Data:**
  - Use the minimum number of parameters to estimate:
  - Geotechnical Parameter: (empty dropdown)
  - Geotechnical Parameter's Value: (empty text box)
  - Buttons: Add / Update, Clear List
  - Table:

Geotechnical Parameter	Value
  - Buttons: Estimate, Cancel

**Figure 5.17** Example of completed sections for the estimation of moisture content using minimum input from the user

If the user unchecks an option to use the minimum number of parameters, the known geotechnical parameters can also be provided to the application and added to the list box in the Geotechnical Data section. Based on the entries by the user, the application uses the proper equation to estimate the parameter of interest.

If the user clicks on the “Estimate” button, a new window will be opened, which contains a summary of data, including the project information, soil type, geophysical data, and geotechnical data, as well as the estimated geotechnical value. Figure 5.18 shows an example of the estimation results and summary of data in the “Result” window. It also contains a chart based on the selected soil type that is developed based on the empirical tests. The Result window also enables the user to easily print the obtained information from the analysis.



**Figure 5.18** Example of the estimation results in the print preview window

In addition to facilitating the computation of the geotechnical parameters using electrical resistivity values from the proposed equations, this application provides handy tools to add new data collected from the laboratory tests to the current database and update the proposed equations based on the new database.

## CHAPTER 6 TRAINING WORKSHOPS

### 6.1. Introduction

This chapter describes the process of performing workshops in the selected districts to convey the information of the electrical resistivity imaging (ERI) technique and share the project's findings with the TxDOT staff.

### 6.2. Performed Training Workshops

The better subsurface characterization, cost-benefit, and data acquisition speed are the three most significant benefits of using geophysical methods in agency transportation projects (Sirles, 2006). However, lack of understanding, non-uniqueness of results, and lack of confidence are the main deterrents of using these geophysical methods (Rosenblad and Boeckmann, 2020). Therefore, training, sharing experiences, and implementing standards are critical to overcome these deterrents and benefit from the geophysical methods. The objectives of the current task are to convey information about the ERI technology to TxDOT staff and share the findings of the current research project. The application of advanced geophysical tools, such as the electrical resistivity imaging technique, could improve site investigations in the TxDOT. The electrical resistivity imaging technique provides continuous assessment of the subsurface condition using a non-invasive, rapid, and cost-effective method that can mitigate cost overruns and delays due to inadequate subsurface information. This lack of sufficient information is due to the inherent limitation of the conventional geotechnical site investigation methods to provide continuous assessment of the subsurface (i.e., these conventional methods only sample and provide information about a small percentage of a total sample space).

The performing agency conducted training workshops in Beaumont, El Paso, Fort Worth, and Paris districts based on the schedule (Table 6.1). Two online workshops were scheduled and performed in the Beaumont and Fort Worth districts in June 2021, and three online workshops were performed in the El Paso, Dallas, and Paris districts in July 2021. Table 6.1 shows the district contact, date, and time of the scheduled workshops for each district.



**Table 6.1** Scheduled workshops in the selected districts

<b>TxDOT District</b>	<b>District Contact</b>	<b>Workshop Scheduled Date</b>	<b>Workshop Time</b>
Beaumont	Kenneth Wiemers	June 17, 2021	2:00 PM to 3:00 PM
Fort Worth	Natnael Asfaw	June 24, 2021	10:00 AM to 11:00 AM
El Paso	Hugo Hernandez	July 12, 2021	11:00 AM to 12:00 PM
Paris	Sydney Newman	July 06, 2021	10:00 AM to 11:00 AM

These workshops focused on (1) significance of subsurface investigations in infrastructure projects, (2) benefits/value of ERI technology in subsurface characterization, (3) deterrents of using ERI technology and practices to overcome those deterrents, (4) presentation of ERI research manual including planning considerations for ERI surveys, safety precautions, and practical considerations regarding different operational environments and extreme weather conditions, (5) the step-by-step procedures and guidelines for performing ERI surveys and processing the field data using the prepared video training material, (6) application of the empirical relationships between the geotechnical and geophysical parameters developed based on extensive data collection (from 5 different districts) and statistical analysis, and (7) interpretation of continuous subsurface resistivity images obtained from the ERI surveys in the selected districts along with the borehole findings. The workshop summary is presented in Appendix C.

## CHAPTER 7 SUMMARY AND CONCLUSION

This research project was mainly concentrated on improving the level of knowledge of TxDOT staff about the Electrical Resistivity Imaging (ERI) technology and providing practical tools for a rapid and continuous assessment of subsurface conditions.

An easy-to-use comprehensive research manual was developed to provide TxDOT staff with the electrical resistivity imaging technique procedures and guidelines for safe and correct implementation of ERI technology. Five TxDOT districts (Beaumont, Corpus Christi, El Paso, Dallas, and Fort Worth) were selected to be the focus of this research for conducting demonstrative electrical resistivity imaging and soil sampling. The gained experiences by demonstrating the electrical resistivity imaging in the selected districts were documented in the research manual to cover practical considerations for surveying in different operational environments and geotechnical conditions. Extensive laboratory testing (soil physical property and laboratory electrical resistivity tests) was performed on the collected samples from different locations in the selected TxDOT districts. The results of the laboratory testing were later analyzed to investigate the relationships between the geoelectrical and geotechnical parameters and to provide sets of empirical equations and charts using linear regression models. A set of empirical equations and charts were developed to provide practical tools for a rapid estimation of geotechnical parameters such as moisture content, dry unit weight, plasticity index, clay content, and percent of fines using electrical resistivity values. An Excel-based application was also developed and introduced to facilitate the computation steps of geotechnical parameters from the proposed equations. Besides, several training workshops were held in the Beaumont, El Paso, Fort Worth, and Paris districts to disseminate the knowledge of the applications, data collection, and data interpretation of electrical resistivity imaging technology to TxDOT staff.

It is expected that this research project's findings will help TxDOT engineers and managers in decision-making by improving site characterization findings using continuous images of subsurface and providing rapid estimates for geotechnical properties using empirical equations and charts. The electrical resistivity imaging technology is beneficial to TxDOT in reducing risk and uncertainty, preventing inadequate/conservative designs, and increasing accuracy in bids.

## REFERENCES

- ABEM Instrument (2010). Instruction Manual Terrameter SAS 4000/SAS 1000.
- Abu-Hassanein, Z. S., Benson, C. H., & Blotz, L. R. (1996). Electrical resistivity of compacted clays. *Journal of geotechnical engineering*, 122(5), 397-406.
- Adhikari, I., Baral, A., Zahed, E., Abedinangerabi, B., & Shahandashti, M. (2021). *Early stage multi-criteria decision support system for recommending slope repair methods*. *Civil Engineering and Environmental Systems*, 1-18.
- Advanced Geoscience Inc. Retrieved from <https://www.agiusa.com/> (Dec 23, 2020).
- Advanced Geosciences Inc., A. (2011). *The Super Sting Automatic Resistivity and IP System. Instructions Manual*.
- Advanced Geosciences, Inc. (2009). *Instruction Manual for EarthImager 2D, Version 2.4. 0*.
- Aizebeokhai, A. P. (2010). 2D and 3D geoelectrical resistivity imaging: Theory and field design. *Scientific Research and Essays*, 5(23), 3592-3605.
- Allied Associates, LTD. (2019). *Tigre resistivity meter User's manual*. Retrieved from <https://www.allied-associates.com/wp-content/uploads/2019/10/Manual-Tigre.pdf>, (2 Oct, 2020).
- Anderson, N. L., Croxton, N., Hoover, R., & Sirles, P. (2008). *Geophysical methods commonly employed for geotechnical site characterization*. *Transportation Research Circular*, (E-C130).
- Anderson, N., & Ismail, A. (2003). *A generalized protocol for selecting appropriate geophysical techniques*. In *Geophysical Technologies for Detecting Underground Coal Mine Voids Forum* (pp. 28-30).
- Anderson, N., Thitimakorn, T., Ismail, A., & Hoffman, D. (2007). *A comparison of four geophysical methods for determining the shear wave velocity of soils*. *Environmental and Engineering Geoscience*, 13(1), 11-23. DOI: 10.2113/gseegeosci.13.1.11.
- Arjwech, R. (2011). *Electrical resistivity imaging for unknown bridge foundation depth determination*. Texas A&M University.
- ASTM D1586/D1586M-18 (2018). *Standard Test Method for Standard Penetration Test (SPT) and Split-Barrel Sampling of Soils*. West Conshohocken, PA; ASTM International, 2018. doi:10.1520/D1586\_D1586M-18, <[www.astm.org](http://www.astm.org)>.
- ASTM D2573/D2573M-18 (2018). *Standard Test Method for Field Vane Shear Test in Saturated Fine-Grained Soils*. West Conshohocken, PA; ASTM International. doi: 10.1520/D2573\_D2573M-18, <[www.astm.org](http://www.astm.org)>.
- ASTM D4318-17e1 (2017). *Standard Test Methods for Liquid Limit, Plastic Limit, and Plasticity Index of Soils*, ASTM International, West Conshohocken, PA, <[www.astm.org](http://www.astm.org)>.
- ASTM D4428/D4428M-07 (2007). *Standard Test Methods for Crosshole Seismic Testing*. ASTM International, West Conshohocken, PA. DOI: 10.1520/D4428\_D4428M-07, <[www.astm.org](http://www.astm.org)>.
- ASTM D5753-18 (2018). *Standard Guide for Planning and Conducting Geotechnical Borehole Geophysical Logging*, ASTM International, West Conshohocken, PA, DOI: 10.1520/D5753-18, <[www.astm.org](http://www.astm.org)>.
- ASTM D5777-00 (2011). *Standard Guide for Using the Seismic Refraction Method for Subsurface Investigation*, ASTM International, West Conshohocken, PA, DOI: 10.1520/D5777-00R11E01, <[www.astm.org](http://www.astm.org)>.

- ASTM D5778-12 (2012). *Standard Test Method for Electronic Friction Cone and Piezocone Penetration Testing of Soils*, ASTM International, West Conshohocken, PA, DOI: 10.1520/D5778-12, <www.astm.org>.
- ASTM D6285-99 (2016). *Standard Guide for Locating Abandoned Wells*, ASTM International, West Conshohocken, PA, <www.astm.org>.
- ASTM D6429-99 (2011). *Standard Guide for Selecting Surface Geophysical Methods*, ASTM International, West Conshohocken, PA, DOI: 10.1520/D6067\_D6067M-17, <www.astm.org>.
- ASTM D6429-99 (2011). *Standard Guide for Selecting Surface Geophysical Methods*, ASTM International, West Conshohocken, PA, DOI: 10.1520/D6067\_D6067M-17, <www.astm.org>.
- ASTM D6431-18 (2018). *Standard Guide for Using the Direct Current Resistivity Method for Subsurface Site Characterization*, ASTM International, West Conshohocken, PA, DOI: 10.1520/D6431-18, <www.astm.org>.
- ASTM D7015-04 (2004). *Standard Practices for Obtaining Undisturbed Block (Cubical and Cylindrical) Samples of Soils*, ASTM International, West Conshohocken, PA. <<https://compass.astm.org/Standards/HISTORICAL/D7015-04.htm>> (Jan 10, 2019).
- ASTM D7400/D7400M-19 (2019). *Standard Test Methods for Downhole Seismic Testing*. ASTM International, West Conshohocken, PA. DOI: 10.1520/D7400\_D7400M-19, <www.astm.org>.
- ASTM D7928-17 (2017). *Standard Test Method for Particle-Size Distribution (Gradation) of Fine-Grained Soils Using the Sedimentation (Hydrometer) Analysis*, ASTM International, West Conshohocken, PA, <www.astm.org>.
- ASTM D854-14 (2014). *Standard Test Methods for Specific Gravity of Soil Solids by Water Pycnometer*, ASTM International, West Conshohocken, PA, <www.astm.org>.
- ASTM G187-05 (2005). *Standard Test Method for Measurement of Soil Resistivity Using the Two-Electrode Soil Box Method*. ASTM International, West Conshohocken, PA, <www.astm.org>.
- Baral, A., Pourmand, P., Adhikari, I., Abediniangerabi, B., & Shahandashti, M. (2021). *A GIS-Based Data Integration Approach for Rainfall-Induced Slope Failure Susceptibility Mapping in Clayey Soils*. *ASCE Natural Hazard Review*, 22(3): 04021026
- Barker, R. D. (1979). Signal contribution sections and their use in resistivity studies. *Geophysical Journal International*, 59(1), 123-129.
- Barton C. A., Tesler L. G., Zoback M. D. (1992). *Interactive Image Analysis of Borehole Televiewer Data*. In: Palaz I., Sengupta S.K. (eds) *Automated Pattern Analysis in Petroleum Exploration*. Springer, New York, NY.
- Baynes, F.J. (2010). Sources of geotechnical risk, *Quarterly Journal of Engineering Geology and Hydrogeology*, 43, 321–331.
- Boeckmann, A. Z., & Loehr, J. E. (2016). *Influence of Geotechnical Investigation and Subsurface Conditions on Claims, Change Orders, and OVERRUNS* (No. Project 20-05, Topic 46-04).
- British Standards Institution, (2010). *Code of Practice for Site Investigation* (revised), BSI, London, England.
- Brunner, I., Friedel, S., Jacobs, F., & Danckwardt, E. (1999). Investigation of a Tertiary maar structure using three-dimensional resistivity imaging. *Geophysical Journal International*, 136(3), 771-780.

- Bureau of Ocean Energy Management (2017). *Geophysical and Geotechnical Investigation Methodology Assessment for Siting Renewable Energy Facilities on the Atlantic*, Retrieved from <<https://www.boem.gov/G-and-G-Methodology-Renewable-Energy-Facilities-on-the-Atlantic-OCS/>> (23 Aug, 2019).
- Campanella, R.G., Robertson, P.K., & Gillespie, D. (1986). *Seismic cone penetration test*, Use of In-Situ Tests in Geotechnical Engineering, S.P. Clemence, Ed., ASCE, GSP 6, pp. 116-130.
- Chen, D. and Scullion, T. (2007). *Using Nondestructive Testing Technologies to Assist in Selecting the Optimal Pavement Rehabilitation Strategy*, Journal of Testing and Evaluation, Vol. 35, No. 2, 2007, pp. 211-219, DOI: 10.1520/JTE100136.
- Christopher, B. R., Schwartz, C. W., Boudreaux, R., & Berg, R. R. (2006). Geotechnical aspects of pavements (No. FHWA-NHI-05-037). United States. Federal Highway Administration.
- Dahlin, T., & Zhou, B. (2004). A numerical comparison of 2D resistivity imaging with 10 electrode arrays. *Geophysical prospecting*, 52(5), 379-398.
- Damnjanovic, I., & Zhang, Z. (2006). *Determination of required falling weight deflectometer testing frequency for pavement structural evaluation at the network level*. Journal of transportation engineering, 132(1), 76-85.
- Desbrandes, R., and Clayton, R. (1994) *Measurement While Drilling*, In Developments in Petroleum Science (Vol. 38, pp. 251-279). Elsevier.
- Dowell, I., & Mills, A. A. *Measurement-While-Drilling (MWD), Logging-While-Drilling (LWD) and Geosteering*. John Wiley & Sons.
- Du, B., Chien, S., Lee, J., & Spasovic, L. (2017). Predicting freeway work zone delays and costs with a hybrid machine-learning model. *Journal of Advanced Transportation*, 2017.
- Edet, A. (2009). *Environmental Monitoring*. Encyclopedia of Life Support Systems. Inyang, H. I., and Daniels, J. L. (Eds.). Oxford, United Kingdom: Eolss Publishers Co. Ltd.
- Ekwue, E. & Bartholomew, J. (2010) *Electrical conductivity of some soils in Trinidad as affected by density, water, and peat content*. *Biosystems Engineering*, 108(2), 95–103.
- Ellis Jr, R. D., Degner, J., O'Brien, W., & Peasley, G. (2003). Review, Analyze and Develop Benefit Cost/return on Investment Equations, Guidelines and Variables (No. UF Proj. 4910 45-04-835,).
- Ellis, R. G., & Oldenburg, D. W. (1994). Applied geophysical inversion. *Geophysical Journal International*, 116(1), 5-11.
- Fenning, P. J., & Donnelly, L. J. (2004). *Geophysical techniques for forensic investigation*. Geological Society, London, Special Publications, 232(1), 11-20.
- FHWA (2018). *Advanced Geotechnical Exploration Methods*. Federal Highway Association. Retrieved from: <[https://www.fhwa.dot.gov/innovation/everydaycounts/edc\\_5/geotech\\_methods.cfm](https://www.fhwa.dot.gov/innovation/everydaycounts/edc_5/geotech_methods.cfm)> (Aug. 18, 2019).
- Fontenot, J. E. (1986). *Measurement While Drilling-A New Tool* (includes associated papers 15328 and 15343). *Journal of petroleum technology*, 38(02), 128-130.
- Furman, A., Ferré, T., & Warrick, A. W. (2003). A sensitivity analysis of electrical resistivity tomography array types using analytical element modeling. *Vadose Zone Journal*, 2(3), 416-423.
- Gazetas, G., 1991, *Foundation Vibrations: Foundation Engineering Handbook*, 2nd Edition, Hsai-Yang Fang, and Editor, 553-593.
- Geogiga Technology Corp. Retrieved from <https://www.geogiga.com/en/rt.php> (Dec 23, 2020).

- Geomative CO., LTD. retrieved from < <https://www.geomative.com/>>, (Oct 2, 2020).
- GeoTomo Software. Retrieved from <http://www.geotomosoft.com/> (Dec 23, 2020).
- Giao, P., Chung, S., Kim, D. & Tanaka, H. (2003) *Electric imaging and laboratory resistivity testing for geotechnical investigation of Pusan clay deposits*. Journal of Applied Geophysics, 52(4), 157–175.
- Gravley, W. (1983). *Review of downhole measurement-while-drilling systems*. Journal of Petroleum Technology, 35(08), 1-439.
- Griffiths, D. H., & Barker, R. D. (1993). *Two-dimensional resistivity imaging and modelling in areas of complex geology*. Journal of applied Geophysics, 29(3-4), 211-226.
- Gucunski, N., & Woods, R. D. (1991). *Use of Rayleigh modes in interpretation of SASW test*.
- Hossain, S., Kibria, G., & Khan, S. (2018). *Site Investigation using Resistivity Imaging*. CRC Press.
- Hunt, R. E. (2005). *Geotechnical engineering investigation handbook*. CRC Press.
- Iliesi, A. T., Tofan, A. L., & Presti, D. L. (2012). *Use of cone penetration tests and cone penetration tests with porewater pressure measurement for difficult soils profiling*. Buletinul Institutului Politehnic din Iasi. Sectia Constructii, Arhitectura, 58(3), 53.
- IRIS Instruments (2018). *Syscal Pro User's Manual*.
- Jongmans, D., & Garambois, S. (2007). *Geophysical investigation of landslides: a review*. Bulletin de la Société géologique de France, 178(2), 101-112.
- Kearey, P., Brooks, M., (1991). *An Introduction to Geophysical Exploration*, second ed. Blackwell Scientific, Oxford Publishing House.
- Kearey, P., Brooks, M., & Hill, I. (2013). *An introduction to geophysical exploration*. John Wiley & Sons.
- Kibria, G. & Hossain, M. S. (2012). *Investigation of geotechnical parameters affecting electrical resistivity of compacted clays*. Journal of Geotechnical and Geoenvironmental Engineering, 138(12), 1520–1529.
- Kibria, G. & Hossain, M.S. (2017). *Electrical resistivity of compacted clay minerals*. Environmental Geotechnics. Retrieved from <<https://doi.org/10.1680/jenge.16.00005>>, ICE.
- Kneisel, C. (2006). *Assessment of subsurface lithology in mountain environments using 2D resistivity imaging*. Geomorphology, 80(1-2), 32-44.
- Kouchaki, B. M., Bernhardt-Barry, M. L., Wood, C. M., & Moody, T. (2018). *A Laboratory Investigation of Factors Influencing the Electrical Resistivity of Different Soil Types*. Geotechnical Testing Journal, 42(4), 829-853.
- Leggio, M. (2012). *Accurate evaluation of the ground impedance of real earthing systems*.
- Lenke, L. R. (2006). *Settlement Issues--Bridge Approach Slabs*.
- Li, Z., Itakura, K. I., & Ma, Y. (2014). *Survey of measurement-while-drilling technology for small-diameter drilling machines*. Electronic Journal of Geotechnical Engineering, 19(2), 10267-10282.
- Libric, L., Jurić-Kačunić, D., & Kovacevic, M. S. (2017). *Application of cone penetration test (CPT) results for soil classification Application of cone penetration test (CPT) results for soil classification*. GRAĐEVINAR. 1. (11-20). DOI: 10.14256/JCE.1574.2016.
- Loehr, E., Lutenegger, A., Rosenblad, B., Boeckmann, A. (2017). *Geotechnical Site Characterization, Geotechnical Engineering Circular NO.5*. National Highway Institute. FHWA NHI-16-072. Federal Highway Administration, Washington, DC.

- Loke, M. H. (1999). *Electrical imaging surveys for environmental and engineering studies. A practical guide to*, 2.
- Loke, M. H. (2004). Tutorial: 2-D and 3-D electrical imaging surveys.
- Loke, M. H. (2015). RES2DINVx64 ver. 4.05: Rapid 2-D Resistivity & IP inversion using the least-squares method. Geotomosoft solutions, Geotomo Software PTY LTD.
- Luna, R., & Jadi, H. (2000). *Determination of dynamic soil properties using geophysical methods*. In Proceedings of the first international conference on the application of geophysical and NDT methodologies to transportation facilities and infrastructure, St. Louis, MO (pp. 1-15).
- Lunne, T., Powell, J. J., & Robertson, P. K. (2002). *Cone penetration testing in geotechnical practice*. CRC Press.
- Mayne, P. W., Christopher, B. R., & DeJong, J. (2002). *Manual on subsurface investigations*. National Highway Institute. Sp. Pub. FHWA NHI-01-031. Federal Highway Administration, Washington, DC.
- Megger Publication (2010). *Getting Down to Earth (A practical guide to Earth Resistance Testing)*.
- Milsom, J. (2003). *Field geophysics (Vol. 31)*. John Wiley & Sons.
- Palacky, G. J. (1988). *Resistivity characteristics of geologic targets*. *Electromagnetic methods in applied geophysics*, 1, 53-129.
- Park, C. B. (1995). *Characterization of geotechnical sites by multi-channel analysis of surface waves (mcasw)*. KGS Fall, 95, 141-148.
- RESISTIVITY.NET Productions. Retrieved from <http://www.resistivity.net/dc2dinvres/> (Dec 23, 2020).
- Reynolds, J. M. (2011). *An introduction to applied and environmental geophysics*. John Wiley & Sons.
- Rinaldi, V.A. & Cuestas, G.A. (2002) *Ohmic conductivity of a compacted silty clay*. *Journal of Geotechnical and Geoenvironmental Engineering*, 128(10), 824-835.
- Rivers, B. S. (2016). *Measurement While Drilling (MWD) [PowerPoint Slides]*. FHWA – Resource Center.
- Robertson, P. K., Campanella, R. G., Gillespie, D., & Rice, A. (1986). *Seismic CPT to measure in situ shear wave velocity*. *Journal of Geotechnical Engineering*, 112(8), 791-803.
- Rogers, J. D. (2009). *Fundamentals of Cone Penetrometer Test (CPT) Soundings*. Missouri University of Science and Technology: USA.
- Rosenblad, B. L., & Boeckmann, A. Z. (2020). *Advancements in Use of Geophysical Methods for Transportation Projects (No. Project 20-05, Topic 50-01)*.
- Roth, M. J. S., & Nyquist, J. E. (2003). *Evaluation of multi-electrode earth resistivity testing in karst*. *Geotechnical Testing Journal*, 26(2), 167-178.
- Samouëlian, A., Cousin, I., Tabbagh, A., Bruand, A., & Richard, G. (2005). *Electrical resistivity survey in soil science: a review*. *Soil and Tillage research*, 83(2), 173-193.
- Sass, O. (2006). *Determination of the internal structure of alpine talus deposits using different geophysical methods (Lechtaler Alps, Austria)*. *Geomorphology*, 80(1-2), 45-58.
- Schepers, R., Rafat, G., Gelbke, C., & Lehmann, B. (2001). *Application of borehole logging, core imaging and tomography to geotechnical exploration*. *International Journal of Rock Mechanics and Mining Sciences*, 38(6), 867-876.
- Schoenleber, J. R. (Ed.). (2005). *Field sampling procedures manual*. Trenton, NJ: The Department of Environmental Protection, Chapter 8.

- Schrank, D., Eisele, B., Lomax, T., & Bak, J. (2015). 2015 urban mobility scorecard. U.S. Department of transportation. (2017). Facts and Statistics – Work Zone Mobility. Retrieved from the Federal Highway Administration website: [https://ops.fhwa.dot.gov/wz/resources/facts\\_stats/mobility.html](https://ops.fhwa.dot.gov/wz/resources/facts_stats/mobility.html)
- Seidel, K., & Lange, G. (2007). *Direct current resistivity methods*. In *Environmental Geology* (pp. 205-237). Springer, Berlin, Heidelberg.
- Seo, J., Ha, H., & Briaud, J. L. (2002). Investigation of settlement at bridge approach slab expansion joint: Numerical simulations and model tests (No. FHWA/TX-03/0-4147-2.).
- Shahandashti, M., Hossain, S., Baral, A., Adhikari, I., Pourmand, P., Abediniangerabi, B. (2020). *Slope Repair and Maintenance Management System* (Report 5-6957-01). Texas Department of Transportation. <https://rip.trb.org/view/1804045>.
- Shrestha, P. P., & Maharjan, R. (2018). Effects of Change Orders on Cost Growth, Schedule Growth, and Construction Intensity of Large Highway Projects. *Journal of Legal Affairs and Dispute Resolution in Engineering and Construction*, 10(3), 04518012.
- Sirles, P. C. (2006). *Use of geophysics for transportation projects* (Vol. 357). Transportation Research Board.
- South Dakota Department of Environment and Natural Resources (2003). Standard Operating Procedure 9, *Drilling Methods*. Retrieved from <<https://denr.sd.gov/des/gw/Spills/Handbook/SOP9.pdf>> (Aug 18, 2019).
- Srinivasamoorthy, K., Sarma, V. S., Vasantavigar, M. P., Vijayaraghavan, K., & Chidambaram, S. (2009). *Electrical imaging techniques for groundwater pollution studies: a case study from Tamil Nadu state, South India*. *Earth Sciences Research Journal*, 13(1), 30-39.
- Suzuki, K., Toda, S., Kusunoki, K., Fujimitsu, Y., Mogi, T., & Jomori, A. (2000). *Case studies of electrical and electromagnetic methods applied to mapping active faults beneath the thick quaternary*. In *Developments in geotechnical engineering* (Vol. 84, pp. 29-45). Elsevier.
- Telford, W. M., Telford, W. M., Geldart, L. P., Sheriff, R. E., & Sheriff, R. E. (1990). *Applied geophysics*. Cambridge university press.
- Texas Department of Transportation (TxDOT), (1999). *Test Procedure for Texas Cone Penetration*. Retrieved from <[http://ftp.dot.state.tx.us/pub/txdot-info/cst/TMS/100-E\\_series/pdfs/soi132.pdf](http://ftp.dot.state.tx.us/pub/txdot-info/cst/TMS/100-E_series/pdfs/soi132.pdf)>. (23 Aug, 2019)
- Texas Department of Transportation (TxDOT), (2013). Geotechnical Investigation Report SH 71 – From East Riverside to SH 130. CSJ No. 0265-01-110. Retrieved from <<https://ftp.dot.state.tx.us/pub/txdot-info/spd/cda/sh71-express/project-documents/geotechnical/geotechnical-report-final-10-31.pdf>> (23 Aug, 2019).
- Texas Department of Transportation (TxDOT), (2013). Geotechnical Investigation Report, Loop 1604 Western Extension. CSJ No. 2452-01-055. Retrieved from <[https://ftp.dot.state.tx.us/pub/txdot-info/sat/loop1604\\_western/rid\\_042613/geotechnical/11c\\_lp1604\\_draft\\_geotechnical\\_report.pdf](https://ftp.dot.state.tx.us/pub/txdot-info/sat/loop1604_western/rid_042613/geotechnical/11c_lp1604_draft_geotechnical_report.pdf)>. (23 Aug, 2019).
- Texas Department of Transportation (TxDOT), (2015). Pavement Design Report, Us 82 from 0.5 Mi. West of SH 121 to 0.5 Mi. East of SH 56. CSJ No.: 0045-20-018.
- Texas Department of Transportation (TxDOT), (2018). *Geotechnical Manual*, Texas Department of Transportation (TxDOT), Retrieved from <<http://onlinemanuals.txdot.gov/txdotmanuals/geo/geo.pdf>>. (23 Aug, 2019).
- Texas Department of Transportation (TxDOT), (2018). Geotechnical Study, IH 20 Frontage Roads from North Main Street to Camp Wisdom Road. CSJ No. 2374-04-060. Retrieved from <

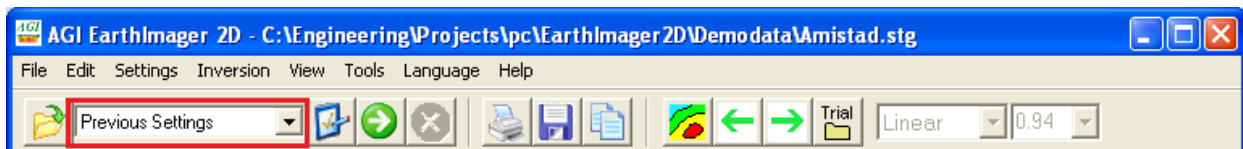


- <https://ftp.dot.state.tx.us/pub/txdot-info/Pre-Letting%20Responses/Dallas%20District/Construction%20Projects/December%202018/Dallas%20County/2374-04-060%20IH20%20Frtdg/DG-13-16563.5%20IH%2020%20Frontage%20Road%20Final%20Geotechnical%20Report%2011-13-18.pdf> >. (23 Aug, 2019).
- Texas Department of Transportation (TxDOT), (2020). Agency Strategic Plan for Fiscal Years 2021-2025. Retrieved from the Texas Department of Transportation website: <https://ftp.txdot.gov/pub/txdot/commission/2020/0528/9.pdf>
- Texas Department of Transportation (TxDOT), (2021). Work Zones. Retrieved from the Texas Department of Transportation website: <https://www.txdot.gov/inside-txdot/media-center/psas/distracted-driving/work-zones.html>
- Tyrrell, A. P., Lake, L. M., & Parsons, A. W. (1983). An investigation of the extra costs arising on highway contracts (No. SR 814 Monograph).
- Vipulanandan, C., Puppala, A. J., Jao, M., Kim, M. S., Vasudevan, H., Kumar, P., & Mo, Y. L. (2008). *Correlation of Texas Cone Penetrometer Test Values and Shear Strength of Texas Soils: Technical Report* (No. FHWA/TX-08/0-4862-1).
- Ward, S. H. (1988). *The resistivity and induced polarization methods*. In *Symposium on the Application of Geophysics to Engineering and Environmental Problems*. (pp. 109-250). Society of Exploration Geophysicists.
- Ward, S. H. (Ed.). (1990). *Geotechnical and Environmental Geophysics: Volume I, Review and Tutorial: Volume I: Review and Tutorial*. Society of Exploration Geophysicists.
- Watanabe, F., & Takeuchi, T. (2004). Application of geophysical methods to engineering and environmental problems: Advisory Committee on Standardization. SEG of Japan.
- Weary, D. J. (2015). The Cost of Karst Subsidence and Sinkhole Collapse in The United States Compared With Other Natural Hazards. 14TH SINKHOLE CONFERENCE.
- Wightman, W., Jalinoos, F., Sirles, P., & Hanna, K. (2004). *Application of geophysical methods to highway related problems* (No. FHWA-IF-04-021).
- Williams, J. H., & Johnson, C. D. (2004). *Acoustic and optical borehole-wall imaging for fractured-rock aquifer studies*. *Journal of Applied Geophysics*, 55(1-2), 151-159. DOI: 10.1016/j.jappgeo.2003.06.009.
- Yang, J.S. (2002) *Three Dimensional Complex Resistivity Analysis for Clay Characterization in Hydrogeologic Study*. Ph.D. thesis, University of California, Berkeley.
- Ye, L., Hui, Y., & Yang, D. (2013). Road traffic congestion measurement considering impacts on travelers. *Journal of Modern Transportation*, 21(1), 28-39.
- Zond Software. Retrieved from <http://zond-geo.com/english/zond-software/ert-and-ives/zondres2d/> (Dec 23, 2020).

## APPENDIX A 2D RESISTIVITY INVERSION SOFTWARE SETTINGS

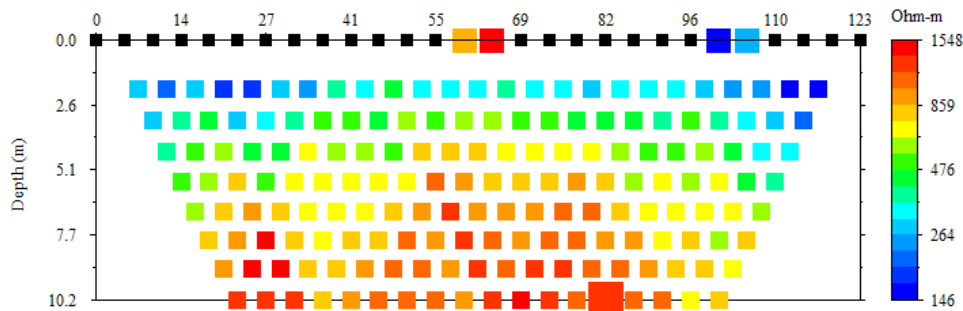
The commonly used software programs for data processing are RES2DINV, EarthImager, and DC2DINVRES (GeoTomo Software, Advanced Geoscience Inc., Resistivity.net Productions). These software programs provide 2D inverted resistivity sections of the subsurface for the field electrical resistivity data. The results obtained by these software programs might be slightly different from each other as they use different techniques in forward and inversion modeling. However, similar settings could be found in these software programs. As an example, details of the available tools in the EarthImager for processing the electrical resistivity data are presented here.

EarthImager is a Windows based software program and requires a license (Advanced Geoscience Inc., 2009). It includes several tools and settings to process the data file from the resistivity meter and to provide an inverted electrical resistivity image of the subsurface in a straightforward process. The type of survey (e.g., surface, borehole, or roll-along) is automatically detected by the EarthImager software program based on the electrode geometry. However, it can be changed from the available toolbar in the EarthImager software program as shown in Figure A.1.



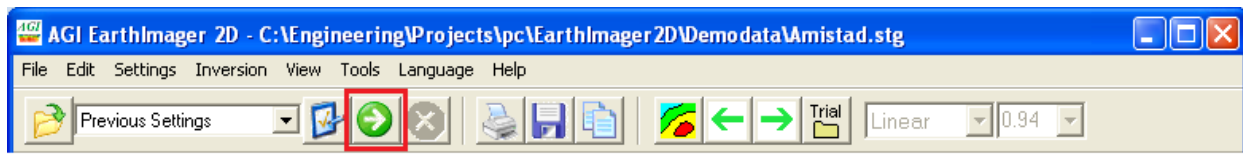
**Figure A.1** Type of survey setting

By loading the data file into the EarthImager software program, it provides a scatter plot of apparent resistivity pseudo-section of the survey. An example of a scatter plot for a data set is shown in Figure A.2. When one clicks on each data point on the scatter plot, the four corresponding electrodes used for the measurement would be highlighted. Also, a noisy data point (shown in black dots) can be manually removed from the scatter plot.



**Figure A.2** Example of a scatter plot for a data set

The EarthImager software program uses the data file to automatically generate a set of parameters for processing of the electrical resistivity data. The data processing can be performed by clicking on the run button (shown in Figure A.3) in the EarthImager software program. Therefore, the electrical resistivity images of the subsurface can be obtained using the default parameters of the software program.



**Figure A.3** Start inversion modeling by clicking on the run button in the EarthImager software program

Although the EarthImager has a set of default parameters, a user can change the default parameters for each data set based on the subsurface (e.g., geometry, minimum and maximum values of material's electrical resistivity) and survey (e.g., minimum voltage, ratio of voltage to transmitted current) characteristics. Here, initial settings, forward modeling, and inversion modeling process settings of the EarthImager software program are presented as examples of the available tools for processing the data to obtain electrical resistivity images of the subsurface.

## A.1. Initial Settings

Criteria for removing the noisy readings and different algorithms for inversion modeling are explained in the following paragraphs.

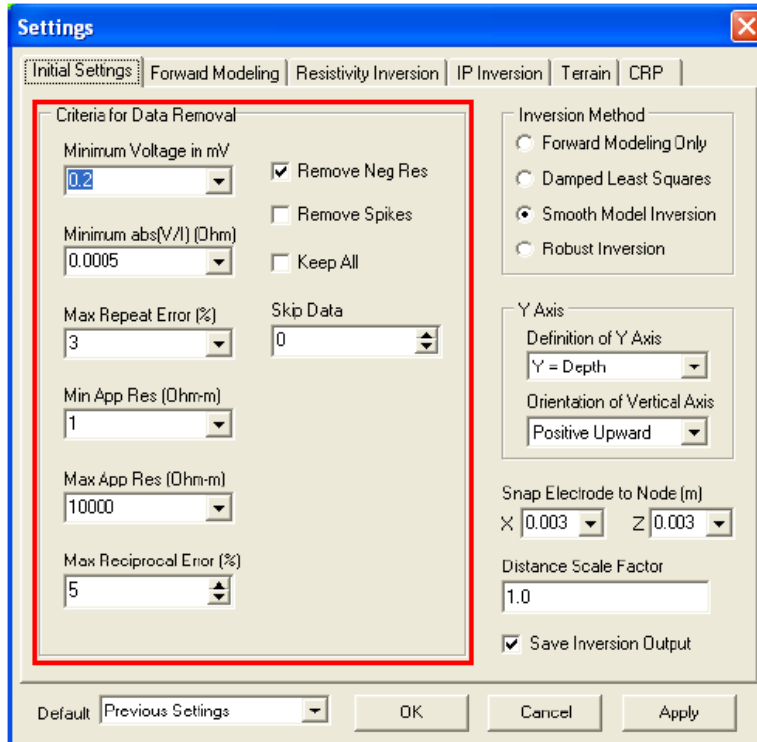
### A.1.1. Criteria for Removing Noisy Readings

The presence of noisy readings (data points) in the data leads to inaccurate models of the subsurface. Systematic and random noises are the two reasons for creating noisy data (Loke, 1999).

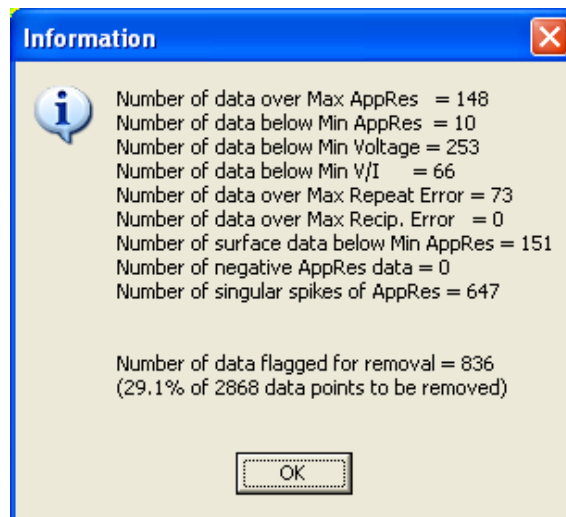
The former refers to a failure during the survey, such as lack of suitable ground contact, breakage in cables, the inappropriate placement of the electrodes, and improper attachment of cables to the electrodes. The data points on the pseudo-section plot and profile plot with unusually high or low electrical resistivity values illustrate noisy readings caused by systematic noise. The latter refers to the telluric currents that affect all the readings.

The random noise is more common for the electrode configurations with large geometric factors (e.g., dipole-dipole and pole-dipole arrays) and very small potentials for the same current compared to other electrode configurations (e.g., Wenner array). The systematic noise can be manually removed from the data sets; however, it is impractical to remove the noisy data points caused by random noise, especially when the data set contains more than a thousand points (Loke, 2004). The available tools in software programs have facilitated removing of poorly-fit data. For example, there are some criteria for removing the noisy readings (before inversion modeling) within the initial settings of the EarthImager software program (Figure A.4). For the surface electrical resistivity surveys, the signals less than 1mV cannot be measured accurately. So, the minimum voltage should be considered around 1mV. Also, the minimum absolute value of  $V/I$  (ratio of the voltage to transmitted current) should be considered in the range of  $2 \times 10^{-4}$  and  $5 \times 10^{-4}$ . The maximum repeat error in the measurements is usually assumed to be between 5% and 10%. It is recommended to use values in the range of 0.1 to 1 for the minimum apparent resistivity and  $1 \times 10^4$  to  $1 \times 10^5$  for the maximum apparent resistivity (Advanced Geoscience Inc., 2009). Therefore, all the negative apparent resistivity values would be removed from the data by these threshold values (negative apparent resistivity values are not allowed for surface electrical resistivity surveys). The maximum reciprocal error, which is usually greater than the repeat error, is essential when the forward and reverse electrical resistivity surveys are performed in the field. To remove the noisy readings that are associated with the anomalous and singular electrodes, “Remove Spikes” should be enabled. The inversion process will use all the data points if “Keep All” is enabled.

Based on these criteria, the program flags the data points beyond these thresholds as noisy readings, which could be removed manually from the data. The quality of a data set based on the data removal threshold may be checked by selecting the editing statistics option in the EarthImager software program, as shown in Figure A.5.



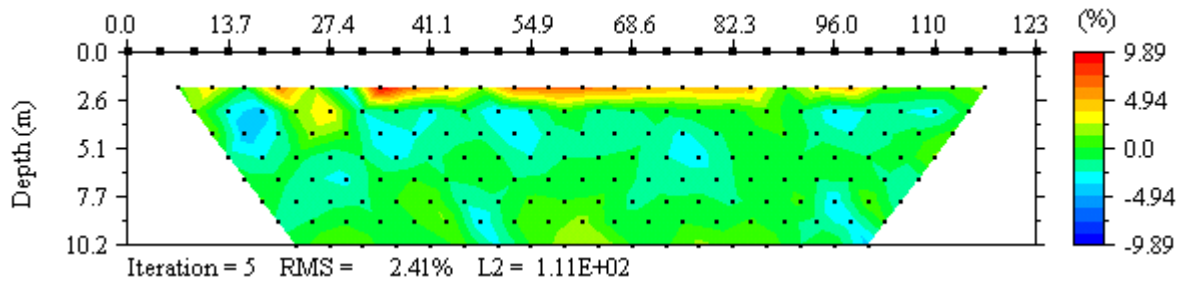
**Figure A.4** Data removal criteria for EarthImager software program



**Figure A.5** Example of the statistics of a data set of the EarthImager software program

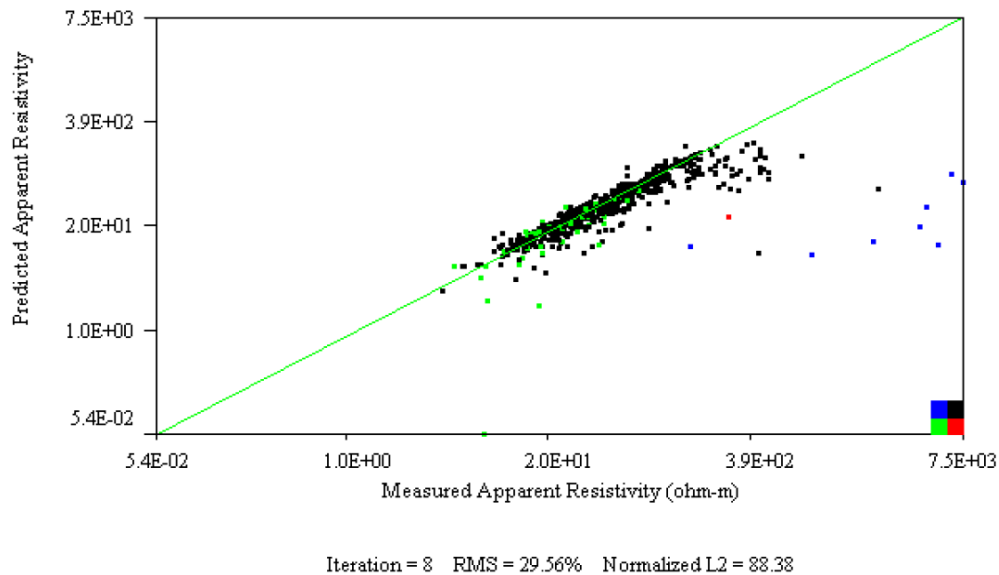
For the surface electrical resistivity data, the relative data error (RMS error) pseudo-section illustrates the relative errors for each data point. The relative data error is defined as the ratio of the difference between calculated and measured electrical resistivity to the measured electrical resistivity. Therefore, the relative data error, which can be negative or positive depending on the magnitude of the calculated electrical resistivity, could be shown on a pseudo-section for all the

data points. Figure A.6 shows an example of a relative data error pseudo-section for a data set using the EarthImager software program.



**Figure A.6** Example of relative data error pseudo-section for a data set using the EarthImager software program

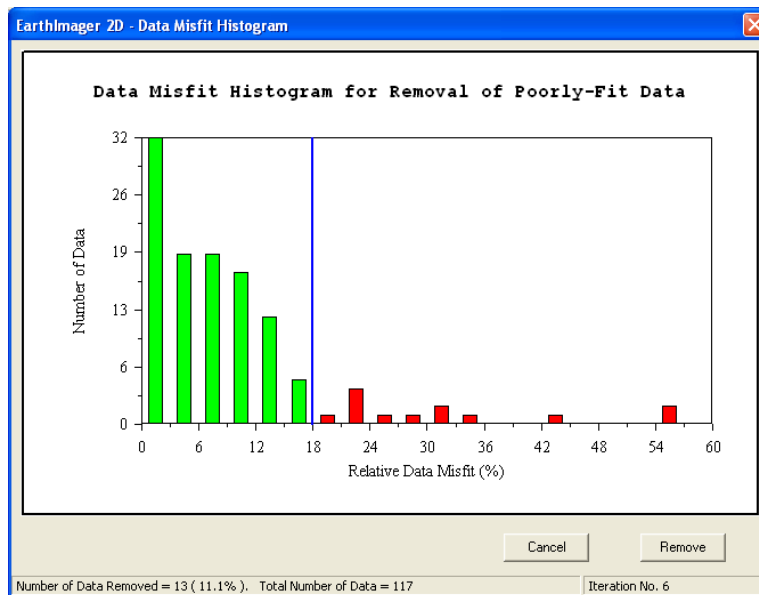
Another way to visualize the data misfit is to use a cross-plot of measured and calculated electrical resistivity data. If the measured and calculated measurements for the data points fit well, the data points will lie on a straight line (green line in Figure A.7). The different colors of the data points in Figure A.7 indicate the signs of the measured and calculated electrical resistivity values. For example, the color is black or green when both the calculated and measured electrical resistivity measurements have positive or negative values, respectively.



**Figure A.7** Cross-plot of measured and calculated electrical resistivity data using the EarthImager software program

After the inversion modeling, the noisy readings could be removed using a data misfit histogram. An example of a data misfit histogram for the EarthImager software program is shown in Figure

A.8. The horizontal and vertical axes present the absolute value of relative data misfit and the number of data points, respectively. In general, the data points with relative data misfit of greater than 50% are assumed as noisy data and should be removed from the dataset (Advanced Geoscience Inc., 2009). The noisy readings can be removed by moving the threshold line (blue line in Figure A.8) to the right or left and clicking the remove button.

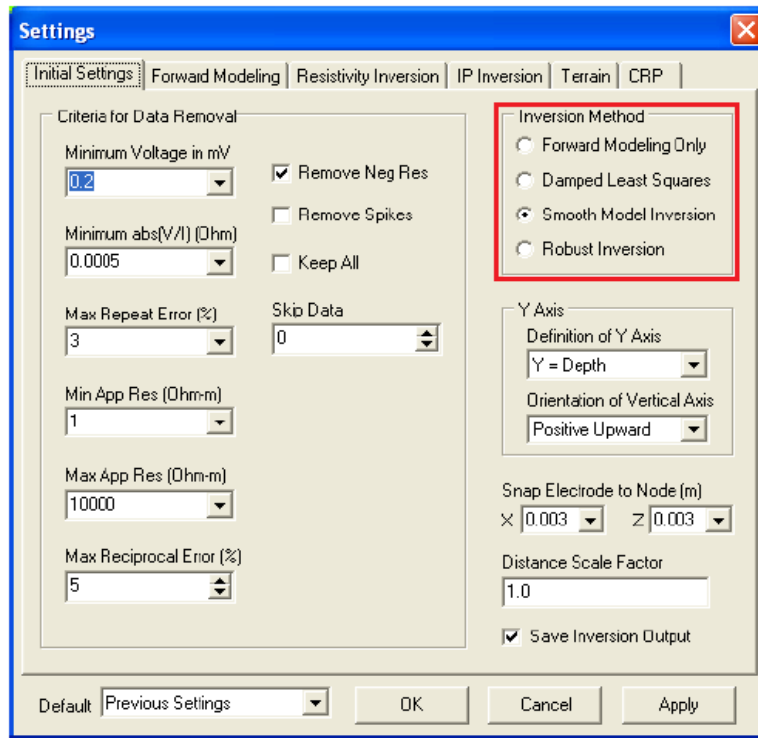


**Figure A.8** An example of a data misfit histogram for the EarthImager software program. Here, the 36% relative data misfit can be considered as a threshold for data removal.

### A.1.2. Inversion Method Selection

There are various methods for the inversion of the electrical resistivity data. The EarthImager software program uses a smooth inversion method (also known as  $l_2$ -norm) by default, which assumes gradual variation in the electrical resistivity of subsurface material (e.g., bedrock with a thick transitional weathered layer) (Arjwech, 2011; Advanced Geoscience Inc., 2009). Figure A.9 shows the inversion modeling methods in the EarthImager software program. However, for creating models of subsurface bodies that are internally homogenous with sharp boundaries (e.g., igneous intrusive in sedimentary rocks), a robust (also known as  $l_1$ -norm or blocky) inversion method is preferred (Ellis and Oldenburg, 1994; Dahlin and Zhou, 2004). Mostly, field data sets lie between the two extremes of the smoothly varying electrical resistivity and discrete geological bodies with sharp boundaries (Loke, 1999). Without prior knowledge about subsurface geometry, the two extreme methods might be utilized to obtain the two possible extreme profiles. Then, the

interpretation will be made based on similar features in both models. The other two alternatives, “Forward Modeling Only” and “Damped Least Squares” are rarely used.



**Figure A.9** Inversion modeling methods of EarthImager software program

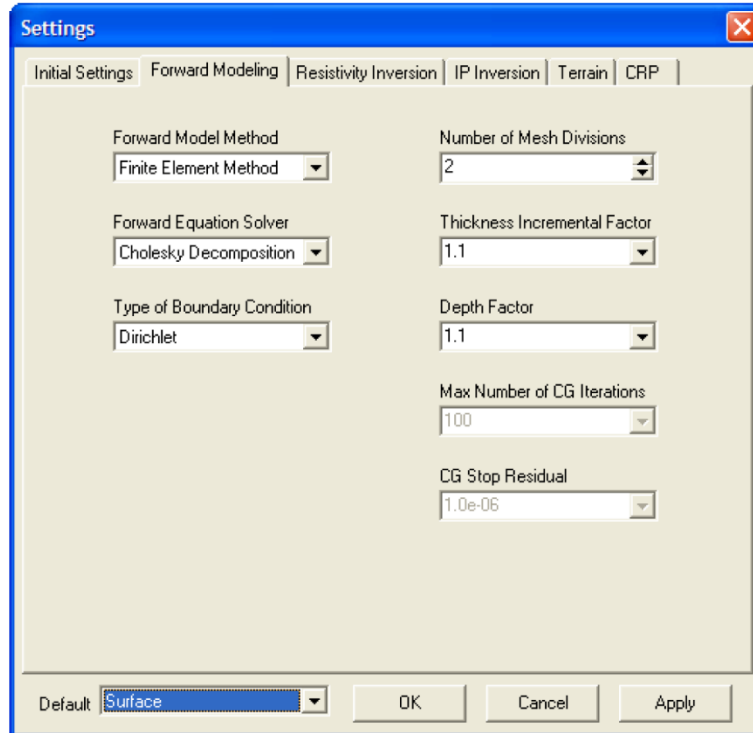
## A.2. Forward Modeling Settings

There are various criteria specific to the forward modeling process in the software program settings. There are two algorithms for performing forward modeling: finite element and finite difference. Although the finite difference is a default setting, the finite element method gives more accurate models of the subsurface (Loke, 2015; Advanced Geoscience Inc., 2009). Also, there are two options for selecting the forward equation solver: Cholesky decomposition and conjugate gradient. However, the Cholesky decomposition method is highly recommended (Advanced Geoscience Inc., 2009). Besides, there are no significant differences between the different boundary condition alternatives.

The number of mesh divisions (minimum number of cells between the two electrodes) affects the accuracy and duration of the forward modeling (a finer mesh produces higher accuracy). It is recommended to set the thickness incremental factor (ratio of the thickness of the lower layer to the thickness of the layer above it) in the range of 1 to 2 to consider the thickening of the subsurface



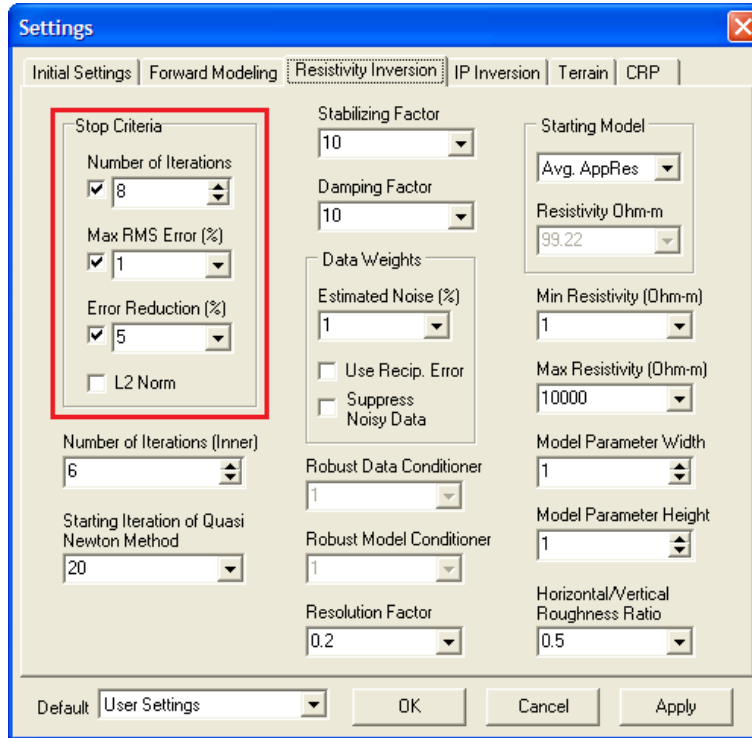
layers through the depth. The depth factor is used to determine the depth of the inverted section, which is recommended to be between 1 and 1.5 (Advanced Geoscience Inc., 2009). Figure A.10 shows the forward modeling settings of the EarthImager software program.



**Figure A.10** Forward modeling settings of the EarthImager software program

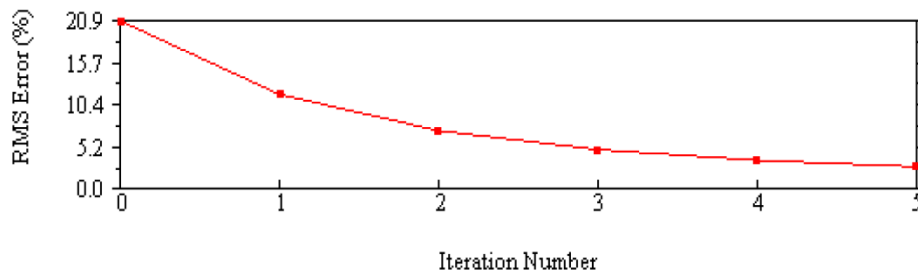
### A.3. Inversion Modeling Settings

There are also several criteria specific to the inversion modeling process in the software program settings. The iterative process is controlled by three parameters: the number of iterations, maximum RMS error, and error reduction. For the surface electrical resistivity survey, the number of iterations should be considered between 8 to 10 (Advanced Geoscience Inc., 2009). The iterative inversion for a nonlinear problem is performed in two steps: converting a nonlinear to a linear problem (outer loop), and solving the linearized problem (inner loop). Therefore, there is an option for the number of iterations (inner loop), which should be considered between 5 and 10. Generally, the maximum RMS error is selected in the range of 1% to 5%. If the RMS errors of the two iterations are less than the error reduction parameter, the inversion will be stopped. It is recommended to select a value of less than 5% for the error reduction (Loke, 2015; Advanced Geoscience Inc., 2009). Moreover, the starting iteration of the quasi-Newton method should not be less than 20. Figure A.11 shows the stop criteria settings of the EarthImager software program.



**Figure A.11** Stop criteria settings of the EarthImager software program

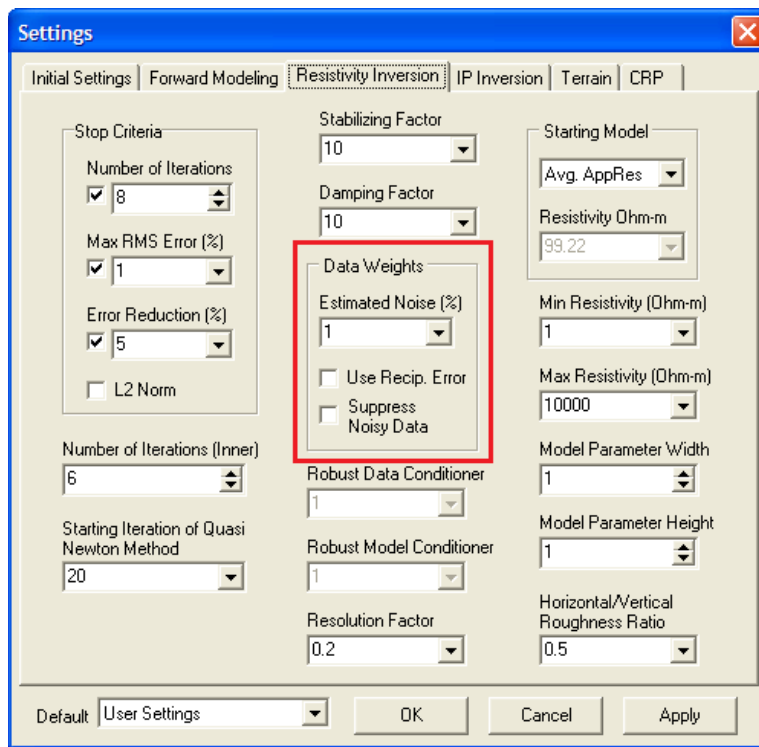
The convergence curve illustrates the RMS error versus the number of iterations. It shows how much the RMS error is reduced in each iteration compared to the previous inversion process until the process stops. An example of a convergence curve for a data set using the EarthImager software program is shown in Figure A.12.



**Figure A.12** Example of a convergence curve for a data set using the EarthImager software program. The inversion process stopped after 5 iterations.

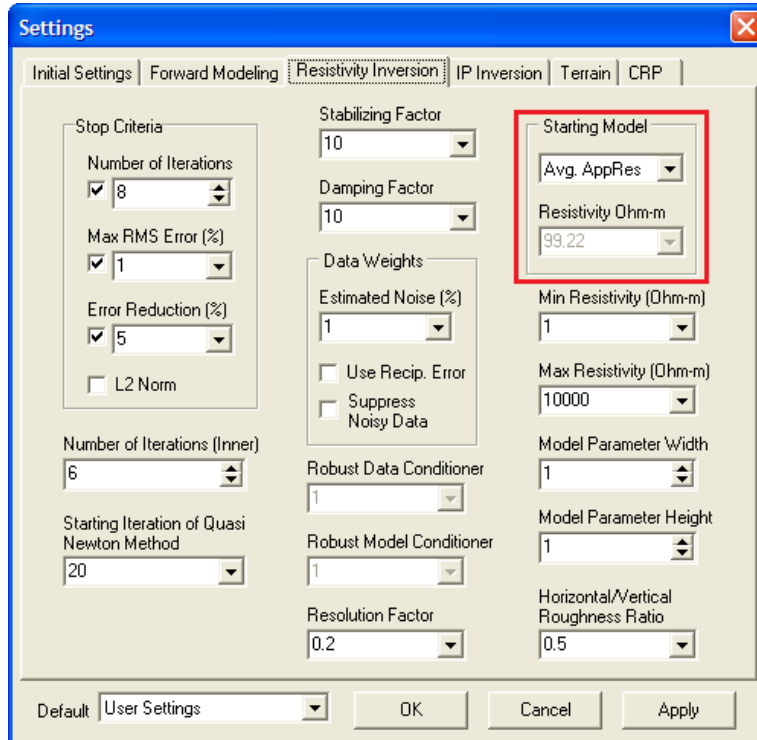
The stabilizing factor, which balances the model constraints and data misfit, is set to 10 by default. Small and large stabilizing factor numbers generate relatively rough and smooth models, respectively. The damping factor, which accelerates the inversion process at the early stages, should be considered the same for the stabilizing factor (Advanced Geoscience Inc., 2009).

When the “L2 Norm” is enabled from the “Stop Criteria” section (L2-norm minimizes a weighted data misfit), the data weights (errors) make a difference in the results. There are three settings in the data weights section: estimated noise, use reciprocal errors, and suppress noisy data. The estimated noise is recommended to be in the range of 1% to 5% (Advanced Geoscience Inc., 2009). When the forward and reverse electrical resistivity surveys are performed in the field, the “Use Recip. Error” needs to be enabled. In the case of having noisy data or a slow convergence, the “Suppress Noisy Data” should be enabled. Figure A.13 shows the data weights settings of the EarthImager software program. The “Robust Data Conditioner” and “Robust Model Conditioner” are only used if the robust inversion method is selected for the modeling (suggested to set 1%).



**Figure A.13** Data weights settings of EarthImager software program

The results of inversion modeling are highly dependent on the type of starting model. There are three different models to select as the starting model for inversion: interpolated pseudo-section, average apparent resistivity (default setting), and custom homogeneous model. Therefore, it is recommended to use interpolated pseudo-section for a good quality surface data set and average apparent resistivity for a noisy surface data set. The use of a custom homogeneous model is not recommended (Advanced Geoscience Inc., 2009). Figure A.14 shows the starting model settings of the EarthImager software program.



**Figure A.14** Starting model settings of the EarthImager software program

The minimum and maximum resistivity values can be changed depending on the typical subsurface resistivity values. If there are layered earth materials, the model parameter width can reduce the lateral variations of electrical resistivity in the inverted section. Also, the resolution of the model in the areas with low sensitivity (refer to Section 2.3.2) can be enhanced by the resolution factor, which is considered in the range of 0 to 0.3 (value of 0 disables this factor). Depending on the geometry of the subsurface, the roughness ratio can have a value greater than 1 (for a survey with high horizontal variations) and less than 1 (for a survey with high vertical variations). Without prior knowledge about the geometry of the subsurface, the roughness factor should be set to 1 (Advanced Geoscience Inc., 2009).

**APPENDIX B BORHOLE LOGS**

**Beaumont District (October 2019)**

GEOTECH BH COLUMNS - GINT STD US LAB.GDT - 4/3/20 01:45 - C:\USERS\MXA0516\ONEEDRIVE - UNIVERSITY OF TEXAS AT ARLINGTON\LAB DOCS\RESISTIVITY IMAGING\TEST RESULTS\SITE RESISTIVITY RESULTS\BEAUMONT\PI1\BORELOG.P1\BORELOG.INFO

<b>LOGO</b>	The University of Texas at Arlington 416 Yates Street 76010	<b>BORING NUMBER P1</b> PAGE 1 OF 1
<b>CLIENT</b> _____		<b>PROJECT NAME</b> _____
<b>PROJECT NUMBER</b> <u>First Visit</u>		<b>PROJECT LOCATION</b> <u>Beaumont</u>
<b>DATE STARTED</b> <u>10/13/19</u> <b>COMPLETED</b> <u>10/13/19</u>		<b>GROUND ELEVATION</b> _____ <b>HOLE SIZE</b> _____ inches
<b>DRILLING CONTRACTOR</b> _____		<b>GROUND WATER LEVELS:</b>
<b>DRILLING METHOD</b> _____		<b>AT TIME OF DRILLING</b> --
<b>LOGGED BY</b> _____ <b>CHECKED BY</b> _____		<b>AT END OF DRILLING</b> --
<b>NOTES</b> _____		<b>AFTER DRILLING</b> --

DEPTH (ft)	GRAPHIC LOG	MATERIAL DESCRIPTION	SAMPLE TYPE NUMBER	RECOVERY % (RQD)	BLOW COUNTS (N VALUE)	POCKET PEN. (tsf)	DRY UNIT WT. (pcf)	MOISTURE CONTENT (%)	ATTERBERG LIMITS			FINES CONTENT (%)
									LIQUID LIMIT	PLASTIC LIMIT	PLASTICITY INDEX	
0												
	[Diagonal Hatching]	(SC) Gray to Brown; Sandy Clay	SS		8-11-3 (14)							
	[Diagonal Hatching]	(CL) Brown to Dark Brown; Clay; Moist										
5	[Diagonal Hatching]	(CH) Brown; Clay	SPT		2-2-2 (4)							
	[Diagonal Hatching]	(CH) Brown; Clay; Moist	ST									
10	[Diagonal Hatching]		SPT		1-2-2 (4)							

Bottom of borehole at 11.5 feet.

GEO TECH BH COLUMNS - GINT STD US LAB.GDT - 4/3/20 01:46 - C:\USERS\WXA0516\ONEEDRIVE - UNIVERSITY OF TEXAS AT ARLINGTON\LAB DOCS\RESISTIVITY IMAGING\TEST RESULTS\BEAUMONT\BP1\BORELOG.INF

<b>LOGO</b>	The University of Texas at Arlington 416 Yates Stress 76010	<b>BORING NUMBER P4</b> PAGE 1 OF 1
<b>CLIENT</b> _____ <b>PROJECT NAME</b> _____		<b>PROJECT NUMBER</b> <u>First Visit</u> <b>PROJECT LOCATION</b> <u>Beaumont</u>
<b>DATE STARTED</b> <u>10/14/19</u> <b>COMPLETED</b> <u>10/14/19</u>		<b>GROUND ELEVATION</b> _____ <b>HOLE SIZE</b> _____ inches
<b>DRILLING CONTRACTOR</b> _____		<b>GROUND WATER LEVELS:</b>
<b>DRILLING METHOD</b> _____		<b>AT TIME OF DRILLING</b> ---
<b>LOGGED BY</b> _____ <b>CHECKED BY</b> _____		<b>AT END OF DRILLING</b> ---
<b>NOTES</b> _____		<b>AFTER DRILLING</b> ---

DEPTH (ft)	GRAPHIC LOG	MATERIAL DESCRIPTION	SAMPLE TYPE NUMBER	RECOVERY % (RQD)	BLOW COUNTS (N VALUE)	POCKET PEN. (tsf)	DRY UNIT WT. (pcf)	MOISTURE CONTENT (%)	ATTERBERG LIMITS			FINES CONTENT (%)
									LIQUID LIMIT	PLASTIC LIMIT	PLASTICITY INDEX	
0												
~1.5		(CL) Light Brown, gray; Silty Clay; Moist;	ST									
~3.5		(CL-CH) Brown to Light Brown; Clay with sand;	ST									
~4.5		(CH) Brown to Dark Brown; Clay;	SPT		1-0-1 (1)							
~6.5			ST									
~8.5		(CH) Brown to Dark Brown; Clay; Moist	ST									
10			SPT		2-1-3 (4)							

Bottom of borehole at 11.5 feet.

GEO TECH BH COLUMNS - GINT STD US LAB.GDT - 4/3/20 01:47 - C:\USERS\MAXA0516\ONE\DRIVE - UNIVERSITY OF TEXAS AT ARLINGTON\LAB DOCS\RESISTIVITY IMAGING\TEST RESULT\BEAUMONT\BORELOG P1\BORELOG INF

<b>LOGO</b>	The University of Texas at Arlington 416 Yates Street 76010	<b>BORING NUMBER P6</b>	PAGE 1 OF 1
CLIENT _____ PROJECT NAME _____		PROJECT NUMBER <u>First Visit</u> PROJECT LOCATION <u>Beaumont</u>	
DATE STARTED <u>10/15/19</u> COMPLETED <u>10/15/19</u>		GROUND ELEVATION _____ HOLE SIZE _____ inches	
DRILLING CONTRACTOR _____		GROUND WATER LEVELS:	
DRILLING METHOD _____		AT TIME OF DRILLING ---	
LOGGED BY _____ CHECKED BY _____		AT END OF DRILLING ---	
NOTES _____		AFTER DRILLING ---	

DEPTH (ft)	GRAPHIC LOG	MATERIAL DESCRIPTION	SAMPLE TYPE NUMBER	RECOVERY % (RQD)	BLOW COUNTS (N VALUE)	POCKET PEN. (tsf)	DRY UNIT WT. (pcf)	MOISTURE CONTENT (%)	ATTERBERG LIMITS			FINES CONTENT (%)
									LIQUID LIMIT	PLASTIC LIMIT	PLASTICITY INDEX	
0												
	[Diagonal Hatching]	(CL) Brown; Silty Clay;	ST									
	[Diagonal Hatching]	(CL) Brown; Clay	ST									
5	[Diagonal Hatching]	(CH) Brown; Clay	SPT		2-2-4 (6)							
	[Diagonal Hatching]	(CH) Dark Brown; Clay	ST									
10	[Diagonal Hatching]				1-1-2 (3)							

Bottom of borehole at 11.5 feet.



GEOTECH BH COLUMNS - GINT STD US LAB.GDT - 4/3/20 01:47 - C:\USERS\IMXA0516\ONE\DRIVE - UNIVERSITY OF TEXAS AT ARLINGTON\LAB DOCS\RESISTIVITY IMAGING\TEST RESULT\BEO\MONTIP\BORELOG\_P17\BORELOG INF

<b>LOGO</b>	The University of Texas at Arlington 416 Yates Stress 76010	<b>BORING NUMBER P17</b> PAGE 1 OF 1
<b>CLIENT</b> _____		<b>PROJECT NAME</b> _____
<b>PROJECT NUMBER</b> <u>First Visit</u>		<b>PROJECT LOCATION</b> <u>Beaumont</u>
<b>DATE STARTED</b> <u>10/14/19</u> <b>COMPLETED</b> <u>10/14/19</u>		<b>GROUND ELEVATION</b> _____ <b>HOLE SIZE</b> _____ inches
<b>DRILLING CONTRACTOR</b> _____		<b>GROUND WATER LEVELS:</b>
<b>DRILLING METHOD</b> _____		<b>AT TIME OF DRILLING</b> ---
<b>LOGGED BY</b> _____ <b>CHECKED BY</b> _____		<b>AT END OF DRILLING</b> ---
<b>NOTES</b> _____		<b>AFTER DRILLING</b> ---

DEPTH (ft)	GRAPHIC LOG	MATERIAL DESCRIPTION	SAMPLE TYPE NUMBER	RECOVERY % (RQD)	BLOW COUNTS (N VALUE)	POCKET PEN. (tsf)	DRY UNIT WT. (pcf)	MOISTURE CONTENT (%)	ATTERBERG LIMITS			FINES CONTENT (%)
									LIQUID LIMIT	PLASTIC LIMIT	PLASTICITY INDEX	
0												
	▨	(CL) Gray to Light gray; Slightly moist; Silty Sand with clay; sand seam	SS		11-9-6 (15)							
	▨	(CL) Gray; Sandy silty clay;										
5	▨	(CL-CH) Gray to brown; Silty Clay	SPT		1-2-4 (6)							
	▨		ST									
	▨	(CL-CH) Gray to brown; silty clay										
10	▨		SPT		2-1-2 (3)							


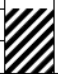
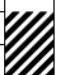
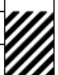
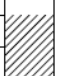
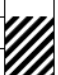
Bottom of borehole at 11.5 feet.

Beaumont District (December 2019)






<b>LOGO</b>	The University of Texas at Arlington 416 Yates Street 76010	<b>BORING NUMBER BR-6A</b>	PAGE 1 OF 4
CLIENT <u>SWIS Lab</u>		PROJECT NAME <u>Md Asif Akhtar</u>	
PROJECT NUMBER _____		PROJECT LOCATION <u>Beaumont</u>	
DATE STARTED <u>12/12/19</u> COMPLETED <u>12/13/19</u>		GROUND ELEVATION _____ HOLE SIZE _____ inches	
DRILLING CONTRACTOR _____		GROUND WATER LEVELS:	
DRILLING METHOD <u>Wash Boring</u>		∇ AT TIME OF DRILLING <u>6.50 ft</u>	
LOGGED BY _____ CHECKED BY _____		AT END OF DRILLING <u>---</u>	
NOTES <u>Wet Rotary set @ 8 ft due to Ground Water Table found at 6.5 ft</u>		AFTER DRILLING <u>---</u>	

DEPTH (ft)	GRAPHIC LOG	MATERIAL DESCRIPTION	SAMPLE TYPE NUMBER	RECOVERY % (RQD)	BLOW COUNTS (N VALUE)	POCKET PEN. (tsf)	DRY UNIT WT. (pcf)	MOISTURE CONTENT (%)	ATTERBERG LIMITS			FINES CONTENT (%)
									LIQUID LIMIT	PLASTIC LIMIT	PLASTICITY INDEX	
0		(CL) Silty Clay; Dark Brown; Moist	ST	88								
5		(CH) Clay; Dark Brown to Light Brown; Moist	ST	89								
	∇	(CH) Very soft clay; Light brown to light grey; Moist	SPT		1-1-1 (2)							
		(CH) Very soft clay; Light brown to light grey; Moist	ST	89								
10		(CL) Slightly Silty Clay; Light brown with some orange and gray; Moist	SPT		6-8-6 (14)							
		(CL) Slightly Silty Clay; Light brown with some orange and gray; Moist	ST	58								
15		(CL) Slightly Silty Clay; Light brown with some orange and gray; Moist	SPT		4-5-9 (14)							
		(SW-SC) Clayey Sand; Reddish-brown; Moist	ST	46								
20		(CL) Silty Clay; Light brown with some orange; Moist and Soft	SPT		7-12-9 (21)							
		(CL) Silty Clay; Light brown with some orange; Moist and Soft	ST	88								
25		(CL) Silty Clay; Light brown with some orange; Moist and Soft	SPT		6-8-8 (16)							
		(CL) Silty Clay; Light brown with some orange; Moist and Soft	ST	100								
30		(CL) Silty Clay; Light brown with some orange; Moist and Soft	SPT		6-6-8 (14)							
		(CL) Slightly Silty Clay; Light brown with some orange; Moist	ST	92								
35												

(Continued Next Page)


 The University of Texas at Arlington 416 Yates Street 76010		<b>BORING NUMBER BR-6A</b> PAGE 2 OF 4										
CLIENT <u>SWIS Lab</u>		PROJECT NAME <u>Md Asif Akhtar</u>										
PROJECT NUMBER _____		PROJECT LOCATION <u>Beaumont</u>										
DEPTH (ft)	GRAPHIC LOG	MATERIAL DESCRIPTION	SAMPLE TYPE NUMBER	RECOVERY % (ROD)	BLOW COUNTS (N VALUE)	POCKET PEN. (tsf)	DRY UNIT WT. (pcf)	MOISTURE CONTENT (%)	ATTERBERG LIMITS			FINES CONTENT (%)
									LIQUID LIMIT	PLASTIC LIMIT	PLASTICITY INDEX	
35			SPT		7-6-6 (12)							
40		(CH) Clay; Gray; Moist	ST	96								
45		(CH) Clay; Gray-Blue Gray; Moist	SPT		5-6-6 (12)							
			ST	90								
			SPT		5-5-6 (11)							
			ST	96								
			SPT		6-6-4 (10)							
			ST	88								
			SPT		4-5-6 (11)							
			ST	60								
			SPT		5-6-5 (11)							
65		(CH) Clay; Gray Moist	ST	81								
			SPT		6-6-4 (10)							
70		(CL) Clay into Clayey Sand; Gray; Moist	ST	73								
			SPT		8-13-15/5"							
75		(CH) Clay; Gray; Moist	ST									

(Continued Next Page)

 The University of Texas at Arlington 416 Yates Street 76010		<b>BORING NUMBER BR-6A</b> PAGE 3 OF 4										
CLIENT <u>SWIS Lab</u>		PROJECT NAME <u>Md Asif Akhtar</u>										
PROJECT NUMBER _____		PROJECT LOCATION <u>Beaumont</u>										
DEPTH (ft)	GRAPHIC LOG	MATERIAL DESCRIPTION	SAMPLE TYPE NUMBER	RECOVERY % (RQD)	BLOW COUNTS (N VALUE)	POCKET PEN. (tsf)	DRY UNIT WT. (pcf)	MOISTURE CONTENT (%)	ATTERBERG LIMITS			FINES CONTENT (%)
									LIQUID LIMIT	PLASTIC LIMIT	PLASTICITY INDEX	
75		(CH) Clay; Gray; Moist <i>(continued)</i>	SPT		8-8-6 (14)							
80			ST	90								
			SPT		6-6-6 (12)							
85			ST	90								
			SPT		6-35-35/0"							
90		Very Little Recover; Sample looks like just cutting	SS									
			SPT		8-35-35/0"							
95		Large Grain Sand with Rock; Gray into White	SS									
			SPT		8-35-35/0"							
100		Large Grain Sand; Gray; Wet	SS									
			SPT		8-35-35/0"							
105		(CH) Shale/ Clay; Blue Gray; Moist	SS									
			SPT		8-16-11/1"							
110		(CH) Shale to Slightly Silty Clay; Blue Gray; Moist	SS									
			SPT		8-17-27/1"							
115		Sandy Clay to Silty Clay; Blue gray; Very Moist	SS									

GEOTECH BH COLUMNS - GINT STD US LAB.GDT - 12/17/19 15:28 - C:\USERS\PUBLIC\DOCUMENTS\BENTLEY\GINT\PROJECTS\GINT STD US LAB.GPJ

(Continued Next Page)

 The University of Texas at Arlington 416 Yates Stress 76010		<b>BORING NUMBER BR-6A</b> PAGE 4 OF 4										
<b>CLIENT</b> <u>SWIS Lab</u>		<b>PROJECT NAME</b> <u>Md Asif Akhtar</u>										
<b>PROJECT NUMBER</b> _____		<b>PROJECT LOCATION</b> <u>Beaumont</u>										
DEPTH (ft)	GRAPHIC LOG	MATERIAL DESCRIPTION	SAMPLE TYPE NUMBER	RECOVERY % (RQD)	BLOW COUNTS (N VALUE)	POCKET PEN. (tsf)	DRY UNIT WT. (pcf)	MOISTURE CONTENT (%)	ATTERBERG LIMITS			FINES CONTENT (%)
									LIQUID LIMIT	PLASTIC LIMIT	PLASTICITY INDEX	
115			▲ SPT		8-35-35/0"							
		Sandy/ Silty Clay; Gray; Moist	▲									
120		Bottom of borehole at 120.0 feet.	▲ SPT		8-35-35/0"							

GEOTECH BH COLUMNS - GINT STD US LAB.GDT - 12/17/19 16:29 - C:\USERS\PUBLIC\DOCUMENTS\BENTLEY\GINT\PROJECTS\GINT STD US LAB.GPJ



The University of Texas at Arlington  
416 Yates Street  
76010

**BORING NUMBER BR-10A**

PAGE 1 OF 3

CLIENT \_\_\_\_\_ PROJECT NAME Beaumont Site Investigation with Electrical Resistivity

PROJECT NUMBER \_\_\_\_\_ PROJECT LOCATION Beaumont (SH 96 and SH69 Intersection)

DATE STARTED 12/12/19 COMPLETED 12/13/19 GROUND ELEVATION \_\_\_\_\_ HOLE SIZE \_\_\_\_\_ inches

DRILLING CONTRACTOR \_\_\_\_\_ GROUND WATER LEVELS:






DRILLING METHOD Wash Boring AT TIME OF DRILLING --

LOGGED BY \_\_\_\_\_ CHECKED BY \_\_\_\_\_ AT END OF DRILLING --




NOTES \_\_\_\_\_ AFTER DRILLING --

DEPTH (ft)	GRAPHIC LOG	MATERIAL DESCRIPTION	SAMPLE TYPE NUMBER	RECOVERY % (RQD)	BLOW COUNTS (N VALUE)	POCKET PEN. (tsf)	DRY UNIT WT. (pcf)	MOISTURE CONTENT (%)	ATTERBERG LIMITS			FINES CONTENT (%)
									LIQUID LIMIT	PLASTIC LIMIT	PLASTICITY INDEX	
0		Dark Brown; Sandy Clay; Organics				1.0						
5		Dark Brown; Clay				1.0						
					0-0-1 (1)	0						
						0						
10						.5						
					0-0-1 (1)							
15												
					4-8-8 (16)	1.0						
20		Gray to Brown; Sandy Clay										
					5-7-7 (14)	2.0						
25		Gray, Brown, Tan; Sandy Clay with White seams										
					3-5-5 (10)							
30												
					5-5-5 (10)	2.0						
35												

(Continued Next Page)

 The University of Texas at Arlington 416 Yates Street 76010		<b>BORING NUMBER BR-10A</b> PAGE 2 OF 3										
CLIENT _____		PROJECT NAME <u>Beaumont Site Investigation with Electrical Resistivity</u>										
PROJECT NUMBER _____		PROJECT LOCATION <u>Beaumont (SH 96 and SH69 Intersection)</u>										
DEPTH (ft)	GRAPHIC LOG	MATERIAL DESCRIPTION	SAMPLE TYPE NUMBER	RECOVERY % (RQD)	BLOW COUNTS (N VALUE)	POCKET PEN. (tsf)	DRY UNIT WT. (pcf)	MOISTURE CONTENT (%)	ATTERBERG LIMITS			FINES CONTENT (%)
									LIQUID LIMIT	PLASTIC LIMIT	PLASTICITY INDEX	
35					3-5-7 (12)	1.75						
40					3-4-4 (8)	1.25						
45		Gray Clay			5-5-5 (10)	1.5						
50					3-4-4 (8)	1.25						
55					3-5-4 (9)	1.25						
60		Gray; Clay Sand			5-4-6 (10)	1.0						
65					5-6-7 (13)	1.5						
70		Gray; Sandy Clay with Organics			4-5-5 (10)							
75		Brown-gray; Clay Sand; Organics										

(Continued Next Page)

 The University of Texas at Arlington 416 Yates Stress 76010		<b>BORING NUMBER BR-10A</b> PAGE 3 OF 3										
CLIENT _____		PROJECT NAME <u>Beaumont Site Investigation with Electrical Resistivity</u>										
PROJECT NUMBER _____		PROJECT LOCATION <u>Beaumont (SH 96 and SH69 Intersection)</u>										
DEPTH (ft)	GRAPHIC LOG	MATERIAL DESCRIPTION	SAMPLE TYPE NUMBER	RECOVERY % (RQD)	BLOW COUNTS (N VALUE)	POCKET PEN. (tsf)	DRY UNIT WT. (pcf)	MOISTURE CONTENT (%)	ATTERBERG LIMITS			FINES CONTENT (%)
									LIQUID LIMIT	PLASTIC LIMIT	PLASTICITY INDEX	
75					3-12-30 (42)	.5						
80		Gray; Sand Clay with wood in Bedded Organics										
85		Tan Gray sand with wood organics in bed			4-3-4 (7)							
90					12-19-36/5"							
95					5-6-23 (29)							
100					12-50-50/0"							
Bottom of borehole at 100.4 feet.					12-50-50/0"							

C:\USERS\PUBLIC\DOCUMENTS\BENTLEY\GINT\PROJECTS\GINT STD US LAB.GPJ




Corpus Christi District (February 2020)

The University of Texas at Arlington 418 Yates Street 76010		<b>BORING NUMBER BR 201</b> PAGE 1 OF 2	
CLIENT _____ PROJECT NAME <u>The University of Texas at Arlington</u>		PROJECT LOCATION <u>Corpus Christi</u>	
PROJECT NUMBER _____		GROUND ELEVATION <u>0 ft</u> HOLE SIZE <u>inches</u>	
DATE STARTED <u>2/25/20</u> COMPLETED <u>2/25/20</u>		GROUND WATER LEVELS:	
DRILLING CONTRACTOR _____		<input checked="" type="checkbox"/> AT TIME OF DRILLING <u>15.00 ft / Elev -15.00 ft</u>	
DRILLING METHOD <u>Wash Boring</u>		AT END OF DRILLING <u>—</u>	
LOGGED BY _____ CHECKED BY _____		AFTER DRILLING <u>—</u>	
NOTES _____			


  

DEPTH (ft)	GRAPHIC LOG	MATERIAL DESCRIPTION	SAMPLE TYPE NUMBER	RECOVERY % (ROD)	BLOW COUNTS (N VALUE)	POCKET PEN. (tsf)	DRY UNIT WT. (pcf)	MOISTURE CONTENT (%)	ATTERBERG LIMITS			FINES CONTENT (%)
									LIQUID LIMIT	PLASTIC LIMIT	PLASTICITY INDEX	
0		LEAN CLAY WITH SAND, (CL) ;Dark Brown;	SS		4-8-5 (11)							
		SILTY SAND, (SM) ;Brown; moist;	SS		4-9-11 (20)							
5		LEAN CLAY WITH SAND, (CL) ;Brown; slightly moist; soft;	SPT		8-7-6 (13)							
		SILTY SAND, (SM) ;Very Pale brown; soft; wet;	SPT		1-5-5 (10)							
			SS		2-2-3 (5)							
15			SPT		2-4-8 (12)							
20		SILTY SAND, (SM) ;Very Pale Brown; Wet;	SPT		4-13-14 (27)							
25		WELL GRADED SAND WITH SILT, (SW-SM) ;Very Pale brown to light gray; soft;	SPT		12-33-50/2"							
30		WELL GRADED SAND, (SW) ;Light Grayish;	SPT		12-33-50/3"							
35		CLAYEY SAND, (SC) ;Light Gray; Stiff;	ST			4.5+						

(Continued Next Page)

 The University of Texas at Arlington 416 Yates Street 78010		<b>BORING NUMBER BR 201</b> PAGE 2 OF 2										
CLIENT _____		PROJECT NAME <u>The University of Texas at Arlington</u>										
PROJECT NUMBER _____		PROJECT LOCATION <u>Corpus Christi</u>										
DEPTH (ft)	GRAPHIC LOG	MATERIAL DESCRIPTION	SAMPLE TYPE NUMBER	RECOVERY % (ROD)	BLOW COUNTS (N VALUE)	POCKET PEN. (tsf)	DRY UNIT WT. (pcf)	MOISTURE CONTENT (%)	ATTERBERG LIMITS			FINES CONTENT (%)
									LIQUID LIMIT	PLASTIC LIMIT	PLASTICITY INDEX	
35			SPT		12-50-50/0"							
			ST			4.5+						
40			SPT		12-34-50/0"							
		LEAN CLAY WITH SAND, (CL) ;Slight Gray; very Stiff with orangeish Stain;	ST			4.5+						
45			SPT		8-33-34/2"							
		LEAN CLAY WITH SAND, (CL) ;Light Gray, Pale Brown; Stiff;	ST			2.5						
50			SPT		12-50-50/0"							
		WELL GRADED SAND, (SW) ;Pale Brown; Wet;	SPT		12-50-50/0"							
55												
		LEAN CLAY, (CL) ;Brown, yellowish strain; very stiff;	ST			4.5+						
60			SPT		8-15-15/4"							
			ST			4.5+						
65			SPT		8-17-20/5"							
		LEAN CLAY WITH SAND, (CL) ;Light Gray;	ST			4.5+						
70			SPT		8-22-28/3"							
75												

Bottom of borehole at 75.0 feet.



The University of Texas at Arlington  
410 Yates Street  
78010

## BORING NUMBER BR 202

PAGE 1 OF 2

---

**CLIENT** \_\_\_\_\_

**PROJECT NUMBER** \_\_\_\_\_

**DATE STARTED** 2/24/20 **COMPLETED** 2/24/20

**DRILLING CONTRACTOR** \_\_\_\_\_

**DRILLING METHOD** Wash Boring

**LOGGED BY** \_\_\_\_\_ **CHECKED BY** \_\_\_\_\_

**NOTES** \_\_\_\_\_

**PROJECT NAME** The University of Texas at Arlington

**PROJECT LOCATION** Corpus Christi

**GROUND ELEVATION** 0 ft **HOLE SIZE** inches

**GROUND WATER LEVELS:**

▽ **AT TIME OF DRILLING** 16.00 ft / Elev -16.00 ft


**AT END OF DRILLING** --

**AFTER DRILLING** --

DEPTH (ft)	GRAPHIC LOG	MATERIAL DESCRIPTION	SAMPLE TYPE NUMBER	RECOVERY % (RQD)	BLOW COUNTS (N VALUE)	POCKET PEN. (tsf)	DRY UNIT WT. (pcf)	MOISTURE CONTENT (%)	ATTERBERG LIMITS			FINES CONTENT (%)
									LIQUID LIMIT	PLASTIC LIMIT	PLASTICITY INDEX	
0												
0-3		LEAN CLAY WITH SAND, (CL) ; Brown Sandy;	SS		4-5-8 (13)							
3-5		LEAN CLAY WITH SAND, (CL) ; Brown; Slightly Moist;	SS		9-10-6 (16)							
5-8		LEAN CLAY, (CL) ; Light Tan, Reddish; Slightly Moist; Stiff;	SPT		1-3-5 (6)							
8-9			SS		3-4-4 (6)							
9-10		WELL GRADED SAND WITH CLAY, (SW-SC) ; Light Tan; Loose; Slightly Moist;	ST			0.5						
10-12		WELL GRADED SAND, (SW) ; Light Tan; Loose; Wet;	SPT		6-8-12 (20)							
12-13			SS		7-8-6 (16)							
13-15			SPT		4-8-9 (17)							
15-17			SS		2-4-7 (11)							
17-18			SPT		8-11-7/2"							
18-19			SS		2-3-6 (9)							
19-21		WELL GRADED SAND WITH GRAVEL, (SW) ; Light Tan; Wet;	SPT		12-35-50/3"							
21-22			SS		5-12-25 (37)							
22-24			SPT		12-50-50/0"							
24-25			SS		16-24-28 (52)							
25-28		WELL GRADED SAND WITH SILT, (SW-SM) ; Light Gray with Small Seam of Sandy Clay; Stiff;	SPT									
28-30			SS									

(Continued Next Page)

LOGO		The University of Texas at Arlington 416 Yates Street 76010		<b>BORING NUMBER BR 202</b>								
CLIENT		PROJECT NAME The University of Texas at Arlington							PAGE 2 OF 2			
PROJECT NUMBER		PROJECT LOCATION Corpus Christi										
DEPTH (ft)	GRAPHIC LOG	MATERIAL DESCRIPTION	SAMPLE TYPE NUMBER	RECOVERY % (RCD)	BLOW COUNTS (N VALUE)	POCKET PEN. (tsf)	DRY UNIT WT. (pcf)	MOISTURE CONTENT (%)	ATTERBERG LIMITS			FINES CONTENT (%)
									LIQUID LIMIT	PLASTIC LIMIT	PLASTICITY INDEX	
35		WELL GRADED SAND, (SW) ; Pale Brown, Light Grayish; Loose; Wet;	SPT		12-50-50/0"							
			SS		5-12-17 (29)							
40		WELL GRADED SAND WITH SILT, (SW-SM) ; Pale Brown; Dense Sand;	SPT		8-28-21/4"							
			SS		4-9-15 (24)							
45		LEAN CLAY WITH SAND, (CL) ; Light Grayish; Pale Brown; Sandy Clay; Stiff;	ST									
			SPT		12-50-50/0"							
50		WELL GRADED SAND, (SW) ; Pale Brown, Grayish; Soft Sand;	SPT		12-50-50/0"							
			SS		23-29-27 (56)							
55		WELL GRADED SAND WITH CLAY, (SW-SC) ; Pale Brown; Very Stiff; Slightly Moist; Seam of Clay	SPT		8-20-13/3"							
			SS		8-12-17 (29)							
60		LEAN CLAY, (CL) ; Pale Brown, Orange;	ST									
			SPT		8-11-20/6"							
65			ST									
			SPT		8-25-27/2"							
70	Bottom of borehole at 70.0 feet.		ST									
			SPT		9-27-27/2"							



The University of Texas at Arlington  
416 Yates Street  
76010

## BORING NUMBER RW 214

PAGE 1 OF 2

---

**CLIENT** \_\_\_\_\_ **PROJECT NAME** The University of Texas at Arlington

**PROJECT NUMBER** \_\_\_\_\_ **PROJECT LOCATION** Corpus Christi

**DATE STARTED** 2/25/20 **COMPLETED** 2/25/20 **GROUND ELEVATION** 0 ft **HOLE SIZE** \_\_\_\_\_ inches

**DRILLING CONTRACTOR** \_\_\_\_\_ **GROUND WATER LEVELS:**




**DRILLING METHOD** Wash Boring  **AT TIME OF DRILLING** 13.00 ft / Elev -13.00 ft

**LOGGED BY** \_\_\_\_\_ **CHECKED BY** \_\_\_\_\_ **AT END OF DRILLING** —


**NOTES** \_\_\_\_\_ **AFTER DRILLING** —

DEPTH (ft)	GRAPHIC LOG	MATERIAL DESCRIPTION	SAMPLE TYPE NUMBER	RECOVERY % (ROD)	BLOW COUNTS (N VALUE)	POCKET PEN. (tsf)	DRY UNIT WT. (pcf)	MOISTURE CONTENT (%)	ATTERBERG LIMITS			FINES CONTENT (%)
									LIQUID LIMIT	PLASTIC LIMIT	PLASTICITY INDEX	
0		LEAN CLAY WITH SAND, (CL) ; Dark Brown sandy Clay;	SS		3-3-3 (6)							
		CLAYEY SAND, (SC) ; Sandy Clay with brown sand;	SS		4-5-8 (13)							
5		CLAYEY SAND, (SC) ; Brown Sand with some clayey Sand;	SPT		5-4-4 (8)							
			SS		4-4-6 (10)							
10		WELL GRADED SAND, (SW) ; Tan; Sand; Moist;	SPT		6-6-7 (13)							
			SS		4-6-8 (14)							
15		WELL GRADED SAND, (SW) ; Tan; Sand followed by Tan Coarse sand with some gravel at 17.5';	SPT		6-6-6 (12)							
			SS		2-3-5 (6)							
20		WELL GRADED SAND WITH SILT, (SW) ; Coarse sand with some gravel; Wet; Dense;	SPT		8-6-5 (11)							
			SS		3-4-4 (6)							
25		LEAN CLAY WITH SAND, (CL) ; Tan; Sandy Clay;	SPT		8-8-8/5"							
			SS		5-7-6 (13)							
30		LEAN CLAY WITH SAND, (CL) ; Tan; Sany Clay followed by Tan Sand;	ST									
			SPT		8-9-9 (18)							
35		WELL GRADED SAND WITH SILT, (SW) ; Tan; Sand;										

(Continued Next Page)

 The University of Texas at Arlington 416 Yates Street 78010		<b>BORING NUMBER RW 214</b> PAGE 2 OF 2										
CLIENT _____		PROJECT NAME The University of Texas at Arlington										
PROJECT NUMBER _____		PROJECT LOCATION Corpus Christi										
DEPTH (#)	GRAPHIC LOG	MATERIAL DESCRIPTION	SAMPLE TYPE NUMBER	RECOVERY % (ROD)	BLOW COUNTS (N VALUE)	POCKET PEN. (tsf)	DRY UNIT WT. (pcf)	MOISTURE CONTENT (%)	ATTERBERG LIMITS			FINES CONTENT (%)
									LIQUID LIMIT	PLASTIC LIMIT	PLASTICITY INDEX	
35			SPT		12-26-50 (78)							
		WELL GRADED SAND WITH SILT, (SW) ; Tan; sand; Wet; Dense;	SS		8-13-18 (31)							
40			SPT		8-19-17 (38)							
		LEAN CLAY WITH SAND, (CL) ; Tan; Silty Sandy Clay with sand seam;	SS		9-12-13 (25)							
Bottom of borehole at 43.0 feet.												

GEOTECH BH COLUMNS - GINT STD US LAB.GDT - 3/5/20 12:21 - C:\USERS\MX\A0516\CONEDRIVE - UNIVERSITY OF TEXAS AT ARLINGTON\LAB DOCS\RESISTIVITY IMAGING\TEST RESULTS\CORPUS CHRISTI\RW 201\BORELOGS\CC\_B0201.GPJ



The University of Texas at Arlington  
416 Yates Street  
76010

## BORING NUMBER RW 215

PAGE 1 OF 2

---

**CLIENT** \_\_\_\_\_

**PROJECT NUMBER** \_\_\_\_\_

**DATE STARTED** 2/25/20 **COMPLETED** 2/25/20

**DRILLING CONTRACTOR** \_\_\_\_\_

**DRILLING METHOD** Wash Boring

**LOGGED BY** \_\_\_\_\_ **CHECKED BY** \_\_\_\_\_

**NOTES** \_\_\_\_\_

**PROJECT NAME** The University of Texas at Arlington

**PROJECT LOCATION** Corpus Christi

**GROUND ELEVATION** 0 ft **HOLE SIZE** \_\_\_\_\_ inches

**GROUND WATER LEVELS:**




∇ **AT TIME OF DRILLING** 13.00 ft / Elev -13.00 ft

**AT END OF DRILLING** \_\_\_\_\_

**AFTER DRILLING** \_\_\_\_\_

DEPTH (ft)	GRAPHIC LOG	MATERIAL DESCRIPTION	SAMPLE TYPE NUMBER	RECOVERY % (ROD)	BLOW COUNTS (N VALUE)	POCKET PEN. (tsf)	DRY UNIT WT. (pcf)	MOISTURE CONTENT (%)	ATTERBERG LIMITS			FINES CONTENT (%)
									LIQUID LIMIT	PLASTIC LIMIT	PLASTICITY INDEX	
0												
0-3		LEAN CLAY WITH SAND, (CL) : Dark Brown; Sandy Clay;	SS		2-4-4 (8)							
3-5		SILT WITH SAND, (ML) : Dark Brown; Sandy Clay followed by Brown Sand;	SS		5-8-9 (17)							
5-7			SPT		7-6-5 (11)							
7-9			SS		3-3-4 (7)							
9-10		LEAN CLAY WITH SAND, (CL) : Brown; Sandy Clay;	ST			3.5						
10-12			SPT		9-6-7 (13)							
12-15		WELL GRADED SAND, (SW) : Tan; Sand; Wet; soft;	SS		6-7-6 (13)							
15-18			SPT		12-8-10 (18)							
18-20			SS		2-3-4 (7)							
20-22			SPT		12-11-10 (21)							
22-25		WELL GRADED SAND, (SW) : Coarse Sand; Wet; Dense;	SS		4-5-6 (11)							
25-30			SPT		12-50-50/0"							
30-32			SS		7-5-16 (21)							
32-34			SPT		12-26-14/5"							
34-35			SS		3-3-4 (7)							


(Continued Next Page)

 The University of Texas at Arlington 416 Yates Street 78010		<b>BORING NUMBER RW 215</b> PAGE 2 OF 2										
CLIENT _____		PROJECT NAME The University of Texas at Arlington										
PROJECT NUMBER _____		PROJECT LOCATION Corpus Christi										
DEPTH (ft)	GRAPHIC LOG	MATERIAL DESCRIPTION	SAMPLE TYPE NUMBER	RECOVERY % (ROD)	BLOW COUNTS (N VALUE)	POCKET PEN. (tsf)	DRY UNIT WT. (pcf)	MOISTURE CONTENT (%)	ATTERBERG LIMITS			FINES CONTENT (%)
									LIQUID LIMIT	PLASTIC LIMIT	PLASTICITY INDEX	
35		LEAN CLAY, (CL-ML) ; Tan; Clay Seam;	SPT		12-24-							
		LEAN CLAY WITH SAND, (CL) ; Slight Recovery; Moist;			16/4"							
40		; Seam of Sand;	SPT		12-45-45							
		LEAN CLAY WITH SAND, (CL) ; Sand Followed by tan clay;	SS		22-20-25	(91)	(45)					
Bottom of borehole at 43.5 feet.												

GEOTECH BH COLUMNS - GNT STD US LAB.G01 - 3/5/20 12:22 - C:\USERS\MKX015\CONEDRIVE - UNIVERSITY OF TEXAS AT ARLINGTON\LAB DOC\SRESISTIVITY IMAGING\TEST RESULT SITE RESULT\CORPUS CHRISTI\RW 2011\BORELOG\CC\_B0201.GPJ



Fort Worth District (July 2019)



**BORING NUMBER BH-1**

PAGE 1 OF 1

---

CLIENT TxDOT - Fort Worth PROJECT NAME Fort Worth Slope Stabilization

PROJECT NUMBER 1 PROJECT LOCATION I30 and Fielder Road (North)

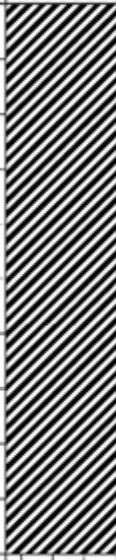
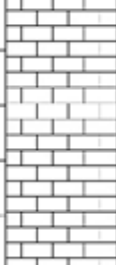
DATE STARTED 6/20/19 COMPLETED 6/20/19 GROUND ELEVATION \_\_\_\_\_ HOLE SIZE \_\_\_\_\_

DRILLING CONTRACTOR \_\_\_\_\_ GROUND WATER LEVELS:

DRILLING METHOD Hollow Stem Auger AT TIME OF DRILLING ---

LOGGED BY UTA CHECKED BY UTA AT END OF DRILLING ---


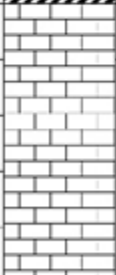
NOTES \_\_\_\_\_ AFTER DRILLING ---


DEPTH (ft)	GRAPHIC LOG	MATERIAL DESCRIPTION	SAMPLE TYPE NUMBER	BLOW COUNTS (N VALUE)	MOISTURE CONTENT (%)
0					
5		Light gray Clay	SH TCP	18-18 (36)	
		Light gray Clay	AU		
		Brown Clay	TCP	50 (5")-50(4")	
10		Light gray Limestone	AU		
		Limestone	TCP		50 (4")-50(3")
15		Bottom of borehole at 15.0 feet.			

GEOTECH BH COLUMNS - GINT STD US GDT - 6/20/19 21:18 - C:\USERS\BDD\1\3\ONE DRIVE - UNIVERSITY OF TEXAS AT ARLINGTON\FORT WORTH INSTALLATION\DRILLING\BHELOG\30 AND FIELDER ROAD - NORTH\50 AND FIELDER ROAD (NORTH)\GPJ

GEOTECH BH COLUMNS - GINT STD US GGT - #2019 21 18 - C:\USERS\PC2051\ONE\DRIVE - UNIVERSITY OF TEXAS AT ARLINGTON\FORTYFOURTH\INSTALLATION\HALLING\BORING\LOG\130 AND FIELDER ROAD (NORTH)\GPJ

<b>Logo</b> uta	<b>BORING NUMBER BH-2</b> PAGE 1 OF 1
CLIENT <u>TxDOT - Fort Worth</u>	PROJECT NAME <u>Fort Worth Slope Stabilization</u>
PROJECT NUMBER <u>1</u>	PROJECT LOCATION <u>I30 and Fielder Road (North)</u>
DATE STARTED <u>6/20/19</u> COMPLETED <u>6/20/19</u>	GROUND ELEVATION _____ HOLE SIZE _____
DRILLING CONTRACTOR _____	GROUND WATER LEVELS:
DRILLING METHOD <u>Hollow Stem Auger</u>	AT TIME OF DRILLING <u>---</u>
LOGGED BY <u>UTA</u> CHECKED BY <u>UTA</u>	AT END OF DRILLING <u>---</u>
NOTES _____	AFTER DRILLING <u>---</u>

DEPTH (ft)	GRAPHIC LOG	MATERIAL DESCRIPTION	SAMPLE TYPE NUMBER	BLOW COUNTS (N VALUE)	MOISTURE CONTENT (%)
0					
		Brown Clay	ST		
5		Brown Clay	TCP	21-25 (46)	
		Gray Clay	AU		
10		Brown Limestone	TCP	40-50 (3')	
		Light gray Limestone	AU		
15		Bottom of borehole at 15.0 feet.	TCP	50 (2')-50(2')	



### BORING NUMBER BH-1

PAGE 1 OF 1

---

CLIENT TxDOT - Fort Worth

PROJECT NUMBER 2

DATE STARTED 6/20/19 COMPLETED 6/20/19

DRILLING CONTRACTOR \_\_\_\_\_

DRILLING METHOD Hollow Stem Auger

LOGGED BY UTA CHECKED BY UTA

NOTES \_\_\_\_\_

PROJECT NAME Fort Worth Slope Stabilization

PROJECT LOCATION I30 and Fielder Road (South)

GROUND ELEVATION \_\_\_\_\_ HOLE SIZE \_\_\_\_\_


GROUND WATER LEVELS:

AT TIME OF DRILLING ---

AT END OF DRILLING ---

AFTER DRILLING ---

---

DEPTH (ft)	GRAPHIC LOG	MATERIAL DESCRIPTION	SAMPLE TYPE NUMBER	BLOW COUNTS (N VALUE)	MOISTURE CONTENT (%)
0					
5		Brown Clay	SH AU TCP	3-5 (8)	
		Reddish brown Clay			
10		Light red Clay	AU ST TCP	12-18 (30)	
		Reddish brown Clay			
		Yellowish brown Clay	AU		
15		Grayish white Limestone	ST		
Bottom of borehole at 15.0 feet.			TCP 50 (2")-50 (2")		

GEOTECH BH COLUMNS - QINT STD US GDT - 8/20/10 21 20 - C:\USER\SPRE33\BONELOGG\AND FIELDER ROAD - SOUTH\CPJ


<b>Logo</b>	uta	<b>BORING NUMBER BH-2</b>	
		PAGE 1 OF 1	
CLIENT <u>TxDOT - Fort Worth</u>		PROJECT NAME <u>Fort Worth Slope Stabilization</u>	
PROJECT NUMBER <u>2</u>		PROJECT LOCATION <u>I30 and Fielder Road (South)</u>	
DATE STARTED <u>6/20/19</u>	COMPLETED <u>6/20/19</u>	GROUND ELEVATION _____	HOLE SIZE _____
DRILLING CONTRACTOR _____		GROUND WATER LEVELS:	
DRILLING METHOD <u>Hollow Stem Auger</u>		AT TIME OF DRILLING <u>---</u>	
LOGGED BY <u>UTA</u>		CHECKED BY <u>UTA</u>	
NOTES _____		AT END OF DRILLING <u>---</u>	
		AFTER DRILLING <u>---</u>	

DEPTH (ft)	GRAPHIC LOG	MATERIAL DESCRIPTION	SAMPLE TYPE NUMBER	BLOW COUNTS (N VALUE)	MOISTURE CONTENT (%)
0					
		Dark brown Clay	ST		
5		Brown Clay	TCP	4-5 (9)	
		Brownish red Clay	SH		
10		Brown Clay	TCP	10-14 (24)	
		Light gray Clay	AU		
15		Light gray Limestone	TCP	50 (2')-50 (2')	

Bottom of borehole at 15.0 feet.

Logo <small>uta</small>		<b>BORING NUMBER BH-1</b>			
		PAGE 1 OF 1			
<b>CLIENT</b> <u>TxDOT - Fort Worth</u>		<b>PROJECT NAME</b> <u>Fort Worth Slope Stabilization</u>			
<b>PROJECT NUMBER</b> <u>3</u>		<b>PROJECT LOCATION</b> <u>1820 and Sun Valley Drive</u>			
<b>DATE STARTED</b> <u>6/21/19</u> <b>COMPLETED</b> <u>6/21/19</u>		<b>GROUND ELEVATION</b> _____		<b>HOLE SIZE</b> _____	
<b>DRILLING CONTRACTOR</b> _____		<b>GROUND WATER LEVELS:</b>			
<b>DRILLING METHOD</b> <u>Hollow Stem Auger</u>		<b>AT TIME OF DRILLING</b> <u>--</u>			
<b>LOGGED BY</b> <u>UTA</u> <b>CHECKED BY</b> <u>UTA</u>		<b>AT END OF DRILLING</b> <u>--</u>			
<b>NOTES</b> _____		<b>AFTER DRILLING</b> <u>--</u>			
DEPTH (ft)	GRAPHIC LOG	MATERIAL DESCRIPTION	SAMPLE TYPE NUMBER	BLOW COUNTS (N VALUE)	MOISTURE CONTENT (%)
0		Dark gray Clay	AU	7-8 (15)	
5		Brown Clay	SH TCP		
10		Dark brownish gray Clay	AU	10-14 (24)	
15		Brown Clay	SH TCP	50 (5.5")- 50(5.5")	
20		Grayish brown Clay with traces of limestone	AU	50 (5.75")- 50(5.5")	
25		Whiteish gray Very stiff clay	SH TCP	50 (6")-50(6")	
Bottom of borehole at 25.0 feet.					

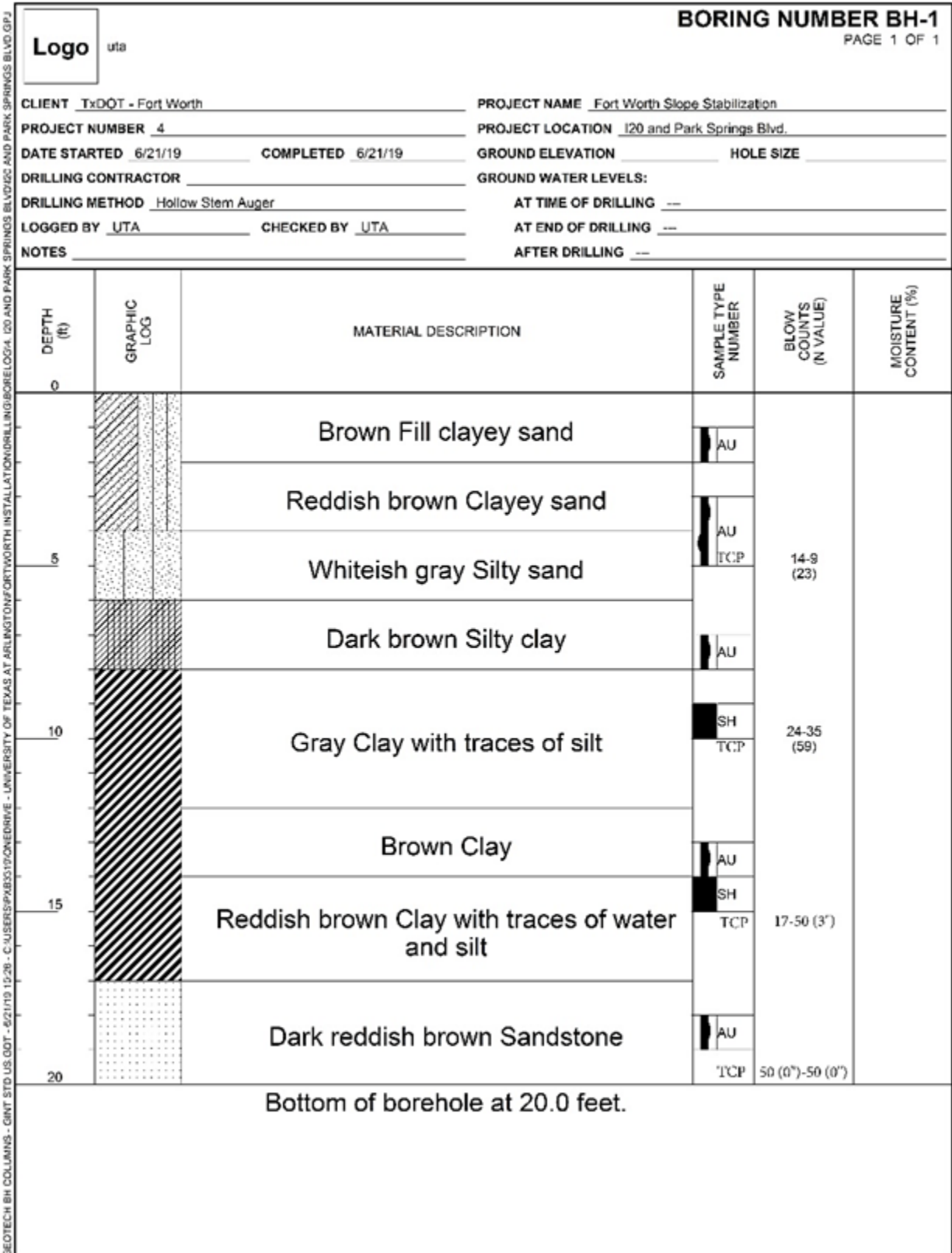
GEO TECH BH COLUMNS - GRF STD US QGT - 6/21/19 10:49 - C:\USERS\PKABO31\CONEDRIVE - UNIVERSITY OF TEXAS AT ARLINGTON\FORT WORTH INSTALLATION\DRILLING\BORELOGS - 1820 AND SUN VALLEY DRIVE\20 AND SUN VALLEY DRIVE\20 AND SUN VALLEY DRIVE.GPJ


		<b>BORING NUMBER BH-2</b> PAGE 1 OF 1			
CLIENT <u>TxDOT - Fort Worth</u>		PROJECT NAME <u>Fort Worth Slope Stabilization</u>			
PROJECT NUMBER <u>3</u>		PROJECT LOCATION <u>1820 and Sun Valley Drive</u>			
DATE STARTED <u>6/21/19</u> COMPLETED <u>6/21/19</u>		GROUND ELEVATION _____		HOLE SIZE _____	
DRILLING CONTRACTOR _____		GROUND WATER LEVELS:			
DRILLING METHOD <u>Hollow Stem Auger</u>		AT TIME OF DRILLING <u>---</u>		AT END OF DRILLING <u>---</u>	
LOGGED BY <u>UTA</u> CHECKED BY <u>UTA</u>		AFTER DRILLING <u>---</u>		_____	
NOTES _____		_____			


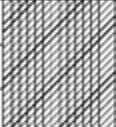

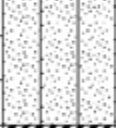

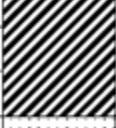
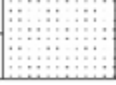
DEPTH (ft)	GRAPHIC LOG	MATERIAL DESCRIPTION	SAMPLE TYPE NUMBER	BLOW COUNTS (N VALUE)	MOISTURE CONTENT (%)	
0						
5		Brown Clay	AU	4-3 (7)		
6			SH TCP			
7			SH			
8			TCP			
10			Light brown Clay	AU	5-11 (16)	
12		SH TCP				
15			Brown Very stiff clay	SH TCP	46-50 (4")	
17		AU				
20				TCP	50 (4")-50 (3")	
25				TCP	50 (1")-50 (0")	
Bottom of borehole at 25.0 feet.						

GEOTECH BH COLUMNS - GW1 STD US GDT - 5/21/19 10:49 - C:\USERS\PA833\B33\ONEDEWIVE - UNIVERSITY OF TEXAS AT ARLINGTON\FORTWORTH INSTALLATION\DRILLING\BORELOG3\_1820 AND SUN VALLEY DRIVE\B20 AND SUN VALLEY DRIVE.GPJ



		<b>BORING NUMBER BH-2</b> PAGE 1 OF 1			
CLIENT <u>TxDOT - Fort Worth</u>		PROJECT NAME <u>Fort Worth Slope Stabilization</u>			
PROJECT NUMBER <u>4</u>		PROJECT LOCATION <u>I20 and Park Springs Blvd.</u>			
DATE STARTED <u>6/21/19</u> COMPLETED <u>6/21/19</u>		GROUND ELEVATION _____      HOLE SIZE _____			
DRILLING CONTRACTOR _____		GROUND WATER LEVELS:			
DRILLING METHOD <u>Hollow Stem Auger</u>		AT TIME OF DRILLING <u>---</u>			
LOGGED BY <u>UTA</u> CHECKED BY <u>UTA</u>		AT END OF DRILLING <u>---</u>			
NOTES _____		AFTER DRILLING <u>---</u>			

DEPTH (ft)	GRAPHIC LOG	MATERIAL DESCRIPTION	SAMPLE TYPE NUMBER	BLOW COUNTS (N VALUE)	MOISTURE CONTENT (%)
0					
		Reddish brown Sandy clay	AU		
5		Reddish brown Silty clay	AU	25-27 (52)	
		Reddish brown Clay	SH		
10		Gray Shally clay	TCP	29-35 (64)	
		Light gray Silty sand			
15		Brown Clay with traces of sandstone	AU SH TCP	50 (0.5')- 50 (0.5')	
20		Dark brown Sandstone	AU TCP	50 (0.75')- 50 (0.5')	
Bottom of borehole at 20.0 feet.					

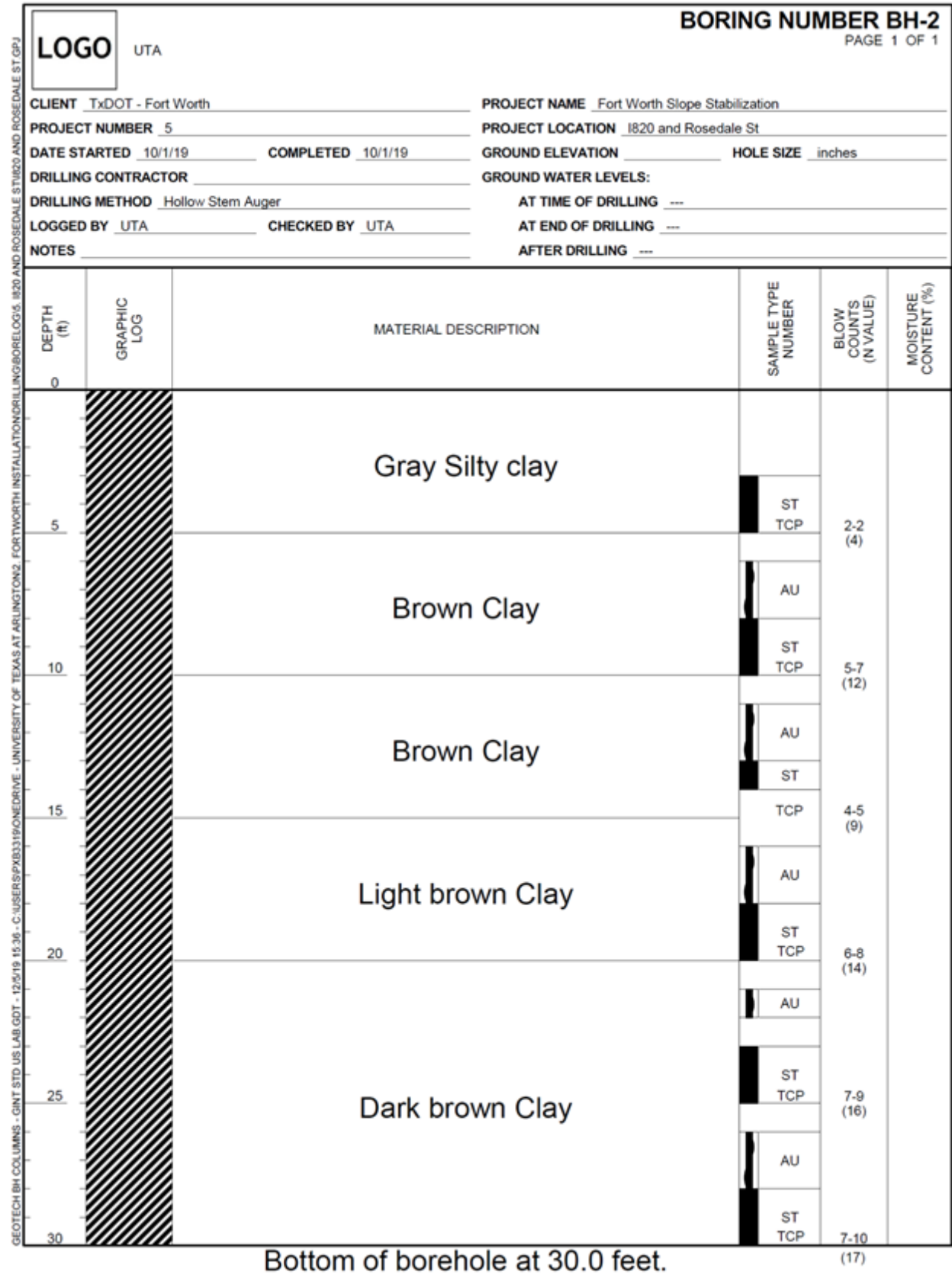


<b>LOGO</b>	UTA	<b>BORING NUMBER BH-1</b>	
		PAGE 1 OF 1	
CLIENT <u>TxDOT - Fort Worth</u>		PROJECT NAME <u>Fort Worth Slope Stabilization</u>	
PROJECT NUMBER <u>5</u>		PROJECT LOCATION <u>I820 and Rosedale St</u>	
DATE STARTED <u>10/1/19</u> COMPLETED <u>10/1/19</u>		GROUND ELEVATION _____ HOLE SIZE _____ inches	
DRILLING CONTRACTOR _____		GROUND WATER LEVELS:	
DRILLING METHOD <u>Hollow Stem Auger</u>		AT TIME OF DRILLING <u>---</u>	
LOGGED BY <u>UTA</u> CHECKED BY <u>UTA</u>		AT END OF DRILLING <u>---</u>	
NOTES _____		AFTER DRILLING <u>---</u>	

DEPTH (ft)	GRAPHIC LOG	MATERIAL DESCRIPTION	SAMPLE TYPE NUMBER	BLOW COUNTS (N VALUE)	MOISTURE CONTENT (%)
0					
5		Gray Silty clay	ST TCP	6-8 (12)	
		Brown Clay with traces of small stones	AU		
10		Brown Clay	ST TCP	9-8 (17)	
		Light brown Clay	AU		
15		Light brown Clay	ST TCP	3-4 (7)	
		Dark brown Clay	AU		
20		Dark brown Clay	ST TCP	8-9 (17)	
		Dark brown Clay	AU		
25		Dark brown Clay	ST TCP	7-10 (17)	
		Dark brown Clay	AU		
30		Dark brown Clay	ST TCP	7-11 (18)	

Bottom of borehole at 30.0 feet.

GEOTECH BH COLUMNS - GINT STD US LAB.GDT - 12/5/19 15:36 - C:\USERS\PX03319\ONE\DRIVE - UNIVERSITY OF TEXAS AT ARLINGTON\2\_FORTWORTH INSTALLATION\DRILLING\BORELOGS\_1820 AND ROSEDALE ST\1820 AND ROSEDALE ST.GPJ



**Fort Worth District (October 2020)**



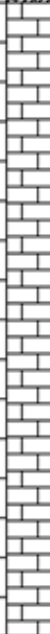
<b>LOGO</b>	University of Texas at Arlington	<b>BORING NUMBER BH-1</b>	PAGE 1 OF 1
CLIENT <u>TxDOT-Forth Worth</u>		PROJECT NAME <u>Forth Worth Slope Stabilization</u>	
PROJECT NUMBER <u>1</u>		PROJECT LOCATION <u>US 67 &amp; W Henderson St (South)</u>	
DATE STARTED <u>10/7/20</u> COMPLETED <u>10/7/20</u>		GROUND ELEVATION _____ HOLE SIZE _____ inches	
DRILLING CONTRACTOR _____		GROUND WATER LEVELS:	
DRILLING METHOD <u>Auger Drilling</u>		AT TIME OF DRILLING <u>---</u>	
LOGGED BY <u>UTA</u> CHECKED BY <u>UTA</u>		AT END OF DRILLING <u>---</u>	
NOTES _____		AFTER DRILLING <u>---</u>	

DEPTH (ft)	GRAPHIC LOG	MATERIAL DESCRIPTION	SAMPLE TYPE NUMBER	BLOW COUNTS (N VALUE)	MOISTURE CONTENT (%)
0.0	[Diagonal Hatching]	Brown clay	ST		
2.5	[Cross-hatching]	Dark grey clay weathered rock	AU		10.4 %
5.0	[Dotted]	Light gray clay with traces of limestone	TCP	50(6")-50(3")	
7.5	[Diagonal Hatching]		AU		10.4 %
10.0	[Dotted]		AU		
	[Diagonal Hatching]		TCP	41-40 (81)	11.7 %

Bottom of borehole at 12.0 feet.

GEOTECH BH COLUMNS - GWAT STD US LAB.GDT - 10/12/20 12:42 - C:\USER\SPUBLIC\DOCUMENTS\BENTLEY\GINT\PROJECTS\US 67 & W HENDERSON ST (SOUTH).GPJ

<b>LOGO</b>	University of Texas at Arlington	<b>BORING NUMBER BH-2</b>	PAGE 1 OF 1
CLIENT <u>TxDOT-Forth Worth</u>		PROJECT NAME <u>Forth Worth Slope Stabilization</u>	
PROJECT NUMBER <u>1</u>		PROJECT LOCATION <u>US 67 &amp; W Henderson St (South)</u>	
DATE STARTED <u>10/7/20</u>	COMPLETED <u>10/7/20</u>	GROUND ELEVATION _____	HOLE SIZE _____ inches
DRILLING CONTRACTOR _____		GROUND WATER LEVELS:	
DRILLING METHOD <u>Auger Drilling</u>		AT TIME OF DRILLING <u>---</u>	
LOGGED BY <u>UTA</u>		CHECKED BY <u>UTA</u>	
NOTES _____		AT END OF DRILLING <u>---</u>	
		AFTER DRILLING <u>---</u>	

DEPTH (ft)	GRAPHIC LOG	MATERIAL DESCRIPTION	SAMPLE TYPE NUMBER	BLOW COUNTS (N VALUE)	MOISTURE CONTENT (%)	
0.0						
2.5		Dark brown clay	ST			
5.0		Light gray clay with traces of limestone	AU	50(1")-50(1")	5.9 %	
			TCP			
7.5		Grey weathered rock	AU	50(0.5")-50(0.5")	10.2 %	
10.0			TCP			
12.5			AU			10.5 %
15.0						

Bottom of borehole at 15.0 feet.



University of Texas at Arlington

**BORING NUMBER BH-3**


PAGE 1 OF 1

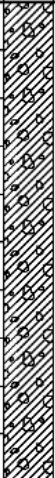

CLIENT TxDOT-Forth Worth PROJECT NAME Forth Worth Slope Stabilization  
 PROJECT NUMBER 1 PROJECT LOCATION US 67 & W Henderson St (South)  
 DATE STARTED 10/8/20 COMPLETED 10/8/20 GROUND ELEVATION \_\_\_\_\_ HOLE SIZE \_\_\_\_\_ inches  
 DRILLING CONTRACTOR \_\_\_\_\_ GROUND WATER LEVELS:  
 DRILLING METHOD Auger Drilling AT TIME OF DRILLING ---  
 LOGGED BY UTA CHECKED BY UTA AT END OF DRILLING ---  
 NOTES \_\_\_\_\_ AFTER DRILLING ---

DEPTH (ft)	GRAPHIC LOG	MATERIAL DESCRIPTION	SAMPLE TYPE NUMBER	BLOW COUNTS (N VALUE)	MOISTURE CONTENT (%)
0					
0-1		Dark brown stiff clay	ST		
1-2		Grey weathered rock	TCP	48-50(3")	6.9 %
2-3		Light gray weathered limestone	AU		
3-4		Light gray weathered limestone	TCP	50(3")-50(1")	6.8 %
4-5		Light gray weathered limestone	TCP	50(3")-50(1")	6.8 %
5-6		Light gray weathered limestone	TCP	50(3")-50(1")	6.8 %
6-7		Light gray weathered limestone	TCP	50(3")-50(1")	6.8 %
7-8		Light gray weathered limestone	TCP	50(3")-50(1")	6.8 %
8-9		Light gray weathered limestone	TCP	50(3")-50(1")	6.8 %
9-10		Light gray weathered limestone	TCP	50(3")-50(1")	6.8 %
10-11		Light gray weathered limestone	TCP	50(3")-50(1")	6.8 %
11-12		Light gray weathered limestone	TCP	50(3")-50(1")	6.8 %
12-13		Light gray weathered limestone	TCP	50(3")-50(1")	6.8 %
13-14		Light gray weathered limestone	TCP	50(3")-50(1")	6.8 %
14-15		Yellow brown stiff clay	AU		10.8 %
15-16		Yellow brown stiff clay	TCP	50(4.25")-50(4.25")	18.6 %
16-17		Yellow brown stiff clay	TCP	50(4.25")-50(4.25")	18.6 %
17-18		Yellow brown stiff clay	TCP	50(4.25")-50(4.25")	18.6 %
18-19		Yellow brown stiff clay	TCP	50(4.25")-50(4.25")	18.6 %
19-20		Yellow brown stiff clay	TCP	50(4.25")-50(4.25")	18.6 %
20-21		Grey brown stiff clay	AU		18.4 %
21-22		Grey brown stiff clay	ST		
22-23		Grey brown stiff clay	ST		
23-24		Grey brown stiff clay	ST		
24-25		Grey brown stiff clay	TCP	50(0.5")-50(0)	18.4 %

G:\GEO\B3\B3\GINT STD. U.S. LAB GDT. - 10/8/20 12:42 - CALISERS\PUBLIC\DOCUMENTS\BENTLEY\PROJECTS\US 67 & W HENDERSON ST (SOUTH).GPJ

Bottom of borehole at 25.0 feet.

	University of Texas at Arlington	<b>BORING NUMBER BH-4</b> PAGE 1 OF 1
CLIENT <u>TxDOT-Forth Worth</u>		PROJECT NAME <u>Forth Worth Slope Stabilization</u>
PROJECT NUMBER <u>1</u>		PROJECT LOCATION <u>US 67 &amp; W Henderson St (South)</u>
DATE STARTED <u>10/8/20</u>	COMPLETED <u>10/8/20</u>	GROUND ELEVATION _____ HOLE SIZE _____ inches
DRILLING CONTRACTOR _____		GROUND WATER LEVELS:
DRILLING METHOD <u>Auger Drilling</u>		AT TIME OF DRILLING ---
LOGGED BY <u>UTA</u> CHECKED BY <u>UTA</u>		AT END OF DRILLING ---
NOTES _____		AFTER DRILLING ---

DEPTH (ft)	GRAPHIC LOG	MATERIAL DESCRIPTION	SAMPLE TYPE NUMBER	BLOW COUNTS (N VALUE)	MOISTURE CONTENT (%)	
0.0		Dark brown stiff clay with gravel				
			ST			
			ST			
2.5				ST		
						17.6 %
5.0						
		Yellow brown clay with crushed limestone	AU TCP	30-26 (56)		
			AU		15.5 %	
7.5			ST		21.8 %	
			TCP	50(3")-39		
10.0			TCP	50(6")-50(6")		

Bottom of borehole at 12.0 feet.

<b>LOGO</b>	University of Texas at Arlington	<b>BORING NUMBER BH-1</b>	PAGE 1 OF 1
CLIENT <u>University of Texas at Arlington</u>		PROJECT NAME <u>TxDOT-Fort Worth</u>	
PROJECT NUMBER <u>1</u>		PROJECT LOCATION <u>US 67 and W Henderson St (North)</u>	
DATE STARTED <u>10/7/20</u> COMPLETED <u>10/7/20</u>		GROUND ELEVATION _____ HOLE SIZE _____ inches	
DRILLING CONTRACTOR _____		GROUND WATER LEVELS:	
DRILLING METHOD <u>Auger Drilling</u>		AT TIME OF DRILLING <u>---</u>	
LOGGED BY <u>UTA</u> CHECKED BY <u>UTA</u>		AT END OF DRILLING <u>---</u>	
NOTES _____		AFTER DRILLING <u>---</u>	

DEPTH (ft)	GRAPHIC LOG	MATERIAL DESCRIPTION	SAMPLE TYPE NUMBER	BLOW COUNTS (N VALUE)	MOISTURE CONTENT (%)
0.0		Brown clay			
	[Hatched Pattern]		ST		
2.5		Light brown clay			
	[Hatched Pattern]		ST		
	[Hatched Pattern]		ST TCP	50(1")-50(1")	
5.0					
	[Hatched Pattern]		ST		21.5 %
7.5					
	[Hatched Pattern]		ST		
	[Hatched Pattern]		ST		
10.0		Weathered limestone	TCP	50(1")-50(0)	
	[Hatched Pattern]				
	[Hatched Pattern]	Grey clay	AU		19.9 %
12.5					
	[Hatched Pattern]		AU		21.8 %
	[Hatched Pattern]	Brown clay	TCP	50(0)-50(0)	
15.0					

Bottom of borehole at 15.0 feet.

GEOTECH BH COLUMNS - GINT STD U.S. LAB GDT - 10/12/20 12:09 - C:\USERS\PUBLIC\CD\DOCUMENTS\BENTLEY\INT\PROJECTS\US 67 & W HENDERSON ST (NORTH).GPJ

<b>LOGO</b>	University of Texas at Arlington	<b>BORING NUMBER BH-2</b>	PAGE 1 OF 1
CLIENT <u>University of Texas at Arlington</u>		PROJECT NAME <u>TxDOT-Fort Worth</u>	
PROJECT NUMBER <u>1</u>		PROJECT LOCATION <u>US 67 and W Henderson St (North)</u>	
DATE STARTED <u>10/8/20</u> COMPLETED <u>10/8/20</u>		GROUND ELEVATION _____ HOLE SIZE _____ inches	
DRILLING CONTRACTOR _____		GROUND WATER LEVELS:	
DRILLING METHOD <u>Auger Drilling</u>		AT TIME OF DRILLING <u>---</u>	
LOGGED BY <u>UTA</u> CHECKED BY <u>UTA</u>		AT END OF DRILLING <u>---</u>	
NOTES _____		AFTER DRILLING <u>---</u>	

DEPTH (ft)	GRAPHIC LOG	MATERIAL DESCRIPTION	SAMPLE TYPE NUMBER	BLOW COUNTS (N VALUE)	MOISTURE CONTENT (%)
0		Dark brown stiff clay with rock	ST	50(1.5")-50(0)	9.9 %
		Light brown clay with traces of limestone	AU		
		Grey clay	AU		
5		Yellow brown clay	TCP		
			AU	14-11 (25)	14.8 %
10			ST		
			AU	15-10 (25)	19.3 %
15			ST		
		Brown clay	AU	21-35 (56)	22.7 %
20			TCP		
				50(0.25")-50(0.125")	

GEOTECH BH COLUMNS - GINT STD U.S. LAB GDT - 10/1/2020 12:08 - C:\USERS\PUBLIC\DOCUMENTS\BENTLEY\PROJECTS\US 67 & W HENDERSON ST (NORTH).GPJ

Bottom of borehole at 22.0 feet.



<b>LOGO</b>	University of Texas at Arlington	<b>BORING NUMBER BH-1</b>	PAGE 1 OF 1
CLIENT <u>TxDOT-Fort Worth</u>		PROJECT NAME <u>Fort Worth Slope Stabilization</u>	
PROJECT NUMBER <u>1</u>		PROJECT LOCATION <u>I35W and W Cotter Ave</u>	
DATE STARTED <u>10/9/20</u> COMPLETED <u>10/9/20</u>		GROUND ELEVATION _____ HOLE SIZE _____ inches	
DRILLING CONTRACTOR _____		GROUND WATER LEVELS:	
DRILLING METHOD <u>Auger Drilling</u>		∇ AT TIME OF DRILLING <u>20.00 ft</u>	
LOGGED BY <u>UTA</u> CHECKED BY <u>UTA</u>		AT END OF DRILLING <u>--</u>	
NOTES _____		AFTER DRILLING <u>--</u>	

DEPTH (ft)	GRAPHIC LOG	MATERIAL DESCRIPTION	SAMPLE TYPE NUMBER	BLOW COUNTS (N VALUE)	MOISTURE CONTENT (%)
0		Brown clay	ST		
			ST		
			ST		
5			ST		
10			AU TCP	6-3 (9)	17.9 %
15			AU ST	9-8 (17)	18.4 %
20	∇		AU ST	5-10 (15)	18.1 % 22.1 %
					21.7 %
		Sandy clay	AU		
25		Gray clay	ST AU	15-18 (33)	
					24.2 %
30			TCP	13-12 (25)	

Bottom of borehole at 30.0 feet.


GEOTECH BH COLUMNS - GINT STD US LAB GDT - 10/7/2020 11:42 - C:\USERS\PUBLIC\DOCUMENTS\BENTLEY\PROJECTS\BENTLEY\PROJECTS\BENTLEY\W.COTTER AVENUE.GPJ

<b>LOGO</b>	University of Texas at Arlington	<b>BORING NUMBER BH-2</b>	PAGE 1 OF 1
CLIENT <u>TxDOT-Fort Worth</u>		PROJECT NAME <u>Fort Worth Slope Stabilization</u>	
PROJECT NUMBER <u>1</u>		PROJECT LOCATION <u>I35W and W Cotter Ave</u>	
DATE STARTED <u>10/9/20</u> COMPLETED <u>10/9/20</u>		GROUND ELEVATION _____ HOLE SIZE _____ inches	
DRILLING CONTRACTOR _____		GROUND WATER LEVELS:	
DRILLING METHOD <u>Auger Drilling</u>		▽ AT TIME OF DRILLING <u>22.00 ft</u>	
LOGGED BY <u>UTA</u> CHECKED BY <u>UTA</u>		AT END OF DRILLING <u>---</u>	
NOTES _____		AFTER DRILLING <u>---</u>	

DEPTH (ft)	GRAPHIC LOG	MATERIAL DESCRIPTION	SAMPLE TYPE NUMBER	BLOW COUNTS (N VALUE)	MOISTURE CONTENT (%)
0		Brown Clay	ST		16.8 %
			ST		
5		Dark Brown Clay	TCP	7-19 (26)	
			ST		
10			AU		
			ST	17-21 (38)	
15		Grey Brown Clayey Sand	AU		
			ST	10-9 (19)	
20			AU		
			TCP ST	13-9 (22)	
25		Yellow Flowing Sand	TCP	10-8 (18)	
			AU		
30	Limestone	TCP	45-50(4.5")	31.9 %	

Bottom of borehole at 30.0 feet.

El Paso District



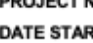
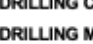
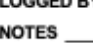

The University of Texas at Arlington  
416 Yates Street  
76010

**BORING NUMBER B-4**  
PAGE 1 OF 2

CLIENT <u>El-Paso</u>	PROJECT NAME <u>El-Paso Soil Sample Collection</u>
PROJECT NUMBER <u>1</u>	PROJECT LOCATION _____
DATE STARTED _____ COMPLETED _____	GROUND ELEVATION _____ HOLE SIZE <u>inches</u>
DRILLING CONTRACTOR _____	GROUND WATER LEVELS:
DRILLING METHOD <u>Hollow Stem Auger 2"</u>	AT TIME OF DRILLING <u>--</u>
LOGGED BY _____ CHECKED BY _____	AT END OF DRILLING <u>--</u>
NOTES _____	AFTER DRILLING <u>--</u>

DEPTH (ft)	GRAPHIC LOG	MATERIAL DESCRIPTION	SAMPLE TYPE NUMBER	RECOVERY % (RQD)	BLOW COUNTS (N VALUE)	POCKET PEN. (tsf)	DRY UNIT WT. (pcf)	MOISTURE CONTENT (%)	ATTERBERG LIMITS			FINES CONTENT (%)
									LIQUID LIMIT	PLASTIC LIMIT	PLASTICITY INDEX	
0												
			SPT		6-5-4 (9)							
			SPT		2-3-2 (5)							
5			SPT		5-4-6 (10)							
			SPT		3-2-3 (5)							
10			SPT		8-18-22 (40)							
			SPT		8-6-8 (14)							
15			SPT		7-7-8 (15)							
			SPT		4-5-5 (10)							
20		SILTY SAND, (SM) Silty Sand (SM); Brown	SPT		8-10-13 (23)							
			SPT		5-7-10 (17)							
25		CLAYEY SAND, (SC) Clayey Sand; Brown;										
			SPT		8-20-16 (36)							
		SILTY SAND, (SM) Silty Sand (SM); Brown;	SPT		9-13-15 (28)							
		CLAYEY SAND, (SC) Clayey Sand (SC); Brown;										
30			SPT		8-18-35 (53)							
			SPT		13-12-9 (21)							
35												

(Continued Next Page)



**APPENDIX C    WORKSHOP SUMMARY****WORKSHOP****Electrical Resistivity Imaging Technique for Geotechnical Analysis**

**The University of Texas at Arlington  
June 2021**

The application of advanced geophysical tools, such as the Electrical Resistivity Imaging (ERI) technique, could improve site investigations in the Texas Department of Transportation (TxDOT). It could mitigate cost overruns and delays due to inadequate subsurface investigations. Electrical Resistivity Imaging provides a unique opportunity to reduce these costs and delays by providing (1) continuous subsurface images along with estimated soil properties and potential anomalies (e.g., karst, void) between the boreholes, and (2) additional information about the required drilling and sampling intervals. The ERI technique provides continuous assessment of the subsurface condition using a non-invasive, rapid, and cost-effective method.

This workshop focuses on:

- Significance of subsurface investigations in infrastructure projects
- Benefits/Value of ERI technology in subsurface characterization
- Deterrents of using ERI technology and practices to overcome those deterrents
- Presentation of ERI research manual developed for TxDOT in RTI Project 0-7008 and its application in practice including:
  - Planning considerations for ERI surveys
  - Step-by-step procedures and guidelines for performing ERI surveys
  - Practical considerations regarding different operational environments and extreme weather conditions
- Interpretation of continuous subsurface resistivity images along with the borehole findings
- Application of the empirical relationships between the geotechnical and geophysical parameters developed based on extensive data collection (from 5 different districts) and statistical analysis
- Demo of the GeoParameter application developed in RTI Project 0-7008 for the estimation of geotechnical parameters using the empirical relationships
- Demonstration of a training video explaining the field data collection procedure and processing the field data using a software

## APPENDIX D VALUE OF RESEARCH ON ADVANCED GEOPHYSICAL TOOLS IN GEOTECHNICAL ANALYSIS

This appendix elaborates on the Value of Research (VoR) by determining the qualitative and economic benefits of electrical resistivity imaging for geotechnical analysis.

Table D.1 presents a summary of the benefit areas related to this project. In this table, the benefit areas are associated with qualitative and economic (quantitative) benefits. Qualitative benefits of transportation research are those benefits that are not directly quantifiable, such as safety (Ellis et al., 2003). On the other hand, the quantitative benefits are those that can be quantified as savings after implementation, such as reduction in construction operations and maintenance costs (Ellis et al., 2003). In the following subsections, the qualitative and economic benefits of this research across various areas are discussed.

**Table D.1** Value of Research (VoR) Form

<i>Benefit Area</i>	<i>Qual.</i>	<i>Econ</i>	<i>Both</i>	<i>TxDOT</i>	<i>State</i>	<i>Both</i>
Reduced Construction Operations and Maintenance Cost		×		×		
Environmental Sustainability	×					×
Level of Knowledge	×			×		
Safety	×					×
Infrastructure Condition	×					×
Material and Pavements	×			×		
System Reliability	×			×		
Increase Service Life	×			×		
Management and Policy	×			×		
Reduced Administrative Costs	×			×		
Traffic and Congestion Reduction	×					×
Customer Satisfaction	×					×

*Notes: Qual.: Qualitative; Econ: Economic; TxDOT: Texas Department of Transportation; State: State of Texas.*


### **D.1. Reduced Construction Operations and Maintenance Cost**

The subsurface investigation costs a few thousand dollars, while the cost of over-conservative designs or costly failures in terms of construction delays, construction extras, shortened design life, increased maintenance, and public inconvenience is typically hundreds of thousands of dollars (Christopher et al., 2006). Texas Department of Transportation (TxDOT) encounters a considerable and yet increasing number of claims and change orders every year that has a detrimental effect on project costs and schedules (Shrestha and Maharjan, 2018). Lack of sufficient and accurate information about the subsurface condition is one of the critical factors that contribute to such cost overruns and delays at project sites in 20 to 50% of all infrastructure projects (Baynes, 2010). This lack of sufficient information is due to the inherent limitation of the conventional geotechnical site investigation methods to provide continuous assessment of the subsurface (i.e., these conventional methods only sample and provide information about a small percentage of a total sample space). A national survey of 55 U.S. transportation agencies showed that the annual cost of change orders resulting from the insufficient subsurface investigation is commonly in order of millions of dollars (Boeckmann and Loehr, 2016).

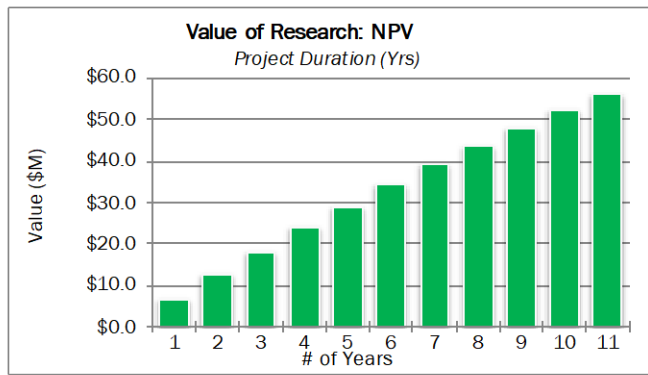
Repairing damages to buildings, highways, and other infrastructure systems resulting from inadequate subsurface information is a significant national cost. For example, the average repairing cost of karst-related damages to the infrastructures was estimated to be at least \$300 million per year in the U.S. (Weary, 2015). As another example, at least \$100 million is spent annually in the U.S. (\$7 million in the TxDOT) on repairs dealing with bridge approach slab problems that mainly resulted from the inadequate subsurface investigation, inadequate analysis, and subsequent stabilization problems (Lenke, 2006; Seo and Briaud, 2002).

This research offers value by providing a unique opportunity to mitigate these costs and limitations of conventional geotechnical site investigation methods. For example, if we assume that TxDOT spends \$7 million annually only for repairing bridges, failed due to inadequate subsurface investigation (Lenke, 2006; Seo and Briaud, 2002), in a 10-year horizon, the present value of avoiding this cost by enriching existing geotechnical investigations with continuous subsurface information using ERI will be over \$55 million considering a discount rate of 5%. Figure D.1 shows how this present value is calculated. In this analysis, the capital cost of ERI equipment is assumed to be around \$20,000, and a total annual salary of \$210,000 is considered for a crew of

three persons to perform the ERI surveys and data analysis. The cost of this research project (with \$269,523 capital cost) has also been taken into account in this analysis.

	<b>Project #</b>		0-7008	
	<b>Project Name:</b>		Advanced Geophysical Tool for Geotechnical Analysis	
	<b>Agency</b>	UTA	<b>Project Budget</b>	\$ 269,523
	<b>Project Duration (Yrs)</b>	2.0	<b>Exp. Value (per Yr)</b>	\$ 6,790,000
<b>Expected Value Duration (Yrs)</b>		10	<b>Discount Rate</b>	5%
<b>Economic Value</b>				
<b>Total Savings:</b>	\$ 67,386,672	<b>Net Present Value (NPV):</b>		\$ 56,140,795
<b>Payback Period (Yrs):</b>	0.039694	<b>Cost Benefit Ratio (CBR, \$1 : \$ ):</b>		\$ 208

Years	Expected Value
0	\$6,744,281
1	\$6,660,176
2	\$6,676,019
3	\$6,790,000
4	\$6,790,000
5	\$6,790,000
6	\$6,790,000
7	\$6,790,000
8	\$6,790,000
9	\$6,790,000
10	\$6,790,000



Years	Expected Value	Expected Value	Expected Value	NPV
0	\$6,744,281	\$6,744,281	\$6.74	\$6.42
1	\$6,660,176	\$13,404,457	\$13.40	\$12.46
2	\$6,676,019	\$20,080,476	\$20.08	\$18.23
3	\$6,790,000	\$26,870,476	\$26.87	\$23.82
4	\$6,790,000	\$33,660,476	\$33.66	\$29.14
5	\$6,790,000	\$40,450,476	\$40.45	\$34.20
6	\$6,790,000	\$47,240,476	\$47.24	\$39.03
7	\$6,790,000	\$54,030,476	\$54.03	\$43.63
8	\$6,790,000	\$60,820,476	\$60.82	\$48.00
9	\$6,790,000	\$67,610,476	\$67.61	\$52.17
10	\$6,790,000	\$74,400,476	\$74.40	\$56.14

**Notes:**

Amounts on Value of Research are estimates.
Project cost should be expensed at a rate of no more than the expected value per year.
This electronic form contains formulas that may be corrupted when adding or deleting rows, by variables within the spreadsheet, or by conversion of the spreadsheet. The university is responsible for the accuracy of the Value of Research submitted.

**Figure D.1** Value of advanced geophysical tools for geotechnical analysis



**D.2. Environmental Sustainability**

This research project offers value by providing essential information about the subsurface condition through a noninvasive geophysical site investigation method. Unlike conventional geotechnical site investigation methods such as drilling, the electrical resistivity imaging technique leaves little if any imprint on the environment. These considerations can be crucial when working in environmentally sensitive areas, contaminated ground, or private properties.

**D.3. Level of Knowledge**

This study improves the level of knowledge by providing a comprehensive, instructive, and practical research manual to offer guidelines and tools for a rapid and continuous assessment of subsurface conditions. The gained experience by demonstrating electrical resistivity imaging surveys in the selected districts is also included in the manual to cover practical considerations for surveying in different operational environments and geotechnical conditions. This research project provides value by offering training workshops in the TxDOT selected districts to disseminate knowledge about the applications, data collection, and data interpretation of electrical resistivity imaging technology.

**D.4. Safety**

Although the failures due to the inadequate subsurface investigation rarely cause danger to human life directly, they affect the performance and structural stability of the infrastructure systems. The process of repairing these failures requires work zones that jeopardize the safety of drivers. TxDOT reported more than 22,000 traffic crashes with 186 fatalities in work zones (TxDOT, 2021). This research project indirectly contributes to highway safety by providing guidelines and tools for a rapid and continuous assessment of subsurface conditions that mitigate failures and subsequently decrease the number of work zones related to these failures.

**D.5. Infrastructure Condition**

Inadequate subsurface information can affect the performance and structural stability of the infrastructure systems or may lead to the failure of these systems. This project offers value by providing guidelines and tools for a rapid and continuous assessment of subsurface conditions, mitigating failures that affect infrastructure systems.

**D.6. Material and Pavements**

This research offers value by providing information about the electrical resistivity imaging technique and practical tools for a rapid and continuous assessment of subsurface conditions to prevent failures and damage to the pavements and ensure the long-term performance of infrastructure systems and construction projects.

**D.7. System Reliability and Increase Service Life**

The inadequate subsurface investigation will lead to long-term problems with the roadway design (Christopher et al., 2006). This research offers value by providing information about the electrical resistivity imaging technique and practical tools to develop procedures in conjunction with the conventional geotechnical site investigation methods to make reliable conclusions about the subsurface condition and potential subsurface anomalies. This information helps conduct a rapid and continuous assessment of subsurface characteristics to prevent inadequate/conservative designs and mitigate risks and unexpected failures due to lack of adequate subsurface investigation.

**D.8. Management and Policy**

This research project provides value by developing a comprehensive research manual to offer guidelines and tools to (1) improve site characterization findings using continuous images of the subsurface, (2) provide rapid estimates for geotechnical properties using empirical equations and charts. The implementation of this manual helps reduce risk and uncertainty, prevent inadequate/conservative designs, and increase accuracy in bids.

**D.9. Reduced Administrative Costs**

Repairing project failures due to inadequate subsurface investigation require administrative tasks, such as project management and paperwork. Reducing the amount of these failures results in a decrease in the costs associated with these administrative tasks. This research provides value with respect to this benefit area by providing guidelines and tools for a rapid and continuous assessment of subsurface conditions, preventing project failures.

This research project creates value by offering training workshops and providing freely available educational materials, such as training text and video materials that can be accessed by TxDOT managers and decision-makers. TxDOT is expected to spend \$1,500,000 on role-based training

programs for fiscal years 2022 and 2023 (TxDOT, 2020). This research project provides the opportunity to reduce the annual educational expenditures by offering training workshops and providing freely available training text and video materials.

#### **D.10. Traffic and Congestion Reduction**

According to an urban mobility report, in 2015, Americans spent 6.9 billion hours in traffic and consumed 3.1 billion gallons of fuel that is equivalent to \$160 billion in time and fuel loss (Schrank et al., 2015). According to the U.S. Department of Transportation (USDOT), about 10% of total delays are attributed to work zones (U.S. Department of transportation, 2017). Therefore, the congestion cost due to work zones is about \$16 billion. This research project contributes to congestion reduction by helping prevent project failures due to insufficient subsurface information and, consequently, reducing the required work zone.

#### **D.11. Customer Satisfaction**

Highway maintenance activities usually require lane closures, frequently disrupt traffic operations, and increase delays because of limited capacity (Du et al., 2016). Congestion is one of the significant factors affecting transportation customer satisfaction (Ye et al., 2013). This research project contributes to congestion reduction by providing means and methods to prevent project failures resulting from insufficient subsurface information and, consequently, reduce the required work zones.

## APPENDIX E TECHNOLOGY READINESS LEVEL ASSESSMENT

This appendix presents the process of assessing the readiness level of the electrical resistivity imaging (ERI) technology to evaluate the readiness and maturity of the electrical resistivity imaging technology to help improve site investigations in TxDOT.

Technology Readiness Levels (TRLs) are formal metrics that support assessments of a particular technology and provide the ability to consistently compare levels of maturity between different types of technologies. The TRL scale was used to determine the development level of the electrical resistivity imaging technology with a targeted TRL 9. The TRL 9 requires the demonstration and refinement of the proven technology (in this case, ERI technology) in operational environments (in this case, job sites of active projects across various TxDOT districts).

A panel consisted of the TxDOT advisory committee appointed to the research project, the Principal Investigator (PI) of the project, and the Co-Principal Investigator (Co-PI) of the project was formed to assess the readiness and maturity of the electrical resistivity imaging technology. Table E.1 lists the panel members and the project manager.

**Table E.1** Panel members and the project manager

<b>Panel Members</b>		
<b>Project Manager</b>	<b>Receiving Agency</b>	<b>Performing Agency</b>
Jade Adediwura	Natnael Asfaw (current)	Mohsen Shahandashti (PI)
	Prakash Chavda (current)	Sahadat Hossain (Co-PI)
	Trenton Ellis (current)	
	Haijian Fan (current)	
	Jimmy Si (former)	
	Boon Thian (former)	

The goals of assessment were discussed in several meetings to make sure that all the panelists agree on these goals. The goals include but are not limited to:

- Development of an easy-to-use comprehensive manual that provides TxDOT staff with the electrical resistivity imaging technique procedures and guidelines for safe and efficient implementation of ERI technology.
- Development of equations and charts to define the relationship between the soil electrical resistivity and geotechnical properties such as moisture content, dry unit weight, plasticity index, clay content, and percent of fines.
- Demonstration of electrical resistivity imaging technique to TxDOT staff in the selected districts.
- Creation of easy-to-use and searchable text and video training materials for learning workshops; enabling TxDOT staff to learn about how to conduct the electrical resistivity imaging and process the field data.

These goals helped assessing the level of the development of the ERI technology.

The performing agency demonstrated the ERI technology in its intended operational environments in the selected districts (27 ERI surveys) to evaluate the performance of the ERI technology to meet its intended use and functionality. The survey planning and implementation procedure were refined during the demonstrations and translated into a step-by-step process elaborated in the ERI research manual. Besides, practical considerations regarding different operational environments and extreme weather conditions were also included in the ERI research manual. Furthermore, sets of equations and charts were developed using extensive laboratory tests and included in the research manual to provide new tools for estimating geotechnical parameters using ERI technology.

The information about ERI technology and the gained experience from the demonstrated surveys were compiled into a comprehensive set of materials, including technical memorandums, electrical resistivity imaging research manual, seven presentations. In addition, an Excel-based application was created to automate the computation of the geotechnical parameters from the proposed equations in the research manual to facilitate the use of the equations. These materials were disseminated to the receiving agency to convey all the required information they need to evaluate

the research project's progress. The results were discussed in two meetings: (December 12, 2020 and September 17, 2020). The timings of the meetings were formalized by the project manager in communication with the panel members. The panel's extensive comments help the research team further improve the electrical resistivity imaging research manual and develop an Excel-based application to facilitate the use of the proposed equations for the estimation of the geotechnical parameters.

The performing agency fully addressed the received comments from panelists by making revisions of the ERI research manual (three revisions). The major additions to the ERI research manual are:

- A section on the intended use of the ERI research manual
- A section of the benefits of the ERI research manual over the existing manuals
- A section on safety hazards and precautions to avoid injury or damage to the equipment
- A section on common mistakes that personnel may encounter in performing a field ERI survey
- A section on limitations of the ERI technology

Besides, according to the panelists' comments, an Excel-based application was created to automate the computation of the geotechnical parameters from the proposed equations in the research manual to facilitate the use of the proposed equations.

The performing agency also created text and video training materials, including presentation slides, a training video, and performed training workshops to convey the information about the ERI technology and share the project's findings with the TxDOT staff. Considering the performing agency's accomplishments, refinements to the ERI research manual, and the successful completed training workshops, the readiness of the ERI technology and research manual is assessed to stand at the TRL 9.